2021

Deep-sea discovery - mining marine environments for novel biologics.

Hesketh-Best, Poppy Jessica

Copyright Statement

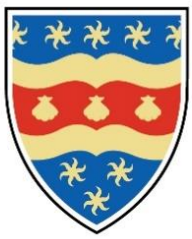

UNIVERSITY OF PLYMOUTH

DEEP-SEA DISCOVERY - MINING MARINE ENVIRONMENTS FOR NOVEL BIOLOGICS

by

POPPY JESSICA HESKETH BEST

A thesis submitted to the University of Plymouth

in partial fulfilment for the degree of

DOCTOR OF PHILOSOPHY

School of Biology and Marine Sciences

September 2021

Acknowledgements

Somehow despite a pandemic, multiple lockdowns, wrist surgery and all the added stresses of a PhD and life, I've managed to complete this thesis. I have so many incredible people to thank for all of this to have been possible.

First of all, to my supervisory panel, thank you so much for trusting me with this project and helping me take the giant leap into a career in research. Kerry Howell and Matthew Upton, your guidance, enthusiasm and vision for this project spanned much further than I could achieve, but both taught me to aim big. To the Upton Lab and Deep-Sea Cru, whose continued support was key for this PhD's outputs. Michelle, your help and guidance helped me get over the terror of writing and submitting that first paper for publication.

A mi amor Dean, I cannot thank you for you enough for all the care and support. For cooking for me all the times I came home from the lab at 11 pm, or making me laugh when it I felt at my lowest. Your support got me through this past year and a half. Te queiro con todo mi corazon, and look forward to traversing the hellscape of life as a postdoc with you.

To my absolute best PhD friend™ Matt, eres lo mejor persona en todo el mundo! Going through this journey with you made it much more bearable. I will miss all the orchestral power metal, Lord of the Rings, and music about evil wizard towers blasting from the lab speakers, and the coffee chats talking about Tolkien and fantasy books. Jack, the second-hand experience of you writing your thesis was awful, but you endured me when I was writing mine. Thank you for all the distracting chats, pub and cinema invites, and drunk sessions eating spicy potatoes outside Favourite Foods. To all the D&D groups and the book

clubs, you provided much-needed escapism from work. Molly and Immy for all the climbing and brownies sessions. Amelia, always ready for a Friday beer. Kim, for all the times you cooked delicious food and then unleashed your parrot onto us. Friedrich for being your usual entertaining grumpiness. To Rachel and Harry, you always managed to call me just when I wanted to gossip and talk nonsense for an hour. Thank you to everyone who let me cat-sit and all the cats that came by to visit our house.

To my wonderful mum, my brothers, and grandparents, thank you all for everything. Without your continued support I probably wouldn't have made it to where I am now. A Puli and Andy, te extrano, quiero y espero el dia cuando reunimonos. To all my friends back home and around the world doing their own PhDs or at new stages of their lives, you were only ever a text or phone away.

Authors Declaration

At no time during the registration for the degree of *Doctor of Philosophy* has the author been registered for any other University award without prior agreement of the Doctoral College Quality Sub-Committee.

Work submitted for this research degree at the University of Plymouth has not formed part of any other degree either at the University of Plymouth or at another establishment. This study was financed with the aid of a studentship from the *University of Plymouth.*

The following external institutions were visited for research and consultation purposes:

- Diving Diseases Research Centre (DDRC) Healthcare, Hyperbaric Medical Centre, Research Way, Plymouth Science Park, Plymouth, Devon, PL6 8BU

Word count of main body of thesis: 38,167

Signed  **Date** 29th September 2021

Research Outputs

Publications

- Chapter 1 – Matthew J. Koch, **Poppy J. Hesketh-Best,** Gary Smerdon, Philip J. Warburton, Kerry Howell and Mathew Upton (TBC) 'Impact of growth media and pressure on the diversity and antimicrobial activity of isolates from two species of Hexactinellid Sponge', *Microbiology*. **(*in press*)**

  This paper was designed and conceived collaboratively between Matthew J. Koch (MJK) and Poppy J Hesketh-Best (PJHB). The collection and analysis of data was evenly divided between MJK and PJHB. MJK drafted the first manuscript. PJHB wrote and conducted to data analysis, graphical presentation, and writing of sections relevant to data collected by PJHB, which is presented in this thesis. GS provided advice and facilities for pressure based cultivation at DDRC. PJW, GS, KH, and MU provided critical review of the work. Funding was acquired by KH and MU.

- Chapter 3 – **Hesketh-Best, P. J.**, Michelle V. Mouritzen, Kayleigh Shandley-Edwards, Richard A Billington, Mathew Upton (2021) '*Galleria mellonella* larvae exhibit a weight-dependent lethal median dose when infected with Methicillin-resistant *Staphylococcus aureus'*, *Pathogens and Disease*. Oxford University Press (OUP). https://academic.oup.com/femspd/article/79/2/ftab003/6121426

This paper was designed and conceived collaboratively between Poppy J Hesketh-Best (PJHB) and Michelle V. Mouritzen (MVM). PJHB and MVM collected the data. PJHB analysed and presented the data, and wrote the manuscript. MVM and additional authors contributed in finalising the manuscript for publication, and provided critical cometary on the analysis and conclusions.

Conference and workshop attendance

- 'Kraken2 to R', online workshop July 5-7th 2021
- 2nd Antimicrobial Discovery Acceleratory Network (ABX) Seminar, online in December 2020 (Session Chair)
- 'Metabarcoding with Mothur' online workshop, Rhodes University, South Africa, March 2021.
- International Meeting for Antimicrobial Peptides in Utrecht Netherlands, August 2019 (poster presentation)
- 1st Antimicrobial Resistance Training Programme's 1st Annual Conference, Bristol UK in August 2018 (poster presentation)
- 15th Deep-sea Biology Symposium, Monterey California in September 2018 (poster presentation)
- An'vio metagenomics workshop, University of Exeter, Penryn. August 2018
- 15th Marine Biological Association Post-graduate Conference, Plymouth UK in April 2018 (oral presentation)

Abstract

Deep-sea discovery - mining marine environments for novel biologics.

Poppy Jessica Hesketh Best

Global antimicrobial resistance will change the face of modern medicine, and the discovery of novel antimicrobials is one of the many solutions to this challenge. Furthermore, expanding antimicrobial natural product discovery to poorly explored ecological habitats may lead to the identification of novel compounds. In this body of work, deep-sea sponges are investigated as a source for bacterially derived antibiotics. Both cultivation dependent and independent strategies were employed to isolate and identify promising bacterial candidates, in addition to further understanding the sponge host microbiome.

Pheronema carpenteri was identified during cultivation efforts as a sponge from which multiple active bacterial strains can be cultivated. The first microbiome of *P. carpenteri* from two aggregations is reported herein. It was observed that *P. carpenteri* contains a bacterial community similar to those previously reported for Hexactinellid sponges and that intra- and inter-aggregation distinction occur.

To establish methodologies for assessing bioactive compounds purified from bacterial isoaltes, the use of *Galleria mellonella* larvae were explored as a rapid and scalable *in vivo* model. Larval weight is demonstrated as a vital parameter to control variability of data when working with pet-food grade larvae. Methodological consideration from working with *G. mellonella* larvae are then

applied to the bioactive compound isoaltes from the strain *Delftia acidovorans* PB091. PB091 was isolated from *P. carpenteri* and demonstrated activity against both methicillin resistant *Staphylococcus aureus* (MRSA) and *Escherichia coli*. Purification of an active compound was achieved, but it displayed only anti-Gram-positive activity, and was identified as delftibactin A. PB091_S70 delftibactin A demonstrated low levels of *in vivo* toxicity and a MIC of 25 µg/ml against multiple strains of MRSA.

In this body of work, *P. carpenteri* sponges are reported as promising organisms for both cultivation dependent and independent investigations for natural product discovery. Metagenomic work here was limited, and future work should build upon early data presented here. Deep-sea sponges continue to be an exciting reservoir of bacterially derived natural products, which may aid in tackling AMR.

Table of Contents

List of Figures

List of Tables

List of Equations

List of Abbreviations

ACN	Acetonitrile
AIA	Actinomycetes isolation agar
ANI(b)	Average nucleotide identifty (BLASTn)
ANOVA	Analysis of Variance
ASW	Artificial Seawater
ATCC	American Type Culture Collection
BGC	Biosynthetic Gene Cluster
CFU	Colony forming units
CV	Column volume
$_{dd}H_2O$	double distilled water
$_{d}H_2O$	distilled water
DNA	Deoxyribonucleic acids
dsDNA	double stranded DNA
DSMZ	German Collection of Microorganisms and Cell Cultures GmbH/ Deutsche Sammlung von Mikroorganismen und Zellkulturen
EDTA	Ethylenediaminetetraacetic acid
EtOH	Ethanol
EUCAST	European Committee on Antimicrobial Susceptibility Testing
FSSW	Filtered Sterilised Seawater
GC	Growth control
HMA	High microbial abundant
IO	Instant Ocean
L50	The smallest number of contigs whose length sum makes up 50% of the total genome length
L75	The smallest number of contigs whose length sum makes up 75% of the total genome length
LB(a)	Luria-Bertani (agar)
LD_{50}	Median lethal dose
LMA	Low microbial abundant
LNHM	Low Nutrient Heterotrophic Media
MA	Marine agar
MALDI-TOF	Matrix-assisted laser desorption ionisation-time of flight
MB	Marine Broth
MeOH	Methanol
MeOH	Methanol
$_{m}EtOH$	molecular grade Ethanol
MH(a)	Mueller Hinton (agar)
$_{m}H_2O$	milliq/molecular grade water

MIC	Minimum Inhibitory Concentration
MRSA	Methicillin resistant *Staphylococcus aureus*
MS	Mass Spectrometry
N	Number of replicas
N50	Sequence length of the shortest contig at 50% of the total genome length
N75	Sequence length of the shortest contig at 75% of the total genome length
NA	Nutrient agar
NB	Nutrient broth
NCTC	National Collection of Type Cultures
NE	North East
NP	Natural Product
NRP	Nonribosomal peptide
NRPS	Nonribosomal peptide synthase
OA	Oatmeal agar
ONT	Oxford Nanopore Technologies
OSMAC	One Strain, Many Active Compounds
p	P-value
PBS	Phosphate buffered saline
PCP	Peptidyl Carrier Protein
PCR	Polymerase Chain Reaction
PKS	Polyketide synthase
R2a	Reasoners 2 agar
RHa	Raffinose-Histidine agar
RiPP	Ribosomally synthesized and post-translationally modified peptides
RNA	Reasoners 2 agar
RRE	RiPP Recognition Element
rRNA	ribosomal Ribonucleic Acid
SAB	Sponge-associated bacteria
SAM	Sponge-associated microbes
SC	Sterility contorl
SEC	Size Exclusion Chromatography
SM	Secondary Metabolite
smBGC	Secondary Metabolite Biosynthetic Gene Cluster
SPE	Solid-phase extract
SSE	Sponge Spicule Extract
T1PKS	Type I Polyketide synthase
T2PKS	Type II Polyketide synthase
TE	Tris-EDTA

TFA	Trifluoroacetic acid
tRNA	Translational RNA
TSB	Tryptic soy Broth

Introduction

General Introduction

The deep sea is the largest biome in the world, occupying 95% of the global biosphere (Herring 2002). The deep sea is generally categorised as depths below 200 m, and at these depths the inability for photosynthesis significantly limits food availability. Deep-sea ecosystems encompass a wide range of habitats and conditions. Pressures range from 20 to over 1,100 atmospheres of pressure. Temperatures vary by depth and geographic location, ranging from -1.8 to 13°C (Yasuhara and Danovaro 2016), except for hydrothermal vent fluids, which can reach 464°C (Koschinsky *et al.* 2008). The deep sea is a challenging ecosystem to access and subsequently investigate, limiting our knowledge of many deep-sea organisms.

Marine sponges (*phylum* Porifera) are an ancient lineage of sessile filter-feeders that dominate the seafloor. The largest megafauna in the deep sea include cold-water sponges and can constitute up to 90% of invertebrate biomass in trawl samples (Klitgaard and Tendal 2004; Murillo *et al.* 2012; Beazley *et al.* 2013). In shallow and deep waters, sponges act as habitat islands for a wide range of fauna (Beaulieu 2001), and as nitrogen and silicon sinks in marine ecosystems (Hoffmann *et al.* 2009; Chu *et al.* 2011; Fiore, Baker and Lesser 2013). They are grouped into four classes: Calcarea, Demospongiae, Hexactinellida and Homoscleromorpha. Deep-sea sponge grounds also function as microhabitats, increasing the overall diversity of fauna on the deep-sea floor (Bett and Rice 1992; Bo *et al.* 2012; Beazley *et al.* 2013).

Sponge bodies are hollow, composed of channels and chambers containing choanoflagellates, cells that generate a water current that pumps water into the sponge and out through the osculum. With these features, sponges pump water

containing nutrients and microbes through the aquiferous sponge system (Yahel, Eerkes-Medrano and Leys 2006; Leys *et al.* 2011). Sponges are frequently the subject of microbiological investigations for two interconnected reasons; they form close associations with microorganisms and are a rich source of natural products (NPs).

Microbes from all domains of life are known to associate with sponges; Bacteria, Archaea and Eukarya (Li *et al.* 2016). Sponges are known to form complex associations with symbionts and associated bacteria, which contribute to holobiont metabolism. Functions include: nutrient cycling, vitamin production and defence compound production; this is reviewed by (Pita et al., 2018). However, there is some hesitancy in referring to sponge residing microbes as symbionts. The term 'sponge-associated bacteria' (SAB) has been suggested in place of 'symbiont' unless symbiosis between the two has been explicitly demonstrated through extensive investigations (Taylor *et al.* 2007; Thacker and Freeman 2012).

Marine sponge research has intensified over the past few decades due to the potential of sponges and their associated microbes to produce secondary metabolites relevant to industry and medicine (Anjum et al., 2016). In addition, secondary metabolites from shallow water sponges have found uses in medicine, including antimicrobial, anti-inflammatory, muscle relaxant, cardiovascular agents, and anti-tumour compounds, to name a few (Anjum *et al.* 2016; He *et al.* 2017). Sponges have historically been regarded as sources for structurally distinc and bioactive metabolitesm and it was the landmark work on the marine sponge *T. swinhoei* that presented through single-cell and metagenomic sequencing the SAB were the source of sponge natural products,

redirecting interest in sponge natural products to the uncultivable majority (Wilson *et al.* 2014). Deep-sea sponges are presented in this thesis to be as promising as their shallow-water counterparts.

The untapped potential of sponges as a source of novel therapeutics is favourable due to the urgent need for novel antimicrobials to tackle global Antimicrobial Resistance (AMR). It is estimated that by 2050 there will be 10 million annual deaths due to AMR (O'Neil 2014); thus, there is considerable emphasis on mobilising global initiatives to tackle AMR. One strategy in addressing this global health crisis is the discovery and development of new antimicrobials.

Deep-sea sponges are explored herein as a reservoir of bacterially derived antibiotics. First, a brief overview of the sponge microbiome is given, followed by the current knowledge of deep-sea sponge microbiomes. Secondly, we explore the sources of antibiotics from bacteria before introducing the deep-sea sponges as a source of antibiotics. Finally, the methodological approaches to antibiotic discovery are covered.

Sponge microbiomes

Sponges can contain bacteria and archaea from across 63 different phyla and candidate phyla (Webster *et al.* 2010; Schmitt *et al.* 2012; Thomas *et al.* 2016; Moitinho-Silva *et al.* 2017). From a global survey of the bacterial 16S rRNA genes of largely shallow-water sponges (Thomas *et al.* 2016), the organisation of the global sponge-microbiome is thought to be driven by abiotic environmental factors via temperature. Furthermore, the core microbiome may also be shaped by host species and the phylogenetic origins of the host, frequently termed as a 'species-specific' sponge microbiome (Lurgi et al., 2019).

The following bacterial phyla frequently dominate the sponge holobiont: Gammaproteobacteria, Alphaproteobacteria, Actinobacteria, Chloroflexi, Cyanobacteria, Nitrospirae, and Poribacteria. Sponge-associated archaea include Euryarchaeota and candidate phylum Thaumarchaeata (Hentschel *et al.* 2012; Thomas *et al.* 2016; Steinert *et al.* 2020).

Furthermore, sponges can be classified into high (MHA) or low microbial abundance (LMA) species, a dichotomy used to describe the density of microbes detected within the sponge microbiome (Weisz, Lindquist and Martens 2008; Giles *et al.* 2013; Erwin *et al.* 2015). Microbial cells constitute a significant proportion of the sponge body, and in extreme cases the nucrobial cells are more abundant than sponge cells, as was observed in *Aplysina aerophoba* and *Spheciospongia vesparium* (Gloeckner *et al.* 2014). HMA sponges are generally reported to contain densities of microbial cells of up to 10^8-10^{10} microorganism per gram of sponge tissue, and LMA sponges are reported to have up to 10^5-10^6 microorganism per gram of sponge tissue (Webster *et al.* 2001; Hentschel *et al.* 2006, 2012; Hentschel, Usher and Taylor 2006; Gloeckner *et al.* 2014).

Bacteria, archaea, and unicellular eukaryotes are thought to compose an essential part of the sponge diet (Reiswig 1975; Leys *et al.* 2017), possibly contributing to carbon and nitrogen cycling and assimilation of dissolved organic matter (DOM) (Leys *et al.* 2017). Microbes are captured during the filtering of seawater before being moved through chambers lined with choanoflagellates, which phagocytose the microbes with the aid of amoebocytes (Fig. 0-1). Sponge filtration is an efficient mechanism, and it is estimated that for the deep-sea sponge *Geodia barretti,* up to 4% of the microbes present in 1 cm^3 of

sponge tissue are being phagocytosed at any given moment (Leys *et al.* 2017). There is some discussion regarding the phagocytosis process, initially regarded as unselective (Hentschel, Usher and Taylor 2006). More recent studies into sponge-associated bacterial genomes and metagenomes have identified eukaryotic-like peptides (Nguyen, Liu and Thomas 2014), signalling peptides (Liu, Kjelleberg and Thomas 2011), and quorum sensing signals (Taylor *et al.* 2004). These were hypothesised to play a role in the recognition as non-food items by the sponge. Metagenomes, for this thesis, are defined as the recovery and sequencing of genetic material extracted directly from environmental samples, creating a metagenome (Huson and Weber 2013). A metagenome is seperate from a 16S rRNA metabarcoding study, which is the sequencing of a single marker gene for the purpose of assessing the bacterial population, this is also refered within this thesis as a 16S rRNA amplicon survey.

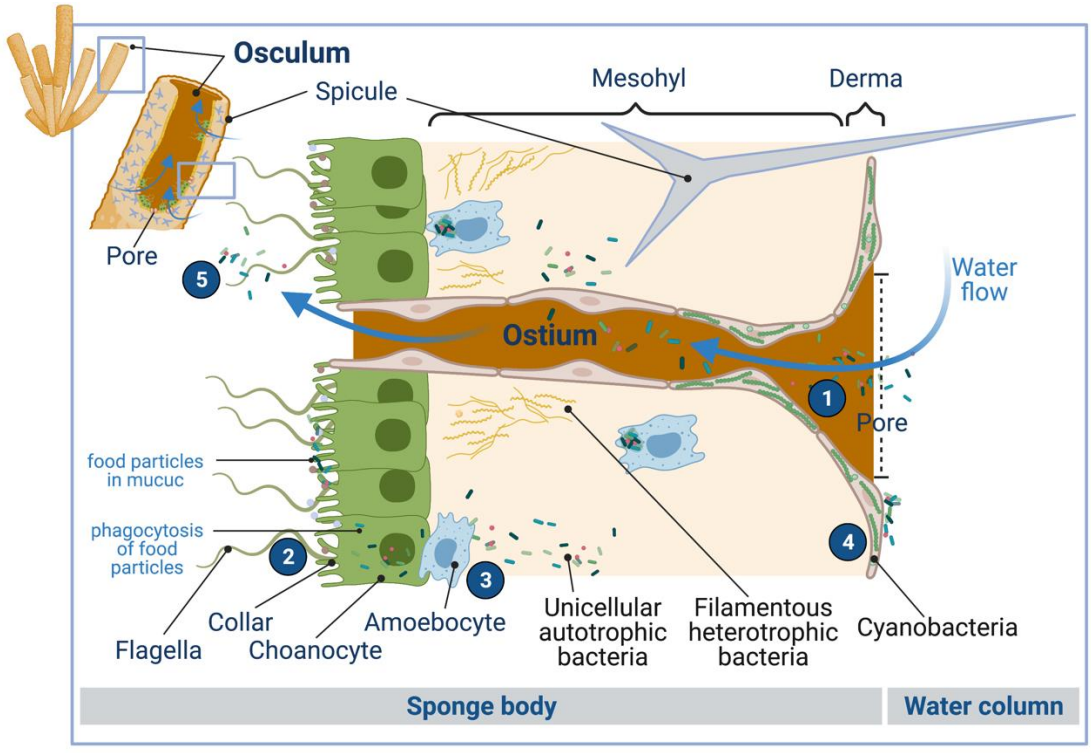

Figure 0-1. Fate of microbial cells in the sponge aquiferous system. (1) Microbial cells from the surrounding water column are sucked into pores and pulled through the ostium by a current generated by the choanocyte flagella. (2) Microbes and food particles are captured in the collar

of the choanocytes. (3) Microbes and food particles are engulfed and phagocytosed by amoebocytes for digestion. (4) Some microbes can avoid or escape amoebocytes; this includes symbiotic bacteria with eukaryotic-like protein markers. Established symbionts can be present intracellularly in the dermal cells such as cyanobacteria, while other unicellular autotrophic and filamentous heterotrophic bacteria will remain present within the mesohyl tissue matrix. (5) A small portion of bacterial matter avoid capture by choanocytes and leave the aquiferous system by the osculum.

Sponges produce a range of metabolic waste products beneficial to their associated microbes. For example, as a result of host phagocytosis, there is likely a high availability of amino acids and carbohydrates (Davy *et al.* 2002), while ammonia waste products favour nitrogen and ammonia oxidising microbes (Bayer, Schmitt and Hentschel 2008). Furthermore, should the microbe avoid ingestion by the host, then a sponge can provide microbial communities with a range of metabolic products, which is especially beneficial in nutrient-limited habitats such as the deep sea (Hentschel *et al.* 2012).

Functional roles of sponge-associated microbes

A variety of roles have been hypothesised for sponge microbiomes: assimilation of nutrients and metabolism (Thomas *et al.* 2010), pathogen defence (Thomas *et al.* 2010), the conversion of DOM and the cycling of nitrogen, carbon and ammonia (Han, Li and Zhang 2013; Li *et al.* 2016; Tian *et al.* 2016, 2017). As mentioned previously, microorganisms from the water column can provide a sponge with most of their carbon (Yahel *et al.* 2003; Yahel, Eerkes-Medrano and Leys 2006). For the deep-water sponge *Aphrocallistes vastus*, heterotrophic bacteria from both terrestrial, oceanic sources and re-suspended sediment were observed to form the primary sources of their diet (Kahn, Chu and Leys 2018).

Stable isotope experiments on the deep-sea sponge *G. barretti* and shallow-water species demonstrate nitrification, denitrification, and ammonium oxidation

reactions (Hoffmann *et al.* 2009). In addition, the transfer of carboxylic acids from anaerobic bacteria to the deep-water sponge *G. barretti* suggests the feasibility of microbial metabolism supplementing the sponge (Hoffmann et al., 2009, 2005). Such symbiosis is also observed in methane-rich deep-sea habitats with chemotrophic bacteria supplementing non-filter feeding sponges (i.e. carnivorous sponges) (Vacelet et al., 1996, 1995).

From metagenomic surveys, high abundances of CRISP-Cas systems have been observed in sponge-associated microbiomes, suggesting a selective pressure against viruses in the sponge microbiome (Horn *et al.* 2016). At the same time, eukaryotic-like genes may come in the form of leucine-rich domains, ankyrin repeats, tetratricopeptide repeats, and protein-protein interaction domains (Fan et al., 2012; Gao et al., 2014; Thomas et al., 2010b; Tian et al., 2014). These are hypothesised to act as 'fingerprints' for the recognition of sponge-symbionts.

Intimate symbiotic relationships were further explored using the sequencing technique of single-cell genomics, which sequenced the genome of a mixotrophic sponge-specific organism belonging to the candidate phylum Poribacteria. The genome contained several eukaryotic-like symbiotic factors previously mentioned, which supports theories of the intimate symbiotic interactions of Poribacteria with sponges (Siegl *et al.* 2011). Whether these are genomic traits exclusive to members of the core microbiome has not been explored in depth.

Several sponge pathogens have also been reported (Webster *et al.* 2002; Mukherjee, Webster and Llewellyn 2009; Luter *et al.* 2017), with most bacterial borne diseases reported from commercial sponge harvesting operations

(Webster 2007). Pathogenic Alphaproteobacteria have been identified, which excrete enzymes responsible for the degradation of sponge spicules in the Great Barrier Reef sponge *Rhopaloeides odorabile* (Webster *et al.* 2002), while overgrowth can lead to blockages in sponge canals (Webster and Taylor 2012). Elsewhere, an enzyme that lyses collagen was isolated from a pathogen of the reef sponge *R. odorabile* (Mukherjee, Webster and Llewellyn 2009).

In response to biological or environmental stressors, sponge-associated microbes (SAMs) may produce a wide range of chemical compounds that may find use in medical or commercial industries. This can be in response to pathogenesis (Ute Hentschel et al., 2006; Schmidt et al., 2000), fouling (Unson, Holland and Faulkner 1994), or environmental stressors (Friedrich *et al.* 2001; Hentschel *et al.* 2003; Thoms *et al.* 2003). Antimicrobials active against clinically relevant pathogens have been isolated from SAMs of the Mediterranean sponges *Aplysina aerophoba* and *Aplysina cavernicola* (Hentschel *et al.* 2006), and the microbial community of *A. aerophoba* has been shown to protect from a range of disturbances such as starvation, antibiotic exposure, and transplantation to a foreign environment (Friedrich *et al.* 2001; Hentschel *et al.* 2003; Thoms *et al.* 2003). The production of antifungals in *Theonella swinhoei* could play a role in sponge defence and immune responses (Schmidt *et al.* 2000).

Data from single-cell genomics have been utilised to identify novel non-ribosomal peptide synthase (NRPS) and polyketide synthase (PKS) genes in sponge-associated *Chloroflexi* (Siegl and Hentschel 2010). While it is was not demonstrated within the study to have antibacterial properties, it does illustrate that novel genomic diversity for secondary metabolite (SM) production can be

found in SAB. Comprehensive reviews offer a much more detailed breakdown of the observed and hypothesised functional roles SAB have within sponge hosts (Taylor *et al.* 2007; Webster and Taylor 2012). It is difficult to characterise the functional role of SAB since they will vary between species and habitat; however, generalised functions have been suggested (Thacker and Freeman, 2012).

Deep-sea sponge microbiomes

The deep sea represents the largest biome in terms of volume. The difficulty in accessing, sampling and studying deep-sea habitats means there is little knowledge regarding deep-sea sponge holobiomes. The majority of existing data were acquired in the last decade using next-generation sequencing. This has focused on Demosponges, with individuals representing 33 distinct Demosponge species investigated, contrasted with individuals representing 11 distinct Hexactinellid species (Fig. 0-2A, B).

Overall, there have been 17 studies involving 16S rRNA gene surveys of deep-sea sponges (Meyer and Kuever 2008; Nishijima *et al.* 2010; Radax *et al.* 2012; Jackson *et al.* 2013; Kennedy *et al.* 2014; Li *et al.* 2014; Borchert *et al.* 2016; Thomas *et al.* 2016; Tian *et al.* 2016, 2017; Luter *et al.* 2017; Verhoeven and Dufour 2017; Verhoeven, Kavanagh and Dufour 2017; Bayer *et al.* 2020; Busch *et al.* 2020b; Steinert *et al.* 2020; Maldonado *et al.* 2021), four whole-metagenome sequencing studies (Li *et al.* 2014; Tian *et al.* 2016, 2017; Rubin-Blum *et al.* 2019), and six cultivation-dependent investigations: two that intended to cultivate bacterial diversity of deep-water SAB (Olson and McCarthy 2005; Williams *et al.* 2020), and five for natural product screening (Romanenko *et al.* 2005, 2008; Xin *et al.* 2011; Borchert *et al.* 2017b; Xu *et al.* 2018). The currently available literature is varied in methodology, range of species covered, geographic locations and study objectives (Fig. 0-2C, and Table S0-1).

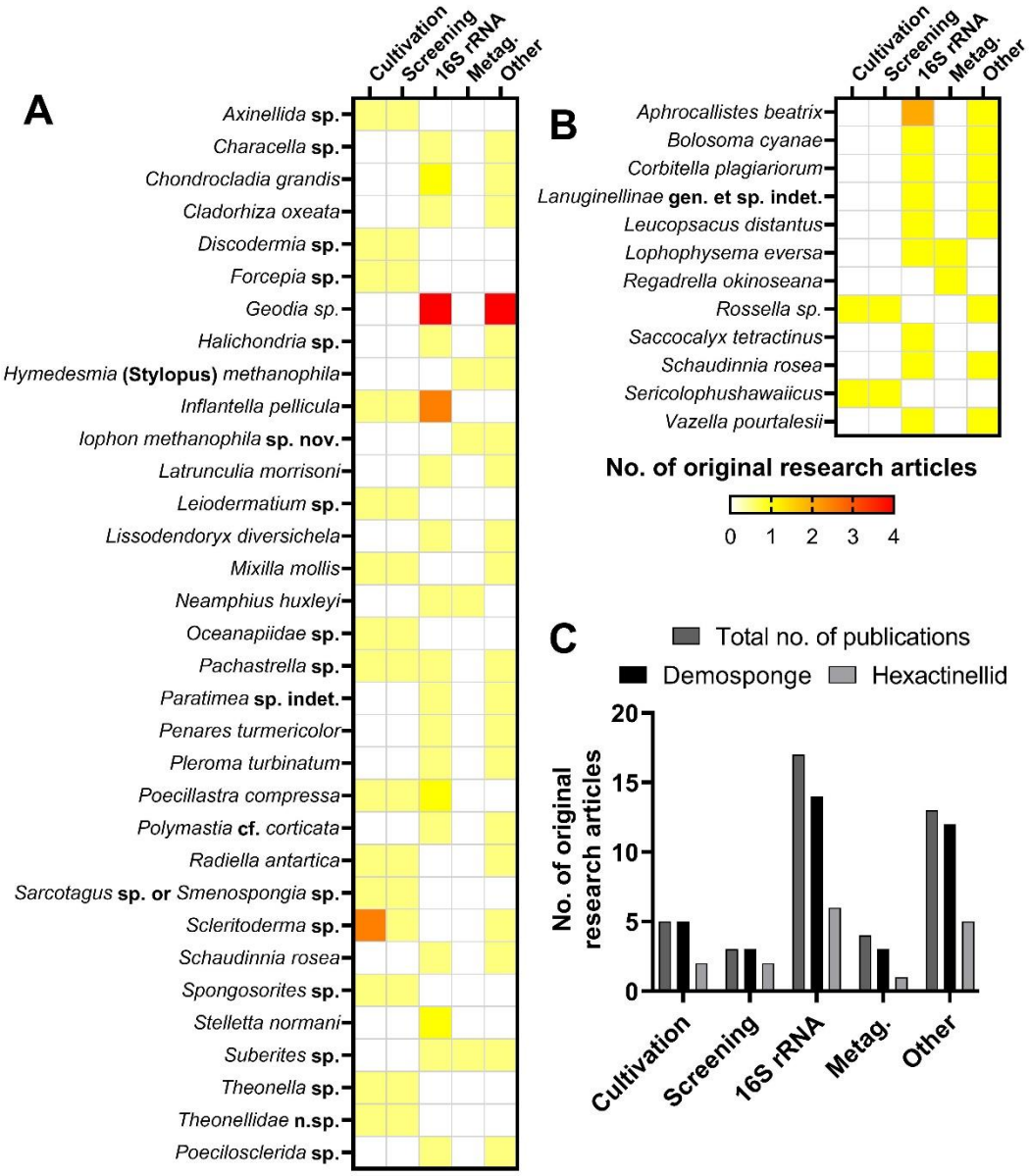

Figure 0-2. Summary of original research articles involving microbiological investigations of deep-sea sponges and the range of methodological exploration performed between 2009 and 2021. Publications were selected because sponges were sampled from depths greater than 200 m, and full or partial taxonomy of the sponges was listed within the publication. Heatmap of the sponge species utilized in microbiological investigations and the methodologies utilized for (A) Demosponges and (B) Hexactinellid sponges; this is summarized in (C). (Cultivation, any attempts to culture microorganisms from the sponge samples; Screening, any screening attempts for natural products, including but not limited to antibiotic discovery; 16S rRNA, amplifying and sequencing the 16S rRNA gene to survey the bacterial diversity; Metag., shotgun metagenome sequencing of sponge metagenomic DNA; and Other, additional methodologies which can be found detailed in Table S0-1).

As previously mentioned, microbiological investigations have primarily occurred using demosponges. Since demosponges can be found across a broader range of depths, this has advantages in studying microbial communities between deep

and shallow-water species. When comparing deep and shallow-water sponge microbiota, similarities in archaeal but distinctions in bacterial populations have been singled out (Kennedy *et al.* 2014). Later work identified several marine demosponges that were very similar to shallow-water sponges. These similarities in bacterial phyla included Proteobacteria, Chloroflexi, Acidobacteria, Bacteriodetes, Nitrospinae, Nitrospirae, and Poribacteria (Bayer, Kamke and Hentschel 2014; Thomas *et al.* 2016; Steinert *et al.* 2020). Likewise, the highly abundant candidate phylum Poribacteria were poorly represented among the deep-sea sponges investigated, except for a *Paratimea* sp. (Steinert *et al.* 2020).

A phylogenetic distinction has been made between cultured bacteria from deep-water Arctic hexactinellid and demosponges, indicating class-specific microbiota (Xin *et al.* 2011); this was later supported by a 16S rRNA amplicon gene survey (Steinert *et al.* 2020). Steiner and colleagues (2020) conducted the most comprehensive study, to date, comparing deep-water species belonging to demosponges and hexactinellids. Deep-water hexactinellid and demosponges demonstrate sponge species-specific microbial communities (Lurgi *et al.* 2019; Busch *et al.* 2020b; Steinert *et al.* 2020), and hexactinellid sponges are suggested to have sponge-individual-specific microbiotas (Busch *et al.* 2020a, 2020b; Steinert *et al.* 2020). Phylogenetically related sponges can display physiological distinctions that lead to differences in microbial community and the functional roles they play within the host, as was noted with *Vazella pourtalesii* and *Schaudinnia rosea* (Hexactinellid) and their assimilation of ammonia/ammonium (Maldonado *et al.* 2021).

Current work indicates that deep-water SAB appear to carry out similar functional roles to that of shallow-water SAB. SAB are implicated in providing essential components to deep-water hosts, such as vitamins, amino acids, and fatty acid precursors (Bayer *et al.* 2020; de Kluijver *et al.* 2021). Among deep-water demosponges, members of *Geodia* are the best studied. This has primarily been focused on understanding the role of deep-water sponges in nitrogen cycling. Taxa involved in nitrification, denitrification and anaerobic ammonia oxidation are well represented in the deep-water sponge *G. barretti*. This is supported by stable isotope experiments (Hoffmann *et al.* 2009) and detection of messenger RNA (mRNA) encoding metabolic enzymes involved in nitrification by ammonia-oxidising archaea (AOA) (Radax *et al.* 2012).

The deep-sea carnivorous sponge *Chondrocladia grandis* has body regions that each support distinct microbial communities. For example, high abundances of *Colwellia* spp. and *Pseudoalteromonas* spp. were found in the sphere (i.e. digestive compartment). Bacterial within these two genera secrete enzymes that hydrolyse the glucose–derived polymer chitin, possibly promoting the digestion of prey with chitin exoskeletons (Verhoeven, Kavanagh and Dufour 2017). A comparison of *C. grandis* individuals from the Arctic and the Gulf of Maine found that geographic location had a lesser effect than body region on *C. grandis* microbial composition (Verhoeven and Dufour 2017).

Three sponges residing near hydrothermal vents, *Characella* sp., *Pachastrella* sp., and an unidentified *Poecilosclerid* were reported to contain thioautotrophic sponge symbionts (Nishijima *et al.* 2010). These chemoautotrophic organisms that feed off sulphur were found in all tissue types of the three sponges and shared 99% DNA sequence identity to the well-characterised symbionts of

Bathymodiolus, the well-studied hydrothermal vent mussel. More recently, two novel species of asphalt seep sponges, *Hymedesmia* (*Stylopus*) *methanophila* sp. nov. and *Iophon methanophila* sp. nov., were found to contain methane-oxidising (MOX) bacteria (Rubin-Blum *et al.* 2019).

Hexactinellid sponges

Hexactinellid sponges typically live in the deep ocean (Leys *et al.* 2004). Data retrieved from the Ocean Biogeographic Information System (OBIS), indicates that hexactinellid sponges account for the majority of Porifera samples collected from trawl data between depths of 1,200 – 1,800 m (Fig. 0-3). This higher frequency of sampling is not reflected in deep-sea microbiological investigations of Hexactinellid sponges, which has limited our understanding of how hexactinellid sponge microbiomes integrate into deep-sea ecosystems. Deep-sea hexactinellids have been the focus of three metagenomic investigation (Tian *et al.* 2016, 2017; Bayer *et al.* 2020), six 16S rRNA gene surveys (Thomas *et al.* 2016; Tian *et al.* 2016; Busch *et al.* 2020b, 2020a; Steinert *et al.* 2020; Maldonado *et al.* 2021), and three culture-based bioprospecting investigations (Mangano *et al.* 2008; Xin *et al.* 2011; Williams *et al.* 2020) (Fig. 0-1B,C).

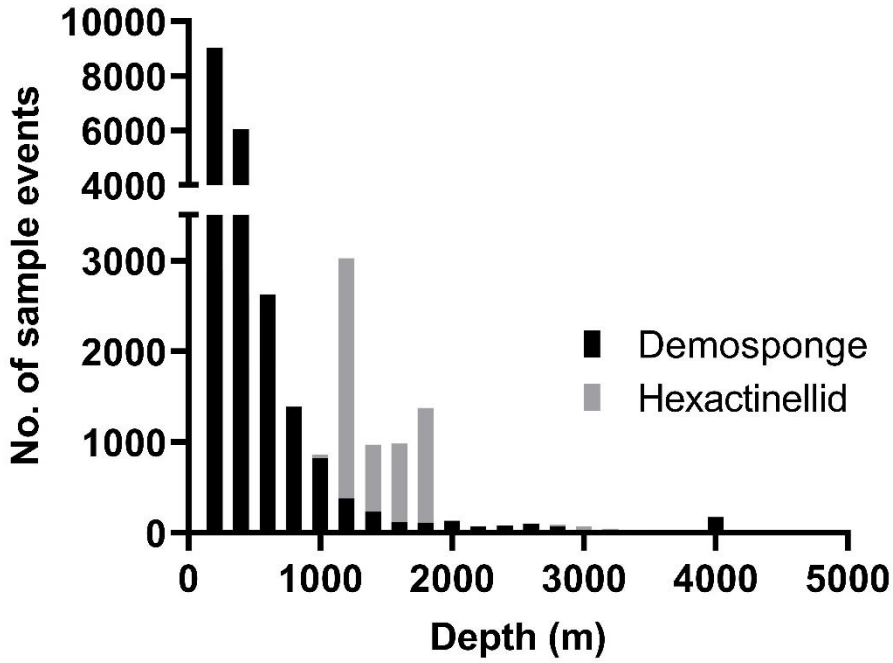

Figure 0-3. Histogram of depth-related patterns in the number of sample events/recordings of Porifera in the North Atlantic within the OBIS database. The frequency of two Porifera (Demosponge and Hexactinellida) from trawl sampling, between the depths of 750 and 5,000 m, was accessed from the Ocean Biogeographic Information System (OBIS) in April 2019. The dataset was cleaned of sampling events with no depths and events outside of the North Atlantic.

Given the higher frequency of recovering a deep-sea Hexactinellid over a Demosponge in depths greater than 1,200 m, it is surprising they are not included in more microbiological investigations. Hexactinellids prefer deep-water and cold habitats (>100 m). Hexactinellids have a morphology, tissue and spicule density distinct from other classes of sponges (Reiswig and Mehl 1991; Tabachnick 1991; Hooper and van Soest 2002; Leys *et al.* 2004). Including distinctive triaxonic (cubic three-rayed) spicules that are held together by syncytia tissue organisation (multinucleate cell) (Leys, Mackie and Reiswig 2007). Furthermore, hexactinellid sponges have diverse morphological structures, displaying complex anatomy and spicule diversity (Hooper and van Soest 2002).

Low temperatures and depth would imply a low availability of suspended food particles for sponges, resulting in different adaptations in metabolic functions

that could result in different microbial communities. In these conditions, the hexactinellids *Aphrocallistes vastus* and *Rhabdocalyptus dawsoni* were hypothesised to be primarily bacteriovores capable of selectively feeding (Yahel, Eerkes-Medrano and Leys 2006). Recent work using transmission electron microscopy (TEM) has identified a novel feature of the hexactinellid *Vazella pourtalessi,* termed a 'bacteriosyncytia' (Maldonado *et al.* 2021). The authors described a bacteriosyncytia as a cytological system specialised for holding microbial cells within membrane-bound vesicles. The bacteriosyncytia were hypothesised by the authors to function as a 'farm' for bacterial symbionts which can be digested or conduct essential nitrogen cycling roles.

The phylogenetic diversity of hexactinellid sponges closely resembled the seawater, such as a high abundance of bacterial members of the class Gammaproteobacteria (Steinert *et al.* 2020). Archaea communities in the two demosponges and hexactinellids were similar, dominated by the ammonia-oxidising genera belonging to the phylum Nitrosopumilaceae. The two sponge classes shared very few unique bacterial features (1.3%) and only slightly more archaeal ones (3.4%) (Steinert *et al.* 2020). The overall alpha diversity of hexactinellids was lower than demosponges, but the highly abundant taxa were typical of global sponge microbiotas (i.e., Proteobacteria, Bacteriodetes and Chloroflexi) (Busch *et al.* 2020b; Steinert *et al.* 2020). This study grouped sponges from vastly different bathymetric depths as biological replicas, ignoring depth and temperature as potentially driving factors on the microbiota structure. In planktonic bacterial communities, changes in vertical gradients (depth) have been observed to be greater than horizontal distances (geographic position) (Sunagawa *et al.* 2015; Li *et al.* 2018b), and current data supports the suggestion that hexactinellid sponge microbiotas closely resemble the

surrounding water column community composition (Thomas *et al.* 2016; Steinert *et al.* 2020).

Busch and colleagues (2020b) pursued this line of questions by investigating the microbiota of deep-water hexactinellid *Schaudinnia rosea* along a gradient on the Schulz Bank seamount in the Atlantic Mid-Ocean Ridge. This study combined a 16S rRNA gene survey of sponges and seawater and quantified dissolved gasses of seawater. A positive relationship was identified between bathymetric depths and the relative abundance of four bacterial phyla (Acidobacteria, Chlamydiae, Kirimatiellaota, Planctomycetes). In contrast, the most abundant phyla within hexactinellids sponges, Proteobacteria, had neither a negative or positive relationship with depth (Busch *et al.* 2020b).

Studies resolving metagenome assembled genomes (MAGs) from hexactinellids repeatedly identify reduced genomes among potential hexactinellid symbionts involved in scavenging strategies for ammonium, nitrogen and sulphur (Tian *et al.* 2016, 2017; Bayer *et al.* 2020). In a study of the deep-water hexactinellid, *Vazella pourtalessi,* the authors hypothesise two microbial strategies between symbionts and host*,* denoted as ‘givers’ and ‘takers’ (Bayer *et al.* 2020). The ‘givers’, which are facultative anaerobes and heterotrophs, secrete amino acids and vitamins for the host, while the ‘takers’ are anaerobes, characterised by reduced genomes and they exploit the other members of the microbial community and the host for resources (e.g. DNA, lipids).

The three MAGs included ammonia-oxidising archaea (AOA), nitrite-oxidising bacteria (NOB), and sulphur-oxidising bacteria (SOB). These organisms were hypothesised to conduct symbiotic roles as nitrite and sulphide scavengers

(Tian *et al.* 2016), likely conducting the role of a ‘taker’ proposed by Bayer and colleagues’ model (2020). MAGs from the sponge *V. pourtalessii* also revealed enzymes operating a complete nitrogen cycle sensitive to anthropogenic impacts (Busch *et al.* 2020a; Maldonado *et al.* 2021).

Deep-water hexactinellids are poorly utilised for NP discovery. *Sericolophus hawaiicus* (E. Borchert et al., 2017) and an individuals belonging to the genera *Rossella.* (Xin *et al.* 2011) have been utilised in culture-dependent strategies to isolate cold-adapted bacteria. From *Rossella nuda,* bioactive strains of *Dietzia* sp. were isolated, which tested positive for the presence of type 1 and 2 PKS genes. At the same time, a strain of *Pseudoalteromonas* sp. was cultivated from *S. hawaiicus* and demonstrated high levels of protease activity.

Further exploration of the microbiomes of hexactinellids is required. Our comparatively limited knowledge of hexactinellid microbiomes possibly excludes a great deal of potential for discovering novel microbial taxa and NP candidates.

Antimicrobial-resistance and drug discovery

Where are the new antibiotics?

We see the reduction in the effectiveness of antimicrobials globally, which will change the face of modern medicine. Antimicrobial resistance (AMR) describes the genetic resistance microbes have towards the antimicrobial chemicals used to prevent growth (i.e. bacteriostatic) and kill cells (i.e. bacteriocidal). Antibiotic use and pollution create selective pressure resulting in the growth of tolerant and resistant strains to existing antibiotics in circulation (Kolář, Urbánek and Látal 2001; Tello, Austin and Telfer 2012). AMR is an inevitability - when high densities of microorganisms are involved, chance and rare advantageous

mutations will occur. Persistent, aggressive use and misuse of antimicrobial therapies in agriculture, aquaculture, and medicine are drivers of this global crisis (Cabello 2006; Penders and Stobberingh 2008; Economou and Gousia 2015). Additionally, mobile adaptive genes conferring resistance to antibiotics are exchanged across entire microbial communities through horizontal gene transfer, even in the absence of antibiotics (Lerminiaux and Cameron 2019). These genetic elements can be mobilised within and between microbial species in a community, creating reservoirs of antimicrobial-resistant genes (Von Wintersdorff *et al.* 2016).

The consequences of global AMR are expected to impact both health and economic structures. It has been estimated that by 2050 we will see 10 million annual global deaths (O'Neil 2014). The United Kingdom government has laid out a five-year plan to tackle AMR, in which the development of new therapeutics was included, together with a statement about the need to establish more robust pipelines in NP mining (Department of Health and Social Care 2019).

In the past three decades, only two new classes of antibiotics have been made publicly available (Talbot *et al.* 2006; Coates, Halls and Hu 2011). In April 2020 there were 41 antibiotics in the clinical pipeline (The PEW Charitable Trusts 2020), of which 18 have the potential to treat priority gram-Negative drug-resistant ESKAPE pathogens identified by the 2019 Antibiotic Resistance (AR) Threat Report (Centre of Disease Control 2019). Promisingly, 1 in 4 of the antibiotic within the pipeline represent a novel drug class or mechanism of action (The PEW Charitable Trusts 2020). However, the challenges still remain, as the costs and challenges of taking a new antibiotic from discovery,

development, clinical trials to commercial availability result in a low probability of the entry of new antibiotics into the market (Payne *et al.* 2007; Gupta and Nayak 2014; Czaplewski *et al.* 2016) (Fig. 0-4). At the same time, the pharmaceutical industry are not investing in research and development efforts that can match the global neds for novel antibiotics (Morel and Mossialos 2010; Renwick and Mossialos 2018). This has led to the antibiotic discovery and development pipeline described as 'running dry' (Gupta and Nayak 2014; Luepke *et al.* 2017).

	1	2	3	4	5	6
	Discovey and Optimisation	Pre-clinical	Phase I	Phase II	Phase III	Registered and Marketed
Probability of Success	0.2-2.5%	3-5%	6-14%	25-30%	50-64%	75-90%
Time	3-7 yrs	1.5-2 yrs	0.5-2 yrs	2-3.5 yrs	2.5-4 yrs	1-2 yrs
Cost	$100-130m	$60-70m	$70-100m	$130-160m	$190-220m	$18-20m

Figure 0-4. Antibiotic discovery and development pipeline is a lengthy and costly process with a low probability of success. (Czaplewski et al., 2016; Payne et al., 2007)

Developing new therapeutics is a challenge, the early discovery and optimisation part of the pipeline more so than the rest, with the lowest chance of compounds progressing beyond the discovery and optimisation stage to the preclinical stage. Increasing and maintaining a high number of compounds entering the pipeline is essential. However, the pharmaceutical industry has shifted away from NP screening, one reason being the high rate of rediscovering known antimicrobial compounds and the subsequent high costs to reach this realisation. One possible way of overcoming this challenge is investigating diverse habitats and isolating strains not previously tested, expanding our reach for newer phylogenetic and chemical diversity.

Bacterially derived antibiotics

Bacteria are a traditional source of novels antibiotics, and to date, 70% of existing antimicrobials in clinical use are derived from bacteria NPs (Newman and Cragg 2012). These compounds serve biological functions for bacteria as tools of predation and competition (Majeed *et al.* 2011; Nedialkova *et al.* 2014; Bhattacharya, Pak and Bashey 2018), providing a selective advantage in the acquisition of nutrient, space or resources (Bibb 2005; Rigali *et al.* 2008).

Bacterial NP biosynthetic pathways are encoded and regulated by biosynthetic gene clusters (BGCs). BGCs are often found in a single large continuous region and can be identified by tools such as the 'antimicrobial Secondary Metabolite Analysis Shell' (antiSMASH;(Blin et al., 2021; Medema et al., 2011). It is predicted that 90% of bacterial BGCs are metabolically inactive under standard laboratory conditions and these are termed 'cryptic genes' (Scherlach and Hertweck 2009; Rutledge and Challis 2015).

Marine bacteria have been readily screened for antimicrobials, with members of marine Actinobacteria (Bull and Stach 2007) and Proteobacteria (Desriac *et al.* 2013) receiving the most attention. The search for novel bacterially derived antibiotics has shifted towards new taxonomic spaces. As a result, marine microbiomes, in particular, have garnered much attention. Numerous lead molecules have been identified from marine invertebrates and symbionts (Piel 2009), with SAB proving to be a rich source of antibacterials (Thoms *et al.* 2003).

Natural product discovery from deep-sea sponge-associated bacteria

Marine sponges over the past two decades have been a growing target for antibiotic discovery (Fig. 0-5A), with the majority of publication focusing on NP discovery for pharmaceuticals (Fig. 0-5B). Sponge NP discovery has historically focused on extracting organic compounds from sponge tissues. When investigators began finding structurally similar compounds from phylogenetically unrelated sponges, it led to the hypothesis that many substances retrieved from sponge were of microbial origin (Piel 2009). This shifted the focus into sampling and exploring the microbial populations for NPs, as it benefits from reducing costs of chemical synthesis, allowing for more sustainable and scalable production from the cultivation of NP producing bacteria (Proksch, Edrada and Ebel 2002; Piel 2009). Exploring new sponge taxonomy has enabled an expansion of the SAB that have been cultivated and screened.

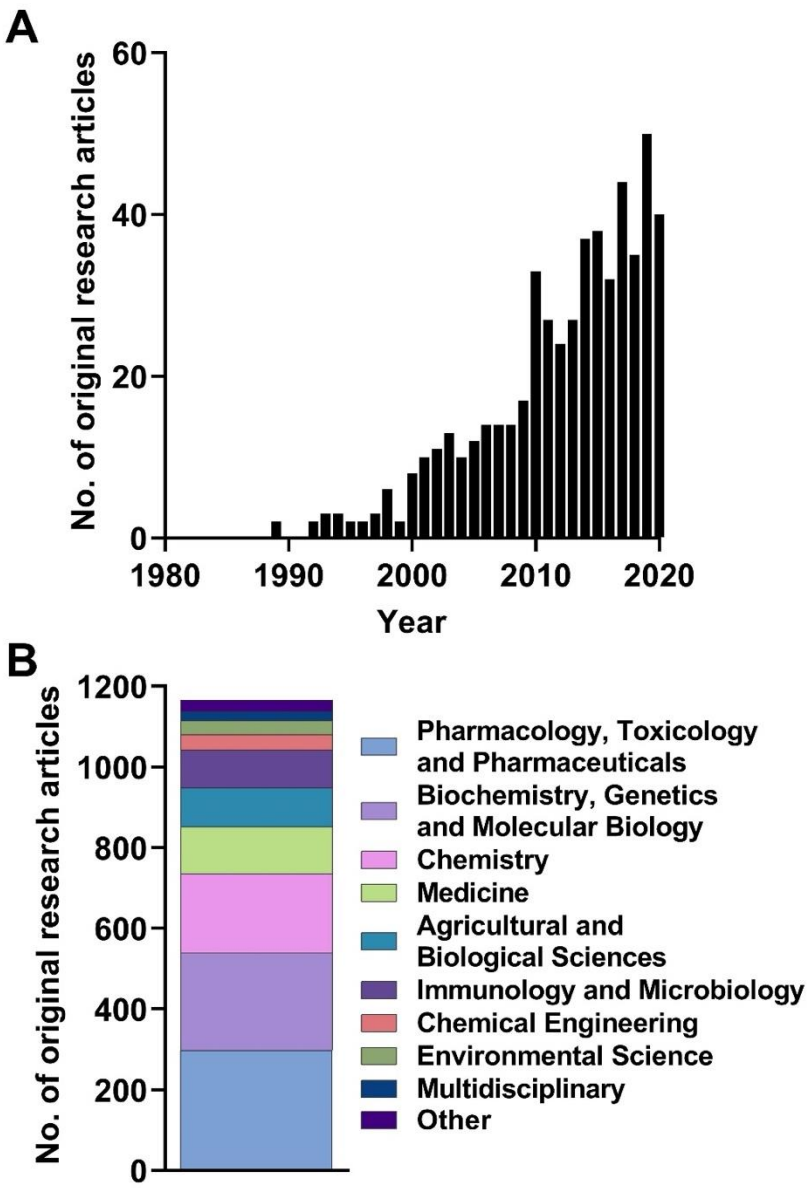

Figure 0-5. Scopus literature search for primary publications on marine sponge natural product research demonstrates a growing interest in research screening for pharmaceuticals.(A) The number of original research articles between 1996 and 2020, (B) the distribution of publications research focus. A literature search of original research articles was done using Scopus (https://www.scopus.com) and the following search terms: sponge AND marine AND Porifera AND natural AND product AND discovery AND antibiotic) AND (LIMIT-TO (DOCTYPE, "ar").

As previously mentioned, bioactive substances from SAB have a range of bioactivity, including anticancer, antimicrobial, anti-inflammatory, to name a few. Furthermore, sponge-derived compounds have successfully make it to clinical and preclinical trials (Blunt *et al.* 2005; Ghareeb *et al.* 2020). For this section, only antimicrobial activity will be discussed. However, a broader view of marine

sponges as sources of drugs and therapeutics can be found in the following reviews: (Thomas, Kavlekar and LokaBharathi 2010; Mehbub *et al.* 2014, 2016; Anjum *et al.* 2016). Additionally, methodological approaches to NP discovery will be discussed later within this chapter.

Antimicrobial discovery from deep-sea SAB

Culture collections dedicated to deep-sea SAB have been used to screen for antibiotic-producing bacteria (Xu *et al.* 2018; Williams *et al.* 2020). A broad culture-dependent investigation of sponge-associated bacteria from 11 different deep-sea sponge species identified multiple compounds from 27 strains of sponge-isolated *Actinobacteria* (Xu *et al.* 2018). These were all observed to have activity against at least one clinically relevant pathogen. This collection is exclusively a marine Actinobacteria collection derived from only demosponges and is maintained by the Harbor Branch Oceanographic Institute (HBOI) Marine Microbial Culture Collection.

Elsewhere, the Bristol Sponge Microbiome Collection (BISECT) is well represented by sponges from three classes (Demosponge, Hexactinellid, and Calcarea). The collection contains bacterial isolates representing four phyla (Actinobacteria, Proteobacteria, Firmicutes, and Bacteriodetes) (Williams *et al.* 2020). Another investigation of deep-water Antarctic sponge isolated phylogenetically diverse Gram-positive strains from the three sponge species representing the two classes demosponge and hexactinellid (Xin *et al.* 2011).

The use of various recovery media and conditions is demonstrated within these cultivation efforts, reflected in the diversity of bacterial isolates (Xin *et al.* 2011; Williams *et al.* 2020). Diverse methods are being utilised in screening, such as utilising ‘one strain, many active compounds’ (OSMAC) principles (Williams *et*

al. 2020) and sequencing approaches (Xin *et al.* 2011; Borchert *et al.* 2016, 2017b), overall utilising a range of approaches to uncover cryptic genes.

A survey of three species of deep-sea demosponges (*Inflatella pellicula*, *Stelletta normani*, and *Poecillastra compressa*) sequencing the subunits of PKS and NRPS demonstrated the genomic diversity of SM genes present within the deep-sea sponge microbiomes (Borchert *et al.* 2016). Other culture-independent strategies have been applied successfully in identifying antimicrobials from bacteria recovered from *Lissodendoryx diversichela* and *I. pellicula*. Whole-genome sequencing of 13 sponge-associated *Streptomyces* spp. identified that the two deep-sea strains were enriched in gene clusters encoding NRPS, while assay based approaches identified activity against clinically relevant pathogens and had an overall greater abundance of BGCs (Jackson *et al.* 2018). More importantly, these BGCs showed little to no homology with previously reported BGCs.

Discobahamin A and B, a peptide extracted from deep-water sponge *Discodermia* sp. is a reported antifungal (Gunasekera, Pomponi and McCarthy 1994), and recently from the same species of sponge 6 strains of bacteria were recovered and demonstrated antimicrobial activity (Xu *et al.* 2018). These strains were closely related to *Pseudonocardia* sp. *Rhodococcus* sp. and *Streptomycetes* sp.

Antibiotic discovery from deep-sea sponges is still in its early days, and there remain a large selection of taxonomically distinct deep-sea sponges to be explored for antibiotic discovery. Already there is much promise, with novel genomic and chemical diversity reported. There are currently no deep-sea

sponge-bacterial derived compounds entering clinical or preclinical pipelines, to the author's knowledge.

Methodological approaches and considerations to sponge natural product discovery

Culture-based approaches are recovering multiple bacterial isolates from sponges with antibacterial and antifungal activity (Xin *et al.* 2011; Bibi *et al.* 2020). These are also effective against many antimicrobial resistant strains, which should be a crucial focus in antimicrobial discovery. However, culture-dependent approaches may overlook cryptic genes encoding novel products. Screening biological samples from diverse habitats for NPs can take two routes: culture-dependent or -independent. Once producer strains have been identified, it is necessary to begin filtering by screening against broad panels and identifying the potency of the compound through various *in vitro* assays before testing the compound *in vivo* in a non-mammalian model (Fig. 0-6).

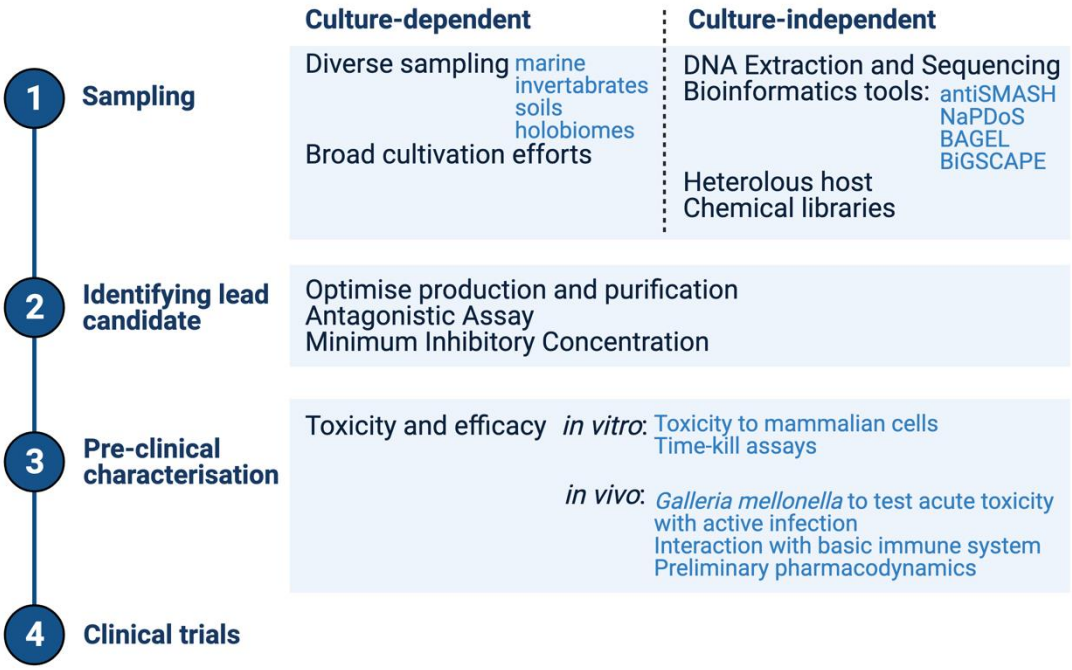

Figure 0-6. Overview of natural product discovery pipeline from sampling to preclinical. Created with BioRender.com.

Culture-independent methods

Initial culture-independent investigations of crude sponge extracts found low levels of antibacterial activity against marine bacteria but a much more significant antibacterial effect on terrestrial bacteria (Amade, Pesando and Chevolot 1982; Amade *et al.* 1987; Uriz, Martin and Rosell 1992; Xue *et al.* 2004). Since sponge bacteria have been difficult to cultivate, most studies have focused on a culture-independent approach. Sponge tissue is soaked or macerated in polar solvents such as ethanol (EtOH), methanol (MeOH), and ethyl acetate (EtOAc) to extract natural compounds. These are typically defined as crude extracts before sequential chromatographic steps gradually remove impurities, select for active compounds and increase purity. Such methods can include Size Exclusion Chromatography (SEC) and High-Performance Liquid Chromatography (HPLC). This is a highly efficient method to facilitate identification of any dissolved compounds in liquid, even in low concentrations.

However, it may not be possible to discriminate between microbial and sponge produced NPs.

Metagenomic-guided drug discovery approaches have been utilised across many organisms and habitats (i.e. soil, marine, etc.) (Li *et al.* 2009; Zerikly and Challis 2009). Major metagenomic studies of sponges have identified PKS and NRPS genes (Piel *et al.* 2004a, 2004b; Schirmer *et al.* 2005; Kim and Fuerst 2006; Kurnia *et al.* 2017). There is one instance where this has been applied to deep-sea sponges, identifying a cold-activate esterase (Erik Borchert et al., 2017). From metagenome-assembled bacterial genomes, it is possible to mine for gene clusters of organisms that cannot be cultivated (Trindade *et al.* 2015); individual bacterial whole-genomes can be assembled from metagenomic data in a similar manner (Adamek *et al.* 2017). This are termed metagenome assembled megenomes (MAGs) (see review (Frioux et al., 2020).

In principle, *'your BGC of interest'* can be identified computationally and cloned into an expression vector (summarised in Fig. 0-7). This is transformed into a host of choice, the expression of the compound of interest is induced, which can then be purified and biologically characterised. This can be done on both uncharacterised BGCs to identify any potential activity or with studied BGCs to increase yield. This process has the advantage of being able to produce large quantities of biological compounds rapidly. However, in practice, it may require significant troubleshooting to achieve sufficient growth of the host or metabolite production.

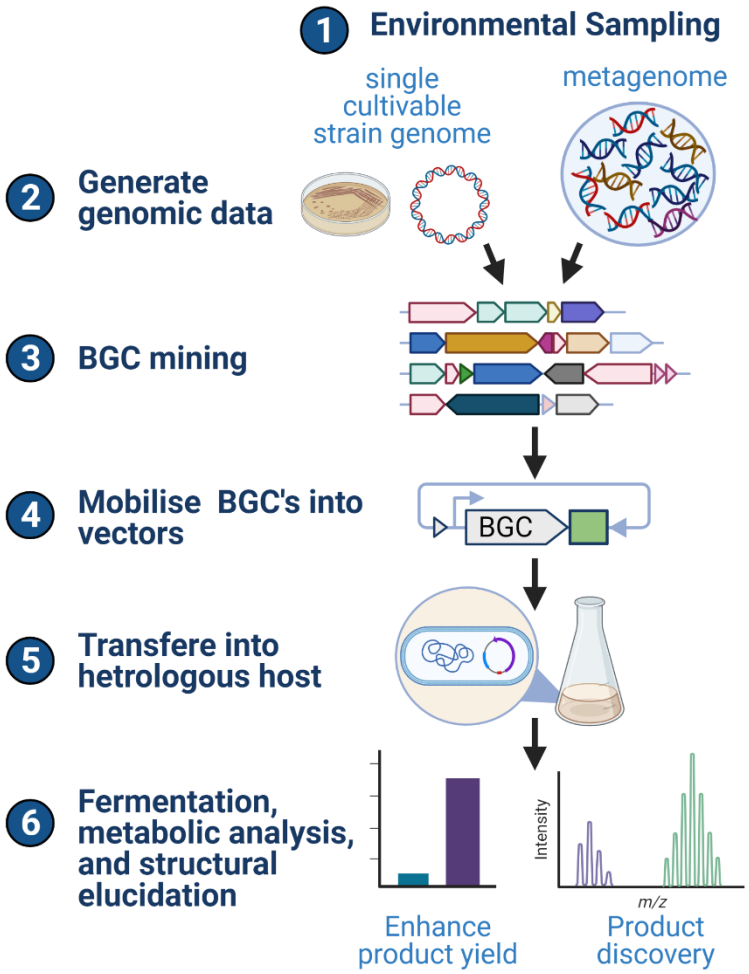

Figure 0-7. Workflow summary of heterologous expression of microbial-derived natural products. Adapted from: (He *et al.* 2018; Huo *et al.* 2019; Ke and Yoshikuni 2020). Created with BioRender.com. (BGCs, biosynthetic gene clusters).

Culture-dependent

A typical method involves the homogenisation and dilution of environmental samples, followed by growth on agar plates or in liquid broth, before isolating into pure culture. A colony of an environmental bacterial isolate is then deposited on a lawn of 'indicator' strains for antagonistic growth to determine bioactivity against clinically relevant bacteria (i.e. *Escherichia coli*, Methicillin-resistant *Staphylococcus aureus*, etc.) (Jackson *et al.* 2018; Xu *et al.* 2018), or overlain with soft-agar containing the indicator strain (Williams *et al.* 2020). An 'indicator' strain defines a bacterial culture to which the compound or bacteria of

interest is challenged to observe any bactericidal or bacteriostatic effect on the growth of the indicator.

NPs can be extracted from bacterial liquid cultures by extracting the organic compounds similar to those mentioned previously (i.e. EtOAc, MeOH, etc.). Alternative approaches involve sequential chromatographic purification and clarification to isolate the NPs from the supernatant of bacterial culture (Fig. 0-8).

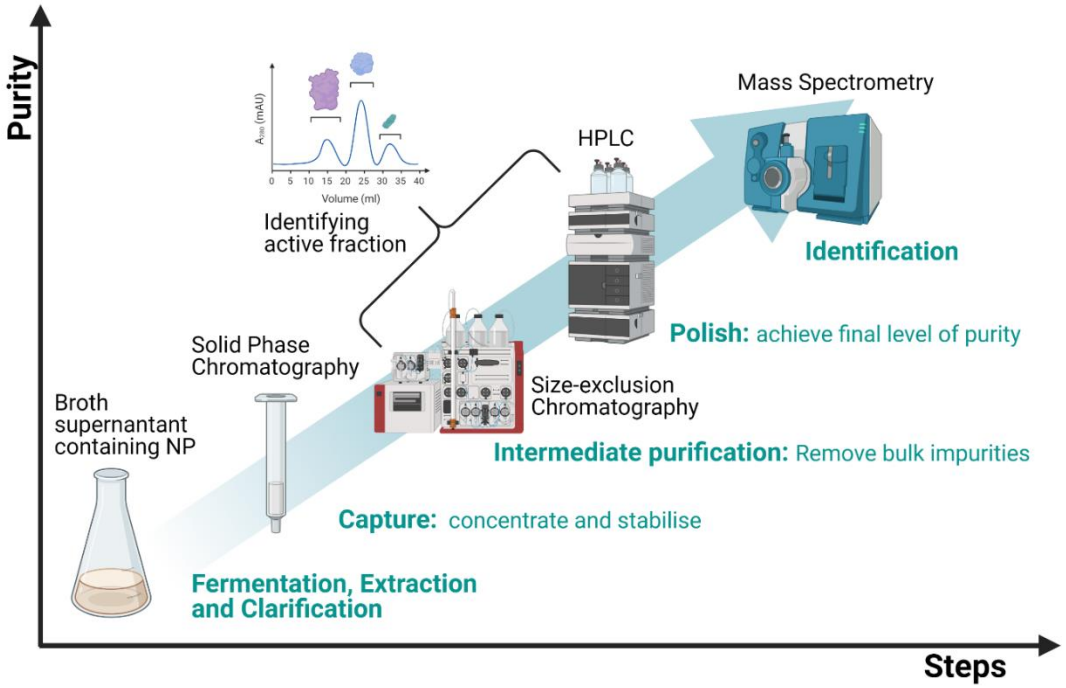

Figure 0-8. Simplified process of the purification and clarification of NPs from bacterial culture media. Created with BioRender.com

The most significant limitation with cultivation-dependent strategies is that our current ability to best cultivate the microbes from environmental samples is poor. Uncultivable bacteria continue to remain a challenge in microbiology, with approximately 99% of bacteria resisting cultivation in laboratory conditions (Amann, Ludwig and Schleifer 1995; Kaeberlein, Lewis and Epstein 2002). Culture media are an important consideration when isolating bacteria. Several culture-dependent approaches have been investigated with sponge-associated

bacteria (Fig. 0-9). Studies have reported on broad comparisons of recovery media for SAB (Sipkema *et al.* 2011; Xin *et al.* 2011; Esteves *et al.* 2016).

Furthermore, there is the issue of cryptid genes in NP discovery. An OSMAC approach has been suggested to overcome this limitation to culture-dependent strategies (Bode *et al.* 2002; Bills *et al.* 2008; Romano *et al.* 2018). SAB have been raised in growth matrix treatments, in which small adjustments are made to the concentrations and sources of carbon, nitrogen and phosphorous; changes in temperature; and orbital shaking (Matobole *et al.* 2017). OSMAC approaches can be used to identify tailored growth conditions in order to induce cryptic BGCs for antibiotic screening.

Incubation conditions (i.e. time, temperature), media and growth matrix are essential considerations when recovering bacteria from any environmental sample and not just sponges. Incubation temperature for SAB recovery has been reported between 13-30°C for a range of time frames (Fig. 0-9). This is interesting as the temperature is a factor that must be carefully considered since ideal recovery and incubation temperatures for bacterial growth are species-dependent (Abdallah *et al.* 2017). Shallow water SAB species are mesophilic, capable of growing between 20 to 45°C (Sipkema *et al.* 2011; Lagier *et al.* 2015; Versluis *et al.* 2017). Whereas psychrophilic sponge-associated bacteria from permanently low-temperature habitats, such as the deep-sea and polar regions, will be selective for low temperatures of 10°C to -20°C (Bowman 2001, 2007; Rothschild and Mancinelli 2001).

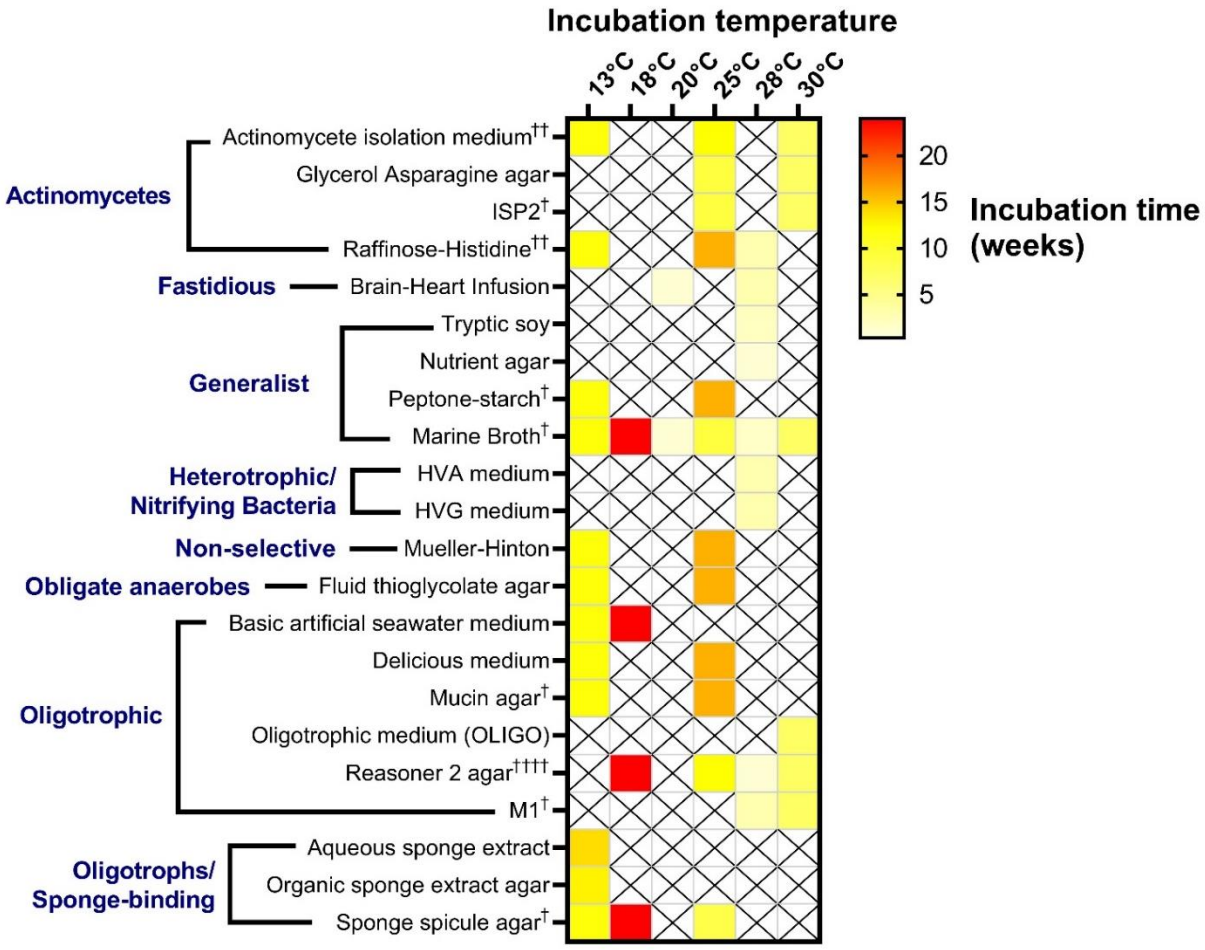

Figure 0-9. Recovery media, incubation temperatures and times used within 13 publications investigating SAB cultivation. Blue text to the left of the media name indicates the target organisms of each media. Full details of the publication used can be found in Table S0-2. (†, denotes the number of publications within the literature that a media was identified as the 'best performing' media; crosses within cells denotes the absence of data).

Growth media is likely the most significant selective factor (Fig. 0-9). This can only be accounted for by employing a broad panel of isolation media, preferably a mixture of high, low nutrient growth and selective media. Diluted growth media has been utilised to cultivate SAB (Esteves *et al.* 2016; Bibi *et al.* 2020). The solidifying agent will also influence the recovery. Using gellan gum as the solidifying agent can improve the recovery of novel members of Proteobacteria and Actinobacteria (Janssen *et al.* 2002; Tamaki *et al.* 2009) and has been used in the recovery of deep-water SAMs (Xin *et al.* 2011). The recovery of deep-water SAB was achieved using solid growth media of gellan gun and

Raffinose-Histidine agar (Xin *et al.* 2011). The use of a broad panel of culture media and relatively simple methods can be enough to recover many undescribed marine bacterial species (Connon and Giovannoni 2002; Cho and Giovannoni 2004; Maldonado *et al.* 2005; Xin *et al.* 2011).

In situ cultivation techniques have been applied for sponge microbiome cultivation. This involves diffusion chambers, which permit for environmentally bioavailable nutrients to diffuse into the agar or liquid media, better simulating the *in situ* conditions for bacterial cultivation, and involving membranes or filters to selectively grown bacteria only (Kaeberlein, Lewis and Epstein 2002). Diffusion chambers have been employed in the form of an isolation Chip (i-Chip) and Tip (i-Tip). The i-Chip has been used in cultivating a potentially novel *Alteromonas* species with 22 BGCs from the shallow water *Xestospongia muta* sponge (Macintyre *et al.* 2019; MacIntyre, Haltli and Kerr 2019). Meanwhile, the use of an i-Tip expanded the phylogenetic diversity of bacteria cultivated from a freshwater sponge (Jung *et al.* 2014). Diffusion chambers are not commercially available, and investigators must fabricate their versions of the chambers. *In situ* cultivation has currently not been applied to deep-sea sponges, as this would be a monumental project to implant and recover the *in situ* cultivation chambers. The value of *in situ* cultivation in marine microbial natural product mining has been reviewed (Jung, Liu and He 2021).

Ultimately, when recovering deep-sea microbes, pressure must be acknowledged. Unfortunately, this is undoubtedly a technologically challenging consideration that has yet to be applied to the recovery of SAB. Multiple approaches have been successfully utilized in recovering obligate piezophiles from seawater and sediment samples. The methods include continuous-flow

bioreactors and pressure vessels, which maintain an in situ pressure, combined with low temperature and low nutrient isolation media (*see review* (Zhang et al., 2018).

Ultimately, a diverse range of culture-independent and dependent techniques is beneficial. This is exemplified by a rifamycin-like compound producing group of sponge-derived bacteria, *Salinispora* spp. (Kim *et al.* 2006). Phylogenetic analysis of PKS gene clusters from sponge-isolated strains of *Salinispora* spp. identified close similarity to rifamycin. Later, multiple sponge-derived *Salinispora* spp. were also found to produce these compounds (Hewavitharana *et al.* 2007). This established an alternate source of rifamycin, which was previously known only to be produced by a soil bacterium.

Identifying lead compounds and preclinical testing

Ideal drug candidates should have an isolation protocol that is straightforward and can generate sufficient concentrations or be amenable to recombinant or synthetic production methods. Low yield is a reoccurring challenge of NP isolation from a bacterial source, as seen with multiple Actinomycete producers (Blodgett, Zhang and Metcalf 2005; Penn *et al.* 2006; Thapa *et al.* 2007; Olano *et al.* 2008). Genetic engineering solutions are frequently required to overcome this pitfall (Nguyen *et al.* 2006; Zhang *et al.* 2016).

The preclinical pipeline involves testing the toxicity and efficacy of novel compounds, both *in vitro* and *in vivo*. Bacterial susceptibility is expressed as the minimal inhibition concentrations (MIC) determined by microbroth dilution techniques recommended by the European Committee on Antimicrobial Susceptibility Testing (EUCAST). Bactericidal and bacteriostatic activity over

time can be determined using Time-kill kinetics assays (American Society for Testing and Materials International 2016).

The toxicity of novel compounds is essential to establish early if the compound is intended for antimicrobial chemotherapy. Cytotoxicity assays using mammalian cell lines (e.g. HaCaT cells) and MTS assays are the most frequently utilised in early cytotoxicity screens. For *in vivo* toxicity screens and antibiotic efficacy assays, the insect model *Galleria mellonella* larvae is a promising cheap and rapid option permitting high-throughput screens (Champion, Wagley and Titball 2016; Singkum *et al.* 2019). However, there is a need for standardisation in methodology with *G. mellonella* assays (Andrea, Krogfelt and Jenssen 2019; Hesketh-Best *et al.* 2021). It is roughly at this stage that a decision will be made on the appropriateness of the compound as a therapeutic candidate to progress.

The compound's identity at this stage may still be unresolved, which may be problematic if it is a known antibiotic. Dereplication of bacterial isolates and compound using mass spectrometry is a feasible option. Matrix-Assisted Lazer Desorption Time Of Flight Mass Spectrometry (MALDI-TOF MS) is used in clinical settings to identify bacteria with high success (Dieckmann *et al.* 2005; Ghyselinck *et al.* 2011; Spitaels, Wieme and Vandamme 2016; Strejcek *et al.* 2018). However, there are not yet sufficient MALDI-TOF spectra databases build using environmental bacteria, but medically relevant bacteria.

Conducting *in silico* investigations can aid in the preliminary identification of bioactive compounds. Using isolate genome and SM gene cluster identification tools, such as antiSMASH v5 (Medema *et al.* 2011; Blin *et al.* 2019) and BAGEL

v4 (de Jong *et al.* 2006; Van Heel *et al.* 2018), can aid in acquiring preliminary identities for the compound.

Current study

There is a knowledge gap regarding the diversity and biomedical potential of the microbiomes of deep-water hexactinellid sponges, and we are still in the early stages of exploring the microbial communities of hexactinellids (Steinert *et al.* 2020). Little is known regarding their microbial communities, yet there is an early demonstration of promise for bioprospecting (Xin *et al.* 2011). This warrants further exploration of sponges belonging to the class Hexactinellida, a central part of this thesis.

The overarching aims of this thesis are to (1) explore the potential of deep-water hexactinellid sponges as a source of novel antimicrobials from culture-dependent and independent approaches; (2) identify promising bacterial producers and purify candidate compounds; (3) explore how *Galleria mellonella* can be used at the early stages of drug discovery and lead compound identification. A brief overview of each chapter is given below:

Chapter 1: Phylogenetically diverse antibiotic-producing bacteria were recovered from two deep-sea sponges

Two deep-water sponges, *Hertwigia* sp. and *Pheronema carpenteri,* are used to survey cultivation conditions to recover antibiotic-producing bacteria. Various incubation temperatures, isolation media and pressures are utilised towards this goal. Phylogenetically diverse antibiotic producing isolates belonging to the Actinobacteria and Proteobacteria are recovered, and

OSMAC strategies uncover previously unobserved biological activity.

Chapter 2: An exploration of the bacteria community composition of two *Pheronema carpenteri* sponge-aggregations from the North Atlantic

Pheronema carpenteri was found to be a strong candidate from which to recover antibiotic-producing bacteria. Next-generation sequencing of bacterial 16S rRNA genes and a single metagenome was used to investigate the diversity and composition of the bacterial communities in *P. carpenteri*. *P. carpenteri* sponges are rich in Actinobacteria and share intra-aggregation similarities and demonstrate an intra-sponge bacterial community structure. Metagenome sequencing reveals an abundance of nitrogen cycling genes, but limited BGCs were detected.

Chapter 3: *Galleria mellonella* larvae exhibit a weight-dependent lethal median dose when infected with Methicillin-resistant *Staphylococcus aureus*

There is an urgent need for a rapid *in vivo* tool to assess the efficacy of crude natural products. The *in vivo* model *Galleria mellonella* larvae are regularly used as a toxicity screen and, to a lesser extent, to measure antibiotic efficacy. The lethal median dose (LD_{50}) for the methicillin-resistant *Staphylococcus aureus* strain NCTC 12493 was determined for larvae of six weight groups between 180-300 mg. The relationship of larvae fat body,

responsible for modulating immune responses, and melanisation was investigated to attempt to understand significant variation seen in mortality of larger weighing larvae (261-300 mg).

Chapter 4: Investigating the antimicrobial production of *Delftia acidovorans* PB091 an isolate from the deep-sea sponge *Pheronema carpenteri*

Delftia acidovorans PB091, recovered from *P. carpenteri,* is explored in detail to identify the medical potential of the compound isolated from this bacterium. PB091 antimicrobial production against clinically relevant Gram-positive and Gram-negative pathogens is assessed. Purification and clarification of only a Gram-positive active compound was achieved. Whole-genome sequencing and BGC analysis identified Delftibactin A/B as the putative Gram-positive compound.

Chapter 1. Phylogenetically diverse antibiotic-producing bacteria recovered from two previously unexplored deep-sea sponges

The content within this chapter contributed to the following publication:

Matthew J. Koch, **Poppy J. Hesketh-Best**, Gary Smerdon, Philip J. Warburton, Kerry Howell and Mathew Upton (TBC) 'Impact of growth media and pressure on the diversity and antimicrobial activity of isolates from two species of Hexactinellid Sponge', *Microbiology*. **(*in press* at time of thesis upload to pearl)**

1.1. Introduction

Antibiotic NP discovery has traditionally involved a culture-dependent approach. Recent years have seen this evolve into a far more refined pipeline that includes strategies to extend antibiotic production using 'cultureomics' and 'one strain, many active compounds' (OSMAC) principles. 'Culturomics' describes a culture-dependent approach that uses multiple culture conditions (i.e. temperature, isolation media) to recover bacteria from difficult to culture samples (Lagier *et al.* 2016). This relatively simple approach has been successful for sponge-associated bacteria (SAB) (Sipkema *et al.* 2011; Xin *et al.* 2011). This strategy can be coupled with de-replication strategies by Matrix-assisted laser desorption ionisation-time of flight mass spectrometry (MALDI-TOF MS) (van Veen, Claas and Kuijper 2010; Spitaels, Wieme and Vandamme 2016), and then sequencing the bacterial 16S rRNA gene.

Tradition NP pipelines implemented on traditional source organisms or habitats (i.e. soils) will likely lead to the isolation of well-known NP chemistry (Pye *et al.* 2017). To reduce this redundancy, NP screening is being directed towards rare sources and taxonomically different spaces in the hopes of isolating novel candidates or 'uncultivable' strains (Silver 2011). Deep-sea sponges could present an opportunity to explore poorly characterised holobiomes, reduce the chances of re-discovery, and increase the possibility of novel compound discovery.

Hexactinellida, commonly known as glass-sponges, are typically found in deep waters >200 m, with only 5 known shallow-water species (Leys, Mackie and Reiswig 2007), and represent 7% of all described Porifera species (Hooper and van Soest 2002). Compared to other classes of sponges (i.e. Demospongiae),

hexactinellid sponges are infrequently included in microbial studies (Mangano *et al.* 2008; Xin *et al.* 2011; Tian *et al.* 2016; Borchert *et al.* 2017b; Steinert *et al.* 2020), and may be a promising unexplored taxonomic space for antibiotic NP discovery.

In culturing SAB, past research has favoured relatively higher temperatures (22-28°C) and short incubation periods (7-28 days) (Olson and McCarthy 2005; Hardoim *et al.* 2009; Axenov-Gribanov *et al.* 2016; Boedeker *et al.* 2017) (Fig 0-8, page 55). For psychrophiles, these conditions can be detrimental to successful recovery (Bowman 2001). Low temperature (12-15°C) and extended incubation periods (>3 months) have additionally been successfully utilised in isolating microbes from shallow-sponges (Sipkema *et al.* 2011). Additional strategies include introducing environmental and or nutritional chemical markers to replicate the host environment, such as sponge spicule extracts, which were highly effective in successfully recovering SAB (Sipkema *et al.* 2011).

Attempts to mimic environmental conditions have not extended to hydrostatic or atmospheric pressure for SAB. Culturing microbes under bathymetric or atmospheric pressure has been attempted on sediments and seawater samples (Jannasch, Wirsen and Winget 1973; Kato, Sato and Horikoshi 1994; Sauer, Glombitza and Kallmeyer 2012). Nevertheless, there is scope to further explore the effects of temperature, nutrient additives and pressure on bacterial cultivation from deep-sea hexactinellid sponges.

There have only been three studies to recover bacteria from hexactinellid sponges and screen them for bioactivity (Mangano et al., 2008; Williams et al., 2020; Xin et al., 2011). Antarctic deep-sea hexactinellid sponges *Rosella nuda* and *Rosella racovitzae* were utilised to recover two Gram-positive isolates.

They were identified to be closely related to a cold-adapted *Dietzia* sp. ice-oil-79 (Xin *et al.* 2011). The same study also reported the presence of polyketide genes (PKS-I and PKS-II) as a marker for potential chemical diversity. From the culture data, the authors also report the presence of phylogenetically distinct hexactinellid and demosponge clusters (Xin *et al.* 2011). An earlier publication compared antagonistic inhibition between the SAB of the shallow-water hexactinellid *Scolymastra joubini* and the demosponge *Lissodendoryx nobilis* (Mangano *et al.* 2008). This study found active isolates among the Proteobacteria, Actinobacteria and, to a lesser extent, Bacteriodetes.

The aims of the current investigation were to: (i) identify a range of culturing conditions that could be used to generate the highest abundance and diversity of antimicrobial-producing candidates from deep-sea sponges; (ii) compare bioactive SAB from two previously unexplored hexactinellid sponges to previously cultivated SAB from the literature, (iii) identify potential bioactive bacterial candidates for further investigation, and (iv) utilise OSMAC strategies to observe previouoslly unseen inhibitory activity.

1.2. Materials and Methods

1.2.1. Sponge collection

Sponge samples were collected from the North Atlantic as part of two different research programmes: the NERC funded DeepLinks Project in 2016 using the RRS James Cook (JC136), and the Sensitive Ecosystem Assessment and ROV Exploration of Reef (SEAROVER) project in 2017 using the Irish Light Vessel Granuaile (GRNL2017) and a second in 2019 on Celtic Explorer (CE19015) (Fig. 1-1A). All cruises conducted sampling of a wide range of deep-sea organisms. Sponges were collected by Remotely Operated Vehicles (ROVs) and photographed *in situ* before removal (Fig. 1-1B-C). Sponges were transferred from the ROV into buckets containing *in situ* seawater and taken into the onboard laboratory for processing. Sponge samples were photographed and a small tissue sample taken for genetic analysis as part of separate investigations. The remaining sponge sample was then placed in a plastic zip-lock bag and frozen at -20°C for the remainder of the cruise. Upon return to land, frozen samples were transported on dry ice back to the University of Galway freezers and maintained at -80°C before being transported on dry ice to the University of Plymouth and maintained at -80°C.

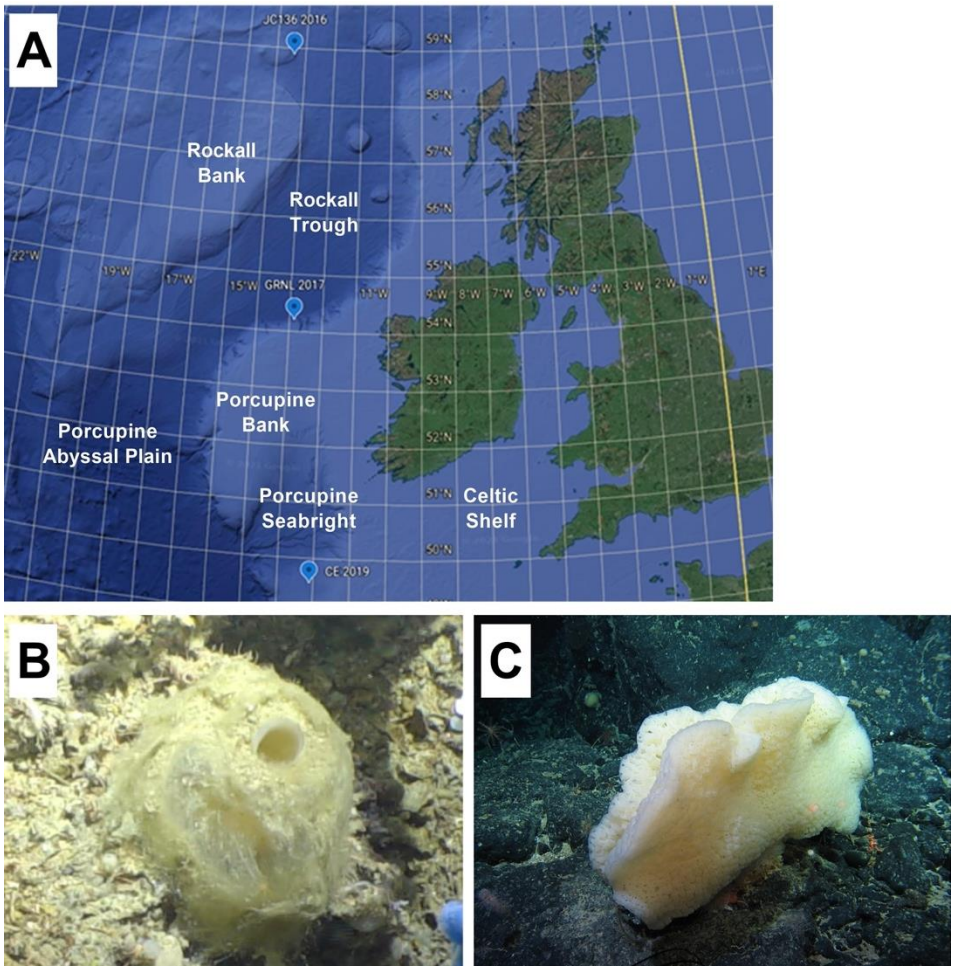

Figure 1-1. Map of sampling sites and sponges used in experimentation. (A) Map of deep-sea sampling points for sponges. Blue marker points from top to bottom, sampling sites for JC136, GRNL and CE. *In situ* images of deep-sea sponges, (B) *P. carpenteri* JC136_125, and (C) *Hertwigia* sp. GRNL_81. Two red laser dots visible illustrate a 10 cm distance.

1.2.2. Sponge Identification

Sponges were identified from the analysis of internal and external morphological features (i.e. body shape, type, size, and arrangement of spicules) following the System Porifera classification system (Hooper and van Soest, 2002). For spicule analysis, under sterile conditions using ethanol washed and flame sterilised scalpels, cuttings of approximately 1 cm^3 were taken, where available, from the three regions on the sponge body: mesohyl, atria, and the prostalia.

Tissues were placed inside Eppendorf tubes (2 ml), covered with 65% Nitric Acid and left for 2 h for spongin tissue to dissolve, then gently centrifuged at 600 x *g* for 2 min. The supernatant was carefully discarded, and the pellet containing spicules re-suspended in water and washed three times to remove all remaining acid. Spicules were then washed in >95% ethanol twice before being left at room temperature for the remaining ethanol to evaporate. Dry spicules were inspected under a compound light microscope and used to identify sponge species (Hooper and van Soest 2002). Manual literature searches were also conducted to identify more recent publications that may help support identification.

1.2.3. Isolation of sponge-associated bacteria

1.2.3.1. *Sample preparation*

Sponges were allowed to thaw at room temperature for up to 30 minutes to facilitate access to the inner tissue layer. To prevent culturing contaminates that may have come in contact with the surface of sponges during sampling, the surface layer (>2 cm deep) of the sponge was not utilised in cultivation. With a flame sterilised scalpel, the outer sponge tissue was cut away and multiple sections of ~0.5 g wet weight of tissue were cut from the inner tissue mass. Tissue cuttings were washed three times by gentle vortexing for 15 s in sterile artificial seawater (ASW; 28.5 g l^{-1} Instant Ocean® Sea Salts).

Washed sponge tissues were homogenised using a sterile mortar and pestle. The homogenate cell suspensions were centrifuged at 4,000 x *g* for 20 min. The supernatant was discarded and the pellet re-suspended in 1 ml ASW. Suspensions were diluted 1:100 in ASW, and 100 µl aliquots of diluted suspension were plated (n=3). Two negative controls were used; 100 µl sterile

artificial seawater and a blank plate. Blank plates were intended for detecting possible contamination during aseptic technique or incubation. Monitoring of cultures involved counting of the colony forming units (CFU) and morphologically distinct colonies (morphotypes).

1.2.3.2. *Incubation conditions*

Cultivation efforts progressed in a sequential experimental design; this can be found summarised in a flow chart.

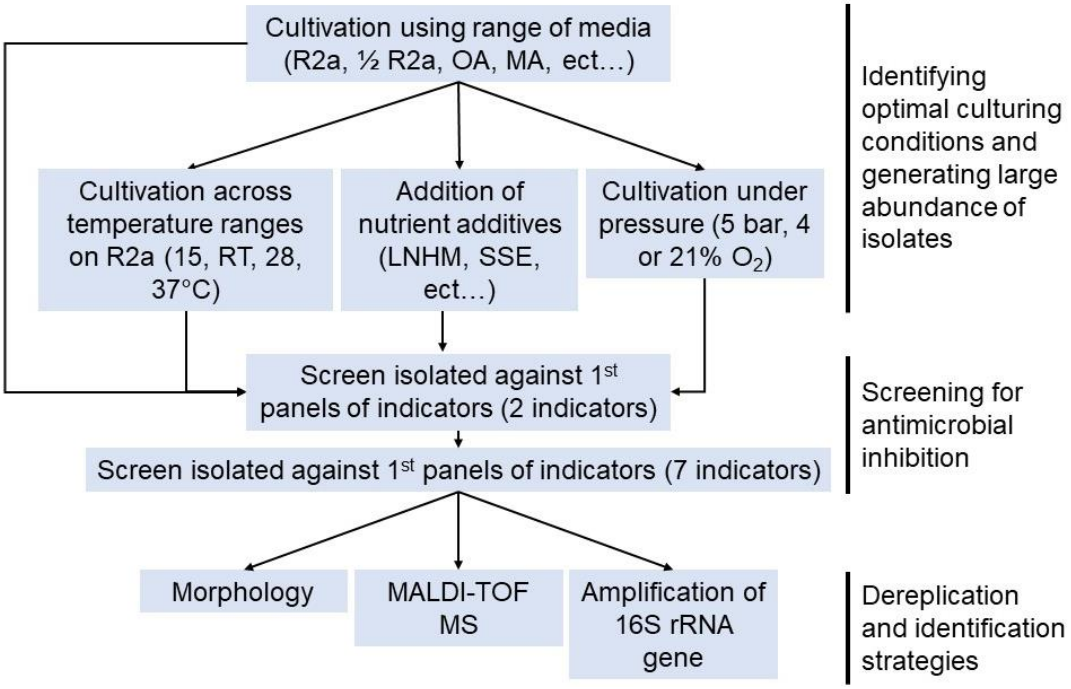

Figure 1-2. Summary of the sequential exeperimental design, from cultring to identification.

1.2.3.2.1. *Recovery media*

A range of growth media was used to assess suitable media for recovery. Details of these can be found in the appendix Table S1-1.

1.2.3.2.2. *Recovery temperature*

In assessing which was the most suitable temperature for incubation, four conditions were used; 4°C, 15°C, room temperature (RT; 22-25°C) or 28°C on

low nutrient ½ R2A (Table S1-1). All cultures were kept in the dark in sterile zip-lock bags to prevent the agar desiccating. Higher temperature (RT and 28°C) treatments were incubated for 41 days and inspected bi-weekly. For lower incubation temperatures, the incubation period was 90 days, and cultures were monitored weekly.

1.2.3.2.3. *Pressurised chambers*

R2a agar plates were inoculated as described above. Plates were incubated inside gas pressurised chambers maintained at 5 bar and room temperature provided by and maintained at the Diving Diseases Research Centre (DDRC Healthcare). The chambers' final oxygen conditions were: (i) 21% O_2/ 5 bar, or (ii) 4% O_2/ 5 bar. Non-pressurised cultures were run in parallel for comparison.

1.2.4. Screening for antimicrobial metabolite production

1.2.4.1. *Antagonistic lawn assay*

All recovered isolates were tested for antagonistic activity against *Escherichia coli* strain NCTC 1048 and an in-house strain of *Micrococcus luteus*. Cultures were diluted in sterile LB media to an OD_{600nm} of 0.10-0.09. The diluted suspension was thoroughly spread, using sterile swabs, over Luria Broth (LB) solidified with 1.5% (w/v) agar. Sterile loops were used to transfer a single colony of recovered SAB isolates onto the bioassay plate. Plates were incubated at 37˚C for 18 h. Clearing zones of the indicator strains were regarded as indicating production of antibacterial activity.

Active strains were then tested in a second-round against a broader panel of indicators; *Staphylococcus aureus* NCTC 12493, an in-house strain of *Streptococcus pyogenes*, *E. coli* 1077, *Klebsiella pneumonia* 681, in-house

strains of *Salmonella enterica* Serovar Typhimurium LT2, *Mycobacterium phlei*, and *Candida albicans*. All screening assays were done in triplicate.

1.2.4.2. *Amplification of biosynthetic gene clusters*

Amplification of secondary metabolite BGCs was carried out for producers and isolates identified as Actinobacteria. The polyketide synthase genes (PSKI and PKSII) and nonribosomal peptide synthase (NRPS) genes were amplified using a set of degenerate primers, as described previously (Palomo *et al.* 2013). Primer sequences and annealing temperatures can be found in the supplementary Table S1-2. PCR products were amplified using a Veriti Thermal Cycler (Applied BioSystems, UK) in a final volume of 50 µl. PCR mixture contained 0.5 µM of each primer, 25 µl 2X Taq PCR Master Mix (Qiagen, UK), and 5 µl of template DNA. The PCR amplification protocols were as follows: initial 5 min denaturation at 95°C, 35 cycles (30 s at 95°C, 2 min at annealing temperatures, and 4 min extension at 72°C); followed by a final extension of 10 min at 72°C. Products were visualised by electrophoresis in 2% (w/v) agarose gel stained with SYBR™ Safe DNA Gel Stain (ThermoFischer, UK). Nuclease-free water was used as a negative control, while an in-house strain of *Streptomyces* strain was used as a positive control owing to multiple PKS and NRPS domains detected through genome sequencing.

1.2.5. OSMAC approach to antibiotic screening

For the induction of different antimicrobial activities, an OSMAC approach in combination with bioautography for screening was followed (Fig. 1-3). A total of 5 isolates were selected, these isolates did not show any antimicrobial activity in the first round of screening, but PCR amplification indicated a presence of BGCs. Isolates were subjected to a matrix incorporating growth modifications

described previously (Matobole *et al.* 2017). The nutrient regimen included varying carbon (mannitol, succinic acid or starch at 5 mM) and nitrogen (NH_4Cl or $NaNO_3$ at 0.02% w/v) sources, and concentrations of phosphorous (KH_2PO_4 at 0.1 µM or 0.5 mM). The base medium was: 2 g/L $MgCL_2$, 0.525 g KCl, 0.075 g/L CaCl, and 2.38 g/L HEPES buffer. The media were made with either 0% or 1.8% w/v NaCl. Bacteria were cultured in 800 µl of liquid culture in 24-well plates at 15°C and room temperature without orbital shaking. The matrix was repeated in triplicate for each bacterial isolate.

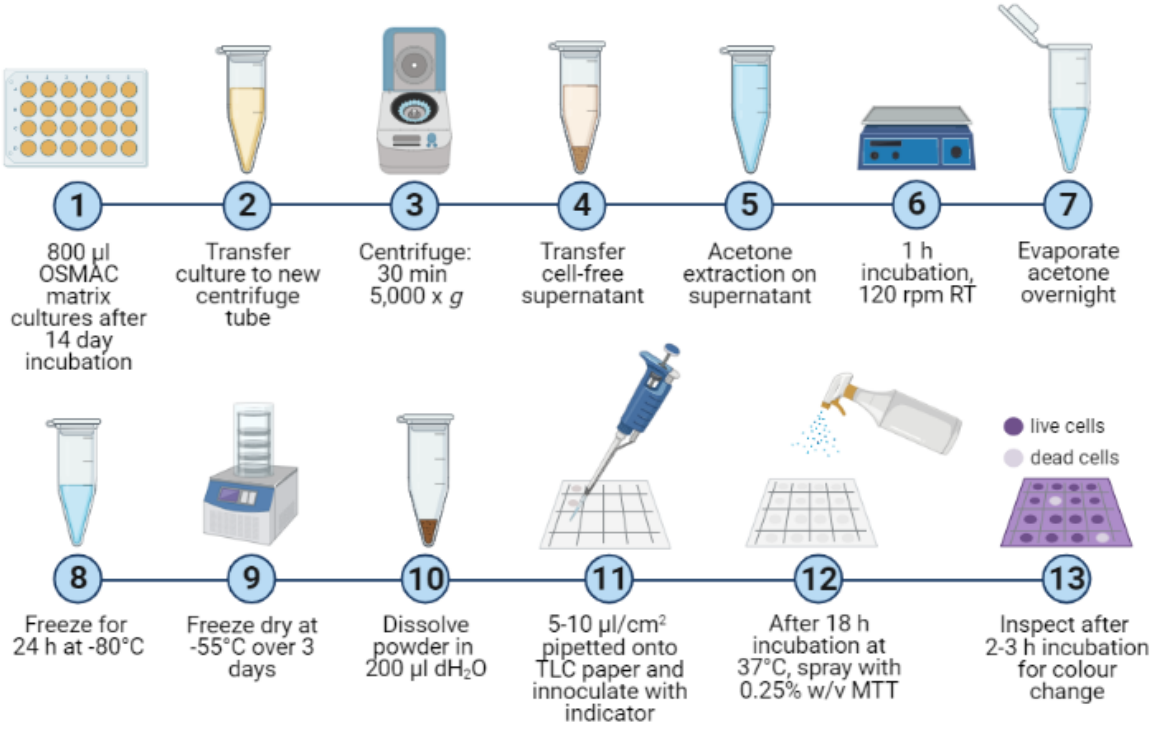

Figure 1-3. Summary of protocol testing OSMAC principles with sponge recovered isolates, including the extraction of culture supernatant and bioautography to screen for antimicrobial activity. Nutrient matrix layout utilised for OSMAC can be seen in Fig. S1-1. ($_dH_20$, distilled water; MTT, Thiazolyl Blue Tetrazolium Blue; OSMAC, one –strain, many active compounds; RT, room temperature; TLC, thin layer chromatography) Created with BioRender.com.

1.2.5.1. *Extraction of OSMAC culture supernatants*

Crude supernatant extraction was achieved as previously described, with modifications (Bills *et al.* 2008). In summary, after 14 days of incubation, micro-cultures were transferred to new centrifugation tubes and centrifuged for 30 min

at 5,000 x *g.* Supernatants were carefully transferred, without disturbing the pellet, to new centrifugation tubes. Cell-free supernatants were treated with 1:2 vol. Acetone (C_3H_6, FisherScientfic, UK). Supernatants were incubated at room temperature for 1 h shaking at 120 rpm. Afterwards, acetone was left to evaporate in a fume hood for 18 h before cultures were frozen at -80°C. After 24 h at -80°C, supernatants were freeze-dried under a vacuum at -55°C for 3 days in a Lablyo mini (Frozen in Time Ltd., UK). Freeze-dried supernatants were re-suspended in 200 µl of sterile distilled water. These were regarded as crude supernatant extracts (CSE).

1.2.5.2. *Bioautography*

This method of bioautography is a variation on previously reported methods (Betina 1973; Dewanjee *et al.* 2015). A grid containing 1 cm^2 squares was drawn in pencil on silica gel and aluminium backed thin layer chromatography (TLC) plates (Whatman, UK). A volume of 5-10 µl CSEs were spotted onto a square and left to dry to completion. Controls included antibiotics (100 µg/ml of Gentamycin, Ciprofloxacin, Vancomycin) and sterile OSMAC media taken through the extraction protocol.

Test bacteria (*S. aureus* NCTC 12493 and *E. coli* C41) were incubated in 5 ml Mueller Hinton (HM) broth, at 37°C and 120 rpm for 18 h. Cultures were adjusted to an OD_{600nm} of 0.5 with sterile media. TLC plates were submerged into the bacterial culture. Plates were placed in a sterile square petri dish lined with blue-roll (tissue) dampened with distilled water to prevent TLC plates from drying out. This was incubated at 37°C overnight. After incubation, TLC were sprayed with 0.25% w/v Thiazolyl Tetrazolium Blue (MTT; Sigma-Aldrich, UK) dissolved in calcium and magnesium free phosphate buffered saline (PBS; 10

mM $NaPO_4$, 2.68 mM KCl, 140 mM NaCl, pH 7.4, Gibco). Plates were incubated at 37°C in the dark for 2-3 h. Sheets were visually inspected for colour change. MTT turns purple when reduced, indicating the presence of living cells. White areas on the plate indicate zones in which the test bacteria were killed.

1.2.6. Dereplication and identification of strains

1.2.6.1. *Matrix-assisted Laser Desorption/Ionisation Time of Flight Mass Spectrometry*

Bacterial isolates demonstrating antimicrobial activity were de-replicated using a Bruker matrix-assisted laser desorption ionisation–time-of-flight mass spectrometry (MALDI-TOF MS) Biotyper. A single colony no more than 24 h old, was smeared in duplicate on MALDI plates and left to dry. Dried colonies were overlain with 1 µl freshly prepared MALDI matrix (10 mg/ml α-Cyano-4-hydroxycinnamic acid (Bruker, UK), 50% Acetonitrile, and 0.05% Trifluoroacetic acid). The MALDI-TOF output included two possible matches between the test organism and those in its database, each with a score indicating the strength of the match. The lowest cuto-off score for identification was set at >1.6. The highest score was used as a preliminary identification of colony.

1.2.6.2. *DNA extraction, 16S rRNA gene PCR amplification and sequencing*

A small density of isolate was suspended into 100 µl of a boil lysate solution (10 mM Tris-Cl, 1 mM EDTA, 0.1% Triton x100, pH 8.0) and heated at 95˚C for 15 min. Suspensions were centrifuged for 2 min at 4,500 x *g*, and the supernatant transferred to a fresh tube. To amplify the bacterial 16S rRNA gene, universal primers 27F (5′-AGAGTTTGATCCTGGCTCAG-3′) and 1492R (5′-

TACGGYTACCTTGTTACGACTT-3′) (Heuer *et al.* 1997; Frank *et al.* 2008) which span nearly the entire length of the bacterial 16S rRNA gene were used. PCR reactions contained; 0.1 µM of each primer, >10% v/v template DNA sample, 50 µl DreamTaq Green PCR MasterMix (2X) (ThermoScientific, UK), and nuclease-free water to a total reaction volume of 50 µl. The amplification program was as follows; 5 min at 94˚C, 35 cycles (30 s denaturing at 94˚C, 30 s annealing at 52˚C, 1.5 min extensions at 72˚C), and final step at 72˚C for 5 min. Products were analysed by electrophoresis on a 2% (w/v) agarose gel and visualised by staining with 1% (v/v) SYBR™ Safe Stain (Invitrogen, UK).

PCR products were purified using the High Pure PCR Cleanup Micro Kit (Roche, UK) following the manufacturer's instructions. DNA yields were analysed using a Nanodrop. Purified PCR products were Sanger sequenced by LGC Genomics (Berlin, Germany). Sequences were trimmed and compared with existing sequences in the National Centre for Biotechnology Information (NCBI) database using BLASTn to facilitate putative identification of isolates.

1.2.6.3. *16S rRNA gene phylogeny*

Using the NCBI database, the 16S rRNA sequences for cultured SAB from the following studies were retrieved: Lafi, Garson and Fuerst, 2005; Kim and Fuerst, 2006; Jiang *et al.*, 2007; Zhang *et al.*, 2008; Mangano *et al.*, 2009; Sipkema *et al.*, 2011; Xin *et al.*, 2011; Bibi *et al.*, 2020. Multiple sequence alignments were performed with MAFFT v. 7.407 using a standard iterative refinement method (Katoh *et al.* 2002; Yamada, Tomii and Katoh 2016). Following a manual curation of the retrieved sequences, highly similar sequences (>98% sequence similarity) from the same study were removed.

Phylogeny was inferred by Maximum Likelihood implementation in RAxML v. 8 using GTR+GAMMA approximation model (Stamatakis 2014; Kozlov *et al.* 2019). RAxML halted bootstrapping automatically. Visualisation of the tree and the addition of metadata (the taxonomy of sponges and detection of antibacterial activity) was done using the interactive Tree Of Life v. 6 (iTOL; (Letunic and Bork 2007, 2019). Final edits to the phylogenetic tree were made using Inkscape v. 1.

1.2.7. Statistical analysis

Two-Way ANOVA's and pairwise comparison of the relative abundance of isolates between sponges and incubation conditions (temperature, nutrient additives, and pressure) were performed using GraphPad Prism v. 9.0.1 for Windows (GraphPad Software, San Diego, California USA; www.graphpad.com).

1.3. Results

1.3.1. Sponge identified as *Pheronema* sp. and *Hertwigia* sp.

Sponges used in this study collected on the JC136 (2016) and CE19015 (2019) cruises were identified as *Pheronema carpenteri* (*order* Amphidiscoside, *family* Pheronematidae) (Table 1-1). Morphological features for *P. carpenteri* include a spherical/hemispherical body with an outer wall formed by long siliceous spicules. Body shapes were more-or-less radially symmetrical. At the top of the sponge, there is a singular large opening, an oscular. The major chromosomal spicules were pentactins (Fig. S1-1A). Monactins were serrated, and microspicules included amphidiscs (macramphidiscs and mesamphidiscs) with smooth teeth (Fig. S1-1B).

Sponges GNRL_81 and GNRL_82 (2017; Fig. 1-1C) were provisionally identified as associated with the sponge *Hertwigia falcifera* (*order* Lyssacinosida*, family* Euplectellidae). Morphological features of sponges GNRL_81 and 82 include a network of canals/tubes ranging in diameter. GNRL_81 and 82 bear morphological resemblance to previously reported sponges identified as belonging to the genera *Hertwigia*, except for colour (Thomas and Watling 2012). Specimens used in this study do not have the distinctive yellow colouration to the sponge body, but this is not always a reported key feature to *Hertwigia* sponges (Tabachnick and Collins 2008). With regards to spicules, loose spicules were rare. The walls were constructed from chromosomal fused spicules, which are reportedly typical for *Hertwigia falcifera* (Tabachnick and Collins 2008). Included among the few loose spicules were sigmatocomes (Fig. S1-2C) and spirodiscohexasters (Fig. S1-2D).

Table 1-1. Summary of hexactinellid sampling metadata and taxonomy used in cultivation efforts. Name prefix refers to the research vessel during which the sponges were collected: CE, RV Celtic Explorer, Republic of Ireland; GRNL, Irish Lights Vessel Granuaile, Republic of Ireland; JC, RSS James Cook, United Kingdom.

Sponge ID	Identity	Sampling Date	Depth (m)	Coordinates (lat, long)	Cruise report
JC136_125	*P. carpenteri*	16/06/2016	1,051	58.85, -13.39	(Howell et al., 2016b)
JC136_134	*P. carpenteri*	16/06/2016	1,054	58.85, -13.39	
JC136_135	*P. carpenteri*	16/06/2016	1,051	58.85, -13.39	
CE_015_09	*P. carpenteri*	13/08/2019	1,209	49.53, -12.09	(O'Sullivan, Healy and Leahy 2019)
CE_015_10	*P. carpenteri*	13/08/2019	1,209	49.53, -12.09	
CE_015_27	*P. carpenteri*	15/08/2019	1,103	50.98, -13.68	
CE_015_29	*P. carpenteri*	15/08/2019	1,103	50.98, -13.68	
GRNL_81	*Hertwigia* sp.	21/07/2017	2,227	54.18, -12.84	(O'Sullivan D., Leahy and Healy 2018)
GRNL_82	*Hertwigia* sp.	21/07/2017	2,175	54.18, -12.84	

1.3.2. No effect observed from incubation temperature, but a significant effect from increased atmospheric pressure

During a continuous effort to culture bacteria isolated from deep-sea hexactinellid sponges, 9 sponge samples covering two genera were utilised. The number of colony forming units (CFU) and morphotypes across all treatments was recorded for the entire incubation period. A total of 1,437 marine bacteria were recovered from the cultivation efforts, 915 bacteria from *P. carpenteri* sponges (N=7) and 522 bacteria from *Hertwigia* sp. sponges (N=2) (Table S1-3). After selectively picking for distinct colony morphology, 800 isolates were successfully transferred to LB agar plates for further processing; no isolate had an absolute requirement of seawater for growth on solid media. This survey observed that at 41 days the appearance of new colonies had slowed. Very few colonies appeared between days 41 and 90, of which most failed to be recovered from the original plate on sub-culture.

A range of conditions tested during the incubation of SAB permitted for an assessment of the effect of media, temperature, enrichment and pressure on the quantity of bacterial isolates recovered (Fig. 1-4). No effect was observed on colony recovery from temperature (F (3, 40) = 0.5524, *p*-value = 0.65) (Fig. 1-4A) or the addition of supplements to ½ R2a (F (3, 40) = 1.818, *p*-value = 0.16) (Fig. 1-4C).

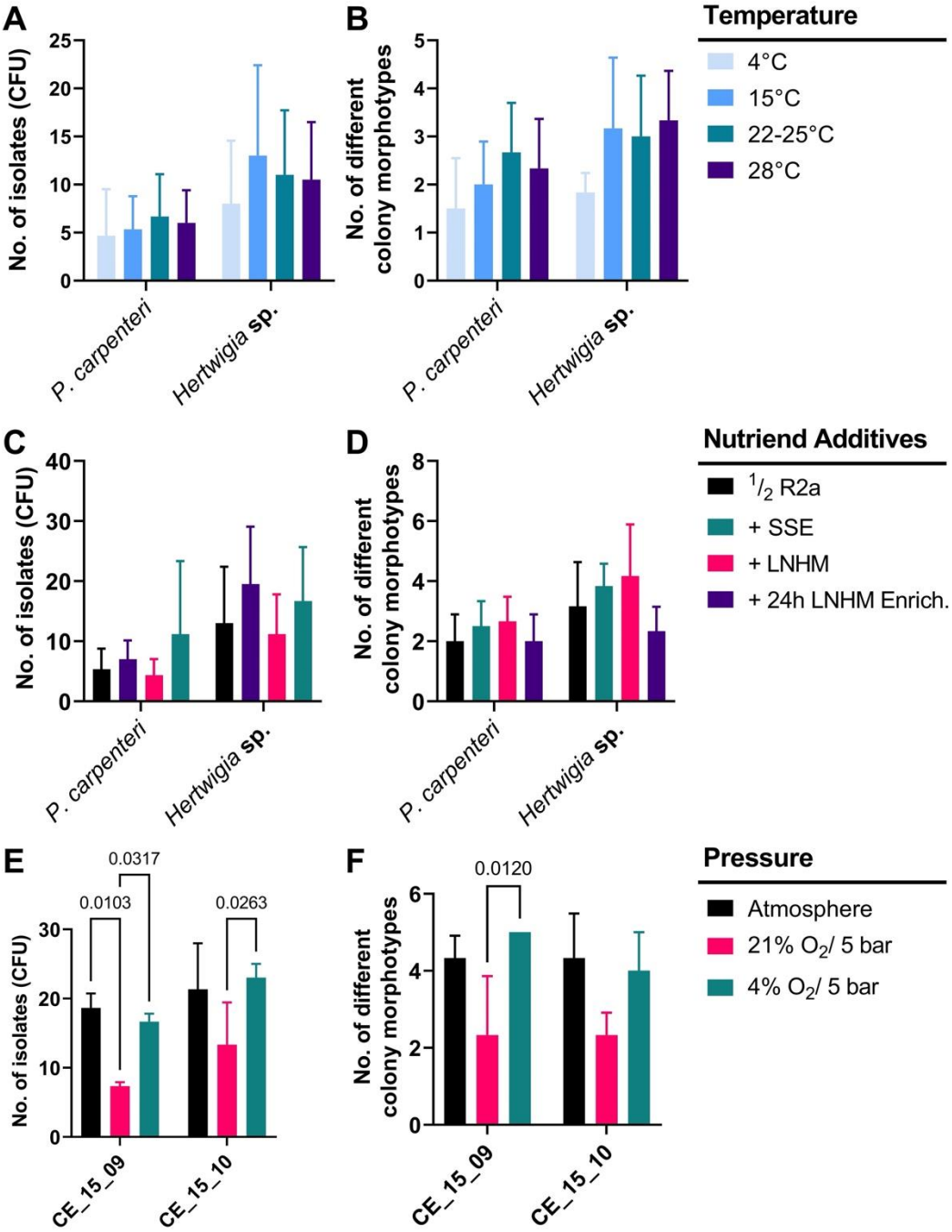

Figure 1-4. Most cultivation conditions did not affect the number of bacterial isolates recovered from the studied sponges. In this survey, the effect of (A-B) temperature, (C-D) nutrient additives to ½ R2a media, and (E-F) pressure was assessed on the recovery of bacterial isolates from *P. carpenteri* and *Hertwigia* sp. The left-hand side shows the number of isolates recovered, and the number of distinct morphotypes on the right-hand side. Data presented as the means of each treatment (N=3), errors bars representing the SD. Significant *p*-values from the posthoc test are depicted within. Complete results of Two-Way ANOVA's can be found in the supplementary (Tables S1-4 to S1-6).

A significant effect was seen in culturing bacteria under pressure (CFU: F (2, 12) = 12.03, *p*-value = 0.001; Morphotypes: F (2, 12) = 9.813, *p*-value = 0.003) (Fig. 1-4E,F). Post-hoc tests show that this effect was prominent in the 21% O_2/ 5 bar treatment; there were fewer colonies and lower morphological diversity than the atmospheric cultures. Statistically significant differences were observed between the means of 4% and 21% O_2/ 5 bar of pressure in the number of colonies recovered (Fig. 1-4E), and in *P. carpenteri* CE_15_09, there was a difference also observed in the diversity of colonies (*p*-value = 0.012) (Fig. 1-4F). No differences were observed between 4% O_2/ 5 bar and the cultures incubated at atmospheric pressure.

One effect observed was a significant difference between the two sponge species, with higher overall recovery of bacteria from *Hertwigia* sp. samples than *P. carpenteri* (Table S1-4 to S1-6). This effect was not observed between the two *Pheronema* sponges used in the cultivation under pressure.

1.3.3. Majority of bioactive isolates were recovered from *Pheronema* sponges.

The plate-based screening effort of 800 bacteria revealed that 77% of bacteria demonstrated no inhibitory activity, and zero isolates exclusively inhibited *E. coli* (Fig. 1-5A). Of the remaining isolates, 15% exclusively inhibited *M. luteus*, and 8% inhibited *M. luteus* and *E. coli*. The sponge JC136_134 had the highest proportion of bacteria with inhibitory activity (34%), followed by *Hertwigia* sp. GRNL_81 (18%). The two remaining *P. carpenteri* sponges performed

approximately the same (14.4% and 14.58%), and GRNL_82 (0.75%) has the lowest proportion of isolates (Fig. 1-5B). Significant variation was observed between individual sponge samples of the same species.

A

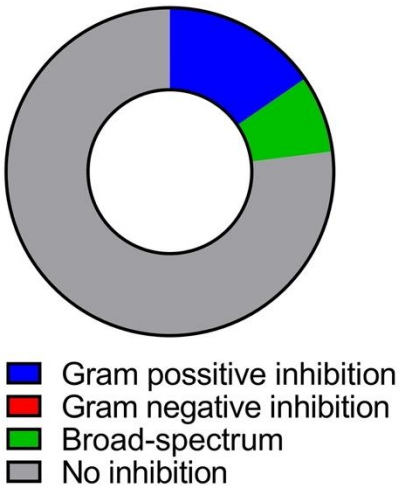

B

Sponge	Sample	% of isolates with antibacterial activity
Pheronema carpenteri	JC136_125	14.49
	JC136_134	33.73
	JC136_135	14.58
	Mean	**20.93 (SD ± 11.08)**
Hertwigia sp.	GRNL_81	17.83
	GRNL_82	0.75
	Mean	**17.05 (SD ± 12.08)**

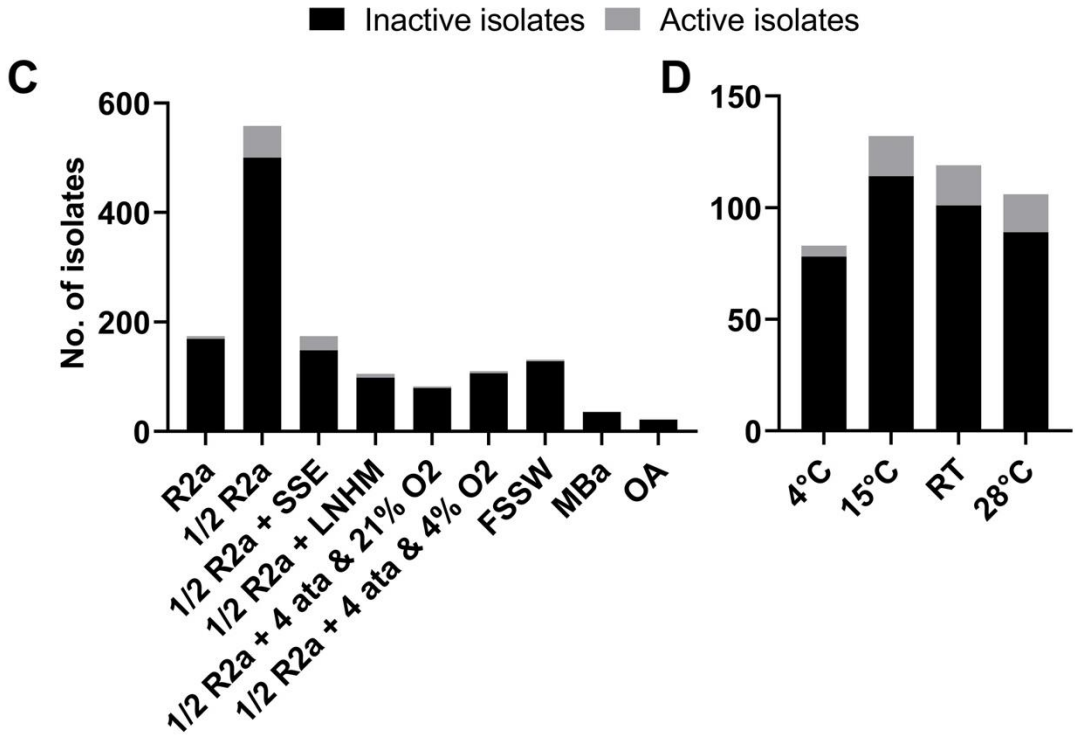

Figure 1-5. Breakdown of the quantity of bacterial isolates from *P. carpenteri* and *Hertwigia* sponges demonstrating antibacterial activity. (A) The proportion of recovered isolates demonstrating activity from the spot assay on a lawn of either *M. luteus* or *E. coli* (n = 734). No solely anti-Gram negative activity was observed from the SAB library. (B) The percentage of isolates with antibacterial activity observed from each sponge samples, as well as showing the mean percentage for each species of sponge (SD, standard deviation (C) Activity from SAB based on isolation media, (D) and on incubation temperature.

Anti-Gram-positive and broad-spectrum activity isolates were screened against a second panel, and 109 bacteria were carried forward. Isolates active exclusively against only *M. luteus* were not carried forward. For the most active isolates that were carried forward, the recovery media and temperature was surveyed. The inclusion of SSE did increase the number of bioactive isolates when supplemented to ½ R2a as compared to other nutritional treatments (Fig. 1-5C). Regarding isolation conditions and activity, we observed that isolates recovered from incubation temperatures of 15°C, RT and 28°C all performed the same (Fig. 1-5D).

The strategy used in this study could be described as an ‘inverted pyramic’, meaning instead of reducing the number of bacterial candidates, and workload, through the process of colony selection, screening and isolate identification, this approach inveribly increased the workload. This could have been adjusted in a number of ways, first by doing one a single screen against a broad panel, this will permit a quick removal of isoaltes with activity that is not expandise, but also allow for ranking isoalteds based on their performance against the wider panel. Secondly, at colony picking stage during cultivation, being far more conservative and selecting only the distinct morphotypes as most of the isoaltes selected here belongued to the same organism.

The pitfalls of this ‘inverted pyramid’ approach become futher apparent when attempts to dereplicate isoaltes begin. There is a fundamental issue with the interpretation of the data generated from the MALDI-TOF MS colony identification which was matched against a databse built from clinical isolates, this presents issues with a limited ability to identify environmental samples. This

strategy inveribly lead to a greater workload and missed opportunities to potentially observe unique inhibitory activity.

1.3.4. Actinobacteria and Proteobacteria isolates with multiple BGCs were recovered from culturing efforts

Preliminary identities of bacterial isolates were determined by MALDI-TOF MS. Following de-replication which included a combination of MALDI-TOF, Gram-staining and morphological characterisation, isolates were identified by amplifying and sequencing the 16S rRNA gene (Table 1-2). Many isolates were identified as closely related to *Delftia* sp., *Pseudomonas* sp., and *Bacillus* sp. as detected by MALDI-TOF spectra identification. Actinobacteria and Proteobacteria constituted the majority of de-replicated isolates selected for 16S rRNA sequencing. Within the phyla of Actinobacteria were bacteria closely related to *Microbacterium*, including *M. paraoxydans*, *M. maritypicum*, *M. luteolum* and *M. oxydans*. Also among the Actinobacteria isolates sequences were most similar to those for *Streptomycetes fulvissimus*, two *Brevundimonas* spp., and *Rhodococcus yunnanensis*. The second most abundant phyla among the isolates were Proteobacteria. Multiple strains of *Delftia acidovorans* were recovered from sponge samples, many demonstrating different antimicrobial activity. There were three *Pseudomonas* sp. strains, one *P. putida,* and two with the closest related species being *P. zhaodongensis*.

In detecting BGCs, 8 Actinobacteria isolates contained PKS-1, and 2 contained both T1PKS and T2PKS (Table S1-4). Only the *S. fulvissimus* and three *Delftia* sp. strains were positive for NRPS genes. Isolates belonging to Proteobacteria were the most diverse in detected BGCs, with the most strains being positive for T1PKS, T2PKS and NRPS. Isolates that did not test positive in the antagonistic

bioassay were positive in the BGC PCR screen, included strains recovered from pressure cultivation: PP-22, PP-23, PP-30, PP-41, PP-42, and PP-43.

Table 1-2. Sponge recovered bacterial isolates demonstrating antimicrobial activity in screening assays or detected during PCR amplification screening. Unique isolates were then identified by amplifying and sequencing the 16S rRNA gene. Isolates were all screened primarily using the plate-based method, phylogenetically distinct isolates were then screened by amplifying a set of PKS genes (+, positive; -, negative). Indicators for metabolic activity are: SA, MRSA NCTC 12493; ST; *S*. Typhimurium LT2; SP, *S. pyogenes*; EC_1, *E. coli* DSM 1077; EC_2, *E. coli* ATCC 11775; KP, *K. pneumoniae*; CA, *C. albicans*. Sponge ID prefix denoted the sponge isolates were recovered from: PP, PB, PC and Act are isolates recovered from *Pheronema carpenteri*, while RC, RE and RG were from *Hertwigia* sp.

Isolate ID	Phylum	Genus	% Match (bp used)	Closest NCBI match	% coverage (*E*-value)	Screening		Detected activity						
						Plate	PCR	SA	ST	SP	CA	KP	EC_1	EC_2
Act-R2a	Actinobacteria	*Streptomycetes*	100 (1,312)	*Streptomycetes fulvissimus*	100.00 (0)	-	+	-	-	-	-	-	-	-
PB-104	Actinobacteria	*Microbacterium*	99.1 (817)	*Microbacterium paraoxydans*	99.76 (0)	-	-	+	-	-	-	-	-	-
PB-125	Actinobacteria	*Brevundimonas*	99.8 (636)	*Brevundimonas* sp.	100.00 (0)	-	+	+	+	-	-	-	+	+
PC-227	Actinobacteria	*Microbacterium*	100 (784)	*Microbacterium maritypicum*	100.00 (0)	-	+	+	-	-	-	-	+	-
PP-23	Actinobacteria	*Microbacterium*	99.2 (1,037)	*Microbacterium keratanolyticum*	100.00 (0)	-	+	-	-	-	-	-	-	-
PP-41	Actinobacteria	*Rhodococcus*	98.1 (1,196)	*Rhodococcus yunnanensis*	100.00 (0)	-	+	-	-	-	-	-	-	-
RC-201	Actinobacteria	*Microbacterium*	98.4 (1,091)	*Microbacterium luteolum*	99.27 (0)	+	+	-	-	+	-	-	-	-
RC-206O	Actinobacteria	*Brevundimonas*	100 (977)	*Brevundimonas* spp.	100.00 (0)	+	+	+	-	-	-	-	-	-
RC-206Y	Actinobacteria	*Microbacterium*	99.7 (1,360)	*Microbacterium oxydans*	100.00 (0)	+	+	+	-	-	-	-	-	-
PP-24	Firmicutes	*Bacillus*	99.5 (953)	*Bacillus pumilus*	100.00 (0)	+	+	+	-	-	-	-	-	-
PP-30	Firmicutes	*Bacillus*	97.6 (535)	*Bacillus toyonensis*	26.00 (0)	-	+	-	-	-	-	-	-	-
PB-091	Proteobacteria (Beta)	*Delftia*	98.3 (1,093)	*Delftia acidovorans*	99.54 (0)	+	+	+	-	-	-	-	+	+
PP-33	Proteobacteria (Beta)	*Dietzia*	99.4 (847)	*Dietzia psychralcaliphila*	100.00 (0)	-	+	-	-	-	-	-	-	-
RC-230	Proteobacteria (Beta)	*Delftia*	100 (1,270)	*Delftia acidovorans*	100.00 (0)	+	+	+	+	-	+	-	+	+
RE-707	Proteobacteria (Beta)	*Delftia*	99.7 (823)	*Delftia acidovorans*	100.00 (0)	+	+	+	+	-	-	-	-	-
PP-21	Proteobacteria (Gamma)	*Pseudomonas*	99.4 (1,397)	*Pseudomonas zhaodongensis*	99.70 (0)	-	+	-	-	-	-	-	-	-
PP-43	Proteobacteria (Gamma)	*Pseudomonas*	96.6 (1,209)	*Pseudomonas zhaodongensis*	99.50 (0)	-	+	+	-	-	-	-	-	+
PB-101	Proteobacteria (Gamma)	*Pseudomonas*	99.5 (1,104)	*Pseudomonas putida*	99.50 (0)	+	+	+	+	-	-	-	+	+
PP-22	Proteobacteria (Gamma)	*Psychrobacter*	98.1 (1,395)	*Psychrobacter aquimaris*	99.86 (0)	-	+	-	-	-	-	-	-	+
RG-453	Proteobacteria (Gamma)	*Stenotrophomonas*	94.5 (911)	*Stenotrophomonas rhizophila*	86.11 (0)	+	+	+	+	-	-	-	+	+

1.3.5. Bacterial cultured from *Hertwigia* and *P. carpenteri* are closely related to previously cultivated hexactinellid SAB

The 16S rRNA sequences for 161 SAB previously described as containing antimicrobial activity were analysed alongside 143 SAB from studies that did not seek to screen for secondary metabolites (Fig. 1-6). In comparing the phylogeny, it was observed that Proteobacteria (54 SAB isolates from 6 studies), Actinobacteria (41 SAB isolates, from 7 studies) and Firmicutes (52 SAB isolates, from 6 studies) are highly represented among previously reported antimicrobial producers. Bacteriodetes had the fewest, only 6 SAB isolates from 2 studies. From the studies selected, demosponges constitute most sponges used in SAB cultivation. This constituted 12 species of sponges, *Haliclona* sp. being the most frequently tested organism. There are 49 SAB cultivated bacteria from hexactinellid sponges with described activity. No single study cultivated from hexactinellids to explore cultivable diversity as was extensively done for demosponges. Of those 49 isolates, there were 20 Proteobacteria, 18 Actinobacteria, 8 Firmicutes, and 3 Bacteriodetes. There were only 4 species of hexactinellid sponges tested.

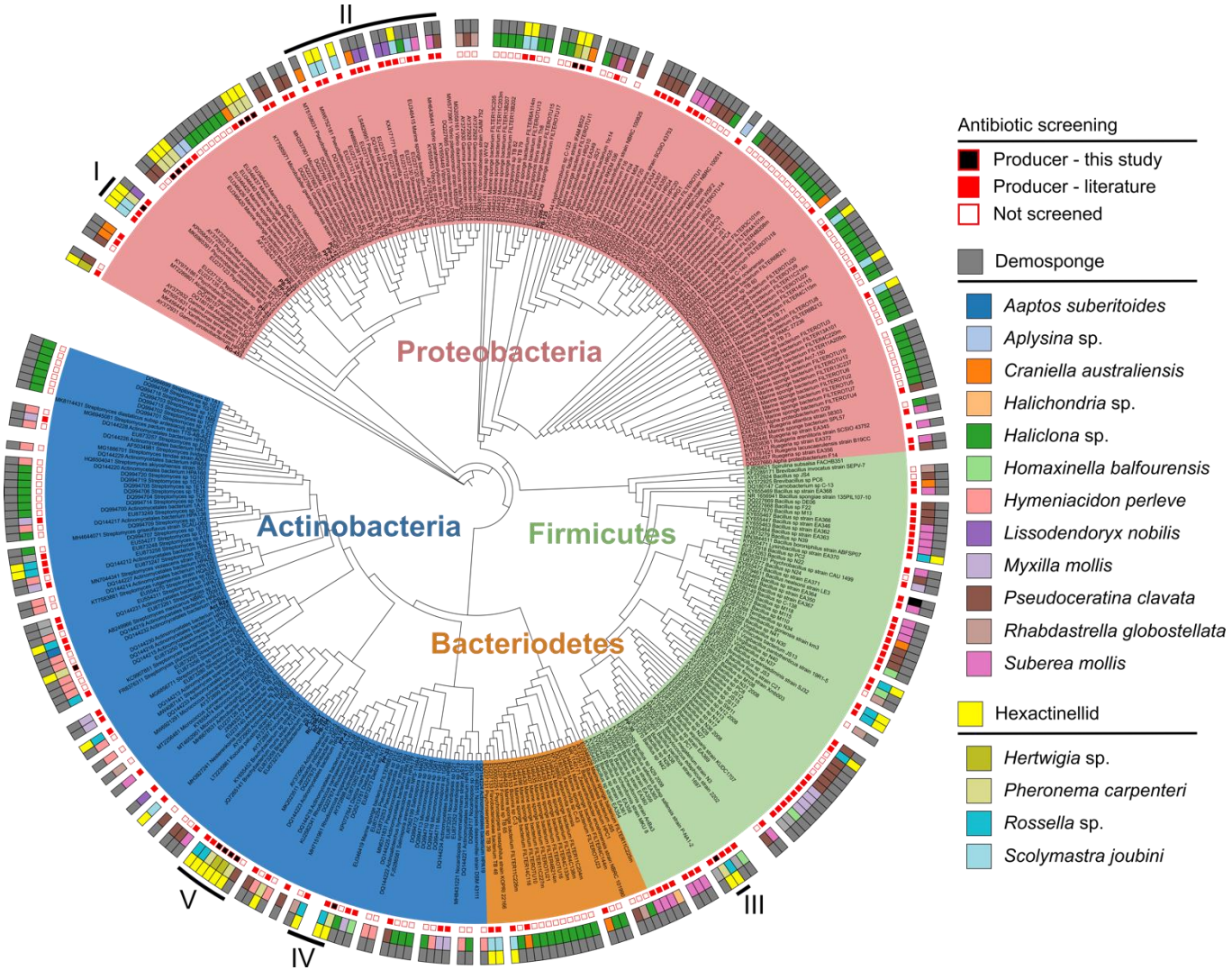

Figure 1-6. Maximum likelihood phylogenetic tree of cultivable SAB showing that antibiotic producers are phylogenetically diverse across all classes and species of sponge. Cultivable sponges presented here include reference organisms, a selection of bacteria cultivated in this study that display antimicrobial activity and from published studies (Lafi, Garson and Fuerst, 2005; Kim and Fuerst, 2006; Jiang *et al.*, 2007; Zhang *et al.*, 2008; Mangano *et al.*, 2009; Sipkema *et al.*, 2011; Xin *et al.*, 2011; Bibi *et al.*, 2020). The inner ring represents whether organisms were screened for antibiotic activity, the middle ring the sponge species from which SAB was cultivated, and the outer ring the class of the sponge. Regions marked I-VI denote regions of interest. Sequence names as part of this study are labelled first with an NCBI accession number and the taxonomic classification and isolate name of the bacterial from the original study. Bacterial isolates from this study are labelled with their unique isolate name in bold (Table 1-2).

Isolates cultivated from both *Hertwigia* (RC-206-Y and RC-201) and *P. carpenteri* (PC-227, PB-104, PP-22, PP-30, PP-33) were closely related to previously cultivated SAB from the hexactinellid sponge *Rossella* sp. from the study conducted by Xin and colleagues (2011) (Fig. 1-6). PP-22 is closely related to *Psychrobacter* sp. TB-40 and TB 55 (I); PP-30 to *Bacillus* sp. N42 (IV); PP-33 with *Dietzia* sp. N11 (V); and PC-227, PB-104, RC-206-Y and RC-201 clustered with *Brevibacterium* sp. and *Brachybacterium* sp (V). A single predominantly hexactinellid-associated bacteria clade is present within Actinobacteria (VI).

Among Proteobacteria, a large clade of metabolically active SAB was found to include organisms closely related to *Pseudoalteronomas* sp., *Shewanella* sp. and *Vibrio* sp. (II). This clade contains bacteria recovered from multiple species of sponges, including both sponge classes. There do appear to be more Firmicutes SAB recovered demonstrating antibacterial activity than those that were not screened. Many of these isolates lack detailed taxonomy and are classified as just *Bacillus* sp. but are placed phylogenetically quite broadly clustering with *Psychrobacillus* sp., *Brevibacillus* sp., and *Virgibacillus* sp.

1.3.6. OSMAC principles identified previously undetected activity

An OSMAC strategy was followed using micro-fermentation combined with bioautography to detect antimicrobial activity, permitting the cultures to be screened on 39 different growth media combinations. Five strains were tested; all were positive in a PCR screen for BGCs, but negative in plate antagonistic assays. Antibacterial activity was observed from all strains but PP-33 (Fig. 1-7). No activity was detected using ISP2, a standard media utilised in Actinomycetes antimicrobial production, or the successful isolation medium R2a. Likewise,

Mannitol was the only carbon sourse with 0% NaCl that did not lead to any antimicrobial metabolite production.

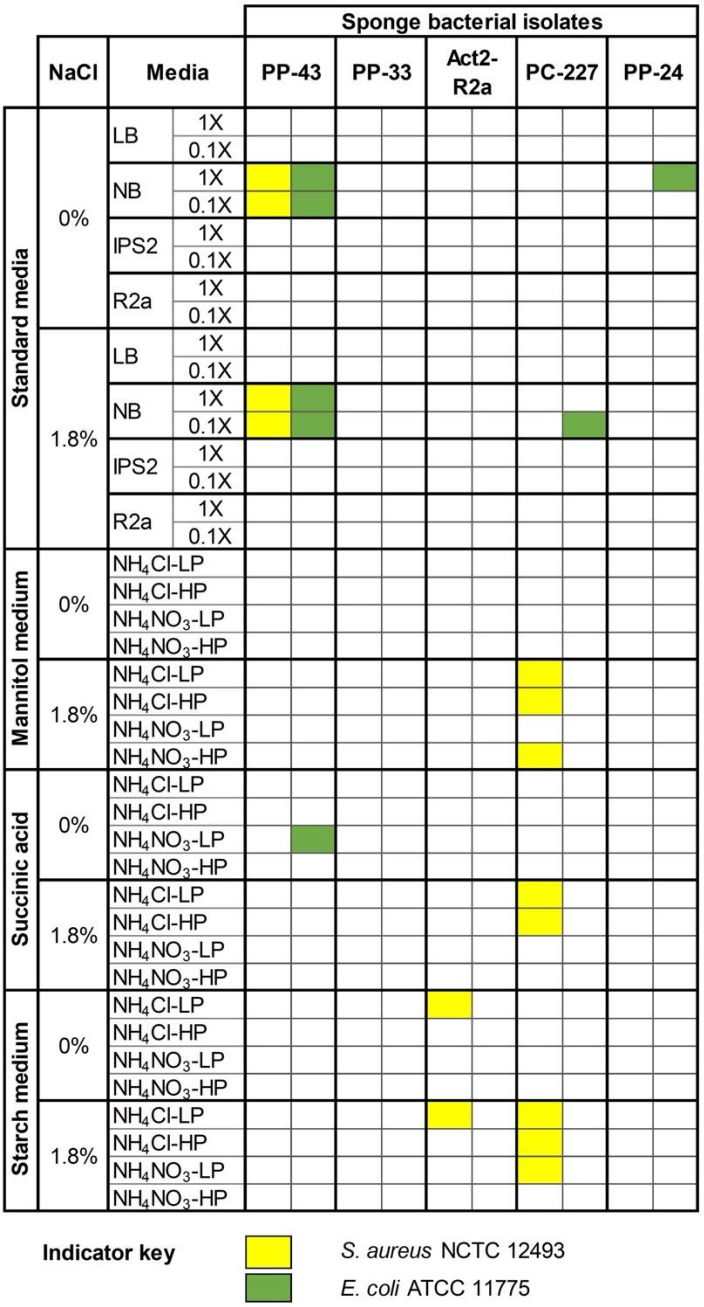

Figure 1-7. An OSMAC approach identified activity in previously non-producing isolates. Indicator strains where activity was detected are indicated in the key, yellow for activity against Methicillin-resistant *S. aureus* NCTC 12493 and green for activity against *E. coli* ATCC 11775. Sponge bacterial isolates were as follows: *Pseudomonas zhaodongensis* PP-43, *Dietzia psychralcaliphila* PP-33, *Streptomycetes fulvissimus* Act2-R2a, *Microbacterium maritypicum* PC-227, and *Bacillus pumilus* PP-24. (LP, low phosphorous 0.1 µM; HP, high phosphorous 5 mM).

Act2-R2a was the only strain to demonstrate Gram-positive-only activity, with the remaining demonstrating activity against both MRSA 12493 and *E. coli* ATCC 11775. PP-43 produced in both 0 and 1.8% NaCl using Nutrient Broth (NB) as the fermentation media, demonstrating activity against both indicator strains. Further activity against *E. coli* was observed from PP-42 grown with succinic acid as the carbon source, with NH_4Cl as the nitrogen source and low phosphorous (0.1 µM KH_2PO_4).

Strain PC-227 antimicrobial activity was observed in 1.8% NaCl. Anti-*E. coli* activity was observed when fermented in 0.1X NB with 1.8% NaCl. Nitrogen source, primarily NH_4Cl, appears to be important in the production of anti-*S. aureus* metabolites. PP-24 demonstrated only anti-*E. coli* activity when incubated in 0.1X NB with 0% NaCl. NB was the only standardised commercial media in which antimicrobial activity was detected, as seen with PC-227 and PP-24.

1.4. Discussion

1.4.1. Sponge identified as *Pheronema* sp. and *Hertwigia* sp.

P. carpenteri forms reefs on fine sediments of the seabed. *P. carpenteri* reefs are proposed to increase the habitat complexity and offer a rigid substrate for colonisation of epifauna (Rice, Thurston and New 1990; Bett and Rice 1992). These reefs are predominantly found in deep waters and have been described at depths between 1,100 – 1,450 m at the Porcupine Seabight (Rice, Thurston and New 1990), Rockall-Hatton Basin (Hughes and Gage 2004), and on the Goban Spur (Duineveld *et al.* 1997; Lavaleye 2002).

The inclusion of *P. carpenteri* into cultivation efforts is benefited by (i) its ecological relevance in soft-bottom deep-sea habitats as a habitat builder; (ii) the availability of this sponge within the North Atlantic region (Howell *et al.* 2016a); (iii) *P. carpenteri* can be confidently identified in-house by morphology and spicule observations alone; and (iv) the availability of prior knowledge, from observational and predictive habitat suitability modelling. With the early observation that *P. carpenteri* individuals generated numerous isolates demonstrating antimicrobial activity, there is further motivation to focus on this species.

Identification of the two *Hertwigia* sponges is less confident due to a lack of current knowledge regarding this genus. *Hertwigia* is a poorly characterised sponge genus, with little reported on the distribution of species or ecological functions. *H. falcifera* is the only accepted species belonging to this genus and it has been identified in the NE Atlantic (Martynov and Litvinova 2008; Ramiro-Sánchez *et al.* 2019) and as a host to crustaceans (Thomas and Watling 2012).

However, in these studies there is little to no description regarding the sponge spicule diversity and the morphological specific features that lead to this taxonomic identification. It was of interest to include a hexactinellid sponge with dense tissue structure, since sponge morphology is an important determining factor to LMA/HMA dichotomy (Gloeckner *et al.* 2014). This may be true for *Hertwigia*, as a greater number of bacteria were recovered from the *Hertwigia* sponges but fewer were bioactive.

Only small subsamples GRNL_81 and 82 were recovered from the larger organisms during sampling with the ROV. As a result, it was not possible to sample the spicule diversity across the whole sponge body. The lack of spicule diversity and sponge morphology only lead to provisional identification. Specimens from this study lacked the distinct yellow colouration of those previously reported, though owing to the limited knowledge of this species, it is not understood if this phenotypic feature removes it from the genus.

1.4.2. No effect observed from incubation temperature, but a significant effect from increased atmospheric pressure on the recovery of bacteria

To assess the effect of incubation temperature and duration on isolate recovery, two ‘low’ and ‘high’ incubation temperatures were utilised. There was no significant temperature effect observed in bacterial cultivation, except for the lowest temperature tested. Incubation temperatures of 15 and 28°C generated the most abundant numbers of isolates for *Hertwigia* sp. and *P. carpenteri* sponges, respectively, but this was not significant. Only a 4°C incubation temperature negatively affected the proportion of bioactive isolates cultivated, and the remaining temperatures all performed similarly.

That 4°C did not yield any promising bioactive isolates was interesting given that the *in situ* temperature for these sponges is approximately 4-5°C. Psychrophilic bacteria bioactivity is frequently described from low temperature environments isolated by low temperature and long incubation periods (4-15°C and >30 days incubation) (Ogata *et al.* 1971; Javani *et al.* 2015; Rafiq *et al.* 2019), but this was not the case for *P. carpenteri* and *Hertwigia* sp. sponges. One factor that might contribute to this is the time between sponge recovery and commencing cultivation. Transportation from cruise ship to institute might act as a pre-selection for microbes that are more tolerant to temperature changes. Furthermore, many psychrophilic bacteria only produce antimicrobial compound at low incubation temperature, which was not attempted in this study.

R2a was the most commonly used commercially available media in the cultivation efforts in this study. The success of R2a is well reported as recovering phylogenetically diverse SAB displaying antimicrobial metabolism (Graça *et al.* 2013; Matobole *et al.* 2017; Liu *et al.* 2019; Bibi *et al.* 2020). The addition of SSE was very successful for recovering isolates with high bioactivity. Supplementation with spicules was previously effective in recovering isolates from *Haliclona* (*gellius*) sp. (Sipkema *et al.* 2011), but these isolates were not screened for bioactivity, so comparisons cannot be drawn.

The most significant effect was noted between the two sponge species, with this study showing that more cultivable and morphologically diverse bacterial isolates can be recovered from *Hertwigia* sp. sponges than *P. carpenteri.* The opposite was observed during screening, with a majority of active isolates cultivated from *P. carpenteri* samples. One sponge species outperforming

another in culture-based investigations has been reported regarding the abundance of bioactive bacteria cultivated, where cultivation from shallow-water *Haliclona* sp. resulted in the most Actinobacteria isolates recovered, as compared to other investigated Demosponges (*Callyspongia* sp. and *Desmacella* sp.) and the Calcarea sponge *Leucaltis* sp. (Liu et al., 2019).

Alternatively, sampling location may impact on the recovery of bacterial phyla with antimicrobial activity. Specific bioactive genera or phyla may dominate the sponges from certain geographical locations. This was noted in a SAB antibiotic screening investigation, which the authors observed that 95% of their bioactive organisms derived from sponges from a single sampling site out of the two tested in South Australia (Anteneh *et al.* 2021). Sponges belonging to the same genera were samples from both sites. With that in mind, it may not be the sponges themselves, but where they were sampled from, this could be related to the fact that hexactinellid sponges are thought to have a holobiome more similar to the local seawater (Steinert *et al.* 2020). Accurate taxonomic, geographical location and bathymetric depth of marine organisms used in bioprospecting could help answer these questions (Leal *et al.* 2016).

The existence of a sponge-specific microbiota is a growing concept within the field, and that this would extend to a holobiont with diverse and easily accessible natural products is not unlikely. The highest observed proportion of bioactive isolates from a single sponge was JC136_134 at 33.7%. This does seem unusually high, likely inflated by the number replicated organisms isolated. However, previous cultivation work from the marine sponge *Erylus discophorus* reported that 31% of cultured SAB produced antimicrobial metabolites (Graça *et al.* 2013) and 41% from *Haliclona* sp. (Anteneh *et al.*

2021). Graça and colleagues did not describe any dereplication, while Anteneh and colleagues (2021) did (morphology and Gram-staining) but this did not include sequencing every single isolate for the 16S rRNA gene, so there could still be an inflated representation of bioactive organisms.

1.4.3. *Actinobacteria* and *Proteobacteria* isolates with multiple BGCs were recovered from culture-based studies

The majority of strains that demonstrated antibacterial activity, or were positive for the amplified genes during PCR of the BGCs, belonged to Actinobacteria and Proteobacteria. Members of the following genera have previously been cultured from sponge samples and demonstrated antimicrobial activity: *Dietzia* (Xin *et al.* 2011), *Psychrobacter* (Mangano *et al.* 2008), and *Microbacterium* (Graça *et al.* 2013; Liu *et al.* 2019). Bioactive strains of *Brevundimonas* sp. and *Delftia* sp. have not previously been reported from sponge samples. One *Delftia acidovorans* strain PB091, identified from culture-based efforts as active against both MRSA and *E. coli*, is investigated further in Chapter 4 of this thesis.

Actinobacteria and Proteobacteria being the abundance organism displaying activity is not a surprising result. Actinobacteria a belonging to the order *Actinomycetales* are responsible for more than 70% of antibiotics approved for clinical use (Newman, Cragg and Snader 2003; Newman and Cragg 2012; Seipke 2015; Qin *et al.* 2017), in particular members of *Streptomycetes* spp. in surveys of the abundance and diversity of specialised metabolites of bacterial genomes illustrate the incredibly potential *Streptomycetes* spp. (Seipke 2015) (Gavrillidou et al 2021; pre-print). Success has been seen with marine Actinomycetes with 80% of novel antibiotics stemming from members of the phyla, which are frequently found associated and cultivable with marine

sponges (Bull and Stach 2007; Laport, Santos and Muricy 2009; Xin *et al.* 2011; Abdelmohsen, Bayer and Hentschel 2014). Actinobacteria represent a small fraction of previously reported sponge microbiomes, while Proteobacteria are present in high relative abundances (Steinert *et al.* 2020). Despite this low relative abundance of Actinobacteria within the microbiota, they are highly prevalent in reported cultivation efforts of marine sponges (Xin *et al.* 2011; Xu *et al.* 2018; Williams *et al.* 2020). While not as historically prolific producers of antibiotics, Proteobacteria are abundant members of the marine sponge microbiomes regardless of their abundance states (Steinert *et al.* 2020), and likewise are valuable sources of marine derived antimicrobial peptides (Desriac *et al.* 2013).

Among the isolated strains from this study are reported producers, including *P. putida* (Marinho *et al.* 2009). Multiple *S. fulvissimus* strains were isolated from a freshwater sponge *Antho dichotoma* and reported to contain multiple BGCs in their whole-genome as detected by antiSMASH (Guerrero-Garzón *et al.* 2020), while culture supernatant demonstrated activity against *E. coli* K12 and *Bacillus subtilis* 188.

P. zhaodongensis has not, to our knowledge, previously been cultivated from sponges. A *P. zhaodongensis* strain SST2 was recovered from the South Shetland Trench at 5,194 m deep on R2a agar supplemented with a fungicide, and the strain demonstrated activity against *Acinetobacter baumanii* (Abdel-Mageed *et al.* 2020). Analysis of the draft genome of SST2 supports the presence of multiple BGCs as detected by antiSMASH. Strain PP-22 only tested positive in PCR screens and not in antagonistic assays, and would

benefit from closer attention to access potential metabolites and an OSMAC approach in addition to draft genome determination.

Strain PP-24, identified as *B. pumilus*, displayed activitiy in the OSMAC screen against only *E. coli.* Distinguishing *B. pumilus* from other species (i.e. *B. safensis, B. stratosphericus, B. altitundinis* and *B. aerophilus*) is difficult by 16S rRNA gene sequencing alone (Guinebretière *et al.* 2013; Liu *et al.* 2013), and *Bacillus* sp. identification should be taken cautiously without the investigation of house-keeping genes. *B. pumilus* strains have been isolated from various marine environments: deep-sea corals (Liu *et al.* 2013), marine sponges (Zhang, Zhang and Li 2009), and sediments (Nithya, Devi and Karutha Pandian 2011). Activity has been seen, such as anti-biofilm activity (Zhang, Zhang and Li 2009), and lipoamides with antimicrobial activity against pathogens and *C. albicans* (Berrue *et al.* 2009).

PCR amplification screening yielded potential producers that were initially not identified using phenotypic methods, highlighting the potentially missed novel activity from utilising a plate-based bioassay alone. This could be resolved by introducing additional stages of screening before deciding to discard inactive bacteria. This can be done by PCR amplification or genome sequencing, but this drives up screening costs. For the approach taken in this study for PCR amplification, the the concentration of DNA was now standardised across all the samples, which may have impacted on the amplification and thus should be taken into consideration in the interpretation of the results. Competition assays are a low-cost option and have been used successfully with marine bacteria from sponges (Mangano *et al.* 2008; Riyanti *et al.* 2020), in which SAB from one sponge is challenged against all other SAB from the same sponge. Bacterial

isolates that inhibit the most strains, the ‘best competitor’, are carried onto to be screened against the best inhibitor from different sponge samples. This approach might be worthwhile carrying out with isolates that initially test as inactive in the preliminary screening stages.

1.4.4. Bacterial cultured from *Hertwigia* and *P. carpenteri* are closely related to previously cultivated hexactinellid SAB

While the bacterial isolates recovered from this study are phylogenetically diverse, compared to existing cultivable SAB, many are similar to those that have previously been reported from the shallow water Antarctic sponges *Rossella* sp. (Xin *et al.* 2011). This adds support to the presence of a distinct hexactinellid cultivable clade proposed from cultivation (Xin *et al.* 2011) and further supported by 16S rRNA gene amplicon surveys (Steinert *et al.* 2020). More cultivation efforts need to occur on multiple species of hexactinellid sponges to confirm these early observations.

Observing that many recovered bacteria with activity belong to the phyla Actinobacteria, culturing strategies more targeted towards Actinobacteria recovery would be beneficial when intending to cultivate bioactive bacteria from *P. carpenteri* and *Hertwigia* sp. This could include heat treatment used to select endospore-forming isolates (Matobole *et al.* 2017). Actinobacteria are historically regarded as prolific producers and frequently the focus of studies intending to screen SAB cultures (Jiang *et al.* 2007; Hameş-Kocabaş *et al.* 2012; Pham *et al.* 2016).

However, in the phylogenetic analysis of previously cultured SAB with and without detected antibacterial activity, it does become apparent that across the three phyla there is an abundance of cultivable SAB with antimicrobial activity.

Proteobacteria and Firmicutes were also heavily present among the bioactive isolates across the literature, which could be overlooked in an Actinobacteria-only focused culturing strategy. Bias towards both spore-forming Firmicutes and Actinobacteria should be expected since spores easily survive sampling, storage and transport, in addition to growing on various standardised media. It can be challenging to compare the phylogenetic diversity of cultivable SAB since media, sponge species, and cultivation conditions will affect the isolates recovered (Sipkema *et al.* 2011).

It is important to iterate that many of the organisms reported in the phylogenetic analysis of cultivable SAB were not screened due to the research goals of the publications. Furthermore, the publications that did screen for antibiotic production did not identify by 16S rRNA sequencing the bacterial isolates that tested negative in screening efforts. The same approach was made in this investigation, accounting for the majority of organisms cultured. There could be valuable undetected antibiotic production or novel taxa among those unidentified and initially bioactivity negative bacterial isolates.

1.4.5. *OSMAC strategy identified previously undetected activity*

An OSMAC strategy permitted the detection of antimicrobial activity that was exhibited by bacterial isolates that were not active during the antagonistic bioassays. A PCR screen aided the selection of strains for the OSMAC matrix for the non-active isolates from pressure cultivation since none demonstrated activity in the plate-based assay. Antimicrobial activity was detected from strains such as PC-227 and PP-43, demonstrating active metabolites under a range of conditions that were active against MRSA and *E. coli*.

The OSMAC strategy employed in this investigation did not extend to physical parameters, such as temperature (Darabpour *et al.* 2012) or the effect of orbital shaking (Geng and Belas 2010; Mitra, Gachhui and Mukherjee 2015), both of which are well-reported inducers of antibiotic metabolism. This may induce antimicrobial metabolite production for PP-33 which did not display any activity during this screen. Using a combination of micro-fermentation and bioautography, the method presented here permits the scalability of an OSMAC approach, and adding more conditions to test the range of activity of selected strains could be implemented.

The OSMAC approach here would have benefitted from quantifying the dry mass of the culture supernatents after freeze dryed. This would have permitted for the content of substance tested at the bioautography step to be normalised and gauged the possibility that activity was not observed due to insufficient concentrations of active substrance. Futher improvements could have occurred to the overall pipeline by including an OSMAC strategy during the screening steps, performed on a larger number of active isoaltes to identify the most promising candidate for futher investigation.

1.5. Conclusion

Here, the first investigation involving two Hexactinellid deep-sea sponges *P. carpenteri* and *Hertwigia* sp. is presented. This culture-based survey has demonstrated that fewer bacterial isolates can be recovered from *Pheronema* sponges than *Hertwigia*, but more *P. carpenteri* SAB demonstrate antimicrobial activity. Future work looking at hexactinellid sponge should explore the *Pheronema* genus for NP discovery. However, this does not indicate that none of the isolates from *Hertwigia* sp. could have activity. OSMAC efforts and

amplification of BGCs demonstrated that isolates that do not initially demonstrate any activity in the primary screen could, under the right conditions, begin producing.

Furthermore, we indicate that an Actinobacteria focused culture-strategy for marine sponges might not benefit broader screening goals. The phylogenetic diversity of SAB antibiotic producers spans Actinobacteria, Proteobacteria and Firmicutes. Finally, various promising strains have been recovered from both *Pheronema* and *Hertwigia* sponges, including several bacterial isolates that have not previously been reported from marine sponges.

Chapter 2. An exploration of the bacterial community composition of two deep-sea *Pheronema carpenteri* sponge aggregations from the North Atlantic

2.1. Introduction

Sponge aggregations are recognised in shallow-water ecosystems for their habitat-building properties and nutrient cycling. These aggregations are regarded as large clusterings of *Pheronema* sponges that form reefs. In the deep-sea, the relatively limited ecological and biological knowledge would suggest the same (Ross and Howell 2013; Howell *et al.* 2016a). The conservation of various deep-sea sponge aggregations has been regarded as a priority by various international bodies (ICES 2016).

Sponges belonging to the class Hexactinellida, are predominantly found and abundant in the mesopelagic at depths greater than 200 m (Leys, Mackie and Reiswig 2007). Hexactinellida have largely been underrepresented in studies focusing on the sponge microbiota. It was even stated that microorganisms are rarely seen in glass sponges (Leys, Mackie and Reiswig 2007). However, there is now evidence to suggest that the general patterns observed in Demosponge microbial compositions, especially those relevant to Low/High Microbial Abundance dichotomy (LMA/HMA), also apply to Hexactinellida (Steinert et al., 2020).

The majority of our knowledge of Hexactinellida at a microbial level currently derives from a culture-based investigation of Rossellid sponges (Xin *et al.* 2011) and *Anoxycalyx joubini* (Mangano *et al.* 2008); 16S rRNA gene amplicon surveys of *Aphrocallistes beatrix* microbiota (Thomas *et al.* 2016), and multiple Hexactinellids belonging to the families of *Euplectellidae*, *Leucopsacidae, Rossellidae* and *Aphrocallistidae* (Steinert *et al.* 2020); and finally metagenome-guided microbial reconstruction of dominant lineages of *Lophophysema eversa* (Tian *et al.* 2016) and *Vazella pourtalesii* bacteria (Bayer *et al.* 2020).

Here, the bacterial community of *Pheronema carpenteri* (*class* Hexactinellida, *family* Pheronematidae) was investigated. *P. carpenteri* aggregations are listed as Vulnerable Marine Ecosystems (VME) (ICES 2016), acting as influential habitat builders with possible functions in biogeochemical cycling (Howell *et al.* 2016a). Nothing has been published to date on its microbiota, and the findings in Chapter 2 indicate that *P. carpenteri* is a promising organism for the cultivation and screening of natural products. Nevertheless, cultivation approaches can only capture a small fraction of the present diversity, and there is further interest in identifying biosynthetic gene clusters present in the *P. carpenteri* bacterial community.

In this study the microbiome of *P. carpenteri* is investigated. Specifically, this chapter aims to test for (i) differences in the microbial community of sponges and that of the neighbouring sediment and water column, and (ii) between site and within site differences in sponge microbiota. Finally, (iii) the functions of associated microbial members are investigated by identified genes using a nitrogen cycling databases.

2.2. Materials and Methods

2.2.1. Collection of sponges and environmental samples

The sponges were collected in August 2019 from the Porcupine Seabight, North Atlantic as part of the Sensitive Ecosystem Assessment and ROV Exploration of Reef (SeaRovers) 2019 research cruise on board the RV Celtic Explorer (Fig. 2-1). Using the remotely operated vehicle (ROV) Holland I, sponges were collected alongside *in situ* sediment and water samples at depths of 1,103 and 1,208 m from east and west sides of the seabight (Table 2-1). At site T7 and T52, *Pheronema carpenteri* sponges (N=3), sediment (N=3), and 1.5 L of seawater were collected using Niskin bottles attached to the ROV.

On surfacing, water samples were filtered through sterile 0.22 µm filter discs. Sediment samples were transferred to sterile falcon tubes. Sponges were rinsed with filter sterilised seawater and placed in sterile zip-lock bags. All samples were stored initially on the ship at -20°C. On return to Galway, sponges were transferred to the University of Galway, and temporarily stored at -80°C before being transported to the University of Plymouth on dry ice and stored on arrival in -80°C freezers.

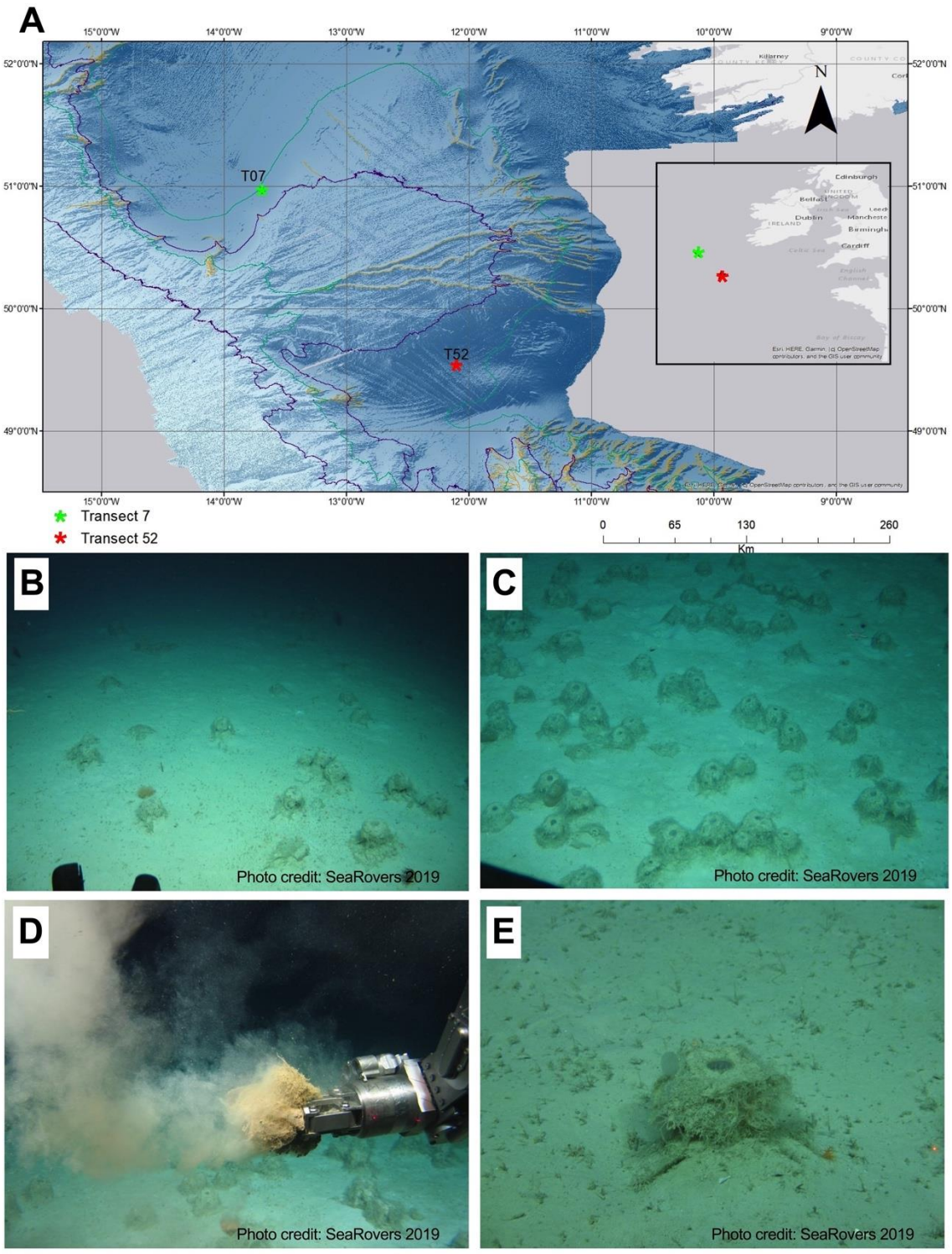

Figure 2-1. Sampling from *Pheronema* sponge grounds. (A) Map of locations in the North-East Atlantic where *P. carpenteri* sponge samples were recovered for microbiome analysis. The map was generated using ArcGIS. *Pheronema* sponge ground from site (B) T07 and (C) T52. (D) *Pheronema* sponge are collected by ROV. (E) *Pheronema carpenteri*. Photos are credited to the Marine Institute of Ireland, Galway and taken on the SeaRovers 2019 cruise.

Table 2-1. Summary of samples, sampling sites and depths, and the number of biological replicates of water volume. (N, the number of replicas taken).

Sample type	Transect site	Unique Sample IDs	N	Latitude	Longitude	Sampling depth (m)
P. carpenteri	T07	Sponge 27 Sponge 28 Sponge 29	3	-13.69	50.96	1,102-1,104
Sediment	T07	Sediment 27 Sediment 28 Sediment 29	3	-13.69	50.96	1,102-1,104
Seawater	T07	Seawater T07	1.5 L	-13.69	50.96	1,102
P. carpenteri	T52	Sponge 09 Sponge 10 Sponge 11	3	-12.11	49.53	1,207-1,209
Sediment	T52	Sediment 09 Sediment 10 Sediment 11	3	-12.11	49.53	1,207-1,209
Seawater	T52	Seawater T52	1.5 L	-12.11	49.53	1,208

2.2.2. Metagenomic DNA extraction

Using a sterile scalpel and working in a laminar flow hood, the sponge's outer dermal layer was removed before cutting into the mesohyl tissue. Cuttings of tissue (0.5 and 0.25 g/ wet weight) were taken from the sponge body. All DNA extractions were carried out using the DNeasy® Powersoil® Kit (Qiagen) as described by the manufacturers. Two masses of sponge tissue were tested (0.5 and 0.25 g of wet sponge tissue) at the bead-beating step. A mass of 0.25 g yielded higher dsDNA concentrations than 0.5 g. A mass of 0.5 g appeared to overload the tube enough to reduce the final DNA yield. All extractions were conducted in triplicate (n = 3 to n = 9) and pooled to account for low DNA yields. Water filters containing seawater filtrate were cut up using sterile forceps into quarters, with each quarter being cut up further and placed into an individual bead-beating tube, final DNA yield was pooled into a single sample. For sediments, 0.25 g of sediment was extracted as instructed by the manufacturers. Prior to selection of DNeasy PowerSoil kit for extraction,

additional methods as described by Simister, Schmitt and Taylor (2011) were attempted. This included a CTAB method with grinding up sponges under liquid nitrogen or over freeze-thaw cycles. They were ultimately utilised due to the persistent low yieldsand high fragmentation of dsDNA from *Pheronema* sponges.

2.2.2.1. *Quantification and quality control of DNA*

DNA purity, concentration, and fragment lengths were determined by various methods. NanoDrop™ 2000 Spectrophotometer (ThermoFisher Scientific) was used for preliminary indication of DNA concentration and purity. Qubit assay (ThermoFisher Scientific) to quantify double-stranded DNA (dsDNA) concentration. Fragment lengths and suitability of DNA for long-read sequencing by Oxford Nanopore technology were determined using Bioanalyzer High Sensitivity DNA Analysis (Agilent Technologies) chips following the manufacturer's instructions. DNA samples with a median fragment length of at least ca. 3 kbp were used in library preparation and sequencing.

2.2.3. 16S rRNA gene amplicon sequencing

The Oxford Nanopore Technologies (ONT) 16S Barcoding Kit (SQK-RAB204) was used following the manufacturer’s instructions with a modification to the number of cycles at the PCR amplification stage. Amplification was carried out using a Veriti 96 Well Thermal Cycler (Applied Biosystems, UK). Clean-up stages were carried out using AMPure XP (Beckman Coulter, UK) magnetic DNA beads and new 75% Molecular Biology Grade Ethanol (Fisher Scientific, UK) prepared on the day.

When amplifying the samples following the ONT protocol, 25 cycles did not generate sufficient amplification so the programme was modified and cycles

increased to 30. This increased amplicon yield as evident by a bright and more visible band when visualised on a 1.5% (w/v) Agarose gel (Fig. S2-1A), which given the low concentration of dsDNA for some samples and the expectation of *P. carpenteri* having low abundance bacteria community, it was deemed practical to have this adjustment. For all samples, 10 ng of HMW dsDNA was amplified using barcoded 16S rRNA primers (27F and 1492R) (Heuer *et al.* 1997; Frank *et al.* 2008). PCR amplification cycle was modified to 30 cycles and was carried out as follows: initial denaturation 1 min at 95°C, 30 cycles (20 secs at 95°C, 30 secs at 55°C and 2 min at 65°C), and a final extension of 5 min at 65°C. To confirm the amplification and library size, finished library 1 (L1) was analysed on the Agilent BioAnalyser, indicating a fragment size of approximately 1,400 bp (Fig. S2-1B).

Each individual amplicon was cleaned using AMPX Pure beads, and resuspended in 10 µl of buffer (10 µl of 10 mM Tris-HCl pH 8.0 with 50 mM NaCl) and quantified by Qubit. Samples were pooled into libraries with a final concentration of 100 ng. The rapid 1D sequencing adaptors were ligated onto the amplicons in the sequencing library, and incubated at room temperature for 5 minutes.

2.2.4. Metagenome sequencing of *Pheronema* sp. CE19-15-029

MinION Ligation Sequencing Kit requires a starting concentration of 21 ng/ µl HMW dsDNA. Due to low DNA metagenomic yield from sponge samples, the DNA was pre-amplified using Ready-to-go™ GenomiPhi™ V3 DNA Amplification Kit (25-6601-24, GE Healthcare Bio-Science, Pittsburgh, PA, USA) as previously described (Brown *et al.* 2017). GenomiPhi™ amplification following the manufacturer's instructions only increased DNA concentration

from 4.70 ng/ µl to 6.10 ng/ µl. In a second reaction, the amplification time at 30°C was increased from 1.5 to 2 h; this resulted in a greater amplification yield to 28 ng/ µl.

The ONT Ligation Sequencing Kit (SQK-LSK110) was then used to construct the sequencing library following the manufacturer's instructions. In summary, first the metagenomic DNA was end repaired and prepped by ligating a dA-tailing Module to the ends of dsDNA strands using the NEBNext® Companion Module for Oxford Nanopore Technologies® Ligation Sequencing (cat # E7180S, New England Bioscience, USA). Secondly, the sequencing adaptors were ligated onto the ends, before finally cleaning up the product and assembling the sequencing library.

2.2.5. Flow-cell set-up sequencing

Brand new R9 flowcells (FLOWMIN-106) were acquired from ONT and fitted into the MinION™ MkIb for quality control. Only flow cells with a minimum of 1,400 active pores were used. An R9 flowcell was removed from storage (4°C) and left equilibrate to room temperature for 15 minutes before use. One millilitre of fresh flowcell priming mix was made (EXP-FLP002; 30 µl flush tether and 970 µl flush buffer). Each flowcell was carefully primed with 800 µl of running buffer through the priming port and left to equilibrate for a minimum of 5 minutes at room temperature. With the SpotON port open, the remaining 200 µl was carefully loaded. The sequencing library was prepared with 11 µl DNA library (≥100 ng for 16S amplicon sequencing and 250 ng for metagenome sequencing), 4.5 µl nuclease-free water, 25.5 µl loading beads, and 34 µl sequencing buffer. The run was performed with a 75 µl DNA sequencing library loaded into the flowcell through the SpotON port. A standard 48 h sequencing

protocol was set using MinKNOWN on a Dell desktop (32 GB RAM, Intel® Core™ i5-7500 CPU, 3.40 GHz), with live base-calling enabled and generating fast5 and fastq files.

2.2.6. Data processing

Bioinformatics analysis was conducted using the Cloud Infrastructure for Microbial Bioinformatics (CLIMB) (Connor *et al.* 2016) on an 18 BioLinux 8 running Ubuntu version 16.04. Various Linux/Ubuntu software was used, and R packages (summarised in Table 2-2). Sequencing was performed using MinKNOWN, generating fast5 files. In some instances, live-base calling was not possible so, after the run, fast5 files were base-called using Guppy v. 3.4.5 (ONT; https://nanoporetech.com). Base-calling and read quality were assessed by NanoPlot (De Coster et al., 2018). Various databases were used in the analysis (summarised in Table S2-1).

Table 2-2. Software and webtools utilised in analysis.

Software	Version	Reference/ GitHub
Clinker	0.0.16	https://github.com/gamcil/clinker
DIAMOND	0.9.24	(Buchfink, Xie and Huson 2014)
Guppy (Oxford Nanopore Technology)	3.4.5	https://nanoporetech.com/
iTOL	5.7	https://itol.embl.de/
Kraken2	2.0.7-beta	(Wood and Salzberg 2014)
meta QUality ASsessment Tool (metaQuast)	4.6.3	(Gurevich *et al.* 2013; Mikheenko *et al.* 2016; Mikheenko, Saveliev and Gurevich 2016)
metaFlye	2.8	(Kolmogorov *et al.* 2019, 2020)
MinKNOWN (Oxford Nanopore Technology)	4.1.22	https://nanoporetech.com/
NanoPack (i.e. NanoFilt, NanoPlot)	1.13.0	(De Coster *et al.* 2018)
phyloseq (R package)	1.1.2.2	(McMurdie and Holmes 2013)
Porechop	0.2.3	https://github.com/rrwick/Porechop
Poretools	0.3	(Loman and Quinlan 2014)
Prodigal	2.6.3	(Hyatt *et al.* 2010)
SeqKit	0.15.0	(Shen *et al.* 2016)
Trimmomatic	0.39	(Bolger, Lohse and Usadel 2014)
Vegan: Community Ecology Package (R package)	2.5-6	(Oksanen *et al.* 2019)
VSEARCH	2.14.2	(Rognes *et al.* 2016)

2.2.6.1. *Bacterial community composition based on 16S rRNA gene amplicon sequencing data*

Demultiplexing was performed by using Porechop, with a quality threshold set at 8 based on the results from NanoPlot. Barcodes and adaptors were trimmed using Porechop. After trimming, reads were filtered and cropped to 1,400 bp using Trimmomatic. A minimum quality score of q =8 was set and read filtered using NanoFilt, as previously described (Heikema *et al.* 2020). Reads were dereplicated and chimeras detected using VSEARCH. Reads were classified by Kraken2 using the SILVA 16S rRNA v. 138 database (Quast *et al.* 2013; Yilmaz *et al.* 2014). Kraken2 classifications were exported with R package Pavian, with general summary tables of Operational Taxonomic Unit (OTU) counts and taxonomy. Taxonomy and representative sequence files were imported into *R studio* and used as an input for the package Phyloseq. Phyloseq was used for

beta and alpha diversity analysis, and generating community composition figures.

2.2.6.2. *Bacterial community composition and functional gene analysis of metagenomic sequencing data*

The assembler metaFlye is designed and intended to be used with raw NanoPore reads; thus, no quality filtering took place. Only contigs greater than 500 bp were used for subsequent analysis; this was filtered using seqkit tools. Quality of contigs was assessed using metaQuast. Open reading frames (ORF) were predicted using Prodigal with the metagenomic parameter (*-p meta*). Taxonomic classification of contigs was predicted by Kraken2 using a pre-built database of RefSeq complete or representative genomes. Both taxonomically classified and unclassified contigs were used for further analysis.

Putative genes from biosynthetic gene clusters (BGCs) were identified and compiled through comprehensive BLASTp searches (E-value ≥ $1x10^{-5}$) (Buchfink, Xie and Huson 2014) against the MiBIG database (Kautsar *et al.* 2020). A reciprocal BLASTp search of identified sequences against a database of Sponge 29 metagenomic proteins and MiBIG database was carried out to identify Reciprocal Best Hits (RBP). RBP were used to classify sequences before phylogenetic analysis.

Functional annotation of key enzymes was conducted by annotating ORFs with four curated databases (Table S2-1) using DIAMOND for a BLASTp algorithm. Homologous sequences were identified when the BLASTp search fulfilled the minimum parameters of E-value ≤ 10^{-5}, and a bit-score > 50 (Pearson 2013).

2.2.6.3. *Statistical Analysis*

Two-Way ANOVA and pairwise comparison of the relative abundance of taxa between sampling sites were performed using GraphPad Prism v. 9.0.1 for Windows (GraphPad Software, San Diego, California USA, www.graphpad.com). Graphical outputs were generated using either GraphPad Prism or R-studio. Final adjustments to figures were made in some cases using Inkscape v. 1.0.

2.3. Results

2.3.1. DNA extraction

Extracting sufficient DNA from *P. carpenteri* mesohyl tissue was a challenge. Between 1.5 and 2.5 g of wet weight, sponge tissue was homogenised in 0.25 g units to yield on average 1072.5 ng dsDNA per g of wet sponge tissue or between 1.15 and 48.8 ng/ µl (Table S2-2). In quantifying DNA, it was found that NanoDrop spectrophotometry overestimated the concentrations in all cases. Bioanalyser fragment analysis showed that for most samples, the protocol generated between 3 and 6 Kbp length fragments (Fig. S2-1B), which was suitable for the 16S rRNA metabarcoding protocol but not the ideal high molecular weight DNA for metagenome sequencing. Extracting similar dsDNA from water-filters proved to be the most problematic, the samples being the most fragmented and having the lowest dsDNA abundances (Fig. S2-2).

2.3.2. 16S rRNA gene amplicon survey

2.3.2.1. *Library preparation, sequencing, and raw read processing*

Fourteen nanograms of dsDNA from nine samples were pooled to construct Library 1 (L1) (Table S2-3). In the case of the remaining five DNA samples (Sponges 09, 10, and 29 and seawater T07 and T52), amplification did not generate sufficient amplicons for library construction. For those samples with low yield, separate amplifications were conducted and pooled with the first to make Library 2 (L2). This yielded less than 8 ng for each sample and still did not meet the minimum dsDNA concentration for library construction, so they were amplified twice with the same amplification programme; first with 27F and 1492R primers (Heuer *et al.* 1997; Frank *et al.* 2008), and a second time with

ONT barcoded 16S rRNA primers provided in the kit. This achieved a maximum of 13 ng dsDNA, and amplicons were pooled into the third library (L3) and sequenced (Table S2-3).

Approximately 5.6 million reads were generated from sequencing. In total, 2.4 million reads remained (42%) after de-multiplexing and chimera removal, filtering reads based on size (> 1,400 bp), and a quality threshold (Q > 8). Kraken2 classification identified across all samples 3,571 OTUs, of which there were 85 distinct phyla and 2,626 genera (Table 2-3). Sediment samples had the highest number of OTUs, followed by *P. carpenteri* and then seawater. The number of OTUs identified are impacted by the number of reads generated from the sequencing and should be taken cautiously especially with respect to the seawater samples which generated the fewest reads. Futhermore, only having three biological replicas from two sampling sites is a small sample size for this sort of investigation.

Table 2-3. Summary of the number of OTUs generated at phyla and genus level.

Sample		Number of OTUs	Number of distinct:	
			Phyla	Genera
P. carpenteri	T07	885	32	655
	T52	1,897	57	1,449
Sediment	T07	3,195	83	2,335
	T52	2,994	80	2,170
Seawater	T07	84	12	62
	T52	435	22	328

Rarefication of OTU counts shows good sampling depths for sediment samples and T52 sponges (Fig. S2-3A, pg 281). Weak sampling depth was achieved for seawater samples and T07 sponges (Fig. S2-3A). Sediment samples had the greatest abundance of taxonomically classified reads, followed by the sponge samples and seawater samples with the lowest, particularly the T52 seawater

sample (Fig. S2-3B). Between the two sampling sites, sponges from T52 had greater OTU diversity and read abundance.

2.3.2.2. *The prokaryotic composition of Pheronema aggregations differed based on the sampling site*

The *P. carpenteri* bacterial community is represented by a high abundance in Proteobacteria (Alpha- and Gamma-), Actinobacteria, and Planctomycetes (Fig. 2-2). Members of the rare phyla (below 0.1% relative abundance) were: Firmicutes, Nitrospirota, Gemmatimodoat, and Spirochaeota (Fig. 2-2). Greater overall diversity was seen in the sediment than the sponges, with sediment samples being relatively uniform between the two transect sites concerning diversity, evenness and abundance of reads (Fig S2-3B). This was not the case for sponge samples, where the two sampling sites saw differences. Sponges from T52 generated the greater mean read abundance, community evenness and diversity (Fig S2-3D).

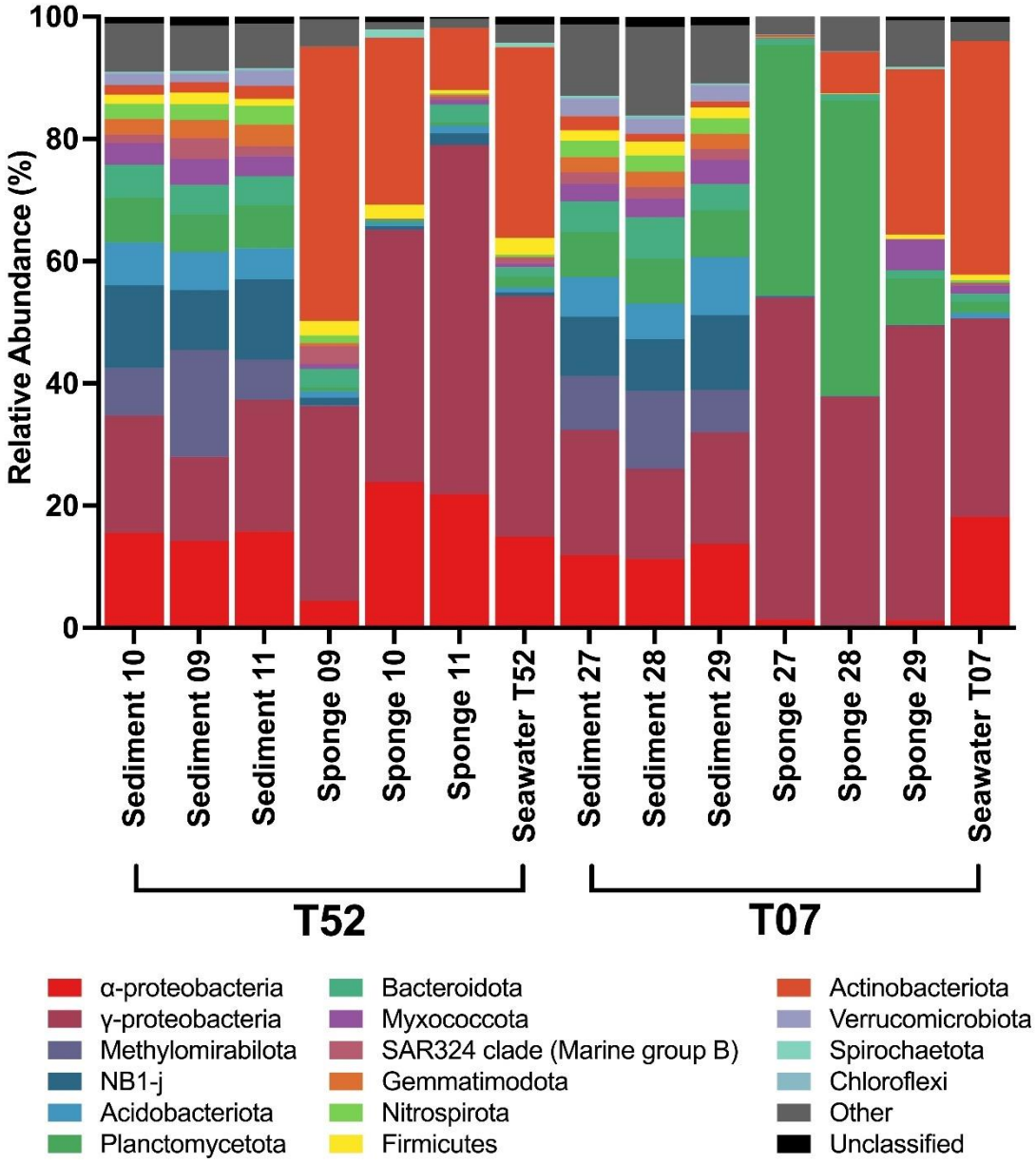

Figure 2-2. The relative proportions of the most abundant bacterial phyla in *P. carpenteri* aggregations, sediment, and water samples from sites T07 and T52. Only the most abundant taxa are shown, with phyla below 0.1% among the samples compiled into 'Other.' Proteobacteria is split into classes (α, Alphaproteobacteria; and γ, Gammaproteobacteria).

Sediment samples were broadly uniform across both sites. Proteobacteria, Methylomirobilota, NB1-j, and Acidobacteriota were the most abundant phyla in these samples. Seawater samples had higher abundance of Proteobacteria and Actinobacteria and shared a greater resemblance to sponge samples than the sediment did. The differences between the bacterial compositions in sponge

individuals was explored (Fig. 2-3). Major differences between sites were seen in the mean relative abundance of Alphaproteobacteria (T07, mean = 0.948 ± 0.67%; and T57, mean = 16.71 ± 10.7%; p = 0.038), Actinobacteria (T07, mean = 11.37 ± 13.97%; and T57, mean = 27.45 ± 17.36%; p = 0.032), and Planctomycetes (T07, mean = 32.29 ± 21.68%, and T57 mean = 0.53 ± 0.15%; p <0.0001), as calculated by a two-way ANOVA (Fig. 2-3B; Table S2-4).

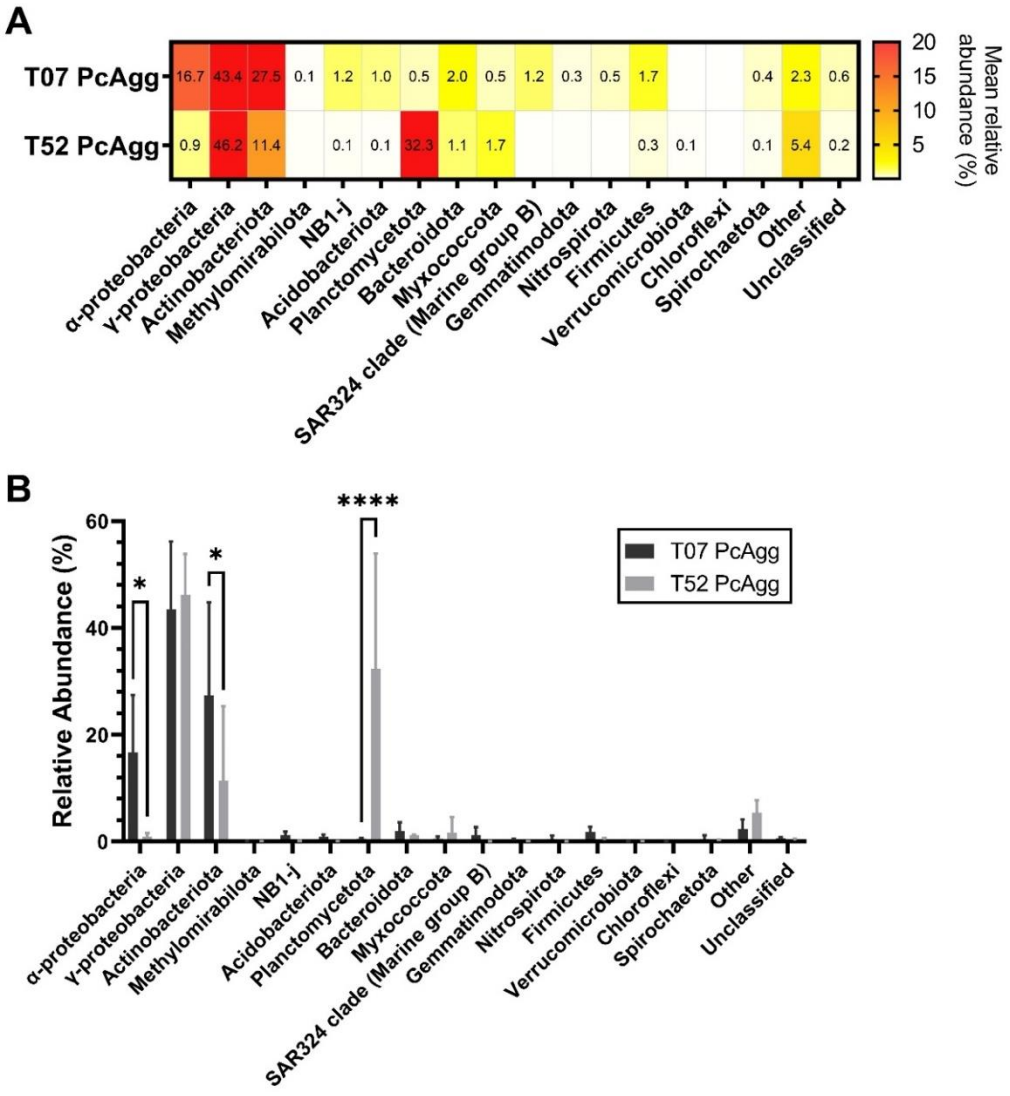

Figure 2-3. Detailed comparison of the prokaryotic composition shows Planctomycetes, Actinobacteria, and Alphaproteobacteria relative abundances are significantly different between T07 and T52 *P. carpenteri* (PcAgg). (A) Mean relative abundance at phyla level, mean relative abundances > 0.1% are shown. (B) Comparing the relative abundances between two *P. carpenteri*, data are shown as mean ± SD (N = 3). (Significant p values from a pairwise comparison are shown in figure: ∗, p < 0.05; ∗∗∗∗, p < 0.0001).

Sediment samples were not found to differ based on the sampling site, as observed with beta diversity calculations (Fig. S2-4C-D, Table S2-5 pg 283-4). The only difference was observed in the collective phylum grouping of 'Other' (T07, mean = 11.59 ± 2.50%; and T52, mean = 7.53 ± 0.35%; p = 0.029) (Fig. S3A-B). The same analysis could not be conducted with the seawater samples due to a lack of sequencing replicas.

2.3.2.3. *Variations in taxa observed between individuals from the same* P. carpenteri

In addition to differences observed between *P. carpenteri*, there were notable differences between the biological replicas from the same *P. carpenteri*. This was noted when comparing the relative read abundances between samples of the same *P. carpenteri* (Fig. 2-3). Ternary plots were used to examine bacterial phyla distribution between the *P. carpenteri* individuals of the same sampling site (Fig. 2-4A). As indicated, specific taxa were nearly exclusive to a single sponge individual from each site, such as Myxococcota and Spirochaete, for Sponge 10 (T52) and Sponge 29 (T07). Proteobacteria were evenly distributed at T07 but less so at T52. Patescibacteria, Actinobacteria, and Bacteriodetes were unevenly distributed at both sampling sites.

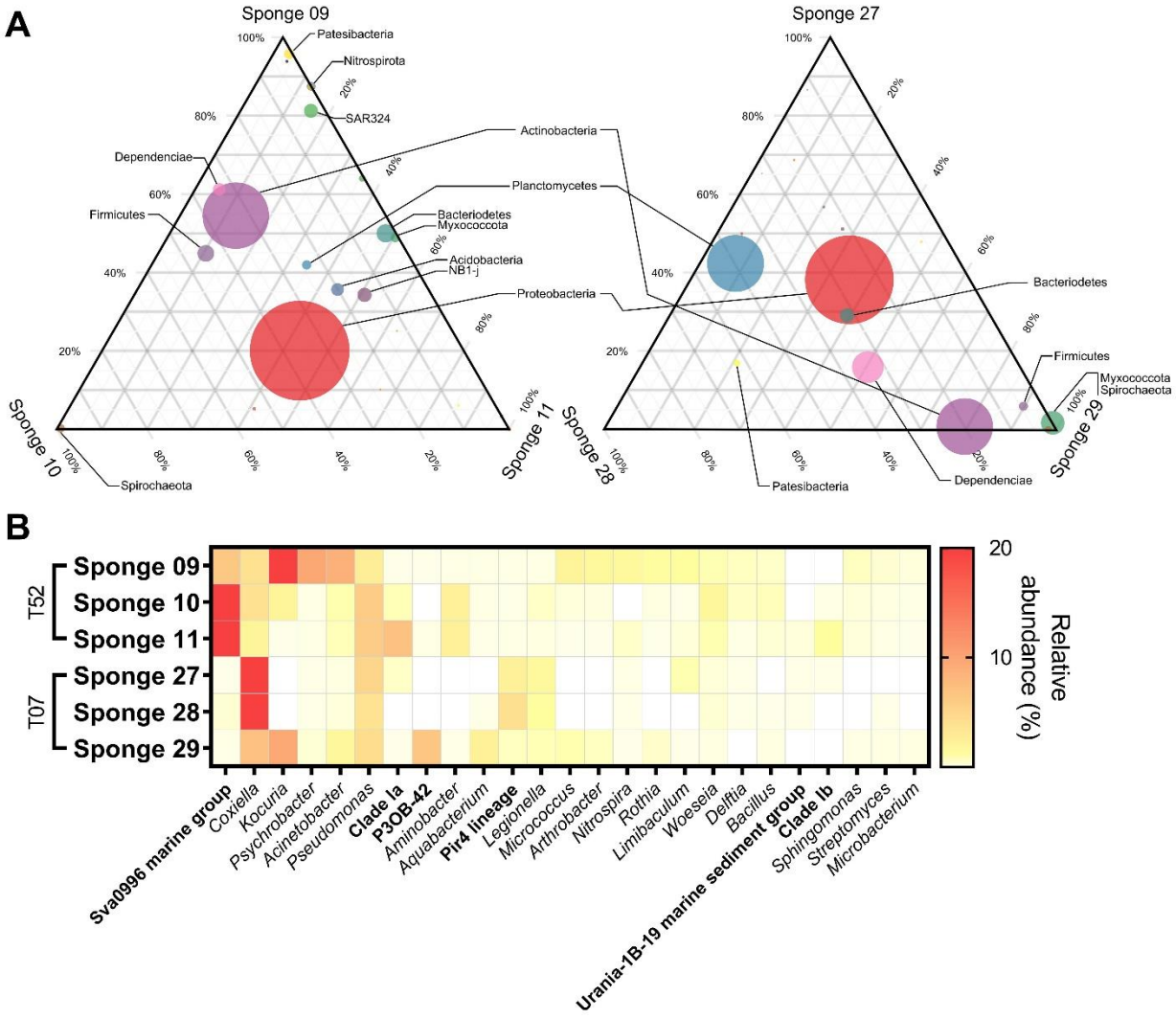

Figure 2-4. Distribution of bacterial taxa between sponge individuals. (A) Ternary plot of the most abundant bacterial phyla. The left ternary plot is for T52 samples, and the right is T07 samples, and circle size indicates the relative abundance of each phylum. (B) Heatmap of relative abundance of genus-level taxa between sponge samples.

At the genus level, *Kocuria, Coxiella, Pseudomonas*, *Woeseia*, and Pir4 lineage were present in all individuals. T52 sponges were rich in Sva0996 marine group bacteria, which were present at lower relative abundances in T07 *P. carpenteri* sponges (Fig. 2-4B). *Aquabacterium* and *Pir4 lineage* abundances were uniform for T07 sponges but not for T52. Lack of uniformity between biological replicas of the same aggregation can be seen in various taxa. Greater overall differences in the taxa were observed from T07 sponges as compared to T52 sponges, which were far more uniform. *Aquabacterium*, *Kocuria*, *Micrococcus*, *Arthrobacteri*, *Rothia,* Clade Ib, *Sphingomonas,* and *Microbacterium* were all present in a single sponge sample from T07. In contrast, the Urania-1B-19 marine sediment group was the only taxa unique to a single sponge sample (Sponge 11) from T52.

2.3.2.4. P. carpenteri *samples share more taxa with seawater samples than sediment*

More significant dissimilarity was seen between sediment samples and the seawater and sponge samples measured by Bray-Curtis Dissimilarity clustering (Fig. 2-5C). UniFrac weighted component analysis shows a clustering of Sponge T52 individuals with both seawater samples (Fig. 2-5B) while also showing a tight clustering of sediment samples from T07 and T52.

Ternary plots were used to examine bacterial taxa distribution between the pooled *P. carpenteri*, sediment, and seawater samples (Fig. 2-5D). As shown in the ternary plot, Proteobacteria, Actinobacteria, Dependentiae, Firmicutes, and Spirochaetota, which make up the most abundant taxa in the *P. carpenteri* sponge samples, were evenly distributed between sponge and seawater. The

remaining taxa were far more abundant in sediment samples. Planctomycetes and *SAR324 Marine Clade* were evenly distributed between all sample types (i.e. sediment, sponge and water). Rare taxa present in sponges (i.e., Nitrospirota, Nitrospinota, Patescibacteria) were far more common in sediment.

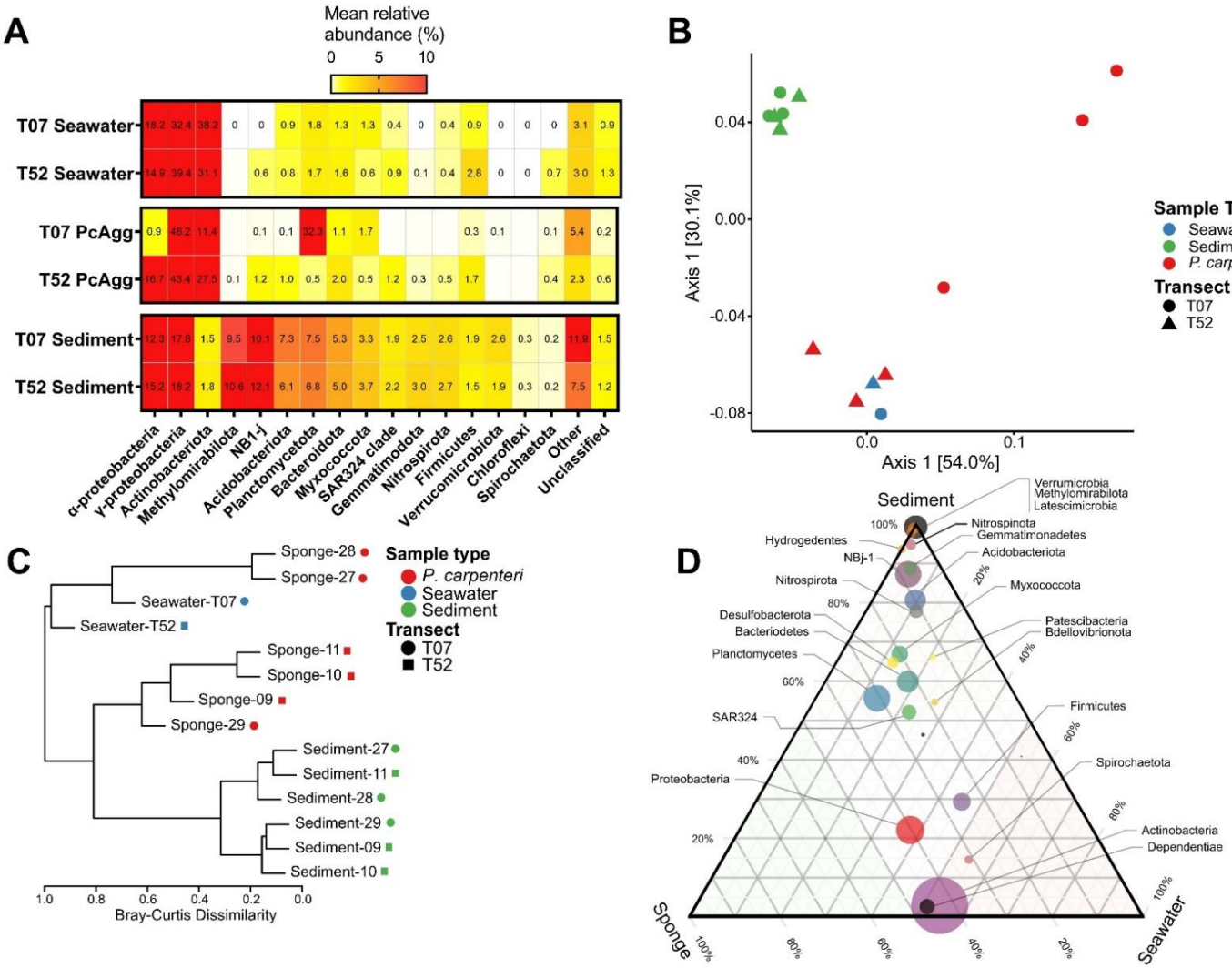

Figure 2-5. Sponge and seawater samples show closer resemblance, while *P. carpenteri* (PcAgg) sampling site and individual taxa are significant factors shaping the bacterial community composition of *P. carpenteri*. Comparison between the relative abundances of (A) all samples at the phylum level and (D) only sponge samples at the genus level. (B) Component analysis using weighted uniFrac distances. (C) Bray-Curtis dissimilarity dendrogram. (D) Ternary plot of pooled samples by biotypes of the most abundant phyla.

2.3.3. Potential functions of microbial members of *P. carpenteri*

2.3.3.1. *Library preparation, sequencing, and raw reads processing*

Sponge 29 was chosen to sequence the metagenome because it had a high enough dsDNA concentration to meet the Ligation Sequencing Kit's required starting material (1 µg of dsDNA). Sponge 29 was sequenced on a 48 h sequence cycle and, using a whole flow cell, generated 232,000 reads. These reads were then cleaned (minimum lengths > 150 bp), from which 3,222 contigs were assembled using metaFlye. The shortest contig was 501 bp and the longest 49 kb (Table S2-6). For evaluating the quality of the assembly, metaQuast was utilised (Fig. S2-5 pg 284), the average GC content of the contigs was 48.86%, and the N50 = 9,106 bp.

2.3.3.2. *Taxonomy of classified contigs showed differences in overall community composition as compared to the 16S rRNA gene amplicon survey*

Contigs were taxonomically assigned using the database and classified with Kraken2. Only 966 of the 3,227 contigs (30%) could be classified using the RefSeq database, of which 966 contigs were taxonomically identified as containing bacterial genes, 7 viral, 26 fungal, and 19 protozoan. Of the bacterial contigs, 48.4% belonged to Proteobacteria and 14.7% to Firmicutes (Fig. 2-6A).

The relative abundance of classified reads between the metagenome and the 16S rRNA amplicon survey was compared (Fig. 2-6B), however it should be noted that it is not entirely fair to compare the two methods of taxonomic identification, owing to the nature of amplicon sequencing and metagenomic sequencing.. Fewer metagenomic contigs were assigned to the phylum

Gammaproteobacteria (-23.6%), Actinobacteria (-17.7%), Dependentiae (-7.3%), and Myxococcota (-5.1%) than amplicon reads. Conversely, more contigs were assigned to Firmicutes (+13.5%), Alphaproteobacteria (+10.1%), Betaproteobacteria (+9.7%), and Bacteriodetes (+5.6%) (Fig. 2-6B). For the entire phyla of Proteobacteria, the proportion of contigs and reads assigned were similar, 48.4% for the bacterial contigs and 49.8% for the 16S rRNA gene amplicon survey.

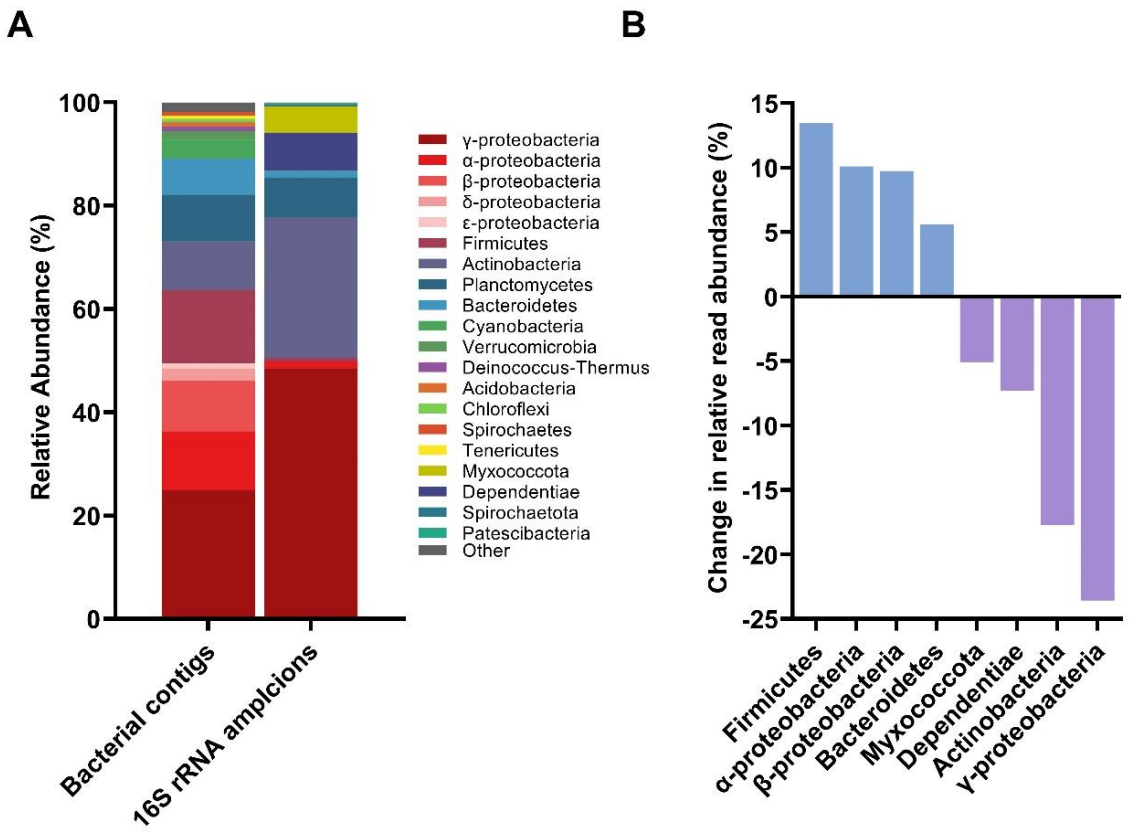

Figure 2-6. Differences were observed in the relative abundance of different taxa between the two sequencing methods. (A) Comparison of the taxonomic assignment of reads generated from the 16S rRNA amplicon gene survey and the metagenome from *Pheronema* sponge 29. (B) Change in abundance of metagenomic reads compared to the 16S amplicon survey data (differences between 5% and -5% were omitted).

2.3.3.3. *Multiple nitrogen cycling protein homologues were present in the* P. carpenteri *29 metagenome*

From the 3,227 contigs, 24,260 protein-coding regions were predicted using Prodigal. Translated amino acid sequences were parsed using BLASTp against both the NaPDoS and NCyc database. There were 21 Best Reciprocal Hits (BRH) against the NaPDoS database (Table S2-7). Against the NaPDoS, the vast majority of BRH were for Fatty Acid Synthesis (FAS) and some Type II PKS. Besides fatty acids, additional predicted products for some of these pipelines were Aclacinomycin, Alnumycin, and spore pigments (Table S2-7). When the contigs were also parsed through the *antiSMASH* v.6 online tools, four clusters were identified: a Type I Polyketide Synthase (T1PKS) region, a Ribosomally synthesised, and post-translationally modified peptide like (RiPP-like) region, and two Arylpolyene regions (Fig. S2-6). Contig_3500 showed 15% similarity to the NRP+T1PKS cluster producing nosperin, related to pederin group members (Kampa et al., 2013). Pederin group members have only been identified from non-photosynthetic bacteria associated with marine sponges and beetles (Robinson *et al.* 2007).

More success was found when parsing the predicted proteins dataset against the NCyc database with 375 BRH identified homologues (Fig. 2-7) (Table S2-8). The majority of BRH were proteins classified under the denitrification pathway, this includes 110 BRH homologues to Nitrite reductase (NO^- forming) (*nir*K). Most of these were identified on contigs which could not be taxonomically classified or were of Proteobacterial origin. A further 64 BRG were Nitrous-oxide reductases (*nos*Z), and 28 BRH were homologues of Nitrite reductases (*nir*S).

Two nitrogen fixation genes were identified; Nitrogenase iron protein NifH (7 BRH) and Nitrogenase-stabilizing/protective protein NifH (6 BRH) (Fig. 2-7).

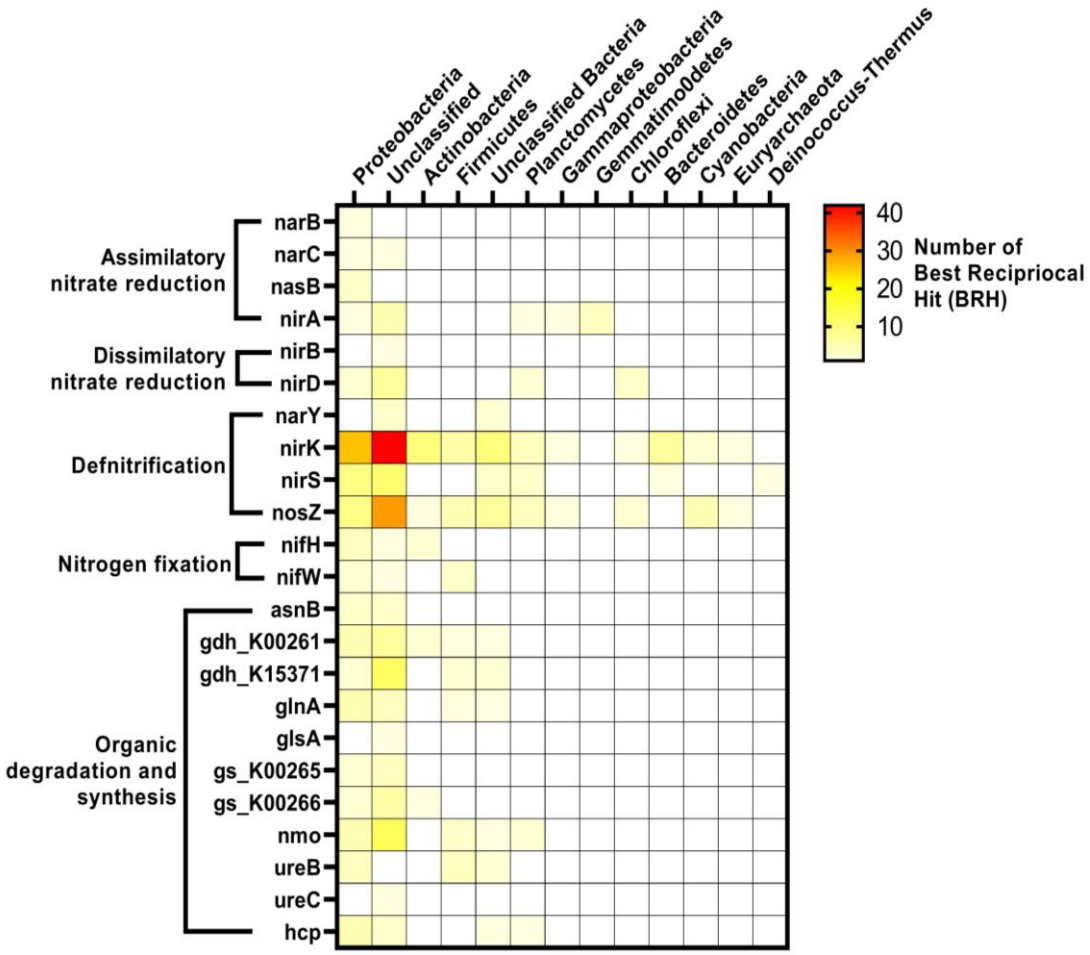

Figure 2-7. Specific functions abundant in *P. carpenteri*-associated bacterial metagenome sequence contigs annotated with COG. The brightness (red) in the heatmap reflects the abundance (number of BRH) of a particular protein in the Sponge 29 metagenome against the NCyc database, white indicates absence. Functional pathways are indicated to the left of the gene name. Full list of COGs identified can be found in Table S2-8.

2.4. Discussion

2.4.1. The microbiome of *P. carpenteri*

P. carpenteri aggregations have been identified across the North East Atlantic at depths of around 1,200 m (Howell *et al.* 2016a; Vieira *et al.* 2020). In the spicule matts of *P. carpenteri* a high diversity of macrofauna can be found (Bett and Rice 1992; Beazley *et al.* 2013), and here we present the first 16S rRNA gene profiling study on the microfauna of *P. carpenteri*. We have identified that *P. carpenteri* has a low diversity of associated bacteria, but the range of phyla observed in this study indicates that *P. carpenteri* has characteristics of both LMA and HMA sponges.

In a seminal piece of work comparing the microbiotas of multiple species of Demosponge and Hexactinellida, Steinert and colleagues (2020) proposed that specific taxa were indicators of LMA and HMA sponges. HMA sponges are enriched in Actinobacteria, Acidobacteria, Chloroflexi, and Poribacteria. Whereas for LMA sponges, it is Proteobacteria, Bacteriodetes, and Planctomycetes. From this investigation, we observed *P. carpenteri* bearing features of HMA and LMA sponges based on microbial diversity. *P. carpenteri* aggregations were enriched in Alphaproteobacteria, Bacteriodetes, and Planctomycetes, all indicative of LMA hexactinellid sponges, but also Actinobacteria, which is indicative of HMA Demosponges sponges.

Beyond this, the Steinert study identified Hexactinellida microbiota as being dominated by Proteobacteria, mainly Alphaproteobacteria and Gammaproteobacteria (Steinert *et al.* 2020). Similar observations were made in our investigation of two *P. carpenteri* aggregations (Fig. 2-3). A low abundance of Chloroflexi, a common taxon observed in sponge microbiomes, was also

characteristic of Hexactinellida (Steinert *et al.* 2020) and in the *P. carpenteri* individuals used in this study. There were some notable differences between our findings and those of Steinert and colleagues (2020), such as the enrichment in Actinobacteria at T07 (Fig. 2-3). Actinobacteria were not so readily abundant in the Hexactinellida sponges but more so in Demosponges (Steinert *et al.* 2020).

2.4.1.1. *The prokaryotic composition of Pheronema aggregations differed based on the sampling site*

One of the sponge species-specific patterns observed previously (Webster *et al.* 2010; Thomas *et al.* 2016), is that different sponge individuals of the same species in the same environment have similar bacterial communities. This is observed to some extent with *P. carpenteri* in the current study. Significant differences in relative abundances of distinct bacterial taxa in *P. carpenteri* from the two sampling sites were observed, notably an enrichment in Planctomycetes in sponges from T52 and Actinobacteria and Alphaproteobacteria in sponges from T07 (Fig. 2-5B). The fact that sponges have species-specific microbiomes is a supported theory from multiple 16S rRNA gene amplicon surveys of a range of marine sponges (Hentschel *et al.* 2003; Thomas *et al.* 2016; Webster and Thomas 2016; Steinert *et al.* 2020), and there is a growing body of evidence to imply differences occur between sponge individuals of the same species (Steinert *et al.* 2020) and sampling sites (Busch *et al.* 2020a).

Differences between sponges of the same species at different sampling sites has been observed between trawled and non-trawled sites (Busch *et al.* 2020a). They report that *Vazella pourtalesii* individuals sampled from fishery-impacted

sites were enriched in Actinobacteria and Planctomycetes instead of individuals from non-trawled sites. We observed the same taxa enrichment, but not from the same *P. carpenteri*, and in the CE2019 cruise report, trawling activity was not reported at either of the sampling sites (O'Sullivan, Healy and Leahy 2019). It would be challenging to connect trawling activities and the observed differences between the *P. carpenteri* in this instance. However, there has been a recent decline in NE Atlantic *P. carpenteri* stocks due to trawling (Vieira *et al.* 2020), so there may be interest in further exploring the impact this may have on the composition of *P. carpenteri* microbiomes.

It has been noted that hexactinellids demonstrated greater variation in bacterial community structure between biological replicas than Demosponges (Steinert *et al.* 2020). That study, like ours, contained at least 3 biological replicas. A more extensive study on 33 individuals of a single species of hexactinellid, *V. pourtalesii,* likewise observed dissimilarity in alpha-diversity between biological replicas from the same sampling site (Busch *et al.* 2020a). We have likewise observed a similar phenomenon at the phyla level (Fig. 2-3B and 2-4A) and even genera (Fig. 2-4B).

In addition to the inter-aggregation differences, intra-aggregation differences were noted, in which sponges from the same aggregation displayed differences in taxonomy. It should be noted that sponges from T07 had less than half the number of OTUs compared to T52 sponges, which can be attributed to the lower proportion of reads sequenced from sponges.

Like the inter-aggregation differences, intra-aggregation or intra-specific differences have been observed. *Petrosia ficiformis*, a shallow-water sponge with a low genetic connectivity, was identified as having microbial communities

less similar across geographic regions (Burgsdorf *et al.* 2014; Díez-Vives *et al.* 2020); within population genetics, this is defined as the transfer of genetic material from one population to another. Later work tested this using geographic location and genetic structure as the parameters, and identified sponges with a low genetic connectivity as having different microbiomes between populations as compared to sponges with a high genetic connectivity (Díez-Vives *et al.* 2020).

Within this thesis, differences were observed in Chapter 1 between technical replicas of the same sponge and the number of colonies recovered. For *P. carpenteri,* the detection of genetic markers such as microsatellites and single nucleotide polymorphisms (SNPs) would need to be performed to begin following this observation. Thus, it may be too early to determine if samples from the same *P. carpenteri* aggregation display entirely different community profiles, and more *P. carpenteri* aggregations should be sampled in future to investigate this further.

2.4.1.2. P. carpenteri *share more taxa with seawater samples than sediment*

P. carpenteri also show closer significant similarity in microbial community composition with seawater samples than the sediment (Fig. 2-2, 2.4); this was observed as a characteristic of hexactinellid microbiota (Steinert *et al.* 2020). *P. carpenteri* individuals are frequently embedded low to the sea-bed and, on sampling, are coated in sediment. This motivated our efforts to remove the derma or outer layer of sponge before extracting mesohyl tissue for DNA extractions and in culturing efforts (Chapter 1). Nevertheless, it would appear that there is little overlap between the sponge and sediment bacterial

compositions, the taxa shared between the two being the rare or low abundance taxa for *P. carpenteri*. Increased sedimentation of the sponge has not been linked with shifts in microbial community profiles for the Great Barrier Reef sponge *Ianthella basta* (Luter, Whalan and Webster 2012) or other shallow-water species (Pineda *et al.* 2017), so it is not surprising to find very little influence of sediment on the *P. carpenteri* associated bacterial composition. It would be interesting to compare inner tissue microbial composition with that out outer tissue layers.

The complications encountered regarding low yields of bacterial 16S rRNA amplicons were unique to most *P. carpenteri* individuals utilised, and did not occur in the sediment samples. Results presented here suggest that future work using ONT MinION be conducted with caution when sequencing low microbial abundance samples. Introducing a second PCR step improved the amplicon yield and made sequencing possible. This methodological change may increase the risk of chimera formation (Sze and Schloss 2019). A combination of a polymerase with a high fidelity and low number of PCR rounds are observed by the authors observed to reduce bias, chimera formation and sequence error. Attempts to control this included the use of a high fidelity polymerase for long-reads (LongAmp Taq 2X Master Mix, NEB), and 30 cycles during PCR. Two rounds of amplification in 16S rRNA gene sequence studies are frequently carried out for Illumina amplicon sequencing projects (Steinert *et al.* 2020). However future work utilising MinION 16S rRNA amplicon sequencing should take caution in this possible source of error and bias.

Low DNA yields are possibly due to the small tissue mass of hexactinellid sponges, given that the majority of their mass composed of the silicon spicules

that make up their skeleton. In addition to the high likelihood that *P. carpenteri* sponges are low microbial abundance sponges, due to the comparatively low microbial diversity and read counts (Fig. S3B-C), as opposed to the sediment samples, will reduce numbers of bacterial cells available for DNA recovery.

2.4.2. Potential functions of microbial members of *P. carpenteri* microbiome

The low number of reads and subsequent contigs generated from this dataset were not enough to make any informed conclusions regarding the presence of BGCs of interest. This dataset revealed a high abundance of possible FAS and Type II PKS genes using the NaPDoS database, none of which aid with any extensive efforts in identifying compounds of interest for NP discovery. More sequencing is needed to facilitate better mining of the *P. carpenteri* metagenome for NPs.

However, this dataset was utilised in identifying multiple protein orthologs using the NCyc database (Tu *et al.* 2019). The microbial mediated cycling of sulphur, phosphorus, carbon, and nitrogen is well reported (see review (Zhang et al., 2019) . For deep-sea species, this is best studied in *G. barretti,* which are reported to conduct microbial nitrification, denitrification and anaerobic ammonium oxidation all occurring within the same sponge (Hoffmann *et al.* 2009). Furthermore, the shallow-water LMA sponge *Dysidea avara* (*class* Demosponge) had notably higher nitrification and denitrification rates than HMA counterparts (Schläppy *et al.* 2010). There is significant interest in better understanding the function of deep-sea sponges in the role of nitrogen cycling.

P. carpenteri contained multiple homologues to the archaeal copper containing nitrate reductase (*nir*K) (Fig. 2-8). AOA are essential players in nutrient cycling, yet little is known regarding NirK in AOA metabolism (Reji *et al.* 2019).

Unfortunately, this study did not focus on archaeal diversity, and as such little can be discussed for the *P. carpenteri* archaeal community. The presence of *nif*H genes encoding nitrogenase, which is a key enzyme for nitrogen fixation, was low (Fig 2-8). If this were to be experimentally verified it could imply a closed nitrogen cycle in *P. carpenteri*. Future work with an interest in exploring nitrogen cycling in deep-sea sponges should expand into the archaeal communities of *P. carpenteri.*

Data presented here suggests future work on microbial nitrogen cycling in *P. carpenteri* should focus on archaeal populations rather than the bacteria. However, due to the limitations of this dataset, bacterial contribution should also not be ruled out until a far more comprehensive metagenome of this sponge species can be produced. Here, we present the first insight into the nitrogen cycling potential of *Pheronema* sponges. A more comprehensive metagenomic investigation coupled with metatranscriptomic studies would provide much-needed data on *P. carpenteri* sponges' ecological functions in the deep-sea and could reveal the biotechnical products these sponges can provide.

2.5. Conclusion

Pheronema carpenteri is an attractive sponge to study for its proposed ecological roles in the deep-sea and, as presented in Chapter 1 of this thesis, a promising species to test for NP discovery. Here, we present the first microbiome of this species of deep-sea sponge and we observe that sponge aggregations can present differences in prokaryotic community profiles, which appear to be driven by a small selection of phyla. We also make the interesting observation that the *P. carpenteri* microbiota contains features thought to represent both HMA and LMA sponges.

A high abundance of Actinobacteria present in *P. carpenteri* 16S rRNA amplicons, in addition to the identification of multiple PKS and NRPS genes, suggests this sponge is a promising candidate for bioprospecting studies. Finally, the observation of a small number of Nitrification and Denitrification genes present in Sponge 29 metagenome suggests that future work should be conducted on *P. carpenteri* and expression analysis could be used to verify this observation.

Chapter 3. *Galleria mellonella* larvae exhibit a weight-dependent lethal median dose when infected with Methicillin-resistant *Staphylococcus aureus*

The entire content of this chapter have been published:

Hesketh-Best, P. J., *et al*. (2021) '*Galleria mellonella* larvae exhibit a weight-dependent lethal median dose when infected with Methicillin-resistant *Staphylococcus aureus'*, *Pathogens and Disease*. Oxford University Press (OUP). doi: 10.1093/femspd/ftab003.

3.1. Introduction

The ability to rapidly test the efficacy of compounds is essential to natural product discovery efforts. *Galleria mellonella* (Greater wax moth) larvae are widely utilised for toxicity screening (Desbois and Coote 2012; Maguire, Duggan and Kavanagh 2016; Coates *et al.* 2019) and to study host-pathogen interactions (Peleg *et al.* 2009; Olsen *et al.* 2011; Junqueira 2012; Wojda and Taszłow 2013). Unlike many insect models, *G. mellonella* can be incubated at 37°C, which facilitates the investigation of human pathogens. This has included most of the ESKAPE pathogens: *Enterococcus faecium* (Chibebe Junior *et al.* 2013; Luther *et al.* 2014); *Staphylococcus aureus* (Brackman *et al.* 2011; Ramarao, Nielsen-Leroux and Lereclus 2012; Sheehan, Dixon and Kavanagh 2019); *Klebsiella pneumoniae* (Wand *et al.* 2013; Diago-Navarro *et al.* 2014); *Acinetobacter baumannii* (Peleg *et al.* 2009); and *Pseudomonas aeruginosa* (Jander, Rahme and Ausubel 2000; Seed and Dennis 2008). Additionally, *Escherichia coli* (Leuko and Raivio 2012; Alghoribi *et al.* 2014; Jønsson *et al.* 2017; Guerrieri *et al.* 2019), *Bulkholderia mallei* (Schell, Lipscomb and DeShazer 2008) and several fungi (Cotter, Doyle and Kavanagh 2000; Reeves *et al.* 2004; Mylonakis *et al.* 2005) have also been studied using *G. mellonella*. Crucially, a positive correlation between the virulence and immune responses between mammalian models and *G. mellonella* has been established for *P. aeruginosa* (Jander, Rahme and Ausubel 2000), *Cryptococcus neoformans* (Mylonakis *et al.* 2005), and *S. aureus* (Sheehan, Dixon and Kavanagh 2019), demonstrating the powerful potential of this invertebrate model.

Antibiotic efficacy at dosages recommended for human use can be tested in *G. mellonella*, in addition to their toxicity correlating with toxicity observed in murine

models (Ignasiak and Maxwell 2017). This has been shown with both natural and synthetic compounds (Gibreel and Upton 2013; Smitten *et al.* 2019), opening up the possibility of a rapid and cheap model for the early stages of discovery and development of natural and synthetic products, without the challenges of ethical approval, specialist training and the difficulties of using mice-models in early-stage drug development. Infections caused by antibiotic-resistant *S. aureus* are of global concern and it is listed as a high priority pathogen for which new antibiotics are urgently needed (The World Health Organisation 2017). Methicillin-resistant *S. aureus* (MRSA) has been utilised with *G. mellonella* for the study of virulence (Mannala *et al.* 2018), pathogenicity (Ebner *et al.* 2016), antimicrobial efficacy of existing antimicrobials (Ba *et al.* 2015; Ferro *et al.* 2016), and for novel candidates (Gibreel and Upton 2013; Jacobs *et al.* 2013; Dong *et al.* 2017) (Table S3-1).

Despite the increased popularity of *G. mellonella*, there is much variability in method application (Andrea, Krogfelt and Jenssen 2019). This includes differences in larval size, storage, infective dose, and injection intervals. In this study, we address larval size and its potential impact in experimental design. In antibiotic efficacy studies, typically the model is infected with a pathogen shortly before the candidate treatment is presented. This has not been standardised with respect to the parameters previously mentioned for *G. mellonella*. In our preliminary experimentation in determining a 50% lethal dose (LD_{50}) for MRSA in *G. mellonella*, it was noted that smaller larvae were more susceptible to infection than larger larvae. This was when using a broad range of larval weights (~200-300 mg), as previously reported (Jacobs *et al.* 2013). Furthermore, the larval weight has been demonstrated to positively correlate with the larval liquid volume, leading to recommendations on how *in vivo*

concentrations of injected compounds and pathogens should be calculated (Andrea, Krogfelt and Jenssen 2019). This led us to hypothesise that the larvae LD_{50} for a pathogen, in our case here MRSA, is directly proportional to the larvae weight and that larvae weight is an essential parameter in experimental design that must be tightly controlled.

When physical and anatomical barriers are breached, the wax moth larvae have an innate immune response relying on germline-encoded factors for the detection and clearance of microbial pathogens (Trevijano-Contador and Zaragoza 2019). There are two branches, cellular and humoral immunity. Cellular immunity is conducted by haemocytes, which are present in an open circulatory system called the haemolymph, which is analogous to vertebrate blood. There are at least six subpopulations of haemocytes which perform similar roles to those of the myeloid lineage in vertebrates (Boman and Hultmark 1987; Lavine and Strand 2002), and they are also associated with digestive system, trachea and fat body (Ratcliffe 1985). Five types of haemocytes were identified in fifth larval instar of *G. mellonella*; prohaemocytes, plasmatocytes, granulocytes, oenocytoids and spherulocytes (Salem *et al.* 2014).The main immune processes include coagulation, phagocytosis and encapsulation (Tojo *et al.* 2000). Circulating haemocyte density increases during pathogenesis due to the release of suspended cells from the fat body (Tojo *et al.* 2000). Haemocyte density and subpopulation variations changes with time of exposure to pathogen and pathogen virulence (Arteaga Blanco *et al.* 2017).

Melanisation additionally occurs in the haemolymph, the process of melanin production resulting in the darkened appearance of the larvae (Tojo *et al.* 2000).

The humoral branch is involved in the production of lytic enzymes (Vogel *et al.* 2011), and antimicrobial peptides (AMPs) that are active against bacterial pathogens (Cytryńska *et al.* 2007; Tsai, Loh and Proft 2016). These molecules are mostly produced by the larval 'fat body', analogous to the mammalian liver, and are released into the haemolymph (Zasloff 2002).

A proteomic investigation has shown *S. aureus* infections lead to an increase in production of proteins such as AMPs and peptidoglycan recognition proteins (Sheehan, Dixon and Kavanagh 2019). Critically, the same study identified similarities between *G. mellonella* and mammal immune response to *S. aureus* infections. What has not been investigated is the physiological change in *G. mellonella* lipid as a result of *S. aureus* infections. For this investigation, we were motivated to quantify the lipid weight, a proxy for the fat body, of the larvae to observe how the fat body might have been affected as a result of MRSA infection.

The aim of the work here is to investigate methodological adjustments which may improve the reproducibility and reliability of using pet-food grade *G. mellonella* as an experimental model. This was achieved by (i) examining the effect of larval weight on the LD_{50} to MRSA infection, and (ii) characterising physiological changes occurring to lipid weight as a result of the larval immune response to MRSA.

3.2. Materials and Methods

3.2.1. Cultivation of MRSA

A single colony of Methicillin-resistant *Staphylococcus aureus* (MRSA) NTCT 12493 was streaked onto fresh Luria broth (LB, Fischer Scientific, UK; Tryptone 10 g/L, yeast extract 5 g/L, and sodium chloride 10 g/L) solidified with 1.5% (w/v) agar (Acros Organics, UK) 24 h before experimentation. Single colonies were suspended in Dulbecco A Phosphate buffered saline (PBS, Oxoid UK) to a range of optical density (OD) read at 600 nm (Eppendorf BioPhotometer, Netherlands). These dilutions were OD_{600} = 0.1 - 1.0 in 0.1 increments. Viable cell counts were made of each dilution.

3.2.2. Determining a weight-based LD_{50} for Galleria mellonella larvae

Larvae were purchased commercially from Livefoods UK Ltd. (Somerset, UK; www.livefoods.co.uk). On receipt, larvae were individually weighed using an accurate scale and grouped into the following weight bands: 180-200, 201-220, 221-240, 241-260, 261-280, and 281-300 mg. Larvae were stored at 4°C for up to 7 days in the dark with no food and water. Healthy larvae were identified by a uniform cream colour, with no indications of melanisation such as spots or markings (Fig. 3-1A) (Li *et al.* 2018a). Larvae were euthanised by chilling them at 4°C for 1 h, before freezing them at -20°C for a minimum of 24 h.

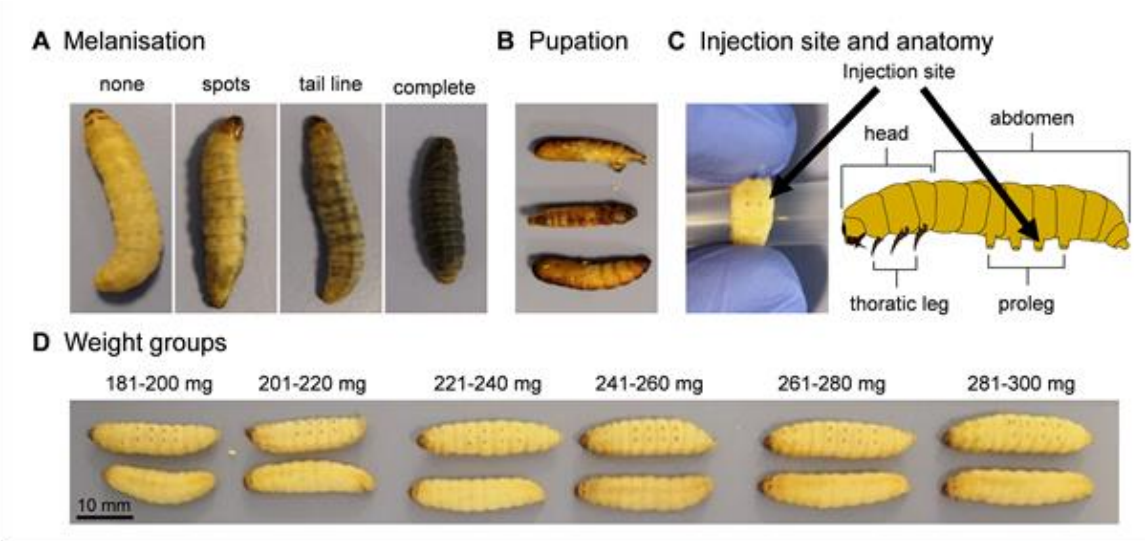

Figure 3-1. Galleria mellonella larvae.(A) Melanisation is a visual indication of the health of the larvae, as larvae progress from none to complete melanisation as a result of stress and/or infection. (B) Larvae pupation. (C) Route of infection for larvae is by intra-haemocoelic injection at the penultimate pro-leg (arrow). (D) Larvae are divided up into six weight groups.

Larvae (n = 10) from each weight band were infected by injecting 10 µl of one of the 10 dilutions of MRSA into the left penultimate pro-leg (Fig. 3-1C), using a 50 µl Hamilton 750 syringe (Hamilton Company, UK) with a removable needle. Injected larvae were placed into Petri dishes lined with tissue paper (KIMTECH, UK). Three independent replicates of this experiment were carried out. Syringes were cleaned before and after each bacterial dilution. Cleaning consisted of taking up and discarding of each wash solution thrice before progressing to the next wash solution. Wash solution order was as follows: distilled H_2O (dH_2O), 70% ethanol, and dH_2O.

After infection, the larvae were maintained at 37°C in the dark without food or water. A placebo control of sterile PBS was used to account for the effect of the physical trauma of injection, along with a non-manipulation (NM) control. After 24 h the live/dead counts were recorded. Larvae were recorded as dead when they met the following: (i) complete melanisation (Fig. 3-1A), (ii) did not respond to touch, and (iii) could not correct itself when rolled onto its back.

Determining the weight-dependent LD_{50}, live/dead counts were converted into percentage mortality at 24 h for each group. For this investigation we have defined LD_{50} as CFU of MRSA per mg of organism resulting in 50% mortality.

To model the dose-response and describe the relationship between increasing the infection dose on survival for each weight group, a non-linear sigmoidal regression curve was plotted. The infection dose, represented as CFU/ mg of total weight of larva, was log-transformed. A non-linear regression curve was calculated to fit best the data generated from three independent replicas. From the equation generated from this curve, the theoretical LD_{50} was calculated along with the standard deviation (SD). Estimated LD_{50} from each weight groups were plotted against the mean larvae weight. A regression line was drawn, and the coefficient of determinant R^2 was calculated.

3.2.3. Correlating larval size with rate of pupation

On the day of receipt, larvae were placed into weight groups in Petri dishes. They were immediately placed at 37°C, in the dark with no food or water and permitted to pupate over 15 days. Larvae were observed daily and pupation events recorded.

3.2.4. Quantifying lipid weight of *G. mellonella*

Following investigation of the LD_{50} for MRSA, the lipid weight for all living and dead larvae was quantified. Live larvae from treatments, the NM and PBS controls were ethically euthanised. Dead larvae were stored at -20°C until needed. Larvae were left to thaw at room temperature for 24 h and were weighed and individually placed in Eppendorf tubes to be dried over 7 days at 55°C, and re-weighed to reveal their dry weight. Larvae were then submerged in ≥99.9% diethyl ether (Sigma-Aldrich, UK) and left for 3 days at 4°C to

dissolve lipid. Diethyl ether was utilised as the lipid extraction solvent (Tzompa-Sosa *et al.* 2014). After, ether was left to evaporate in a fume hood for 24 h. Once dried, larvae were weighed again to acquire the post-ether weight. Quantities are then presented as followed: 'total weight' is the weight of the larvae pre-experimentation; 'water weight' (Equation 3-1); 'lipid weight' (Equation 3-2).

Equation 3-1. Calculating the larval water weight.

$$water\ weight = pre\text{-}experimentation\ weight - dry\ weight$$

Equation 3-2. Calculate the larval lipid weight.

$$lipid\ weight = dry\ weight - post\text{-}ether\ weight.$$

3.2.5. Statistical analysis

All statistical analysis was performed using PRISM GraphPad 8.4.2 (GraphPad Software, San Diego, CA, USA). One-Way ANOVA (two-tailed), Two-Way ANOVA, and Pearson's correlation coefficients were used when applicable to compare treatment groups. Log-rank Mantel-Cox tests compared survival curves for antimicrobial efficacy tests and pupation. A *p*-value of: < 0.05 ($*$), < 0.01 ($**$) or < 0.001 ($***$), < 0.0001 ($****$) was considered to be significantly different.

3.3. Results

3.3.1. Larval weight affects LD_{50}

To begin testing our hypothesis, LD_{50} values were determined for each weight group. A sigmoidal non-linear model best fit the dose-dependent response of the data, resulting in an LD_{50} calculated for each weight group (Fig. 3-2). When adjusted to the number of cells injected into each larvae per one unit of body weight (CFU/mg), the resulting LD_{50} ranged from 1.19 $x10^7$CFU/mg, for the 180-200 mg group, to the highest LD_{50} which was 8.97 $x10^7$ CFU/mg for the 261-280 mg group (Table 1). The LD_{50} increased across weight groups except for the 281-300 mg group, which had a lower LD_{50} than the 261-280 mg weight group. Throughout this experiment, we encountered some difficulties when handling larvae from the two higher weight-bands (261-280 and 281-300 mg), such as high variation in mortality at the lowest infective dosages (0-40% mortality) and highest dosages (60-100% mortality). Nevertheless, we were able to calculate an LD_{50} with the final data.

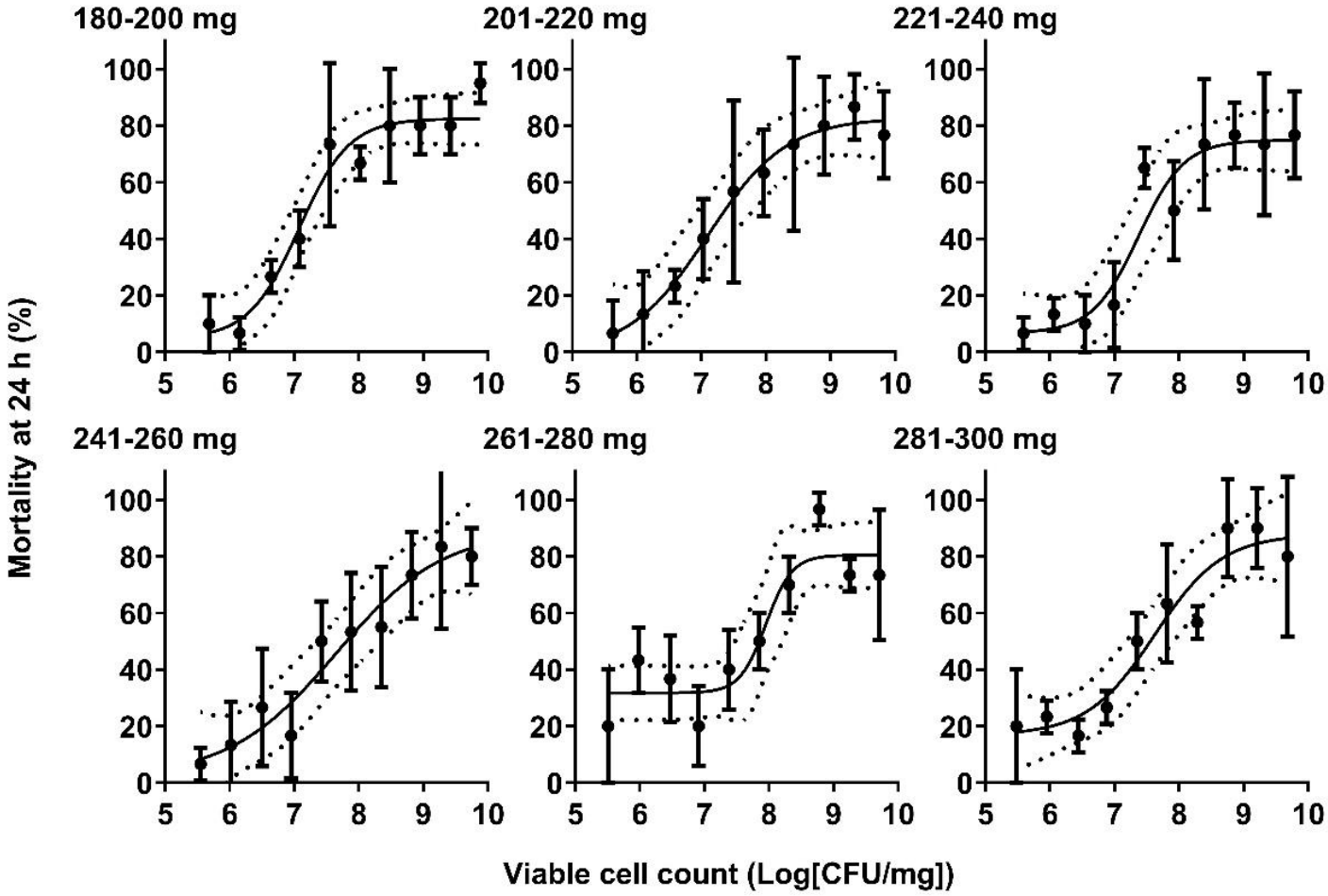

Figure 3-2. Sigmoidal non-linear logistic regressions best fit the dose-dependent response observed when calculating an LD_{50} for MRSA. LD_{50} was calculated for each weight group with 10 larvae/group. Data are shown as mean ± SD (n = 10) of three independent replicas.

Table 3-1. Summary of the LD_{50}s as calculated by non-linear models for each weight group (N, number of replicas; R^2, coefficient of determination).

Weight group (mg)	LD_{50} (CFU/mg)[(a)]	SD (CFU/mg)	N	R^2
180-200	1.19 x10^7	1.47	30	0.85
201-220	1.26 x10^7	2.45	30	0.77
221-240	2.34 x10^7	1.57	30	0.80
241-260	4.40 x10^7	3.35	30	0.76
261-280	8.97 x10^7	1.46	30	0.69
281-300	4.19 x10^7	1.81	30	0.78

We observed a positive correlation between weight of the larvae and LD_{50}, as calculated by Pearson correlation test (r = 0.87, p = 0.025, n = 18). A linear regression model arriving at an equation ($y = 0.007966x + 5.548$) was used to estimate LD_{50} (Fig. 3-3A). The LD_{50} values, as estimated by our model, were tested *in vivo*, demonstrating an approximate 50-56% (± 5.7 – 10%) survival for four of the weight groups (Fig. 3-3B). Survival at 24 h for the weight groups 261-280 and 281-300 mg was 30% (± 0%) and 43% (±15.3%), respectively.

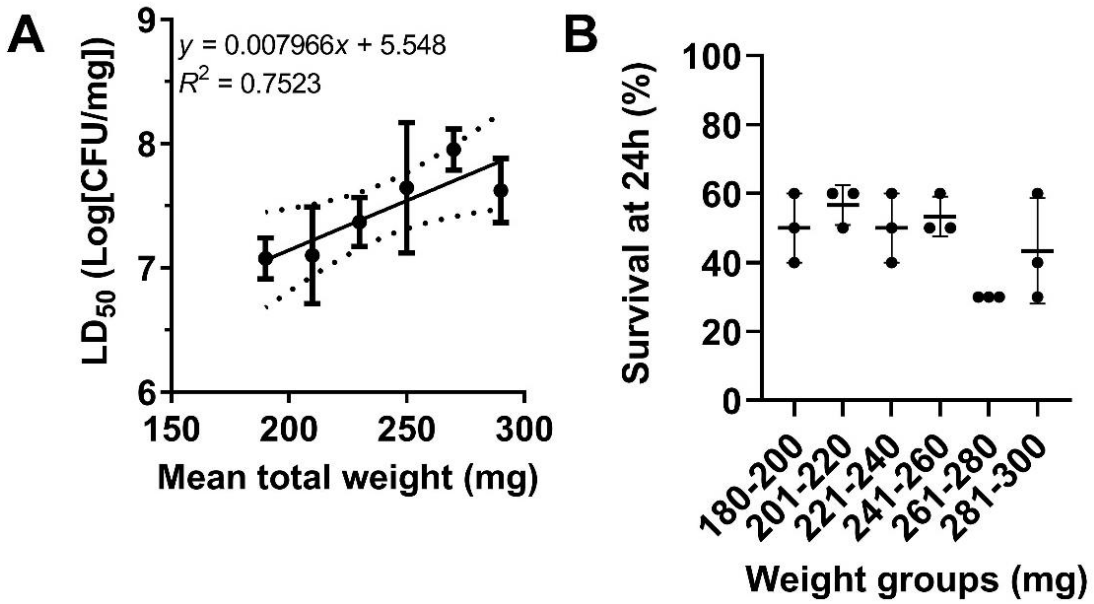

Figure 3-3. LD_{50} as calculated by non-linear regression models positively correlated with weight and was validated *in vivo* for all but the two highest weight groups.(A) Calculated LD50 by non-linear models correlation positively with total weight. (B) LD50 value as calculated by the model was validated by injecting into larvae and observing mortality. Data are shown as mean ± SD (n=10) of three independent replicas.

3.3.2. MRSA infection leads to a reduction in lipid weight

With the NM group, we assessed the overall relationship between total weight, dry weight, and lipid weight and length of the larvae (Fig. 3-4). Determined by Pearson's correlation test, we found a positive correlation between the total and dry weight, ($r = 0.972$, $p < 0.0001$, $n = 83$) (Fig. 3-4A), and total and water weight ($r = 0.989$, $p < 0.0001$, $n = 83$) (Fig. 3-4B). These two results support the findings of previous research (Andrea, Krogfelt and Jenssen 2019). Two additional positive correlations were observed between total weight and lipid ($r = 0.788$, $p < 0.0001$, $n = 83$) (Fig. 3-4C), and total weight and length ($r = 0.9944$, $p < 0.0001$, $n = 252$) (Fig. 3-4D).

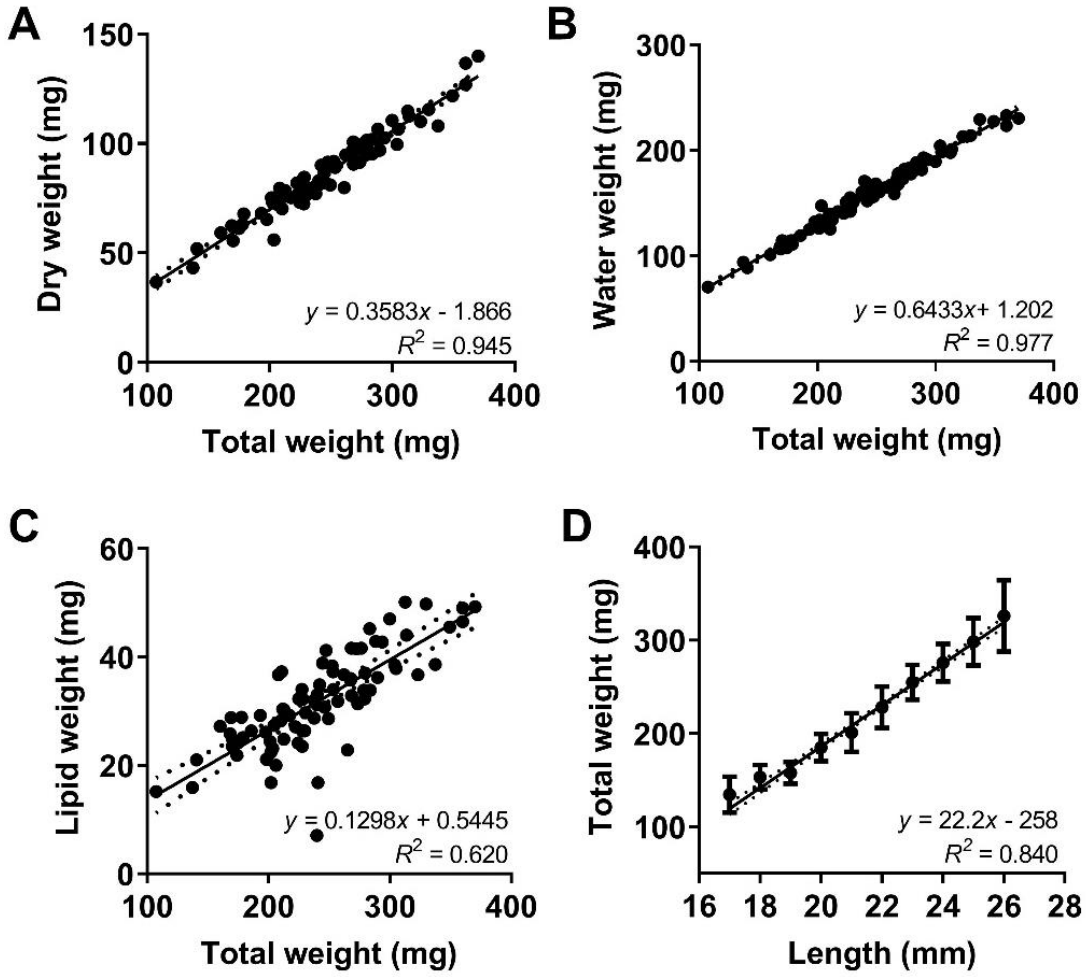

Figure 3-4. Multiple correlations observed between larvae total weight and dry weight, water weight, lipid weight, and larvae length. Non-manipulated (NM) larvae were used to analyse the relationships between (A) total weight and dry weight, (B) total weight and the lipid weight after here presented as lipid weight, (C) total weight and lipid weight as proportional to the total weight, water weight, and (D) total weight and larvae length where data is presented as mean ± SD (n = 252).

We also investigated the effect of infection on the lipid weight of all the larvae used in determining the LD_{50} for MRSA (Fig. 3-5). As calculated by one-way ANOVA, injection with MRSA resulted in an overall decrease in the lipid weight for both dead (18.7 mg ± 8.541, $p < 0.0001$, n = 573) and live larvae (22.4 mg ± 6.556, $p < 0.0001$, n = 524), when compared to the NM control (31.92 mg ± 8.815, n = 83) (Fig 3-5A). When compared to one another, live larvae had a significantly greater lipid weight compared to dead larvae (p <0.0001). There was no significant reduction in the lipid weight between NM and PBS control (27.81 mg ± 5.825, $p > 0.999$, n = 50) (Fig 3-5A and Table S3-2).

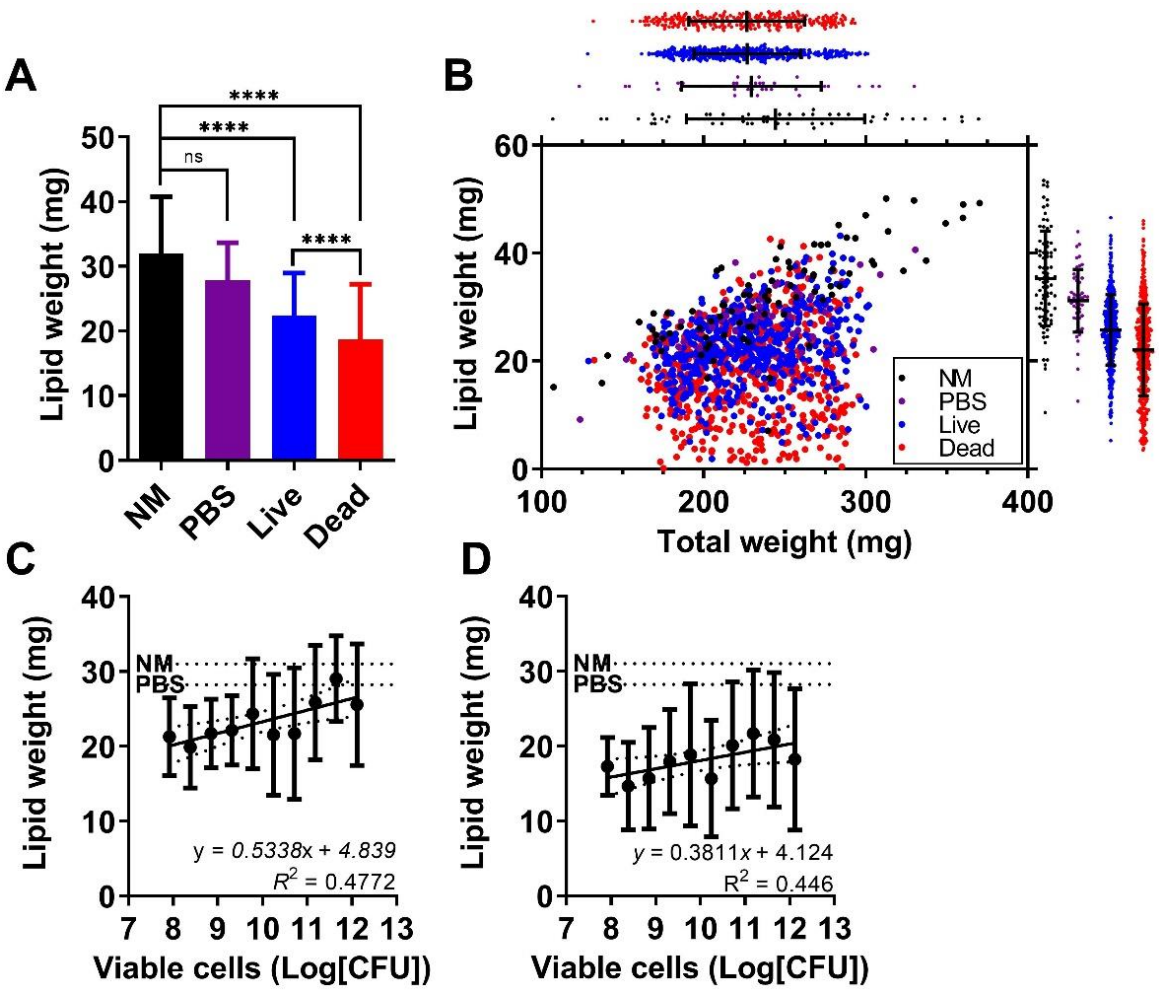

Figure 3-5. Injection of the larvae with MRSA results in an overall decreased in the lipid weight of the larvae.(A) Statistical results from a one-way ANOVA are illustrated above the bars as compared to the NM control. Summary of multiple analysis can be found in Table S3-2. (B) Box-plots above and to the right of the scatter plot are to illustrate the distribution of the data. Colours are as follows: black, NM control; purple, PBS control; blue, live larvae; and red, dead larvae 24 h post-MRSA infection. Correlations of infective dose and lipid weight for (C) living and (D) dead larvae. Data is presented as Log[CFU], as the infective doses are not adjusted for larvae weight. Data presented as mean ± SD (n = 10) of three independent replicas.

Finally, we observed that at a high infective dosage of MRSA, the larvae had a lipid weight close to the mean of the NM and PBS controls compared to the lower dosages (Fig. 3-5C,D). This was supported by a positive correlation between lipid weight and infective dose for both live (r = 0.778, p = 0.008) (Fig. 3-5C) and dead larvae (r = 0.669, p = 0.035) (Fig. 3-5D).

3.3.3. Pupation is unaffected by weight

To explore whether larger larvae were closer to the final instar stage (pupae) in which they begin to pupate into adult moths, an observational experiment was performed. NM larvae were left to pupate at 37°C, and it was observed that 80-100% of larvae pupated within the 15 day incubation period, independent on their weight grouping, as calculated by Log-rank (Mantel-Cox) test ($X^2(5, N = 60) = 4.004$, $p = 0.549$) (Fig. 3-6).

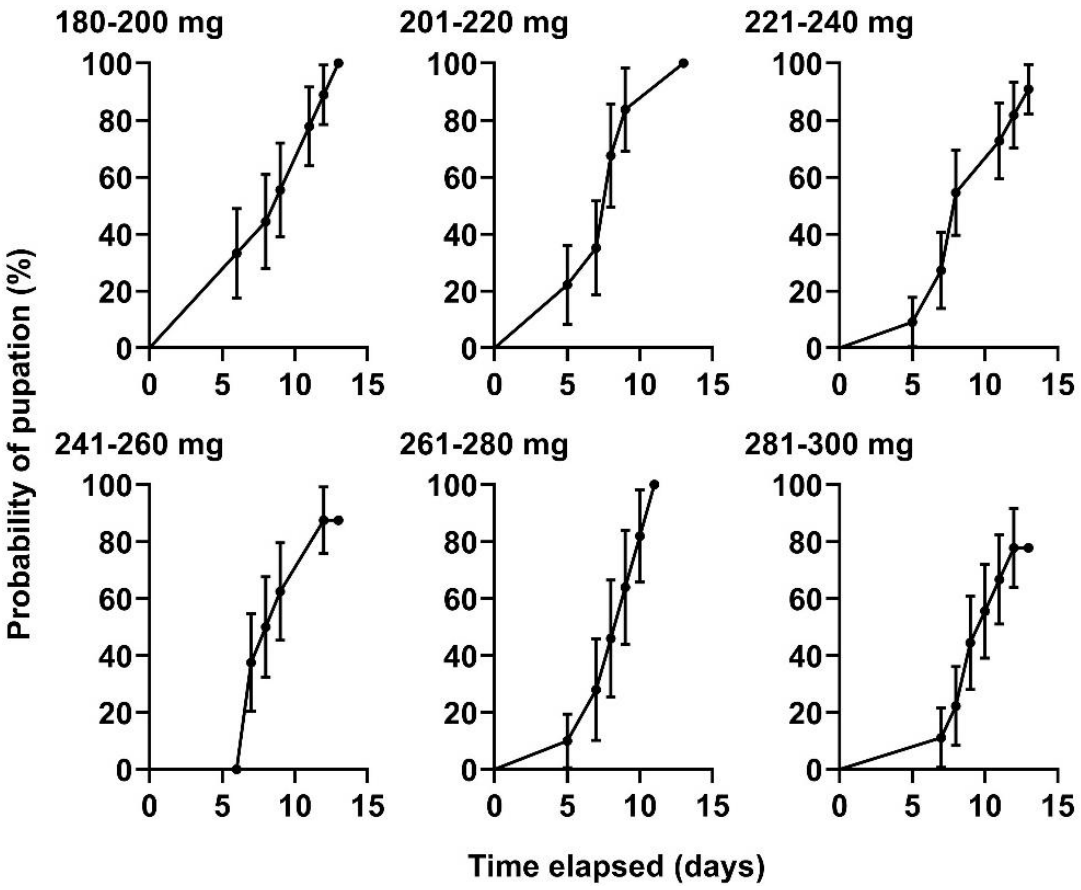

Figure 3-6. The weight did not influence the probability of pupation of NM larvae. NM larvae were incubated at 37ºC for 15 days and observed daily for pupation events. No significant difference was found between the weight group and the probability of pupation as calculated by a Log-rank Mantel-Cox test (p = 0.5489). Data are shown as mean ± SD (n = 10) repeated twice.

3.4. Discussion

3.4.1. MRSA exhibits a weight-dependent LD_{50}

In this study, we have demonstrated it is possible to develop a model in which a LD_{50} can be predicted based on the weight of the larvae, and that the prediction can be experimentally validated (Fig. 3-3). The linear model correlating total and water weight (Fig. 3-4B) imply that in increasingly larger larvae, the *in vivo* dilution of MRSA increases requiring a greater density of pathogen to reach the LD_{50}. Likewise for the positive correlation confirmed with total and lipid weight (Fig. 3-4C), the presence of a larger fat body that can be degraded for the production of immune factors, may well be why we observe the weight-dependent effect on LD_{50}. The LD_{50}s (1.19 – 8.97 $x10^7$ CFU/mg) for the MRSA strain was not within range of infective dosages utilised in previously investigated MRSA and Methicillin-sensitive *S. aureus* (MSSA) strains (0.8 – 5.0 $x10^6$ CFU) (Table S3-1). However, a direct comparison may not be appropriate given the variation in reporting densities as in our study the LD_{50} was adjusted to account for *in vivo* dilution in the larvae as described in (Andrea et al., 2019), but this is not always done.

During the process of this investigation, we found two of the largest weight groups (261-280 and 281-300 mg) to be unreliable, which hindered progress. This was consistent across multiple batches of larvae orders. LD_{50}, as calculated by our model for 261-280 and 281-300 mg larvae, resulted in less than 50% survival at 24 h (Fig. 3-3B), indicating that our model for a weight-dependent LD_{50} had overestimated the LD_{50}. Our first assumptions were that larger larvae were older and closer to pupation than the smaller weight groups, as larvae increase in size until pupation (Jorjão *et al.* 2018), which might

somehow impact on survival. Given the difficulty in identifying an age for each larva, it is a difficult hypothesis to test beyond quantifying the number of days it took for NM larvae from each weight group to pupate.

When this was conducted, we found that larval size did not influence the probability of pupation (Fig. 3-6), and we conclude that the larvae received from the supplier had an 80-100% probability of pupating within 15 days if kept at 37°C, regardless of weight. It would appear that larger larvae were not likely to be closer to pupation than smaller ones, so the reason for our observed decrease in LD_{50} for large larvae remains unknown. Since larvae were kept without food, this may be a reason for the observed similar pupation times across all weight groups as lack of food source may be forcing the larvae into pupation. Feeding regimes are not the standard protocol when investing antibiotic efficacy, as such we feel this best represented the conditions larvae would be exposed to at the start of experimentation.

Using *G. mellonella* does have drawbacks, one such being the functional equivalent of adaptive immunity termed ‘immune priming’ (Little and Kraaijeveld 2004; Sadd and Schmid-Hempel 2006). Individual larvae that survive infection or exposure to a particular pathogen may exhibit increased immune resistance against the same or similar pathogens. Priming with heat-killed pathogens was observed to result in increased larval survival (Wu *et al.* 2014). Ultimately there will be no control over the immune history of the larvae and this should always be recognised when working with pet-food grade *G. mellonella.* Across the literature, a wide range of weight bands have been utilised: 150-200 mg (Mannala *et al.* 2018); 300-700 mg (Ebner *et al.* 2016); 200-300 mg (Jacobs *et al.* 2013); and in other studies this is not declared (Ba *et al.* 2015; Jorjão *et al.*

2018). Our results suggest that choosing weight ranges as wide as 300-700 mg and 200-300 mg could result in inconsistent data. While a weight range of only 20 mg is likely a conservative approach, ranges such as 100 mg or greater in our weight-dependent LD_{50} model for MRSA indicates that there would be significant differences in survival (Fig. 3-3A).

Weighing individual larvae is a time-consuming procedure. This study also demonstrated that larvae length is reasonable proxy for the weight (Fig. 3-4D). Larval length has been previously used to characterise larvae for experimentation where larvae of 15-25 mm were utilised (Bazaid *et al.* 2018). Like total weight, a large length grouping may also encounter similar challenges. A 20 mg weight grouping would equate to roughly 1 mm, for example, 180-200 mg would be 20-21 mm. Measuring length may be a preferred alternative to accurately weighing all larval. When sourcing larvae from our supplier, we frequently found that larvae belonging to the weight groups 201-220 and 221-240 mg were most abundant, which will inevitably be the practical determining factor in weight group selection. Our findings would support selection of larvae in this range.

3.4.2. Lipid metabolism occurs in response to MRSA infection

MRSA infection leads to a decreased lipid weight in the larvae after 24 h, whether they died or survived the infection (Fig. 3-5A). The reduction in lipid weight is likely the result of lipolysis during an immune response. This is to be expected, the fat body of the larvae produce many defence compounds essential to the larvae's immune response (Cytryńska *et al.* 2007; Tsai, Loh and Proft 2016). This reaction can be rapid, in some models showing production of AMPs within the first 4 to 6 h post-infection (Sheehan, Dixon and Kavanagh

2019; Trevijano-Contador and Zaragoza 2019). This is supported by proteomic work, which demonstrated that at 6 and 24 h post-*S. aureus* infection larvae had increased expression of AMPs (Sheehan, Dixon and Kavanagh 2019).

On exposure to the infecting pathogen, there may be a rapid metabolism of the fat body to provide the required energy to fight the infection. Larvae with larger lipid weight before infection might be more likely to survive, as seen with the surviving larvae having a greater lipid weight than dead larvae (Fig. 3-5A). Within this experimental design, the larvae are not fed before or during the experiment, and therefore they cannot be acquiring more lipid. Where lipid weight was seen as closer to the NM and PBS control baseline, as observed in the trend of lipid weight positively correlating with infective dose (Fig. 3-5C,D), it is more likely that lipid metabolism has been compromised.

What could reasonably be expected is that lipolysis of the fat body occurs to increase the production of AMPs and additional defence compounds. When *Drosophila* are stimulated by a systemic infection with *S. aureus*, signalling from the Toll receptor increases, which leads to increased production of AMPs and reduced accumulation of lipids (Liu *et al.* 2016; Lee and Lee 2018). This could suggest that for larvae surviving high infective dosages, there are additional immune responses that do not deplete the fat body.

We intended to quantify the larval lipid weight to aid in understanding the weight-dependent LD_{50} effect and the observed unreliability of the two largest weight groups (261-280 and 281-300 mg). We report several observations regarding the lipid weight and MRSA infection; however, none can fully explain the irregularity we encountered for the largest weight groups. Analysing larval lipid weight has proved some insight, but would benefit from further

investigation, though alternative methods to estimate lipid mass would be required.

3.4.3. Overall assessment of *G. mellonella* as a model

There remains a lack of widely available and cheap standardised stocks of larvae reared under controlled conditions. Temperature (Mowlds and Kavanagh 2008), diet (Banville, Browne and Kavanagh 2012; Jorjão *et al.* 2018), past infections (Fallon, Kelly and Kavanagh 2012), and antibiotics and hormones in the feed (Büyükgüzel and Kalender 2008) are all reported to influence laboratory experimentation. Most larvae currently used are acquired from commercial insect food providers (Andrea, Krogfelt and Jenssen 2019), where it is understood that use of antibiotics and hormones in the culture medium is common practice, and acquiring accurate information regarding the conditions in which the larvae are reared is challenging. All of which may vary between larvae suppliers, which is a challenge that warrants caution.

Ultimately from our investigation, it would appear that lipid deposits are essential in *G. mellonella* response to MRSA. Prior investigation has evaluated the effect of nutrient deprivation on larvae (Banville, Browne and Kavanagh 2012), and the selection of diet (Jorjão *et al.* 2018), which both influence susceptibility to *S. aureus* infection. This emphasises the issues associated with a having lack of knowledge of rearing conditions used by suppliers and how they will influence experimental results. TruLarv™ (BioSystems Technology, UK) currently provide the only standardised *G. mellonella* in the UK. While cheap compared to murine models, it is considerably costlier (£1.20 per larvae) than purchasing larvae from commercial pet food providers.

However for pet-food grade larvae to be reliably used in research, more significant consideration should be taken over the parameters that can be controlled, and in this study, we emphasise that such experiments can be reproducible and reliable. We recommend that investigators consider the potential variability associated with using different larval weight as we have shown herein. We would recommend using weight groupings as a means to control this. Our data suggests that all larvae used should be within 10 mg of the mean weight of all larvae to provide consistency. Additionally, larvae of >260 mg should be avoided.

3.5. Conclusion

In this work, several linear regression curves are presented that could be used as tools to aid in experimental design, such as the linear model for LD_{50} (Fig. 3-3A), weight and lipid content (Fig. 3-4C), and length (Fig. 3-4D). Finally, we demonstrate that the lipid weight is reduced as a result of MRSA infection, identifying a potentially new measure in which to understand the immune response. Similarities between *G. mellonella* and mammals in response to *S. aureus* infections can be used to study the efficacy and interactions of novel antimicrobials, even at early development stages. By refining and standardising methodologies in which to handle and select *G. mellonella* for study, it can improve the reliability of this powerful model for multiple purposes

Chapter 4. Investigating the antimicrobial production of *Delftia acidovorans* strain PB091, an isolate from the deep-sea sponge *Pheronema carpenteri*

4.1. Introduction

A single sponge-associated bacterium was isolated from the deep-sea hexactinellid *Pheronema carpenteri* and investigated for natural products. The sponge was sampled in 2016 on the RSS James Cook off the coast of the Republic of Ireland. This isolate PB091 was identified, by sequencing the 16S rRNA gene, as *Delftia acidovorans* (Table 1-2, pg 85). This strain was found to produce a SMs that had antimicrobial activity against *Escherichia coli* and *Staphylococcus aureus*. This strain was further investigated to characterise antimicrobial productivity and the results are reported in this chapter. The selection of PB091 as a candidate was benefited due to its production of antimicrobial substance occurred in liquid culture, and was not reliant on artificial marine salts; and for the production of antimicrobial substance.

Delftia species are Gram-negative, straight or slightly curved rods, strictly aerobic, non-fermentative and chemo-organotrophic (Wen *et al.* 1999). The genus comprises environmental microorganisms with a wide geographical distribution, and members have previously been isolated from fresh and marine waters, soils, deserts, rhizopheres, plants, active sludge and clinical samples (Wen *et al.* 1999). The genus currently contains six recognised species *Delftia acidovorans* (Wen *et al.* 1999), *D tsuruhatensis* (Shigematsu *et al.* 2003), *D. lacustris* (Jørgensen *et al.* 2009), *D. litopenaei* (Chen *et al.* 2012), *D. deserti* (Li *et al.* 2015) and *D. rhizosphaerae* (Carro *et al.* 2017).

Delftia species are involved in the biodegradation of toxic carbon compounds such as phenols (Juárez-Jiménez *et al.* 2010, 2012) and anilines (Zhang *et al.* 2008, 2010); the bio-mineralisation of metals (Johnston *et al.* 2013; Wyatt, Johnston and Magarvey 2014); and they form part of the bacterial rhizosphere flora that promotes

plant growth (Han *et al.* 2005; Morel *et al.* 2011; Cagide *et al.* 2018). They have also been found to be members of the gut microbiome of healthy populations of fish such as sea bream (Nikouli *et al.* 2018), Atlantic salmon (Gajardo *et al.* 2016) and rainbow trout (Rimoldi *et al.* 2019; Pérez-Pascual *et al.* 2021). In contrast, they are rarely reported in humans, appearing to be an opportunistic pathogen in immunocompromised individuals (Mahmood *et al.* 2012; Bilgin *et al.* 2015; Ranc *et al.* 2018).

The broad potential of *Delftia* species for agriculture, bioremediation and bioproduct synthesis has previously been reviewed (Braña, Cagide and Morel 2016). Identifying a *Delftia* species as a potential producer of antimicrobials is a recent addition, first being noted in the whole genome of *D. tsuruhatensis* MTQ3, where multiple genes involved in antibiotic production were identified (Hou *et al.* 2015).

More recently, the supernatant of a novel *Delftia* sp. strain demonstrated antibacterial properties against Gram-positive and Gram-negative drug-resistant pathogens, including Methicillin-resistant *Staphylococcus aureus* (MRSA) and *Acinetobacter baumannii* (Tejman-Yarden *et al.* 2019). A nonribosomal peptide (NRP) delftibactin-A was proposed as the active molecule. NRPs are synthesised by large multimodular enzymes, nonribosomal peptide synthases (NRPSs), during bacterial and fungal secondary metabolism (Walsh 2008). The structural versatility of NRPs is the reason that they can generate a large pool of biologically active NRPs with medical applications and, as NRPSs are not limited to the 20 proteogenic amino acids, over 500 monomers, such as nonproteogenic amino acids, fatty acids, α-hydroxyl acids have all been identified as NRPs building blocks (Caboche *et al.* 2008; Flissi *et al.* 2020).

Data presented in the following chapter demonstrates the antimicrobial action of PB091_S70, a putative small molecule isolated from the supernatant of *D. acidovorans* PB091. Initial screening of PB091 demonstrated activity against a panel of Gram-negative and Gram-positive bacterial indicators, including *Escherichia coli* and MRSA. In this chapter, the aims were to 1) isolated and purify the bioactive compound from PB091; 2) assemble preliminary data to determine how promising the PB091-derived compound is for therapeutic use using both *in vitro* and *in vivo* assays; and 3) identify and characterise the active compound(s) by sequencing the whole genome of PB091 using both long and short-read sequencing platforms. A combination of *in silico, in vivo* and *in vitro* techniques are employed towards achieving these aims.

4.2. Materials and Methods

4.2.1. Culture and incubation conditions

Unless stated otherwise, seed cultures were made by suspending 3-5 individual colonies from a bacterial strain grown on agar plates into 5 ml of growth media, incubated overnight (minimum 18 h) at either room temperature or 37°C, with shaking at 120 rpm. Subsequent broths were inoculated using 10% (v/v) of the overnight seed culture. Liquid cultures were grown with and without orbital shaking at 150 rpm and room temperature. Growth was monitored by measuring the OD_{600nm}. The culture media used included: Luria broth (LB) medium (Sigma-Aldrich, UK); Nutrient-Broth (NB; ThermoFisher, UK); Tryptic-Soy Broth (TSB; ThermoFisher, UK) (Table 4-1), and unless stated otherwise, all broth were solidified with 1.5% (w/v) Agarose (Thermo-Fischer, UK) for use in agar plates. Various strains were used in antagonism assays and determining the minimum inhibitory concentration (Table 4-2).

Table 4-1. Summary of culture media.

Media	Content	Source (product code)
Luria-Bertani (LB)	10 g/L peptone, 5 g/L yeast extract, 5 g/L NaCl	FischerScientific, UK (11345992)
Nutrient Broth (NB)	5 g/L peptone, 2 g/L yeast extract, 5 g/L NaCl, 1 g/L 'Lab-Lemco' powder	Oxoid, UK (CM0001)
Tryptic Soy Broth (TSB)	17 g/L casein peptone (pancreatic), 2.5 g/L K_2HPO_4, 2.5 g/L glucose, 5 g/L NaCl,	Sigma-Aldrich, UK (22092)
Mueller Hinton broth (MH)	2 g/L beef infusion solids, 17.5 g/L casein hydrolysate, 1.5 g/L starch	Sigma-Aldrich, UK (70192)
Reasoners' 2 agar (R2a)	0.5 g/L yeast extract, 0.5 g/L proteose peptone, 0.5 g/L casein hydrosate, 0.5 g/L glucose, 0.5 g/L starch, 0.3 g/L K_2HPO_4, 0.024 $MgSO_4$, 0.3 g/L sodium pyruvate, pH 7.2 ± 0.2 at 25°C	Oxoid, UK (CM0906)

Table 4-2. Summary of indicator strains used in detecting antimicrobial activity and determining the minimum inhibitory concentration.

Gram reaction	Organism	Strain(s)	Notable characteristic
Positive	*Staphylococcus aureus*	NCTC 12493	Methicillin-resistant (*mec*A positive)
		NCTC 6571	
		M1281	In-house strain
		UoP strain-17	Methicillin-resistant (*mec*A positive), In-house clinical isolate
		UoP strain-9	Methicillin-resistant (*mec*A positive), In-house clinical isolate
Positive	*Micrococcus luteus*	UoP strain	In-house strain
Positive	*Streptococcus pyogenes*	UoP strain	In-house strain
Positive	*Enterococcus sp.*	UoP strain	In-house strain
Negative	*Escherichia coli*	NCTC 11560	TEM-1 Beta lactamase producer

UoP strain, University of Plymouth culture collection strain

4.2.2. Isolation of *D. acidovorans* strain PB091

D. acidovorans strain PB091 was recovered from a *P. carpenteri* sample collected from the North Atlantic. PB091 was recovered on ½ R2a solidified with 1.5% w/v agarose, supplemented with 33.3 g/L Instant Ocean™ (IO) and incubated at 15°C for 3 months. A single colony was picked and re-streaked until a pure culture was achieved. PB091 was successfully transferred to LB media and continued to demonstrate the same antimicrobial activity without the addition of IO.

4.2.3. Antagonistic well-diffusion assays

Antagonism assays were carried out on LB agar seeded with 1 ml (OD_{600} ~ 0.500) of the indicators *Micrococcus luteus* or *Escherichia coli* per 49 ml of molten agar (~40°C). The seeded agar was gently inverted 5 times before pouring. Plates were left in a sterile environment for up to 1 h to dry. Six-millimetre diameter wells were cut into seeded agar, and >50 µl of PB091 supernatant or purified compound were allowed to diffuse into the agar for up to 2 h at 4°C. Plates were incubated at 37°C for 18 h before being inspected for zones of inhibition; this would look as

demonstrated below (Fig. 4-1B). Antimicrobial activity was detected with this method at each purification step and with every batch to confirm activity continuously.

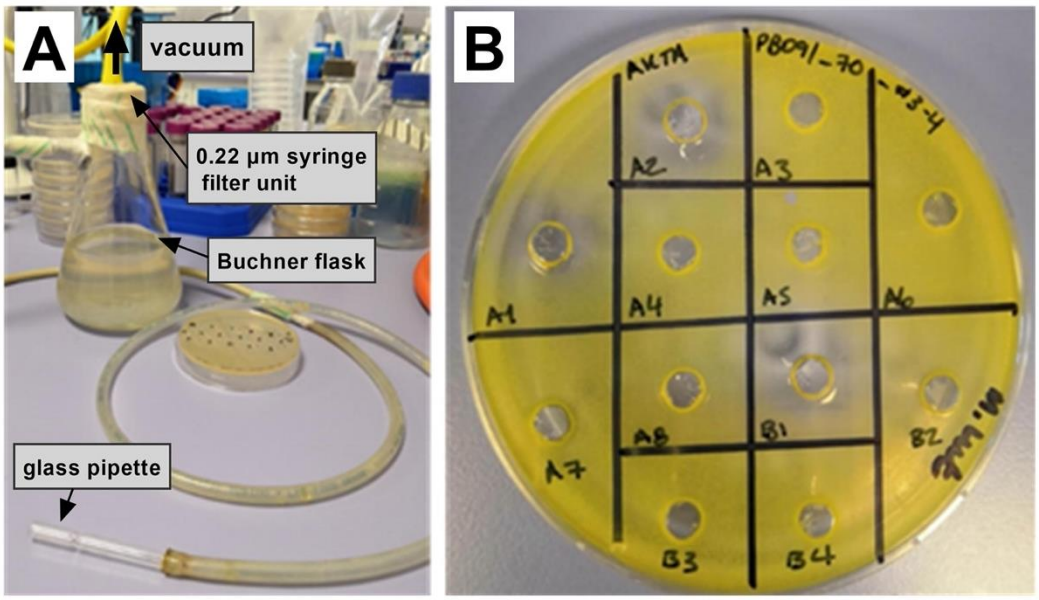

Figure 4-1. Well-diffusion assay plate seeded with *M. luteus*. (A) A filtering/Buchner flask was attached to a vacuum and filled with water. Rubber tubing is attached to a glass pipette that can be flame sterilised. The vacuum is created, and the device is used to punch holes out of the agar. (B) Example of a well-diffusion plate showing zones of inhibition for samples A1, A2 and B1.

4.2.4. Purification of a potential antibacterial agent from culture supernatants

4.2.4.1. *Crude organic extraction*

Five hundred millilitres of a three-day room temperature culture of PB091 was transferred to screw-top bottles and centrifuged at a speed of 5,500 x *g* for 40 minutes (Avanti J-26S Series, Beckman Coulter Inc.) using a fixed-angle rotor (J-LITE®JLA-10.500, Beckman Coulter Inc.). The supernatant was then filtered through pre-sterilised 0.22 µm pore-filter bottle-top vacuum filtration units (514-0332P; VWR International, UK). The filtered supernatant was regarded as the crude broth extract and progressed to Solid-Phase Extraction (SPE).

4.2.4.2. *Solid-phase Extraction*

Crude broth extracts were subjected to SPE using a 500 mg Strata Column C18-E (Phenomenex) cartridge and eluted using a MeOH + 0.01% Trifluoroacetic acid (TFA)/H_20 step gradient (tot. vol. 240 ml; 50%, 70%, and 90% MeOH + TFA). A 50 µl aliquot of each fraction was tested in well-diffusion assays. Fractions with no activity were discarded, fractions containing activity were concentrated to ~2 ml using a rotatory evaporator (Biotage® V-10 Touch, Biotage, UK).

4.2.4.3. *Reverse-phase Flash Chromatography*

Up to 2 ml of active crude extract from the SPE step were loaded onto a C18 Snap cartridge (10 g, Biotage) and subjected to reverse phase flash chromatography on an Isolera One system (Biotage). A H_2O/0.01% TFA-ACN gradient was used (H_2O/TFA-ACN; 1:1, 3 column volumes (CV); 1:5, 19.5 CV; 2:5, 1 CV; and 0:1, 5 CV), generating up to 60 fractions, all of which were tested for activity. Active fractions were combined and concentrated.

4.2.4.4. *Size-exclusion Chromatography*

Size-exclusion Chromatography (SEC) was conducted on an AKTA™ Pure system (GE Healthcare, Sweden). Analyses of the extract were carried out using a Superdex 10/300GL Peptide column (GE Healthcare). One millilitre of the concentrated compound was loaded onto the column and eluted in 150 mM NaCl. Fraction volumes were collected in a 96-well plate. All fractions were tested in well-diffusion assays and active fractions combined and concentrated. SEC was repeated multiple times to improve the purity of the compound.

4.2.4.5. *Quantifying putative mass of the compound*

Putative masses of purified compounds were determined using Matrix-Assisted Laser Desorbtion/Ionization Time of Flight Mass Spectrometry (MALDI-TOF MS) at The University of Bristol, UK. Samples were prepared by pipetting 1 µl of the compound onto a MALDI plate, permitting it to dry to completion before adding 1 µl of matrix (Bruker; 10 mg/ml α-Cyano-4-hydroxycinnamic acid; 50% v/v Acetonitrile, and 0.05% v/v Trifluoroacetic acid).

4.2.5. Experimental characterisation of antimicrobial compound PB091_S70

4.2.5.1. *Minimum Inhibitory Concentration (MIC)*

Following the manufacturer's instructions, the Pierce™ BCA Protein Assay Kit (ThermoScientific, UK) was used to determine the concentration of purified PB091_S70. Once quantified, the Minimum Inhibitory Concentration (MIC) was determined using the standardised broth microdilution method described by the European Committee on Antimicrobial Susceptibility Testing (EUCAST; (Wiegand et al., 2008). A positive control of Gentamicin (ThermoFisher Scientific, 50 mg/ml) was used at a final concentration of 100 µg/ml in MH broth.

To prepare the bacterial inoculation standard, indicator strains were streaked onto LB plates and incubated at 37°C. Five CFUs were suspended in 10 ml of MHb and incubated at 37°C for a minimum of 3 hours. A suspension with the same OD_{600nm} of a 0.1 McFarland standard was prepared using a 1 mL solution of culture (OD_{600nm} = 0.065), and this was diluted 1:100 in MHb, and 5 µl used to inoculate the wells. The standard was used within 15 minutes of preparation. Plates were left to incubate for 18 h at 37°C, with no orbital shaking. Wells were visually inspected for signs of growth of indicator strains in order to determine the MIC. Three technical replicates

were performed, and MICs re-measured with every new purification run of PB091_S70 to confirm the consistency of batches.

4.2.5.2. Galleria mellonella *infection assay*

The compound's preliminary *in vivo* investigation was performed using the Greater Wax Moth (*Galleria mellonella*) larvae. Larvae were infected with MRSA and then treated with PBS or PB091_S70, and survival recorded over 5 days. Detailed methodology and lethal median dose (LD_{50}) for *S. aureus* NCTC 12493 can be found in Chapter 3. Thirty healthy larvae of similar weight (220-240 mg) were uniform in creamy colouration with no dark marking (Fig. 3-1A, page 143) were used for each treatment. Larvae were injected with the LD_{50} at t = 0 h into the penultimate left pro-leg (Fig. 3-1C, page 143). Two hours post-infection, 10 µl of SEC purified compound was injected (Hamilton 1705 Gastight Syringe, 50 µL, 2" conical tip) into the penultimate right pro-leg. Syringes were cleaned between groups with three washes in a cycle of sterile distilled H_20 (dH_2O), 75% EtOH and distilled dH_20, discarding each wash. After injection, the larvae were maintained at 37˚C in the dark. Sterile PBS was used in 'manipulation control groups' to account for the effect of the physical trauma of injection (N =30), along with a no manipulation control (N =10). Larvae that began to pupate (Fig. 3-1B, page 143) during the investigation were not included in the analysis.

Over 120 h (5 days) at every 24 h time point, the number of larvae surviving were counted and the deceased ones discarded. Survival data were used to plot survival curves. Larvae were regarded alive when they were responsive to touch. If responsiveness was weak or not obvious, the larvae were then placed onto their backs, and if they were capable of correcting their position, they were marked as alive. The larva liquid volume (V_l) was determined using the total larva weight (M_l)

(Eq. S4-1). To calculate the *in vivo* concentration of compound ($C_{in\ vivo}$), the sum of the V_l, the concentration ($C_{comp.}$) and volume of compound injected ($V_{comp.}$), 10 µl in this case, are needed (Eq. S4-2) (Andrea, Krogfelt and Jenssen 2019).

4.2.5.3. *Time-kill assay*

Time-kill assays were performed using three concentrations of isolated compound: 0.5, 5 and 10 X MIC. A 30 µl aliquot of a suspension equivalent to a 0.5 McFarland standard, as described previously, was prepared and diluted in 15 ml of antibiotic-free and pre-warmed (37°C) MHb, and 90 µl of inoculum was dispersed into round-bottom 96-well plates (VWR, UK). Plates were pre-incubated for 4 h at 37°C and shaking at 150 rpm. After the pre-incubation, 10 µl of compound (or PBS for the controls) was added to the well containing 90µl inoculum to a final concentration of 24 and 46 µg/ml. This resulted in eight identical rows for each time point (-4, 0, 1, 2, 3, 4, 5, 6 h). A singular well was serially diluted at each consecutive time point and 10 µl pipetted onto a LB agar plate to enumerate the CFU/ml.

4.2.6. Whole-genome sequencing

Analysis of *D. acidovorans* genome was conducted using the Cloud Infrastructure for Microbial Bioinformatics (CLIMB) (Connor *et al.* 2016) on an 18 BioLinux 8 running Ubuntu version 16.04. Various Linux/Ubuntu software and online web tools were utilised (Table 4-3).

Table 4-3. Web tools and software used in the genomic analysis of *D. acidovorans* strain PB091.

Software/Web-tools	v.	Reference/Github
antiSMASH	5.0	(Medema *et al.* 2011; Blin *et al.* 2019)
BAGEL4	4.0	(de Jong *et al.* 2006; Van Heel *et al.* 2018)
Biosynthetic Gene Similarity Clustering and Prospecting Engine (BiGSCAPE)	NA	https://git.wageningenur.nl/medema-group/BiG-SCAPE/-/wikis/home
BWA-MEM	0.7.15	(Li and Durbin 2009; Li 2013)
CheckM	1.0.18	(Parks *et al.* 2015)
Clinker	0.0.16	https://github.com/gamcil/clinker
CORe Analysis of Syntenic Orthologs to prioritise Natural Product-Biosynthetic Gene Cluster (CORASON-BGC)	NA	https://github.com/nselem/corason/wiki
Guppy	3.2.4	https://nanoporetech.com/
Interactive Tree of Life (iTOL)	5.7	https://itol.embl.de/personal_page.cgi
JSpecies Web Service (JSpeciesWS)	NA	(Richter *et al.* 2016)
Kraken	2.0	(Wood and Salzberg 2014; Wood, Lu and Langmead 2019)
MinKNOWN		https://nanoporetech.com/
MUMmer	3.0	(Kurtz *et al.* 2004)
PhyloSift	1.0.1	(Darling *et al.* 2014)
Porechop	0.2.4	https://github.com/rrwick/Porechop
Prokka	1.14.5	(Seemann 2014)
RiPPER (RiPP Precursor Peptide Enhanced Recognition)	1.1	(Santos-Aberturas *et al.* 2019; Moffat *et al.* 2021)
SPAdes	3.8.1	(Bankevich *et al.* 2012)
Trimmomatic	0.30	(Bolger, Lohse and Usadel 2014)
Type (Strain) Genome Server (TYGS)	1.0	(Meier-Kolthoff and Göker 2019)
Unicycler	0.4.8	(Wick *et al.* 2017)

4.2.6.1. *Short-read Illumina sequencing and bioinformatics provided by MicrobesNG*

PB091 was cultured on an LB agar plate and incubated at room temperature for 5 days before being transferred to a cryo-tube provided by Microbial Genomics Ltd. (MicrobesNG; http://www.microbesng.uk), which is supported by the BBSRC (grant number BB/L024209/1). The data is currently embargoed. MicrobesNG performed the DNA extraction, library preparation and sequencing using an Illumina platform. Their methods are described on their website and can be found here: https://microbesng.uk/documents/5/MicrobesNG_Methods_Document_-_PDF.pdf.

MicrobesNG additionally processed raw sequencing data as followes: 1) sequencing adapters were trimmed using Trimmomatic 0.30, 2) reads filtered based on a quality score cutoff of > Q15, 3) Kraken2 was used for identifying a reference genome, 4) reads were then mapped to the reference genome to assess the data quality using BWA-MEM, 5) *de novo* assembly was completed using SPAdes, 6) contigs were generated using MUMmer v. 3.0, and 7) contigs were annotated by using Prokka.

4.2.6.2. *Long-read MinION sequencing*

PB091 was grown in LB medium in a shaking incubator at room temperature and 140 rpm until the late log phase. The DNeasy PowerSoil Kit (12888, Qiagen, UK) was used for DNA extraction, with one alteration. The buffer in the bead-beating tube was replaced with 1 ml of culture of log-phase culture before proceeding with the manufacturer's instructions. Finally, 100 µ of DNA was eluted in low TE buffer (10 mM Tris-HCl, 0.1 mM EDTA, pH 8.0).

Genomic DNA was sequenced on the MinION sequencing platform (Oxford Nanopore Technologies) using a one-dimensional (1D) flow cell (FLO-MIN106). Genomic DNA was repaired and end-prepped following the 1D Genomic DNA ligation protocol (with SQK-LSK109) using a NEBNext Ultra II End-Repair/dA tailing module. The DNA was then barcoded and library assembled following the 1D Native barcoding Genomic DNA protocol (with EXP-NBD103 and SQK-LSK108). End-prepped and barcoded samples were pooled into a single library, and an adapter was ligated using NEBNext Quick T4 DNA ligase (New England Biolabs, USA). After each enzymatic reaction (end-repair, barcoding, and adapter ligation), the DNA was cleaned using AMPureXP beads (Beckman Coulter, Inc.) and quantified by using the Qubit™ Fluorometer with a Qubit dsDNA High Sensitivity assay Kit (Invitrogen, UK).

The DNA library for loading included 14 µl DNA library (16.0 ng/µl), running buffer and loading beads. Using MinKNOWN, the library was sequenced following the standard parameters, deactivating live base-calling. Quality control detected 1568 active pores for sequencing.

4.2.6.3. *Whole-genome analysis*

After sequencing, FAST5 files were base-called using Guppy v.3.2.4. Base-called FASTQ files were de-multiplexed based on the ONT barcodes, and the adapters were trimmed using Porechop. Unicycler was used in order to map long MinION reads to Illumina generated contigs.

For taxonomic classification of PB091, the genome-wide Average Nucleotide Identify using *BLAST*+ (ANIb) and tetranucleotide usage patterns (TETRA) for all pairwise comparisons of 13 publicly available *Delftia* genomes were calculated using the JSpecies Web Service (JSpesciesWS) online tool (Richter *et al.* 2016). The threshold to ascribe one species for ANIb is 95% of genome sequence similarity, and for TETRA is 0.997 (Richter and Rosselló-Móra 2009). Publicly available complete, draft and metagenome-assembled genomes (MAGs) of *Delftia* spp. were retrieved from the National Centre for Biotechnology Information (NCBI) in July 2020. Table S4-1 reports the accession numbers and other information about the genome type and level of completion.

For the detection and annotation of secondary metabolite Biosynthetic Gene Clusters (BGCs), the antiSMASH v.5. web tool was utilised. Clinker was used to generate reader-friendly gene-arrow maps of BGCs, and these were further annotated in Inkscape v. 1.0.

4.2.7. Statistical Analysis

Two-Way ANOVA and Tukey's pairwise comparison of *G. mellonella* and time-kill assay were performed using GraphPad Prism v. 9.0.1 for Windows (GraphPad Software, San Diego, California USA, www.graphpad.com). Graphical outputs were generated using GraphPad Prism.

4.3. Results

4.3.1. Optimisation of compound production and isolation

Delftia acidovorans strain PB091 was grown for 5 days in LB, TSB, NB, and MB, and supernatants tested for antimicrobial activity. Production was achieved in LB, and weaker activity observed in NB. No production was observed in TSB and MB. Anti Gram-positive activity was detected in the 70% MeOH fraction eluted from a Strata column. This is referred to as PB091_S70 (Fig. 4-2). After quantification with BSA, typically, 500 ml of broth would yield on average >900 µg of PB091_S70 with an approximate volume of 3 ml. Despite PB091 demonstrating activity against *S. aureus* and *E. coli* in early screening (Chapter 1), no Gram-negative activity was observed during the process of purifying potential antimicrobial compounds from this strain.

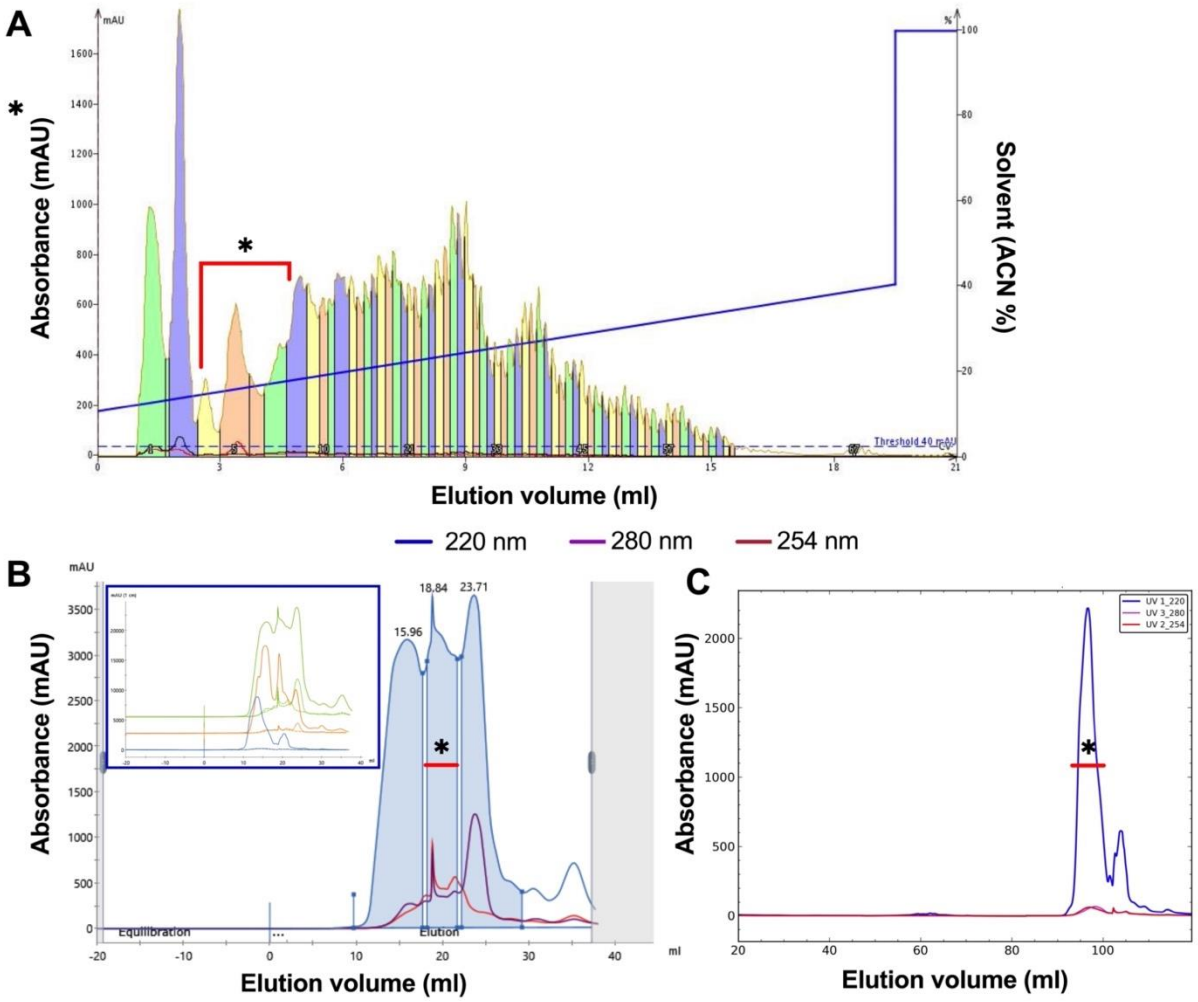

Figure 4-2. Chromatography and MALDI-TOF MS spectra of PB091_S70. Chromatographs of the of 70% MeOH purification Strata fraction. Active fractions are denoted by an asterisk (✱). (A) Flash Chromatography shows trace UV absorbance at 210 nm, fractions eluted in a gradient of H_2O + 0.1%:ACN + 0.1% TFA. (B) SEC shows trace UV absorbance at 210, 250 and 268 nm, factions eluted in 150 mM NaCl + 0. 1% TFA. Active fractions are named (B) PB091_S70. Small chromatographs in the blue box illustrate a degree of consistency of methods over multiple extractions. (C) The subsequently purified spectra of PB091_S70.

4.3.2. Minimum Inhibitory Concentration

MICs were carried out by microbroth dilution with gentamicin as a positive control. PB091_S70 showed consistency in MIC against multiple indicator strains (Table 4-4). The lowest MIC was against *M. luteus* at 13.0 µg/ml, and the highest values were against *S. aureus* strains. PB091_S70 has a mean MIC of 25 µg/ml against the five *S. aureus* strains.

Table 4-4. Minimum inhibitory concentration of PB091_S70. SD of MICs from replicas are presented in parenthesis, where none is present indicates that MIC did not vary between replicas and extractions. No effect indicates that no concentration tested that inhibited growth of the indicator.

Indicator		**Mean MIC (µg/ml)**	
Organism	**Strain**	**Gentamycin**	**PB091_S70**
S. aureus	NCTC 12493	0.60	25.0
S. aureus	NCTC 6571	0.20	25.0
S. aureus	M1281	0.35	25.0
S. aureus	UoP strain - 17	37.5 (± 17.6)	25.0 (± 25.0)
S. aureus	UoP strain - 9	0.39	25.0
Str. pyogenes	UoP strain	6.3	15.6 (± 7.36)
Enterococcus sp.	UoP strain	1.6	20.8
M. luteus	UoP strain	0.25	13.0

4.3.3. PB091_S70 compound displayed no toxicity in *Galleria mellonella* and a slight bacteriostatic effect

To determine any toxic effect and investigate the efficacy of PB091_S70 as an antimicrobial treatment, *G. mellonella* were employed. A volume of 10 µl containing 200 µg/ml of PB091_S70 was used to treat larvae infected with MRSA strain NCTC 12493; this was the highest concentration of PB091_S70 available. PB091_S70 displayed no toxicity in *G. mellonella* over a 120 h period compared to the no-manipulation control (p = 0.863, N =30) (Fig. 4-3B). There was no improvement in using PB091_S70 as an antibiotic treatment *in vivo* in *G. mellonella* over a 120 h incubation (Fig. 4-3A). The *in vivo* concentration achieved of PB091_S70 for the G*. mellonella* assay was 5.89 µg/ml. At 120 h, the mean survival of treated larvae (LD_{50} + PB091_S70) was 20% (± 7.3 %, N =30) and in untreated larvae survival was 6.67% (± 4.55 %, N =30). At 120 h there was no significant difference between the two treatment groups as calculated by One-Way ANOVA (p = 0.290, N =30) (Fig. 4-3B).

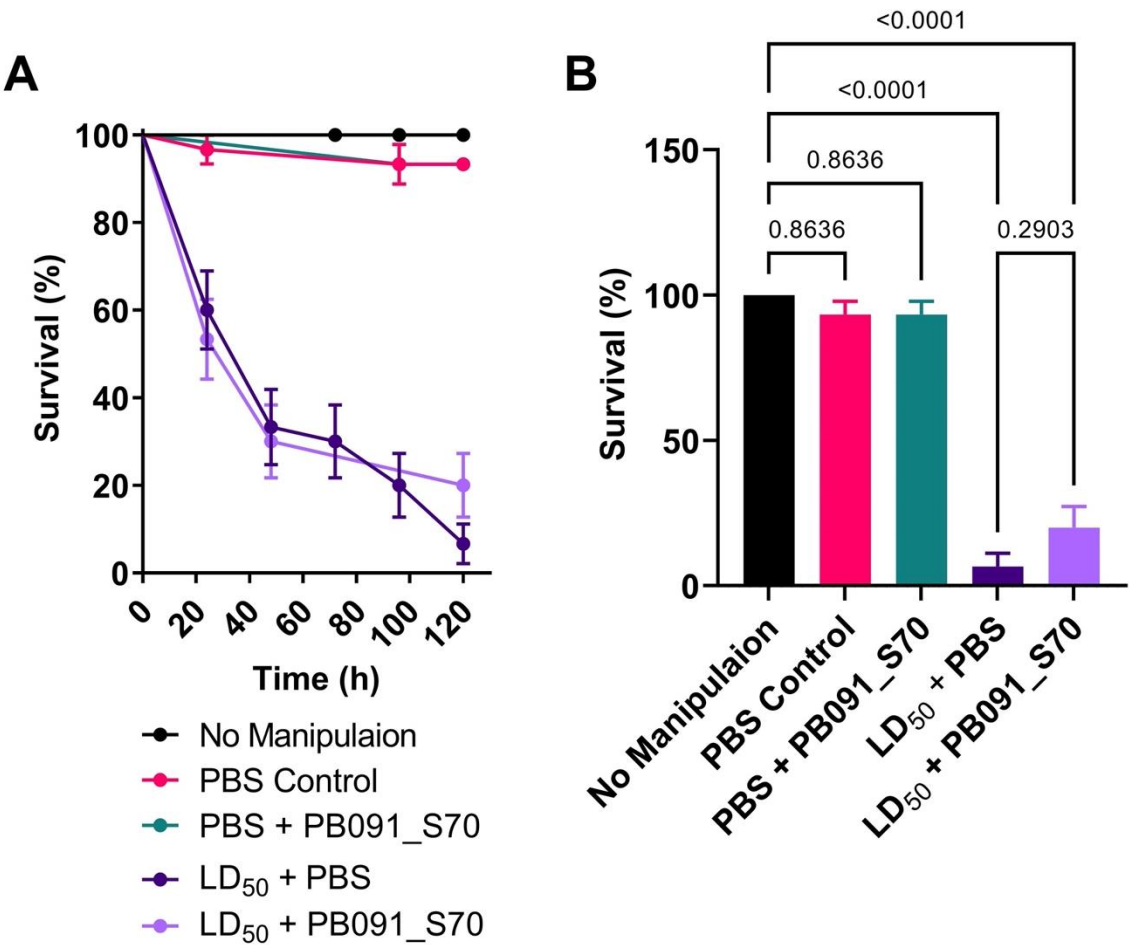

Figure 4-3. *Galleria mellonella* efficacy assay using PB091_S70 as a treatment for larvae infected with the MRSA strain NCTC 12493 (A) Survival curve of treated larvae over 5 days. (B) Differences between treatment groups at 120 h. *P*-values of a One-Way ANOVA comparing the treatment groups against the PBS control are indicated in the graph. Complete results of Two-Way ANOVA can be found in Table S4-2. Error bars represent the SD. (PBS + PB091_S70, larvae injected with PBS and 2 h later treated with PB091_S70; LD_{50} + PBS, larvae infected with MRSA and injected with PBS 2 h later; and LD_{50} + PB091_S70, larvae infected then 2 h later treated with PB091_S70).

In addition to there being no *in vivo* efficacy, *in vitro* efficacy in a time-kill assay likewise demonstrated no effective control of MRSA while using the highest concentration of compound available (25 and 43.7 µg/ml) (Fig. 4-4). At 8 h there was no difference in viable cell counts of MRSA between the treatment groups with any concentration of PB091_S70 as compared to the PBS control, as measured by a One-Way ANOVA (25 µg/ml: mean = 1.73 x 10^8 CFU/ml, p = 0.623, N =3; and 43.7 µg/ml: mean = 7.40 x 10^7 CFU/ml, p = 0.565, N =3) (Fig. 4-4B).

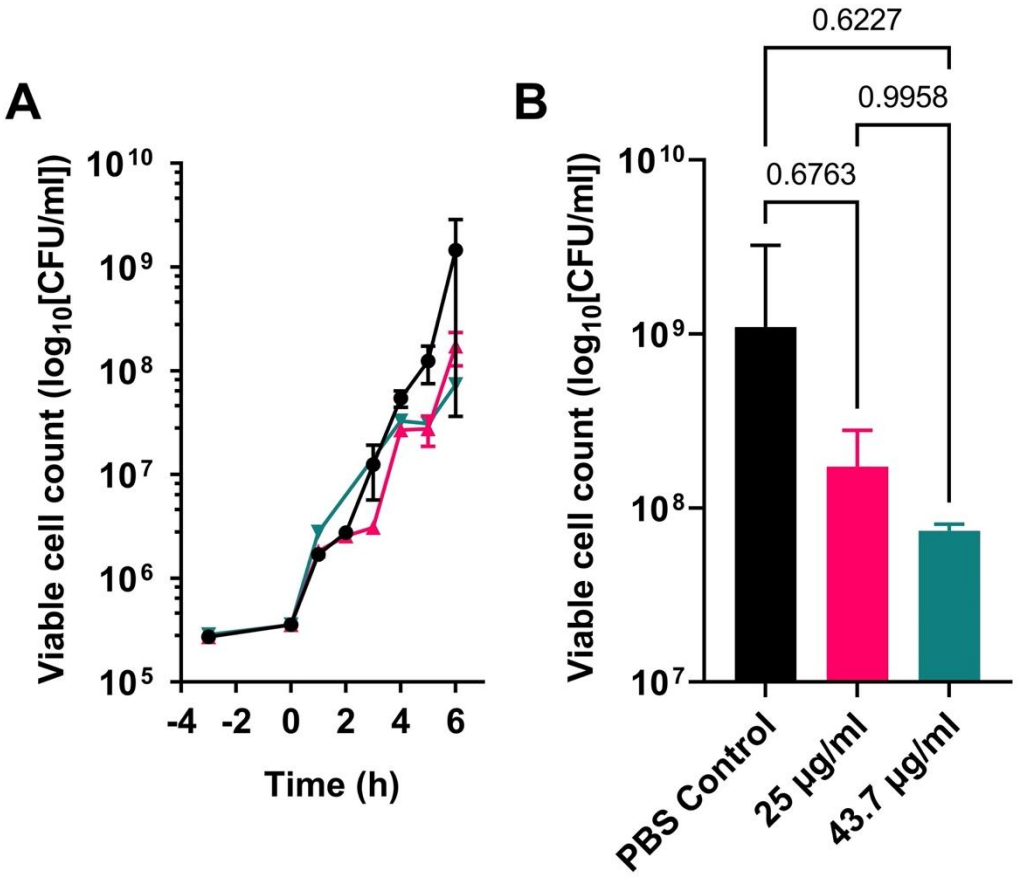

Figure 4-4. Time-kill assay of PB091_S70 incubated with the MRSA strain NCTC 12493.(A) Time-kill assay of PB091_S70 at two concentrations (1X and 1.8X MIC), and (B) the differences between treatment at the final time-point (6 h). *P*-values of a One-Way ANOVA comparing the treatment groups against the PBS control are indicated in the graph. Complete results of Two-Way ANOVA can be found in Table S4-2.

4.3.4. Sequencing and hybrid assembly

PB091 was identified in Chapter 1 as *D. acidovorans* by sequencing the 16S rRNA gene sequencing and the phylogenetic placement of the strain in the Comamoadaceae family (Fig. S4-1). Long-read minion sequencing generated 190K reads, and after filtering to a Q ≧ 8 there were 125K reads remaining with a mean length of 10 Kbp. Shot-read Illumina MiSeq whole-genome sequencing by MicrobesNG generated 1.6 million reads, achieving 30X coverage. Illumina MiSeq reads were assembled into 190 contigs, had a GC content of 66.69%, and a total length of 6.7 Mbp (Table 4-5).

Table 4-5. PB091 draft genome assembly statistics of Illumina and the hybrid Illumina-MinION assembly. (GC-content, guanine-cytosine content; N50/75, sequence length of the shortest contig at 50/75% of the total genome length; L50/75, smallest number of contigs whose length sum makes up 50/75% of genome size).

	Illumina	Illumina-MinION Hybrid
contigs (≥ 0 bp)	190	5
contigs (≥ 1,000 bp)	121	4
Total length (≥ 0 bp)	6,736,708	6,680,119
Total length (≥ 1,000 bp)	6705894	6,679,712
contigs	128	4
Largest contig	393,018	6,059,722
Total length	6,710,814	6,679,712
GC-content (%)	66.69	66.71
N50	85800	6059722
N75	52361	6059722
L50	24	1
L75	49	1
Completeness (%)	99.85	99.85
Contamination (%)	0.25	0.21

Long-read MinION sequences where scaffolded to the genome assembly generated by Illumina sequencing data. The hybrid assembly improved the overall completeness of the genome and reduced the number of contigs from 190 to 5 (Table 4-5). The hybrid assembly had a total length of 6.67 Mbp. The draft hybrid assembly features five contigs with a total length of 6,680,119 bp, G+C content of 66.7%, and no plasmids were detected. The genome was annotated and predicted to have 6,129 protein-coding genes, 77 tRNAs, and 12 rRNA. CheckM, estimated genome completeness as 99.85% and with no detectable level of contamination, the hybrid assembly did not impact on the genome completeness or contamination levels (Parks *et al.* 2015).

The draft whole-genomes of the 14 publicly available *Delftia* spp. were considered further for genome-wide ANIb using the JSpeciesWS online tool. There were multiple ANIb hits above the assignment species threshold (95%), indicating that *D.*

acidovorans strain PB091 is not an uncharacterised species (Table S4-1). The closest match was to *Delftia* sp. RIT313, which shows 97.64% sequence identity, and the highest sequence identity to a *D. acidovorans* type strain was to NBRC 14950 at 97.30%.

4.3.5. *Delftia acidovorans* strain PB091 genome displayed minimal hits using antiSMASH as compared to other members of the *Delftia* genus

The genome was mined for genes potential encoding bioactive secondary metabolites using antiSMASH v5, which detects similarity between BGCs in terms of gene content and synteny. The antiSMASH results showed four potential secondary metabolite clusters (Fig. 4-5A), as follows: 1) a NRPS that shows 100% similarity to Delftibactin-A/B; 2) an unspecified ribosomally synthesised and post-translationally modified peptide product (RiPP) cluster and potential bacteriocin; 3) a resorcinol cluster; and 4) a terpene cluster (Fig. 4-5A). All 4 BGCs identified in PB091 were conserved across multiple *Delftia* species (Table S4-4, Fig. S4-2). In comparison to D-2189, PB091 contains an additional ORF (Fig. 2-5B), this is reported in more detail below. When the publicly available genomes for known *Delftia* spp. strains were accessed and parsed through antiSMASH (Table S4-1), it was found that the four BGCs identified in PB091 were largely ubiquitous among individuals belonging to the genus *Delftia* (Table S4-1 and Fig. S4-2).

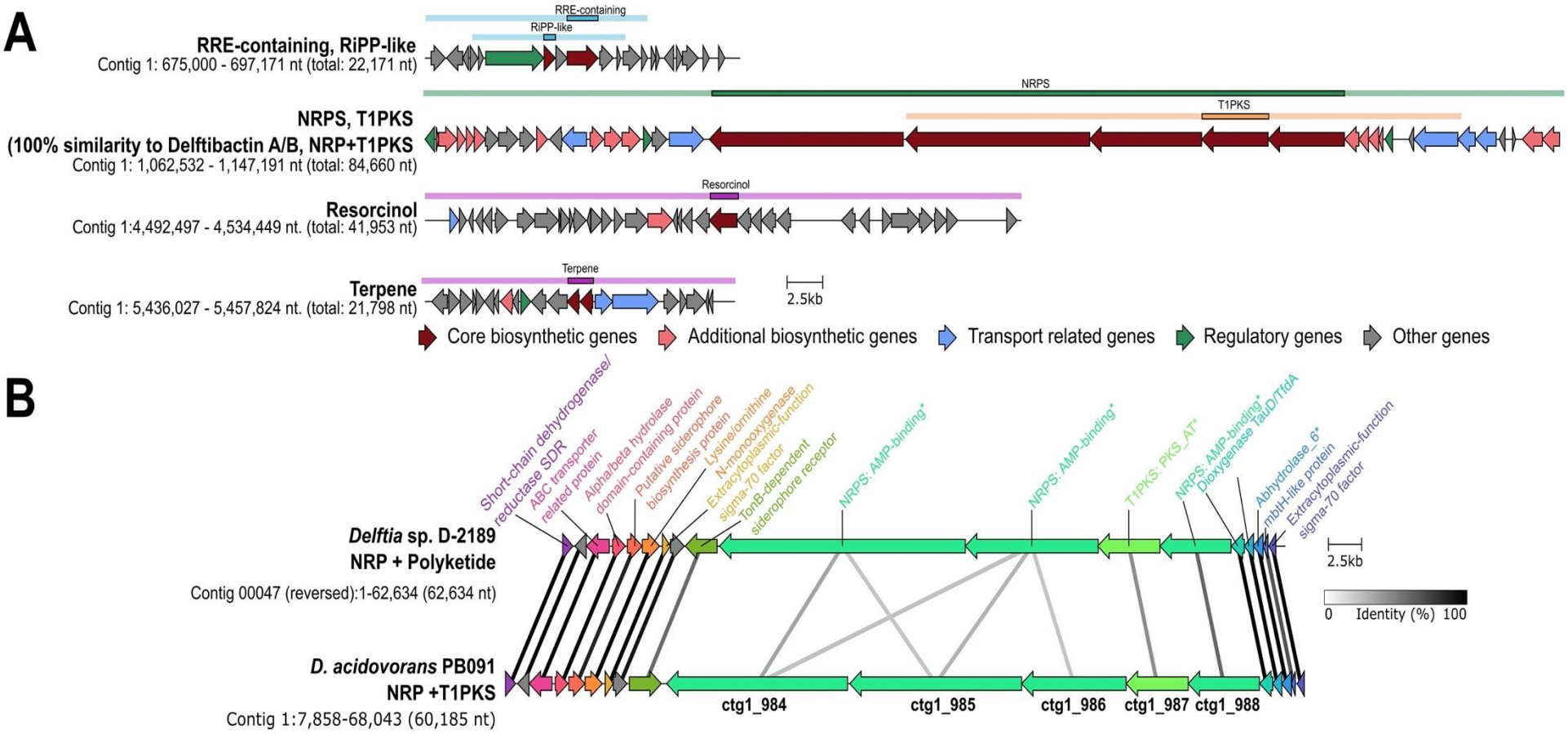

Figure 4-5. antiSMASH v.5 predicted secondary metabolite biosynthetic clusters for PB091. (A) Four BGCs were detected in PB091. Localisation and length of the cluster can be found below the cluster hit name. Cluster type (i.e T1PKS, RiPP-like) is indicated above each gene map. (B) Comparison of PB091 and D-2189 Delftibactin-A/B clusters, showing low (<67% nt. identity) identity between the core biosynthetic genes, and greater similarity (>67% nt. Identity) between additional, transport and regulatory genes. Lines between ORF indicate the sequence identity from alignment. The antiSMASH hits were downloaded in GenBank file format (.gbk) and visualised in using Clinker. Figure was then further annotated in InkScape v. 1.0. (RRE-containing, RRE-element containing cluster; RiPP-like, Ribosomally synthesised and post-translationally modified peptides-like; NRPS, Non-Ribosomal Peptide Synthetase; T1PKS, Type 1 Polyketide Synthetase; ✱, gene annotations detected by rules-based-clusters in antiSMASH).

From the antiSMASH output there were no known clusters or subcluster hits against the resorcinol, terpene or RiPP-like BGC (Table 4-6). Comparison against the Minimum Information about a Biosynthetic Gene cluster (MiBIG) database by antiSMASH showed low similarity scores (>0.70) against core BGC genes for all three. The highest hits were for delftibactin A/B, which will be reported in more detail below. Terpene BGC core gene was most similar to a terpene from *Xanthobacter autotrophicus* Ps2 reported to produce zeaxanthin, a carotenoid pigment (Larsen *et al.* 2002). The RiPP-like protocluster closess hit was to the cluster synthesising aclacinomycin (0.30), an anthracycline antibiotic and antitumor compound from *Streptomycetes galilaeus* (Ylihonko *et al.* 1994). The resorcinol BGC had the poorest similarity score to any known resorcinol, the two highest (0.13 and 0.15) were to bartolosides from the cyanobacteria *Synechocystis salina*. Bartolosides represent a novel family of glycolipids (Afonso *et al.* 2016).

Table 4-6. MIBiG database comparisons of core biosynthetic genes identified from PB091.

Type	PB091 contig and gene ID	MIBiG Reference	Similarity Score	Type	Compound(s)	Organisms
RRE-containing, RiPP-like	ctg_621	BGC0000193.1	0.30	Polyketide	aclacinomycin	*Streptomyces galilaeus*
		BGC0000477.1	0.26	RiPP	patellin 2/3	uncultured *Prochloron* sp. 06037A
		BGC0000483.1	0.26	RiPP	aeruginosamide B/C	*Microcystis aeruginosa* PCC 9432
NRPS, T1PKS	ctg1_984-988	BGC0000984.1	0.91	NRP, Polyketide	delftibactin A/B	*Delftia acidovorans* SPH-1
	ctg1_984 and 985	BGC0000389.1	0.80	NRP	massetolide A	*Pseudomonas fluorescens* SS101
		BGC0002071.1	0.76	NRP	virginiafactin	*Pseudomonas* sp. QS1027
Resorcinol	ctg1_3936	BGC0001526.1	0.15	Other	bartolosides E/F/G/H/I/J/K	*Synechocystis salina* LEGE 06099
		BGC0001525.1	0.13	Other	bartoloside 2/3/4	*S. salina* LEGE 06155
		BGC0000838.1	0.06	Polyketide	flexirubin	*Flavobacterium johnsoniae* UW101
Terpene	ctg1_4756	BGC0000656.1	0.58	Terpene	zeaxanthin	*Xanthobacter autotrophicus* Py2
		BGC0000634.1	0.53	Terpene	carotenoid	*Brevundimonas* sp. SD212
		BGC0000643.1	0.53	Terpene	carotenoid	*Brevundimonas vesicularis*

4.3.6. Delftibactin-A as the putative compound displaying antimicrobial effect

A *Delftia* sp. isolate D-2189 has previously been described as a producer of an antimicrobial peptide from the delftibactin A/B cluster (Tejman-Yarden *et al.* 2019). When the D-2189 delftibactin cluster is compared to the equivalent region in the PB091 genome, a lower nucleotide identity was observed between the core genes (<60%) compared to the additional genes encoding biosynthetic, transport and regulatory functions (>80%) (Fig. 4-6). Futhermore there was an additional open reading frame (ORF) in PB091 as compared to D-2189 (Fig. 405B). The delftibactin cluster is 84,660 nt long and is identified as a hybrid NRPS-T1PKS.

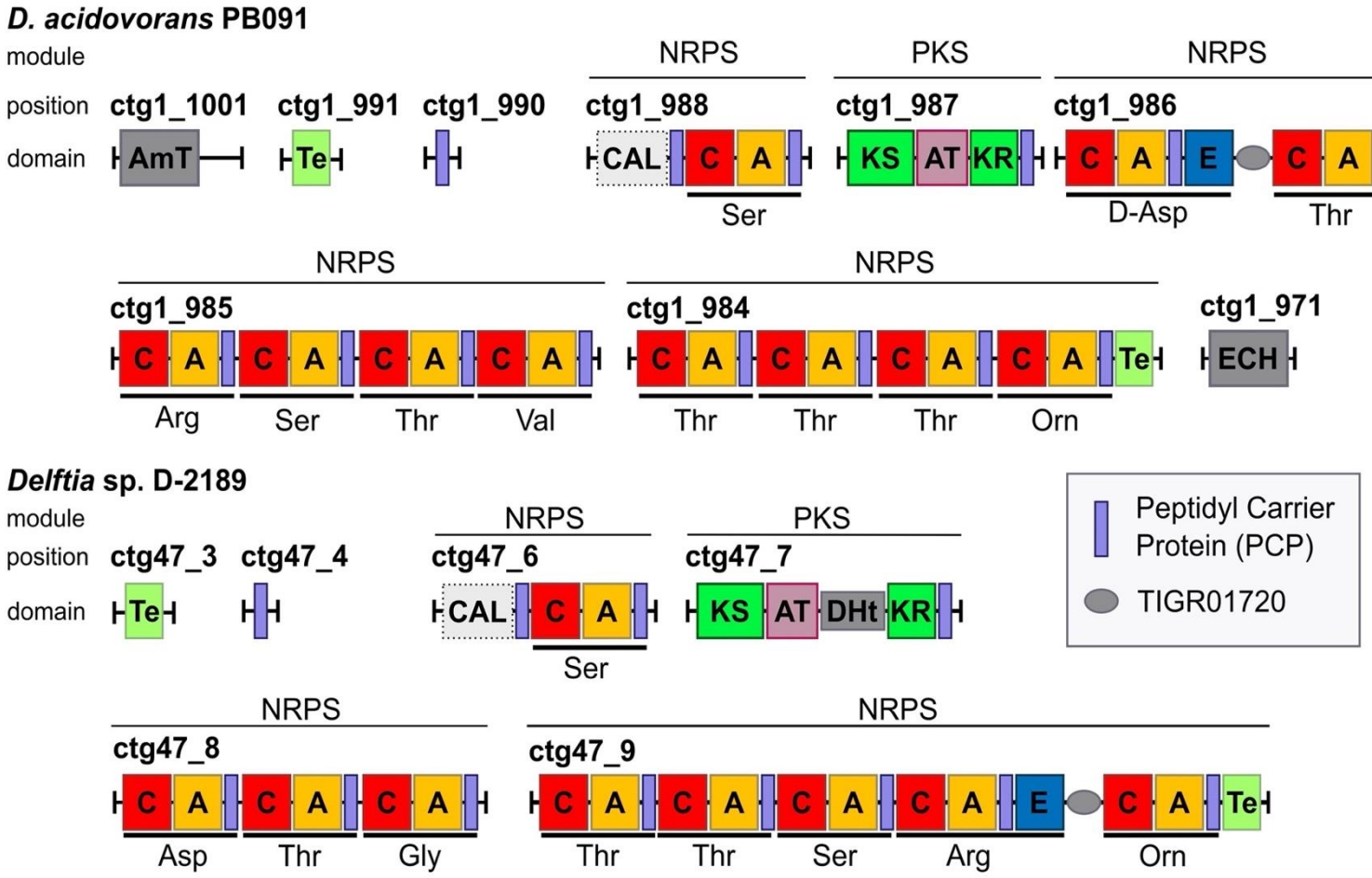

Figure 4-6 Domain architecture of *D. acidovorans* PB091 and *Delftia* sp. D-2189 NRPS-T1PKS. Consensus schematic representation of the NRPS-T1PKS hybrid domain structure based on the PFAM database and antiSMASH results. The PB091 cluster is reversed in this figure to portray the likely orientation of the NRPS-T1PKS hybrid. See Table S4-5 for details on the coordinates and residues in binding pocket resulting in the predicted amino acid. Module domains are listed as follows: A, adenylation; AT, acyltransferase; AmT, aminotransferase; C, condensation; CAL, Co-enzyme A ligase; DHt, dehydratase; E, epimerisation; ECH, enoyl-CoA hydratase/isomerase; KR, ketoreductase; KS, ketosynthase; Te, thioesterase. Labels that could not fit, PCP and the InterPro domain TIGR01720, are described within the figure.

Thioesterase domains (TE) are usually located in the final NRPS module facilitating peptide release (Strieker, Tanović and Marahiel 2010), indicating that ctg1_984 of the PB091 cluster is likely the terminal NRPS module (Fig 4-6). The hybrid NRPS-T1PKS was composed of four NRPSs and one PKS. A single NRPS module is followed by a single T1PKS module, then three NRPS. The PKS module in PB091 contains three domains, a ketosynthase (KS) and acyltransferase (AT), followed by a ketoreductase (KT)

Three prominent structural differences are observed in the NRPS-T1PKS domains between PB091 and D-2189: 1) PB091 has an additional NPRS domain as compared to D-2189; 2) the D-2189 PKS domain contains a dehydratase domain (DHt) which is absent from PB091; 3) D-2189 lacks an aminotransferase (AmT) module, although this could be possibly a result of the D-2189 contig_47 being not spanning the entire BGC. Both clusters contain the conserved domain TIGR01720, which belongs to the family NRPS-para261. The InterPro domain TIGR01720 is classified as a model and implicated in post-condensation modification events (Lu *et al.* 2020).

Substrates of adenylation domains (A) in the NRPS modules were predicted based on residues in the binding pocket (Stachelhaus, Mootz and Marahiel 1999) (Table S4-5, Fig. 4-7). The predicted consensus peptide from NRPSPredictor2 and UMaryland NRPS/PKS analyst tools for PB091 was the following 11 amino acid (aa) long peptide: H-Ser-Asp-Thr-Arg-Ser-Thr-Val-Thr-Thr-Thr-Orn-NH_2 (1,184 g/mol). This differs from D-2189 prediction, which was the following 9 aa long peptide: H-Ser-Asp-Thr-Gly-Thr-Thr-Ser-Arg-Orn-NH_2 (956 g/mol).

The predicted delftibactin-A peptide differs slightly from the 10 aa long peptide resolved by NMR from the clarified supernatant of D-2189 and subsequently synthesised: H-Ala-Ser-Asp-Thr-Gly-Thr-Orn-Ser-Arg-Orn-NH_2 (1,058 g/mol) (Tejman-Yarden *et al.* 2019). There are two differences between the synthesised peptide and predicted one: (i) the synthesised peptide contains an additional Alanine at the start of the chain; and (ii) at position 7 of the synthesised peptide, there is a nonproteogenic aa Ornithine in place of a Threonine.

The spectra from MALDI-TOF MS using a SEC purified fraction of active compound had a dominant peak at 919.2 *m/z* (Fig. 4-7). Unfortunately, there were several other peaks making the determination of an exact mass not possible in this instance.

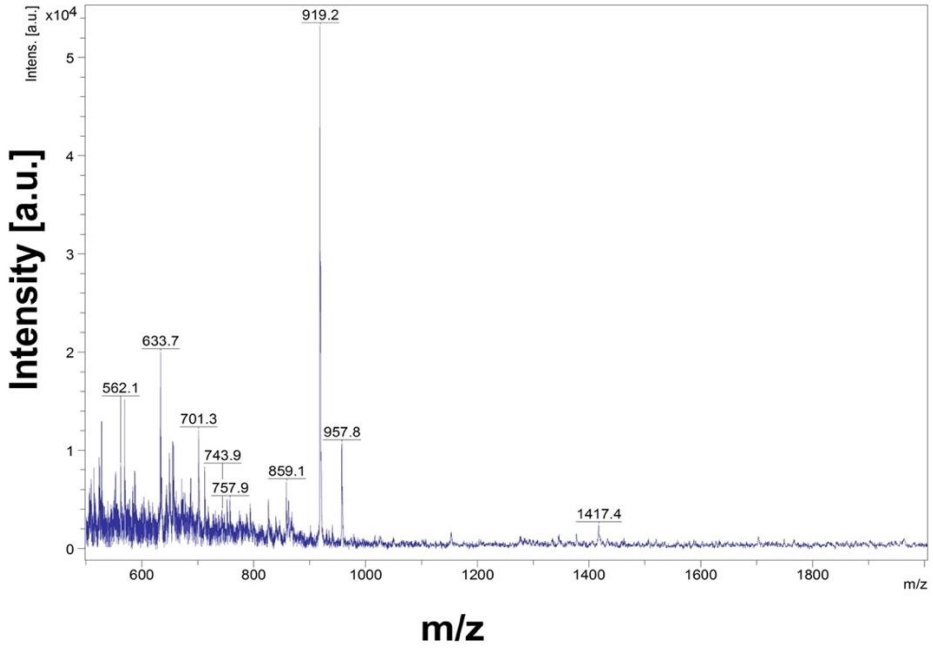

Figure 4-7. MALDI-TOF MS spectra of PB091_S70.

4.4. Discussion

4.4.1. Delftibactin-A as the putative compound displaying antimicrobial effect

It is most likely that PB091_S70 is a delftibactin, similar to that described from *Delftia* sp. D-2189 (Tejman-Yarden *et al.* 2019). This is informed by: 1) the spectrum in antibacterial activity originally detected from PB091 is similar to D-2189; 2) similar extraction protocols for the isolation of PB091_S70 and D-2189 delftibactin-A; and 3) the MALDI-TOF MS spectra indicating a strong peak at 919 *m*/*z* suggesting the compound is likely a short peptide.

Early screening of PB091 by plate-based antagonism assays revealed activity against MRSA, *E. coli*, and *K. pneumoniae* (Chapter 2). Delftibactin A was observed to have activity against Gram-positive pathogens MRSA and Vancomycin resistant *Enterococcus* (VRE), in addition to the Gram-negative pathogens *A. baumannii* and *Klebsiella pneumoniae* (Tejman-Yarden *et al.* 2019). Elsewhere, a delftibactin-like BGC was detected in *Acidovorax paradox* KB5, an organism with antagonistic activity against *Pseudomonas syringae*, a tomato pathogen (Hong *et al.* 2017). However, only Gram-positive inhibitory activity was observed from the supernatant of PB091 when cultivated in liquid media. There does remain the potential for isolating an anti-Gram-negative compound from PB091. This may be a secondary compound, not captured with the method presented here or a compound that had become deactivated during the process of liquid fermentation.

PB091_S70 was isolated in different conditions to D-2189 delftibactin A. PB091 was incubated at room temperature, while D-2189 was incubated at 30°C and 37°C but the extraction protocol here and for D-2189 did not include orbital shaking (Tejman-Yarden *et al.* 2019). The authors note that Delftibactin A

production was temperature dependent. This could be a possible reason for PB091_S70 having only Gram-positive activity, while D-2189 delftibactin A displayed both Gram-positive and Gram-negative activity.

Possibly due to lacking any post-translational modifications, a synthetic delftibactin A did not inhibit the same as the supernatant extractions (Tejman-Yarden *et al.* 2019). Furthermore, the delftibacin A/B cluster on the MiBIG resource only has the minimum level of annotation, most of which are predicted proteins. Further investigation is needed to provide a deeper understanding of the production of delftibactin A/B, such as better characterising the BGC and identifying a means of scaling production.

Two of the four antiSMASH results were singled out as promising identities for PB091_S70. These were the RiPP-like RRE containing cluster, which was identified as producing a putative bacteriocin, and the NRPS-T1PKS hybrid producing the siderophore delftibactin A/B. Bacteriocins vary in size, microcins for examples are <10 kDa in size (Duquesne *et al.* 2007), while colicin-like bacteriocins can be >20 kDa (Baquero and Moreno 1984). NRPSs are much smaller, generally ~10 amino acids in length (Montavon and Bruner 2010). In addition to what was observed in the MALDI-TOF MS, this knowledge would indicate that PB091_S70 is more likely to be an NRPs since the two highest charges were 957 and 1,417.4 *m*/*z*.

Fourteen *D. acidovorans* strains were analysed using antiSMASH v.5. The software identified 4 putative BGCs for PB091, which is not a high number of BGCs for organisms belonging to the genus *Delftia*. Members such as *D. tsuruhatensis* have 10 BGCs, while strain *D. acidovorans* NBRC 14950 has 7 (Table S4-1). Regarding the diversity of BGCs, other strains of *D. acidovorans*

deserve closer inspection to explore further the diversity of delftibactins and other BGCs within this genus. The whole genome of PB091 demonstrated that PB091 delftibactin is not structurally identical to the delftibactin A from Tejman-Yarden and colleagues (2019) investigation, based on sequence identity and peptide structure. Exploring the structural diversity of delftibactin BGC in addition to the predicted delftibactin peptide structures from *Delftia* organisms may aid in understanding this peptide in greater detail.

Delftia spp. are primarily reported as being isolated from terrestrial habitats. Recent metagenomic studies of various habitats are resolving MAGs of *D. acidovorans* that indicate that this organism can be found in Amazonian rivers and as part of the gut microbiota of Rainbow Trout (Rimoldi *et al.* 2019; Pérez-Pascual *et al.* 2021). Here, we report the first hybrid draft whole-genome of a *D. acidovorans* strain isolated from a deep-sea sponge, indicating that the habitat range of this organism is broader than initially thought.

4.4.2. Purification of *D. acidovorans* strain PB091 derived antibacterial compound was hampered by low yields

The most significant drawback to the purification strategy was the low yield of compound from PB091. The low productivity of PB091_S70 made extensive investigation laborious and time consuming, with the majority of the time invested in the purification steps. An additional alternative would be to synthesise peptides for investigation, but this would require extensive investigation of the structure of BGCs and the mass spectrometry data on the active compound itself. And this has been previously attempted to no success (Tejman-Yarden *et al.* 2019). Heterologous expression could be the alternative

approach to achieving sufficient yields for further characterisation and analysis of this compound (Olano *et al.* 2008; He *et al.* 2018).

Low yield could be the result of the purification method or the fermentation media utilised in the production of PB091_S70. In PB091 fermentation orbital shaking did not have a noticeable effect on production, which is in contrast to what was observed for D-2189 where the inclusion of orbital shaking impeded production (Tejman-Yarden *et al.* 2019). Furthermore, the authors reported improved production at 30°C as opposed to 37°C. PB091 was always fermented at room temperature, as such the effect of temperature on production cannot be comment. Since PB091 was isolated from a cold-water habitat (4-5°C) effort was not directed to cultivating PB091 at higher temperatures.

PB091, and other *Delftia* isolates, would benefit from applying OSMAC (one strain, many active compounds) (Romano *et al.* 2018) principles in identifying an optimum fermentation media, or a condition post-fermentation, for maximal production. PB091 was observed to produce the antimicrobial activity in LB and, to a lesser extent NB. Adjustments to incubation temperatures, shaking speeds, trace metal concentrations and vitamin additives can lead to identification of a fermentation process that can generate greater yields. This approach has found success in fungi and bacteria using growth nutritional arrays (Bills *et al.* 2008; Matobole *et al.* 2017). Given the reported delftibactin A functional role in detoxifying gold (Johnston *et al.* 2013; Wyatt, Johnston and Magarvey 2014), it would be of interest to test if the presence of gold particles during fermentation increased PB091_S70 production.

Greater attention to production conditions may also identify conditions in which the putative bacteriocin identified using antiSMASH could be produced. Finally,

the lack of Gram-negative activity in purified S70 fractions from PB091 is notable; this activity was detected on plate assays (Chapter 2) but not in liquid cultivation. While not reported in this chapter, efforts were made to extract Gram-negative active compounds from agar cultures using solvents (MeOH, ACN) to no success. The above-mentioned methods could lead to conditions in which a compound exhibiting Gram-negative activity was recovered.

4.4.3. PB091_S70 compound displayed no toxicity in *Galleria mellonella* and a slight bacteriostatic effect

Before any natural product can be considered for therapy, any toxic effect must be reported. Here we report that PB091_S70 at concentrations of > 200 µg/ml is non-toxic to *G. mellonella* larvae (Fig. 4-4). The MICs against the tested Gram-positive strains were all less than 50 µg/ml. This was initially promising, however, survival of larvae treated with PB091_S70 after infection with *S. aureus* NTCT 12493 did not improve as a result of treatment with PB091_S70. Despite the maximum concentration available being administered, when accounting for the internal dilution on injection into larvae this was only 0.2 X MIC. The same issue is relevant for the time-kill assay. These assays would be worth revisiting with higher PB091 concentrations to determine if the dose-dependent effect observed in the time-kill assay can lead to the identification of an effective *in vivo* and *in vitro* concentration for PB091_S70.

Results from the *G. mellonella* infection assay with MRSA 12493 are inconclusive, given that a high enough concentration of PB091_S70 could not be recovered to run the assay at a high concentration of PB091_S70. The assay could be improved by reducing the time between infection and treatment, as reducing the interval from 2 h to 30 minutes can increase the potency of

antimicrobial peptides (Gibreel and Upton 2013). It is currently not known how PB091_S70 interacts with the larval haemolymph, and degradation of the compound should not be ruled out as a possibility, limiting the bioavailability of PB091_S70 to treat MRSA infection.

This is a very minimal investigation of the potential fo PB091_S70 as an antibiotic substance. Future works should expand on this, first prioritising increased production in addition to identifying means by which to access the gram-negative inhibitory activity that was observed in plate-assays in Chapter 1. Next work should the progress to attaining an accurate mass and predictive structure of PB091_S70, to futher corroborate with the genomic data presented here. Finally with increased access to more active substance, work should then be directed to additional bioassays, such as its efficacy in hemolysis assays, lysisng of human cells lines. Should activity still not be optimal, changes to the peptide chain could be introduced by syntehsising new versions of PB091_S70 with the goal of improving efficacy.

4.5. Conclusion

In this study we purified an antimicrobial from *D. acidovorans* PB091, identified here as PB091_S70 which is likely a delftibactin. Presented is a hybrid whole-genome sequencing using short- and long-read platforms generating a near complete genome with no detectable contamination. We conducted a comprehensive phylogenetic analysis, genome comparison and biosynthetic potential analysis of PB091 and related *Delftia* species. This investigation has expanded on existing knowledge on the antimicrobial potential of *Delftia acidovorans.*

PB091_S70 was demonstrated to be non-toxic at 200 µg/ml, but not an effective treatment against MRSA 12493 during an *in vitro* time-kill assay, under the conditions employed here. In this investigation, it has been identified that the PB091 delftibactin NRPS-PKS hybrid differs from the one previously reported in strain D-2189. It should be noted that existing understanding of *Delftia* secondary metabolite pathways is still very limited. While the strain PB091 might not generate a compound at sufficient concentrations for further investigation, other *D. acidovorans* strains isolated from various habitats could be explored further or alternative approaches to accessing BGC encoded compounds could be attempted.

General Discussion

Introduction

Natural product discovery for bacterially-derived antibiotics is burdened with low success rates, and exploring taxonomically new spaces such as the deep-sea Hexactinellid sponges *Pheronema carpenteri* and *Hertwigia* sp. presented unique opportunities to screen bacterial cultivated from previously untested organisms. The aims of this thesis were: (1) to cultivate multiple bacterial isolates testing positive in antibiotic assay screens; (2) to conduct an *in silico* survey of the bacterial community of *P. carpenteri* and an attempt to identify biosynthetic gene clusters (BGCs) through metagenomic sequencing; (3) to identify promising bioactive candidates to be carried forward; and finally (4) refining an existing *in vivo* antibiotic efficacy assay utilising *Galleria mellonella*. The main findings of this body of work are herein discussed.

Pheronema carpenteri as a source of bacterially-derived antibiotics

Summary of findings

The scope of this thesis was to explore deep-sea hexactinellids for antibiotic NPs. The first research question presented was: can hexactinellid sponges be good organisms to screen for bacterially derived antibiotics? This was approached by testing 9 individual hexactinellid sponges belonging to *Hertwigia* and *Pheronema carpenteri*. In summary, it was observed that lower abundances of bacteria were recovered from *P. carpenteri* than *Hertwigia* sponges, but a higher proportion of those isolates demonstrated antibacterial activity. A focus was identifying incubation conditions that lead to increased recovery of antibiotic-producing SAB. There was no clear answer to the

questions posed as multiple factors influenced the outcomes, including (i) individual sponge sample, (ii) screening method, and (iii) recovery conditions (media, temperature, and pressure).

Of the bacteria recovered, taxonomically similar organisms were retrieved from North Atlantic *P. carpenteri* as the Antarctic hexactinellid sponge *Rossella nuda*, such as *Dietzia* sp. (Xin *et al.* 2011). Many other bacteria recovered from *P. carpenteri* and *Hertwigia* sp. demonstrated activity, including five isolates previously unobserved in plate-based antagonistic assays that were stimulated to produce antimicrobial activity during an OSMAC screen following PCR screening by amplifying PKS and NRPS genes. One active strain in particular that initially looked promising was *Delftia acidovorans* PB091, recovered from *P. carpenteri* and displaying antimicrobial activity against *Escherichia coli* and Methicillin-resistant *Staphylococcus aureus* (MRSA). Further comments for this strain follow below.

When the community composition of *P. carpenteri* was further explored, several observations were made: (i) bioactive isolates recovered from cultivation efforts belong to the genera that constitute the low abundance organisms; (ii) *P. carpenteri* microbiota displays both intra- and inter-species uniqueness, particularly with the relative abundances of Actinobacteria and Planctomycetes; and (iii) *P. carpenteri* prokaryotic community shows similarity to both LMA and HMA sponges.

Wider implications

Data presented in this thesis adds to the growing body of work focused on Hexactinellid sponges. The 16S rRNA amplicon sequencing investigation expands on another species of deep-water sponge that was previously

unexplored. The literature reports on a sponge-individual-specific microbiome within hexactinellid sponges (Busch *et al.* 2020a; Steinert *et al.* 2020), and within those studies, the implication of this specificity impacts ecological function, and the work presented in this thesis suggests that this likewise has an impact on NP screening efforts.

The 'one strain, many active compounds' (OSMAC) strategy employed in this thesis demonstrated the effect of cryptic gene expression for SMs. A similar outcome was previously reported for SAB (Matobole *et al.* 2017). Work presented in Chapter 1 emphasises the necessity to employ a range of screening techniques to capture a wide range of potential antibacterial activity from isolated bacteria.

An exciting observation was that *P. carpenteri* aggregations have community structures similar to low and high microbial abundance (LMA/HMA) sponges. Hexactinellids are only beginning to be discussed in terms of the LMA/HMA dichotomy and have generally been classified as LMA sponges (Steinert *et al.* 2020), so it is interesting to begin identifying sponge species that do not entirely follow this established dichotomy.

Overall limitations

The observation from 16S rRNA gene sequence data that cultivation efforts with *P. carpenteri* are only capturing the low abundance organisms has been previously observed on shallow-water sponges (Esteves *et al.* 2016). However, in the study by Esteves and colleagues, the abundance of cultivated bacteria represented within the host was highly variable (0.5-92% of total relative abundance), while from *P. carpenteri,* it was only 0.1-0.5%. A recent codon usage bias analysis of publicly available genomes (isolates, single-cell amplified

genomes (SAGs), and metagenome-assembled genomes (MAGs)) illustrated that the majority of the highly abundant secondary metabolite genes for cell defence was found in slow-growing oligotrophic bacteria primarily present within the MAGs and SAGs (Weissman, Hou and Fuhrman 2021). The study by Weissman and colleagues illustrated a niche that could not be exploited by traditional means of cultivation. Slow growing oligotrophs are challenging to cultivate, and the usage of 4°C and 90 days incubation did not yield any promising bacterial isolates from the deep-sea sponges utilised.

Sequencing the metagenome of a *P. carpenteri* sample using the Oxford Nanopore MinION sequencing platform was unsuccessful in identifying BGCs due to the low number of reads sequenced. Sequencing a *P. carpenteri* metagenome was limited by the difficulty in achieving the high DNA concentration to prepare the sequencing library (1 mg dsDNA), regardless of which sponge samples were utilised. Metagenomic sequencing to screen for BGCs can be improved.

The ONT sequencing technique is optimised for long strands of DNA, and the DNeasy PowerSoil Kit (Qiagen) used in this study resulted in fragmentation of metagenomic DNA. An alternate option could be to use the Field Sequencing Kit (ONT; SQK-LRK001) instead of the Ligation Sequencing Kit (ONT; SQK-LSK110). The Ligation Sequencing Kit requires a minimum of 1 mg of dsDNA starting material, and during the clean-up steps of the library preparation, there is frequently a loss of DNA (Tyler *et al.* 2018). In this study, Sponge 29 metagenome was sequenced with less than the recommended starting material, which may have impacted the number of reads generated. The Field Sequencing Kit recommended input is 400 ng dsDNA and this may have suited

low DNA yielding samples better; this would not address the high fragmentation but may increase the number of reads sequenced. One final methodological change reported to work well for low DNA samples was to run a duplicated second library after 1 h of sequencing (Tyler *et al.* 2018).

Future directions

This body of work focused on hexactinellid sponges, a highly unrepresented class of deep-water sponges. The continued inclusion of hexactinellid sponges in culture-based and culture-independent microbiological studies will benefit our broader understanding of sponge microbiomes. Likewise, this should also be extended to the additional classes of sponges Calcarea and Homoscleromorpha. This will help address questions around the differences in bacterial producers isolated from different sponge classes and how cultivation strategies might be adjusted to cater to the separate sponge classes.

More 16S rRNA gene amplicon surveys of hexactinellid sponges, which constitute most deep-water sponges, can only widen our understanding of the deep-sea sponge holobiome and how it may be explored for NP discovery. Included within this should be more investigations of *Pheronema* sponges and how their aggregations, which can display distinct microbial communities, may be utilised for bacterial NPs.

This study was unsuccessful in utilising metagenomic sequencing as a tool for NP discovery. A much more comprehensive investigation into the diversity of bacterial genes in the *P. carpenteri* microbiome should still be explored. With a more comprehensive dataset, BGC screening and identification could begin for this species, which would uncover the biotechnical potential of the uncultivable majority.

The OSMAC pipeline described within this body of work can detect a broader range of biological activity by combining micro-fermentation of bacterial isolates with bioautography based antibacterial screening. This permits scalability and some degree of automation that could lead to rapid detection of candidate isolates for future work. Coupling the OSMAC approach with robust chemical dereplication will concentrate effort in identifying and investigating new natural products. Methods utilising liquid chromatography-Mass Spectrometry (LC-MS) have demonstrated this as a rapid tool for analysing products of 149 marine *Salinipora* and *Streptomyces* strains (Crüsemann *et al.* 2017). LC-MS is one of many approaches proposed as effective methods for NP dereplication (Hubert et al., 2017).

This body of work has led to the recovery of several bacterial isolates from deep-sea hexactinellids that displayed, on either a plate-based assay, OSMAC or PCR screen, the potential for antimicrobial production. This is a valuable resource that should be further explored. Screening of existing culture collections may reveal new insight into the taxa of bacteria that are and are not bioactive.

Galleria mellonella larvae is a powerful tool for identifying lead compounds

Summary of findings

The third research question posed was: how can early compound discovery be coupled with *in vivo* assays to facilitate selecting a lead compound with high efficacy? This was achieved in Chapter 3 by exploring the commonly utilised insect larvae model *Galleria mellonella*. The study outcomes were: (i) that

reliability and standardisation of pet-food grade *G. mellonella* larvae can be improved by controlling larvae weight, and (ii) that lipid metabolism of the larvae fat body during infection could be a potentially new measure to determine antimicrobial efficacy. Several linear regression models were implemented as potential tools in guiding experimental design with *G. mellonella*.

Wider implications

G. mellonella has gained widespread scientific interest as an insect model (Junqueira, Mylonakis and Borghi 2021). This study has immediate methodological implications that are easy to incorporate into any *G. mellonella* assay. Linear models correlating larvae weight with the lethal median dose (LD_{50}) impact study design when testing antimicrobial efficacy, while linear models correlating larvae length vs weight present a potentially quicker alternate method of separating larvae into weight categories. It likewise highlights the importance of reporting on larvae weight used in investigations, something not always done (Andrea, Krogfelt and Jenssen 2019), as this parameter can impact study outcomes.

Overall limitations

This study was only limited to using Methicillin-resistant *Staphylococcus aureus* NCTC 12493, which illustrates the scope of expanding such work to multiple pathogens and observing differences between different strains of the same organism. Pet-food grade larvae are broadly used in microbiological investigations (Andrea, Krogfelt and Jenssen 2019). Sourcing larvae this way is limited immensley by the many unknowns of the rearing conditions of the larvae. Larvae in this investigation were not left to acclimatise before experimentation, reported between 1 h and 2 days at 37°C (Andrea, Krogfelt

and Jenssen 2019; Sheehan, Dixon and Kavanagh 2019; Fredericks *et al.* 2020). However, acclimatisation is not always a reported strategy, or where it is, the recommended acclimatisation occurs over one or more life cycles of the larvae (Firacative *et al.* 2020). There is currently no clear indication of how the acclimatisation length and temperature might impact experimentation design.

This also links back to unknown rearing conditions of the larvae before receipt from the breeder, and larvae may well be kept at warm temperatures before arrival. Finally, investigating the relationship between pupation time and larvae weight could have been expanded to include larvae treated with a placebo of phosphate-buffered saline (PBS), observing how the stress of injection interferes with pupation times.

Future directions

Future work may wish to expand on the range of organisms a weight-dependent LD_{50} can be achieved for testing on low and high pathogenic strains and expanding to additional microorganisms that are of interest in antibiotic efficacy screening. *G. mellonella* has been validated as an infection model for > 65 strains of bacteria and fungi (Tsai, Loh and Proft 2016), and it would be of value to understand if different pathogens also lead to this lipolysis immune response observed when infected with MRSA.

The finding that lipid content can be a measure of health post-infection could be a promising new means by which to detect the effect of antibiotic efficacy *in vivo* accurately. The detected lipolysis immune response in *G. mellonella* larvae could be employed to detect whether the tested antibiotic reduces lipid depletion as the infection is treated. Furthermore, there remains the uncertainty

of inconsistencies observed with higher weight group larvae that could be further explored.

With a whole-genome sequence of *G. mellonella* available (Lange *et al.* 2018), *G. mellonella* work begins to enter a 'molecular age' of genomics, transcriptomics and proteomics work (Dinh *et al.* 2021). This new phase will continue to aid in better understanding this model. The low entry requirements to begin working with *G. mellonella* makes the future use of *G. mellonella* as a widely used microbiological model highly promising.

A Delftibactin A-like compound is a promising candidate from *Delftia acidovorans* strain PB091, requiring further characterisation and optimisation

Summary of findings

While not a research question exactly, the thesis's focus was to take a promising candidate and progress the SM through an early characterisation pipeline. This was done in Chapter 4 with the *P. carpenteri* cultivated SAB *Delftia acidovorans* strain PB091. Delftibactin A/B was hypothesised as the active compound, supported by similar work on an environmentally isolated *Delftia* sp. (Tejman-Yarden *et al.* 2019). PB091_S70 was active only against Gram-positive bacteria, primarily various Methicillin-resistant *Staphylococcus aureus* (MRSA) strains. PB091_S70 was identified as being a delftibactin peptide by analysing the whole genome of the isolate. PB091_S70 has a mean MIC of 25 µg/ml again multiple MRSA strains, was non-toxic in *G. mellonella* but did not improve the survivability of larvae during *in vivo* (*G. mellonella*) infection and displayed a slight bacteriostatic effect during *in vitro* (time-kill) assays.

There was evidence to suggest that poor performance during *in vitro* time-kill assay was due to low concentration.

Wider implications

Work presented here expands on the reported habitat range of *Delftia* sp. organisms. They are reported as ubiquitous environmental organisms, having been cultivated from various habitats. This work here is the first report of a *Delftia* sp. organism from a deep-sea sponge, detected both in cultivation efforts and in the 16S rRNA gene survey of *P. carpenteri* (Chapter 2). This work also supports the current position of delftibactin A/B as a promising antimicrobial (Tejman-Yarden *et al.* 2019), extending the biological functions of this siderophore beyond biomineralisation (Johnston *et al.* 2013; Wyatt, Johnston and Magarvey 2014).

The draft whole genome generated during this study has use in future research due to only a small number of complete genomes of *Delftia* species. PB091 whole-genome consist of only 5 contigs, is assembled from both long and short-read sequencing and contains no detectable contamination, so there is value in the hybrid-assembled genome as a future reference genome for the genus especially when the only other draft genome of an antibiotic producing *Delftia* strain is currently composed of 110 contigs.

Overall limitations

The work on *D. acidovorans* presented here was limited by low product yield and low bioactivity observed in assays. To entirely rule out PB091_S70 as a suitable *in vivo* candidate, more efforts should be made to purify higher concentrations for the *in vivo* experimentations. Unfortunately, high concentrations of PB091_S70 could not be achieved during this work with

PB091. While not reported in the chapter, unsuccessful attempts were made to identify the anti-Gram-negative activity, such as re-suspending PB091 bacterial in organic solvents (Methanol, Acetate, and Acetonitrile), and macerating agar plates with PB091 and incubating it in organic solvents. PB091_S70 was never purified by High-Performance Liquid Chromatography (HPLC), which resulted in unclear Mass Spectra of which peak is the active compound, thus determining an accurate mass was not possible from MALDI-TOF MS. No attempts were made to apply OSMAC principles on PB091 to identify nutrient conditions that may have induced anti-Gram-negative activity in liquid culture. If PB091 is continued to be limited by the quantity of SM that can be harvested from it, alternative directions will need to be taken.

Future directions

D. acidovorans PB091 and related strains displaying antimicrobial activity are worthy of closer inspection. Future work will likely need to take the form of further characterising the BGC *in silico*. Within the National Centre for Biotechnology Information (NCBI), there are 26 *D. acidovorans* draft genomes recovered from a range of environments. This is a good set of data to begin working towards better characterising the delftibactin A/B cluster. With PB091 in particular, future work should focus on purifying the anti-Gram-negative activity, which can be observed on plate-based assays but not expressed in liquid cultures. A persistent pitfall within working with delftibactin A and PB091_S70 was the low product yields. Synthetic production of delftibactin-A has previously been unsuccessful (Tejman-Yarden *et al.* 2019), so future work could focus on heterologous expression.

Bibliography

Abdallah RA, Beye M, Diop A *et al.* The impact of culturomics on taxonomy in clinical microbiology. *Antonie van Leeuwenhoek, International Journal of General and Molecular Microbiology* 2017;**110**:1327–37.

Abdel-Mageed WM, Lehri B, Jarmusch SA *et al.* Whole genome sequencing of four bacterial strains from South Shetland Trench revealing biosynthetic and environmental adaptation gene clusters. *Marine Genomics* 2020:100782.

Abdelmohsen UR, Bayer K, Hentschel U. Diversity, abundance and natural products of marine sponge-associated Actinomycetes. *Natural Product Reports* 2014;**31**:381–99.

Abdelmohsen UR, Pimentel-Elardo SM, Hanora A *et al.* Isolation, Phylogenetic Analysis and Anti-infective Activity Screening of Marine Sponge-Associated Actinomycetes. *Marine Drugs* 2010;**8**:399–412.

Adamek M, Spohn M, Stegmann E *et al.* Mining bacterial genomes for secondary metabolite gene clusters. *Methods in Molecular Biology* 2017;**1520**:23–47.

Afonso TB, Costa MS, Rezende De Castro R *et al.* Bartolosides E-K from a Marine coccoid cyanobacterium. *Journal of Natural Products* 2016;**79**:2504–13.

Alghoribi MF, Gibreel TM, Dodgson AR *et al. Galleria mellonella* infection model demonstrates high lethality of ST69 and ST127 uropathogenic *E. coli*. *PLoS One* 2014;**9**:e101547–e101547.

Amade P, Charroin C, Baby C *et al.* Antimicrobial activities of marine sponges from the Mediterranean Sea. *Marine Biology* 1987;**94**:271–5.

Amade P, Pesando D, Chevolot L. Antimicrobial activities of marine sponges from French Polynesia and Brittany. *Marine Biology* 1982;**70**:223–8.

Amann RI, Ludwig W, Schleifer KH. Phylogenetic identification and in situ detection of individual microbial cells without cultivation. *Microbiol Rev* 1995;**59**:143–69.

American Society for Testing and Materials International. *Standard Guide for Assessment of Antimicriobial Activity Using a Time-Kill Procedure*., 2016.

Andrea A, Krogfelt KA, Jenssen H. Methods and Challenges of Using the Greater Wax Moth (*Galleria mellonella*) as a Model Organism in Antimicrobial Compound Discovery. *Microorganisms* 2019;**7**:85.

Anjum K, Abbas SQ, Shah SAA *et al.* Marine sponges as a drug treasure. *Biomolecules and Therapeutics* 2016;**24**:347–62.

Anteneh YS, Yang Q, Brown MH *et al.* Antimicrobial Activities of Marine Sponge-Associated Bacteria. *Microorganisms* 2021;**9**:171.

Arteaga Blanco LA, Crispim JS, Fernandes KM *et al.* Differential cellular immune response of *Galleria mellonella* to *Actinobacillus pleuropneumoniae*. *Cell and Tissue Research* 2017;**370**:153–68.

Axenov-Gribanov D, Rebets Y, Tokovenko B *et al.* The isolation and characterization of Actinobacteria from dominant benthic macroinvertebrates endemic to Lake Baikal. *Folia Microbiol (Praha)* 2016;**61**:159–68.

Ba X, Harrison EM, Lovering AL *et al.* Old drugs to treat resistant bugs: Methicillin-resistant *Staphylococcus aureus* isolates with mecC are susceptible to a combination of penicillin and clavulanic acid. *Antimicrobial Agents and Chemotherapy* 2015;**59**:7396–404.

Bankevich A, Nurk S, Antipov D *et al.* SPAdes: A new genome assembly algorithm and its applications to single-cell sequencing. *Journal of Computational Biology* 2012;**19**:455–77.

Banville N, Browne N, Kavanagh K. Effect of nutrient deprivation on the susceptibility of *Galleria mellonella* larvae to infection. *Virulence* 2012;**3**:497.

Baquero F, Moreno F. The microcins. *FEMS Microbiology Letters* 1984;**23**:117–24.

Bateman A, The UniProt Consortium. UniProt: a worldwide hub of protein knowledge. *Nucleic Acids Research* 2018;**47**:D506–15.

Bayer K, Busch K, Kenchington E *et al.* Microbial Strategies for Survival in the Glass Sponge *Vazella pourtalesii*. *mSystems* 2020;**5**, DOI: 10.1128/msystems.00473-20.

Bayer K, Kamke J, Hentschel U. Quantification of bacterial and archaeal symbionts in high and low microbial abundance sponges using real-time PCR. *FEMS Microbiology Ecology* 2014;**89**:679–90.

Bayer K, Schmitt S, Hentschel U. Microbial nitrification in Mediterranean sponges: possible involvement of ammonium-oxidizing Betaproteobacteria. Museu Nacional, 2008.

Bazaid AS, Forbes S, Humphreys GJ *et al.* Fatty Acid Supplementation Reverses the Small Colony Variant Phenotype in Triclosan-Adapted *Staphylococcus aureus*: Genetic, Proteomic and Phenotypic Analyses. *Scientific Reports* 2018;**8**, DOI: 10.1038/s41598-018-21925-6.

Beaulieu SE. Life on glass houses: sponge stalk communities in the deep-sea. *Marine Biology* 2001;**138**:803–17.

Beazley LI, Kenchington EL, Murillo FJ *et al.* Deep-sea sponge grounds enhance diversity and abundance of epibenthic megafauna in the Northwest Atlantic. *ICES Journal of Marine Science* 2013;**70**:1471–90.

Berrue F, Ibrahim A, Boland P *et al.* Newly isolated marine *Bacillus pumilus* (SP21): A source of novel lipoamides and other antimicrobial agents. *Pure and Applied Chemistry*. Vol 81. De Gruyter, 2009, 1027–31.

Betina V. Bioautography in paper and thin-layer chromatography and its scope in the antibiotic field. *Journal of Chromatography A* 1973;**78**:41–51.

Bett BJ, Rice AL. The influence of hexactinellid sponge (*Pheronema carpenteri*) spicules on the patchy distribution of macrobenthos in the Porcupine Seabight (Bathyal NE Atlantic). *Ophelia* 1992;**36**:217–26.

Bhattacharya A, Pak HTY, Bashey F. Plastic responses to competition: Does bacteriocin production increase in the presence of nonself competitors? *Ecology and Evolution* 2018;**8**:6880–8.

Bibb MJ. Regulation of secondary metabolism in *Streptomycetes*. *Current Opinion in Microbiology* 2005;**8**:208–15.

Bibi F, Yasir M, Al-Sofyani A *et al.* Antimicrobial activity of bacteria from marine sponge *Suberea mollis* and bioactive metabolites of *Vibrio* sp. EA348. *Saudi Journal of Biological Sciences* 2020;**27**:1139–47.

Bilgin H, Sarmis A, Tigen E *et al. Delftia acidovorans*: A rare pathogen in immunocompetent and immunocompromised patients. *Canadian Journal of Infectious Diseases and Medical Microbiology* 2015;**26**:277–9.

Bills GF, Platas G, Fillola A *et al.* Enhancement of antibiotic and secondary metabolite detection from filamentous fungi by growth on nutritional arrays. *Journal of Applied Microbiology* 2008;**104**:1644–58.

Blin K, Shaw S, Kloosterman AM *et al.* AntiSMASH 6.0: Improving cluster detection and comparison capabilities. *Nucleic Acids Research* 2021;**49**:W29–35.

Blin K, Shaw S, Steinke K *et al.* antiSMASH 5.0: updates to the secondary metabolite genome mining pipeline. *Nucleic Acids Research* 2019, DOI: 10.1093/nar/gkz310.

Blodgett JAV, Zhang JK, Metcalf WW. Molecular cloning, sequence analysis, and heterologous expression of the phosphinothricin tripeptide biosynthetic gene cluster from *Streptomyces viridochromogenes* DSM 40736. *Antimicrobial Agents and Chemotherapy* 2005;**49**:230–40.

Blunt JW, Copp BR, Munro MHG *et al.* Marine natural products. *Natural Product Reports* 2005;**22**:15–61.

Bo M, Bertolino M, Bavestrello G *et al.* Role of deep sponge grounds in the Mediterranean Sea: A case study in southern Italy. *Hydrobiologia* 2012;**687**:163–77.

Bode HB, Bethe B, Hofs R *et al.* Big effects from small changes: possible ways to explore nature's chemical diversity. *Chembiochem* 2002;**3**:619–27.

Boedeker C, Schuler M, Reintjes G *et al.* Determining the bacterial cell biology of *Planctomycetes*. *Nat Commun* 2017;**8**:14853.

Bolger AM, Lohse M, Usadel B. Trimmomatic: A flexible trimmer for Illumina sequence data. *Bioinformatics* 2014;**30**:2114–20.

Boman HG, Hultmark D. Cell-free immunity in insects. *Annual review of microbiology* 1987;**41**:103–26.

Borchert E, Jackson SA, O'Gara F *et al.* Diversity of Natural Product Biosynthetic Genes in the Microbiome of the Deep Sea-Sponges *Inflatella pellicula*, *Poecillastra compressa*, and *Stelletta normani*. *Front Microbiol* 2016;**7**:1027.

Borchert E, Knobloch S, Dwyer E *et al.* Biotechnological Potential of Cold Adapted *Pseudoalteromonas* spp. Isolated from "Deep Sea" Sponges. *Mar Drugs* 2017a;**15**, DOI: 10.3390/md15060184.

Borchert E, Selvin J, Kiran SG *et al.* A novel cold active esterase from a Deep-Sea Sponge *Stelletta normani* Metagenomic Library. *Frontiers in Marine Science* 2017b;**4**, DOI: 10.3389/fmars.2017.00287.

Bowman JP. Methods for psychrophilic bacteria. *Methods in microbiology* 2001;**30**:591–614.

Bowman JP. Bioactive compound synthetic capacity and ecological significance of marine bacterial genus *Pseudoalteromonas*. *Marine Drugs* 2007;**5**:220–41.

Brackman G, Cos P, Maes L *et al.* Quorum sensing inhibitors increase the susceptibility of bacterial biofilms to antibiotics in vitro and in vivo. *Antimicrobial Agents and Chemotherapy* 2011;**55**:2655–61.

Braña V, Cagide C, Morel MA. The Sustainable Use of *Delftia* in Agriculture, Bioremediation, and Bioproducts Synthesis. *Microbial Models: From Environmental to Industrial Sustainability*. Springer Singapore, 2016, 227–47.

Brown BL, Watson M, Minot SS *et al.* MinION™ nanopore sequencing of environmental metagenomes: a synthetic approach. *Gigascience* 2017;**6**, DOI: 10.1093/gigascience/gix007.

Buchfink B, Xie C, Huson DH. Fast and sensitive protein alignment using DIAMOND. *Nature Methods* 2014;**12**:59–60.

Buck JD. Effects of medium composition on the recovery of bacteria from sea water. *Journal of Experimental Marine Biology and Ecology* 1974;**15**:25–34.

Bull AT, Stach JEM. Marine actinobacteria: new opportunities for natural product search and discovery. *Trends in Microbiology* 2007;**15**:491–9.

Burgsdorf I, Erwin PM, López-Legentil S *et al.* Biogeography rather than association with cyanobacteria structures symbiotic microbial communities in the marine sponge *Petrosia ficiformis*. *Frontiers in Microbiology* 2014;**5**, DOI: 10.3389/fmicb.2014.00529.

Busch K, Beazley L, Kenchington E *et al.* Microbial diversity of the glass sponge *Vazella pourtalesii* in response to anthropogenic activities. *Conservation Genetics* 2020a;**21**:1001–10.

Busch K, Hanz U, Mienis F *et al.* On giant shoulders: How a seamount affects the microbial community composition of seawater and sponges. *Biogeosciences* 2020b;**17**:3471–86.

Büyükgüzel E, Kalender Y. *Galleria mellonella* (L.) Survivorship, Development and Protein Content in Response to Dietary Antibiotics. *Journal of Entomological Science* 2008;**43**:27–40.

Cabello FC. Heavy use of prophylactic antibiotics in aquaculture: A growing problem for human and animal health and for the environment. *Environmental Microbiology* 2006;**8**:1137–44.

Caboche S, Pupin M, Leclère V *et al.* NORINE: A database of nonribosomal peptides. *Nucleic Acids Research* 2008;**36**, DOI: 10.1093/nar/gkm792.

Cagide C, Riviezzi B, Minteguiaga M *et al.* Identification of plant compounds involved in the microbe-plant communication during the coinoculation of soybean with *Bradyrhizobium elkanii* and *Delftia* sp. strain JD2. *Molecular Plant-Microbe Interactions* 2018;**31**:1192–9.

Carro L, Mulas R, Pastor-Bueis R *et al. Delftia rhizosphaerae* sp. Nov. isolated from the rhizosphere of *Cistus ladanifer*. *International Journal of Systematic and Evolutionary Microbiology* 2017;**67**:1957–60.

Centre of Disease Control. *Antibiotic Resistance Threats in the United States, 2019*. Atlanta, GA, 2019.

Champion OL, Wagley S, Titball RW. *Galleria mellonella* as a model host for microbiological and toxin research. *Virulence* 2016;**7**:840–5.

Chen WM, Lin YS, Sheu DS *et al. Delftia litopenaei* sp. nov., a poly-β-hydroxybutyrate- accumulating bacterium isolated from a freshwater shrimp

culture pond. *International Journal of Systematic and Evolutionary Microbiology* 2012;**62**:2315–21.

Chibebe Junior J, Fuchs BB, Sabino CP *et al.* Photodynamic and Antibiotic Therapy Impair the Pathogenesis of *Enterococcus faecium* in a Whole Animal Insect Model. *PLoS ONE* 2013;**8**:55926.

Cho JC, Giovannoni SJ. Cultivation and growth characteristics of a diverse group of oligotrophic marine *Gammaproteobacteria*. *Appl Environ Microbiol* 2004;**70**:432–40.

Chu JWF, Maldonado M, Yahel G *et al.* Glass sponge reefs as a silicon sink. *Marine Ecology Progress Series* 2011;**441**:1–14.

Coates AR, Halls G, Hu Y. Novel classes of antibiotics or more of the same? *British Journal of Pharmacology* 2011;**163**:184.

Coates CJ, Lim J, Harman K *et al.* The insect, *Galleria mellonella*, is a compatible model for evaluating the toxicology of okadaic acid. *Cell Biology and Toxicology* 2019;**35**:219–32.

Connon SA, Giovannoni SJ. High-throughput methods for culturing microorganisms in very-low-nutrient media yield diverse new marine isolates. *Applied and Environmental Microbiology* 2002;**68**:3878–85.

Connor TR, Loman NJ, Thompson S *et al.* CLIMB (the Cloud Infrastructure for Microbial Bioinformatics): an online resource for the medical microbiology community. *Microbial Genomics* 2016;**2**, DOI: https://doi.org/10.1099/mgen.0.000086.

De Coster W, D'Hert S, Schultz DT *et al.* NanoPack: visualizing and processing long-read sequencing data. *Bioinformatics* 2018;**34**:2666–9.

Cotter G, Doyle S, Kavanagh K. Development of an insect model for the *in vivo* pathogenicity testing of yeasts. *FEMS Immunology & Medical Microbiology* 2000;**27**:163–9.

Crüsemann M, O'Neill EC, Larson CB *et al.* Prioritizing Natural Product Diversity in a Collection of 146 Bacterial Strains Based on Growth and Extraction Protocols. *Journal of Natural Products* 2017;**80**:588–97.

Cytryńska M, Mak P, Zdybicka-Barabas A *et al.* Purification and characterization of eight peptides from *Galleria mellonella* immune hemolymph. *Peptides* 2007;**28**:533–46.

Czaplewski L, Bax R, Clokie M *et al.* Alternatives to antibiotics-a pipeline portfolio review. *The Lancet Infectious Diseases* 2016;**16**:239–51.

Darabpour E, Ardakani MR, Motamedi H *et al.* Isolation of a potent antibiotic producer bacterium, especially against MRSA, from northern region of the Persian Gulf. *Bosnian Journal of Basic Medical Sciences* 2012;**12**:108–21.

Darling AE, Jospin G, Lowe E *et al.* PhyloSift: Phylogenetic analysis of genomes and metagenomes. *PeerJ* 2014;**2014**:e243.

Davis HC, Guillard RR. Relative value of ten genera of micro-organisms as foods for oyster and clam larvae. 1958.

Davy SK, Trautman DA, Borowitzka MA *et al.* Ammonium excretion by a symbiotic sponge supplies the nitrogen requirements of its rhodophyte partner. *J Exp Biol* 2002;**205**:3505–11.

Department of Health and Social Care. *Tackling Antimicrobial Resistance 2019–2024*., 2019.

Desbois AP, Coote PJ. Chapter 2 - Utility of Greater Wax Moth Larva (*Galleria mellonella*) for Evaluating the Toxicity and Efficacy of New Antimicrobial Agents. In: Laskin AI, Sariaslani S, Gadd GM (eds.). *Advances in Applied Microbiology*. Vol 78. Academic Press, 2012, 25–53.

Desriac F, Jégou C, Balnois E *et al.* Antimicrobial peptides from marine proteobacteria. *Marine Drugs* 2013;**11**:3632–60.

Devi P, Wahidullah S, Rodrigues C *et al.* The Sponge-associated Bacterium *Bacillus licheniformis* SAB1: A Source of Antimicrobial Compounds. *Marine Drugs* 2010;**8**:1203–12.

Dewanjee S, Gangopadhyay M, Bhattacharya N *et al.* Bioautography and its scope in the field of natural product chemistry. *Journal of Pharmaceutical Analysis* 2015;**5**:75–84.

Diago-Navarro E, Chen L, Passet V *et al.* Carbapenem-resistant *Klebsiella pneumoniae* exhibit variability in capsular polysaccharide and capsule associated virulence traits. *Journal of Infectious Diseases* 2014;**210**:803–13.

Dieckmann R, Graeber I, Kaesler I *et al.* Rapid screening and dereplication of bacterial isolates from marine sponges of the sula ridge by intact-cell-MALDI-TOF mass spectrometry (ICM-MS). *Appl Microbiol Biotechnol* 2005;**67**:539–48.

Díez-Vives C, Taboada S, Leiva C *et al.* On the way to specificity - Microbiome reflects sponge genetic cluster primarily in highly structured populations. *Molecular Ecology* 2020;**29**:4412–27.

Dinh H, Semenec L, Kumar SS *et al.* Microbiology's next top model: *Galleria* in the molecular age. *Pathogens and disease* 2021;**79**:6.

Dong CL, Li LX, Cui ZH *et al.* Synergistic effect of pleuromutilins with other antimicrobial agents against *Staphylococcus aureus* in vitro and in an experimental *Galleria mellonella* model. *Frontiers in Pharmacology* 2017;**8**:553.

Duineveld GCA, de Wilde PAWJ, Berghuis EM *et al.* Benthic respiration and standing stock on two contrasting continental margins in the western Indian Ocean: The Yemen-Somali upwelling region and the margin off Kenya. *Deep-Sea Research Part II: Topical Studies in Oceanography*. Vol 44. 1997, 1293–317.

Duquesne S, Destoumieux-Garzón D, Peduzzi J *et al.* Microcins, gene-encoded antibacterial peptides from enterobacteria. *Natural Product Reports* 2007;**24**:708–34.

Ebner P, Rinker J, Nguyen MT *et al.* Excreted cytoplasmic proteins contribute to pathogenicity in *Staphylococcus aureus*. *Infection and Immunity* 2016;**84**:1672–81.

Economou V, Gousia P. Agriculture and food animals as a source of antimicrobial-resistant bacteria. *Infection and Drug Resistance* 2015;**8**:49–61.

Erwin PM, Coma R, Lopez-Sendino P *et al.* Stable symbionts across the HMA-LMA dichotomy: low seasonal and interannual variation in sponge-associated bacteria from taxonomically diverse hosts. *FEMS Microbiol Ecol* 2015;**91**:fiv115–fiv115.

Esteves AI, Amer N, Nguyen M *et al.* Sample Processing Impacts the Viability and Cultivability of the Sponge Microbiome. *Front Microbiol* 2016;**7**:499.

Fallon J, Kelly J, Kavanagh K. *Galleria mellonella* as a Model for Fungal Pathogenicity Testing. *Methods in Molecular Biology* 2012;**845**:469–85.

Fan L, Reynolds D, Liu M *et al.* Functional equivalence and evolutionary convergence in complex communities of microbial sponge symbionts. *Proceedings of the National Academy of Sciences* 2012;**109**:E1878–87.

Ferro TAF, Araújo JMM, dos Santos Pinto BL *et al.* Cinnamaldehyde Inhibits *Staphylococcus aureus* Virulence Factors and Protects against Infection in a *Galleria mellonella* Model. *Frontiers in Microbiology* 2016;**7**:2052.

Fiore CL, Baker DM, Lesser MP. Nitrogen Biogeochemistry in the Caribbean Sponge, *Xestospongia muta*: A Source or Sink of Dissolved Inorganic Nitrogen? *PLoS One* 2013;**8**:e72961.

Firacative C, Khan A, Duan S *et al.* Rearing and maintenance of *Galleria mellonella* and its application to study fungal virulence. *Journal of Fungi* 2020;**6**:1–13.

Flissi A, Ricart E, Campart C *et al.* Norine: Update of the nonribosomal peptide resource. *Nucleic Acids Research* 2020;**48**:D465–9.

Frank JA, Reich CI, Sharma S *et al.* Critical evaluation of two primers commonly used for amplification of bacterial 16S rRNA genes. *Applied and Environmental Microbiology* 2008;**74**:2461–70.

Fredericks LR, Lee MD, Roslund CR *et al.* The design and implementation of restraint devices for the injection of pathogenic microorganisms into *Galleria mellonella*. *PLoS ONE* 2020;**15**:e0230767.

Friedrich AB, Fischer I, Proksch P *et al.* Temporal variation of the microbial community associated with the mediterranean sponge *Aplysina aerophoba*. *FEMS Microbiol Ecol* 2001;**38**:105–15.

Frioux C, Singh D, Korcsmaros T *et al.* From bag-of-genes to bag-of-genomes: metabolic modelling of communities in the era of metagenome-assembled genomes. *Computational and Structural Biotechnology Journal* 2020;**18**:1722–34.

Gajardo K, Rodiles A, Kortner TM *et al.* A high-resolution map of the gut microbiota in Atlantic salmon (*Salmo salar*): A basis for comparative gut microbial research. *Scientific Reports* 2016;**6**, DOI: 10.1038/srep30893.

Gao ZM, Wang Y, Tian RM *et al.* Symbiotic Adaptation Drives Genome Streamlining of the Cyanobacterial Sponge Symbiont “Candidatus *Synechococcus spongiarum*". *mBio* 2014;**5**, DOI: 10.1128/mBio.00079-14.

Geng H, Belas R. Expression of tropodithietic acid biosynthesis is controlled by a novel autoinducer. *Journal of Bacteriology* 2010;**192**:4377–87.

Ghareeb MA, Tammam MA, El-Demerdash A *et al.* Insights about clinically approved and Preclinically investigated marine natural products. *Current Research in Biotechnology* 2020;**2**:88–102.

Ghyselinck J, Van Hoorde K, Hoste B *et al.* Evaluation of MALDI-TOF MS as a tool for high-throughput dereplication. *Journal of Microbiological Methods* 2011;**86**:327–36.

Gibreel TM, Upton M. Synthetic epidermicin NI01 can protect *Galleria mellonella* larvae from infection with *Staphylococcus aureus*. *Journal of Antimicrobial Chemotherapy* 2013;**68**:2269–73.

Giles EC, Kamke J, Moitinho-Silva L *et al.* Bacterial community profiles in low microbial abundance sponges. *FEMS Microbiol Ecol* 2013;**83**:232–41.

Gloeckner V, Wehrl M, Moitinho-Silva L *et al.* The HMA-LMA dichotomy revisited: an electron microscopical survey of 56 sponge species. *Biol Bull* 2014;**227**:78–88.

Graça AP, Bondoso J, Gaspar H *et al.* Antimicrobial Activity of Heterotrophic Bacterial Communities from the Marine Sponge *Erylus discophorus* (Astrophorida, Geodiidae). Schlievert PM (ed.). *PLoS ONE* 2013;**8**:e78992.

Guerrero-Garzón JF, Zehl M, Schneider O *et al. Streptomyces* spp. From the Marine Sponge *Antho dichotoma*: Analyses of Secondary Metabolite Biosynthesis Gene Clusters and Some of Their Products. *Frontiers in Microbiology* 2020;**11**:437.

Guerrieri CG, Pereira MF, Galdino ACM *et al.* Typical and Atypical Enteroaggregative *Escherichia coli* Are Both Virulent in the *Galleria mellonella* Model. *Frontiers in Microbiology* 2019;**10**:1791.

Guinebretière MH, Auger S, Galleron N *et al. Bacillus cytotoxicus* sp. nov. is a novel thermotolerant species of the *Bacillus cereus* group occasionally associated with food poisoning. *International Journal of Systematic and Evolutionary Microbiology* 2013;**63**:31–40.

Gunasekera SP, Pomponi SA, McCarthy PJ. Discobahamins A and B, new peptides from the bahamian deep water marine sponge discodermia sp. *Journal of Natural Products* 1994;**57**:79–83.

Gupta SK, Nayak RP. Dry antibiotic pipeline: Regulatory bottlenecks and regulatory reforms. *Journal of Pharmacology and Pharmacotherapeutics* 2014;**5**:4–7.

Gurevich A, Saveliev V, Vyahhi N *et al.* QUAST: Quality assessment tool for genome assemblies. *Bioinformatics* 2013;**29**:1072–5.

Hameş-Kocabaş EE, Uzel A, Hames-Kocabas EE *et al.* Isolation strategies of marine-derived Actinomycetes from sponge and sediment samples. *Journal of Microbiological Methods* 2012;**88**:342–7.

Han J, Sun L, Dong X *et al.* Characterization of a novel plant growth-promoting bacteria strain *Delftia tsuruhatensis* HR4 both as a diazotroph and a potential biocontrol agent against various plant pathogens. *Systematic and Applied Microbiology* 2005;**28**:66–76.

Han M, Li Z, Zhang F. The ammonia oxidizing and denitrifying prokaryotes associated with sponges from different sea areas. *Microb Ecol* 2013;**66**:427–36.

Hardoim CC, Costa R, Araujo F V *et al.* Diversity of bacteria in the marine sponge *Aplysina fulva* in Brazilian coastal waters. *Appl Environ Microbiol* 2009;**75**:3331–43.

He F, Mai LH, Garderes J *et al.* Major Antimicrobial Representatives from Marine Sponges and/or Their Associated Bacteria. *Prog Mol Subcell Biol* 2017;**55**:35–89.

He Y, Wang B, Chen W *et al.* Recent advances in reconstructing microbial secondary metabolites biosynthesis in *Aspergillus* spp. *Biotechnology Advances* 2018;**36**:739–83.

Van Heel AJ, De Jong A, Song C *et al.* BAGEL4: A user-friendly web server to thoroughly mine RiPPs and bacteriocins. *Nucleic Acids Research* 2018;**46**:W278–81.

Heikema AP, Horst-Kreft D, Boers SA *et al.* Comparison of illumina versus nanopore 16s rRNA gene sequencing of the human nasal microbiota. *Genes* 2020;**11**:1–17.

Hentschel U, Fieseler L, Wehrl M *et al.* Microbial Diversity of Marine Sponges. In: Müller WEG (ed.). *Sponges (Porifera)*. Berlin, Heidelberg: Springer Berlin Heidelberg, 2003, 59–88.

Hentschel U, Piel J, Degnan SM *et al.* Genomic insights into the marine sponge microbiome. *Nature Reviews Microbiology* 2012;**10**:641–54.

Hentschel U, Schmid M, Wagner M *et al.* Isolation and phylogenetic analysis of bacteria with antimicrobial activities from the Mediterranean sponges *Aplysina aerophoba* and *Aplysina cavernicola*. *FEMS Microbiology Ecology* 2006;**35**:305–12.

Hentschel U, Usher KM, Taylor MW. Marine sponges as microbial fermenters. *FEMS Microbiol Ecol* 2006;**55**:167–77.

Herring P. *The Biology of the Deep Ocean*. Oxford, UK: Oxford University Press, 2002.

Hesketh-Best PJ, Mouritzen M V, Shandley-Edwards K *et al. Galleria mellonella* larvae exhibit a weight-dependent lethal median dose when infected with methicillin-resistant *Staphylococcus aureus*. *Pathogens and Disease* 2021;**79**, DOI: 10.1093/femspd/ftab003.

Heuer H, Krsek M, Baker P *et al.* Analysis of actinomycete communities by specific amplification of genes encoding 16S rRNA and gel-electrophoretic separation in denaturing gradients. *Applied and Environmental Microbiology* 1997;**63**:3233–41.

Hewavitharana AK, Shaw PN, Kim TK *et al.* Screening of rifamycin producing marine sponge bacteria by LC–MS–MS. *Journal of Chromatography B* 2007;**852**:362–6.

Hoffmann F, Larsen O, Thiel V *et al.* An anaerobic world in sponges. *Geomicrobiology Journal* 2005;**22**:1–10.

Hoffmann F, Radax R, Woebken D *et al.* Complex nitrogen cycling in the sponge Geodia barretti. *Environ Microbiol* 2009;**11**:2228–43.

Hong CE, Jo SH, Jo lH *et al.* Draft genome sequence of the endophytic bacterium *Variovorax paradoxus* KB5, Which has antagonistic activity against a phytopathogen, *Pseudomonas syringae* pv. tomato DC3000. *Genome Announcements* 2017;**5**, DOI: 10.1128/genomeA.00950-17.

Hongoh Y, Yuzawa H, Ohkuma M *et al.* Evaluation of primers and PCR conditions for the analysis of 16S rRNA genes from a natural environment. *FEMS Microbiology Letters* 2003;**221**:299–304.

Hooper J, van Soest R. *Systema Porifera: A Guide to the Classification of Sponges*., 2002.

Horn H, Slaby BM, Jahn MT *et al.* An Enrichment of CRISPR and Other Defense-Related Features in Marine Sponge-Associated Microbial Metagenomes. *Frontiers in Microbiology* 2016;**7**:1751.

Hou Q, Wang C, Guo H *et al.* Draft Genome Sequence of *Delftia tsuruhatensis* MTQ3, a Strain of Plant Growth-Promoting Rhizobacterium with Antimicrobial Activity. *Genome announcements* 2015;**3**:e00822-15.

Howell K-L, Piechaud N, Downie A-LL *et al.* The distribution of deep-sea sponge aggregations in the North Atlantic and implications for their effective spatial management. *Deep Sea Research Part I: Oceanographic Research Papers* 2016a;**115**:309–20.

Howell K-L, Taylor M, Crombie K *et al. RRS James Cook, Cruise No. JC136, 14th May – 23rd June, DEEPLINKS: Influence of Population Connectivity on Depth-Dependent Diversity of Deep-Sea Marine Benthic Biota.*, 2016b.

Hubert J, Nuzillard JM, Renault JH. Dereplication strategies in natural product research: How many tools and methodologies behind the same concept? *Phytochemistry Reviews* 2017;**16**:55–95.

Hughes DJ, Gage JD. Benthic metazoan biomass, community structure and bioturbation at three contrasting deep-water sites on the northwest European continental margin. *Progress in Oceanography* 2004;**63**:29–55.

Huo L, Hug JJ, Fu C *et al.* Heterologous expression of bacterial natural product biosynthetic pathways. *Natural Product Reports* 2019;**36**:1412–36.

Huson DH, Weber N. Microbial community analysis using MEGAN. *Methods in Enzymology*. Vol 531. Academic Press Inc., 2013, 465–85.

Hyatt D, Chen GL, LoCascio PF *et al.* Prodigal: Prokaryotic gene recognition and translation initiation site identification. *BMC Bioinformatics* 2010;**11**:119.

ICES. *Report of the Workshop on Vulnerable Marine Ecosystem Database (WKVME), 10–11 December 2015, Peterborough, UK. ICES CM 2015/ACOM:62. 42 Pp*., 2016.

Ignasiak K, Maxwell A. *Galleria mellonella* (greater wax moth) larvae as a model for antibiotic susceptibility testing and acute toxicity trials. *BMC Research Notes* 2017;**10**, DOI: 10.1186/s13104-017-2757-8.

Jackson SA, Crossman L, Almeida EL *et al.* Diverse and abundant secondary metabolism biosynthetic gene clusters in the genomes of marine sponge derived *Streptomyces* spp. Isolates. *Marine Drugs* 2018;**16**:67.

Jackson SA, Flemer B, McCann A *et al.* Archaea appear to dominate the microbiome of Inflatella pellicula deep sea sponges. *PLoS One* 2013;**8**:e84438.

Jacobs AC, DiDone L, Jobson J *et al.* Adenylate kinase release as a high-throughput-screening-compatible reporter of bacterial lysis for identification of antibacterial agents. *Antimicrobial Agents and Chemotherapy* 2013;**57**:26–36.

Jander G, Rahme LG, Ausubel FM. Positive correlation between virulence of *Pseudomonas aeruginosa* mutants in mice and insects. *Journal of Bacteriology* 2000;**182**:3843–5.

Jannasch HW, Wirsen CO, Winget CL. A bacteriological pressure-retaining deep-sea sampler and culture vessel. *Deep Sea Research and Oceanographic Abstracts* 1973;**20**:661–4.

Janssen PH, Yates PS, Grinton BE *et al.* Improved culturability of soil bacteria and isolation in pure culture of novel members of the divisions

Acidobacteria, Actinobacteria, Proteobacteria, and Verrucomicrobia. *Applied and Environmental Microbiology* 2002;**68**:2391–6.

Javani S, Marín I, Amils R *et al.* Four psychrophilic bacteria from Antarctica extracellularly biosynthesize at low temperature highly stable silver nanoparticles with outstanding antimicrobial activity. *Colloids and Surfaces A: Physicochemical and Engineering Aspects* 2015;**483**:60–9.

Jiang S, Sun W, Chen M *et al.* Diversity of culturable actinobacteria isolated from marine sponge Haliclona sp. *Antonie van Leeuwenhoek, International Journal of General and Molecular Microbiology* 2007;**92**:405–16.

Johnston CW, Wyatt MA, Li X *et al.* Gold biomineralization by a metallophore from a gold-associated microbe. *Nat Chem Biol* 2013;**9**:241–3.

de Jong A, van Hijum SA, Bijlsma JJ *et al.* BAGEL: a web-based bacteriocin genome mining tool. *Nucleic Acids Res* 2006;**34**:W273-9.

Jønsson R, Struve C, Jenssen H *et al.* The wax moth *Galleria mellonella* as a novel model system to study Enteroaggregative *Escherichia coli* pathogenesis. *Virulence* 2017;**8**:1894–9.

Jørgensen NOG, Brandt KK, Nybroe O *et al. Delftia lacustris* sp. nov., a peptidoglycandegrading bacterium from fresh water, and emended description of *Delftia tsuruhatensis* as a peptidoglycan-degrading bacterium. *International Journal of Systematic and Evolutionary Microbiology* 2009;**59**:2195–9.

Jorjão AL, Oliveira LD, Scorzoni L *et al.* From moths to caterpillars: Ideal conditions for *Galleria mellonella* rearing for in vivo microbiological studies. *Virulence* 2018;**9**:383–9.

Juárez-Jiménez B, Manzanera M, Rodelas B *et al.* Metabolic characterization of a strain (BM90) of *Delftia tsuruhatensis* showing highly diversified capacity to degrade low molecular weight phenols. *Biodegradation* 2010;**21**:475–89.

Juárez-Jiménez B, Reboleiro Rivas P, Gonzalez Lopez J *et al.* Immobilization of *Delftia tsuruhatensis* in macro-porous cellulose and biodegradation of phenolic compounds in repeated batch process. *Journal of Biotechnology* 2012;**157**:148–53.

Jung D, Liu L, He S. Application of in situ cultivation in marine microbial resource mining. *Marine Life Science & Technology* 2021;**3**:148–61.

Jung D, Seo EY, Epstein SS *et al.* Application of a new cultivation technology, I-tip, for studying microbial diversity in freshwater sponges of Lake Baikal, Russia. *FEMS Microbiol Ecol* 2014;**90**:417–23.

Junqueira JC. *Galleria mellonella* as a model host for human pathogens: Recent studies and new perspectives. *Virulence* 2012;**3**, DOI: 10.4161/viru.22493.

Junqueira JC, Mylonakis E, Borghi E. *Galleria mellonella* experimental model: advances and future directions. *Pathogens and Disease* 2021;**79**, DOI: 10.1093/femspd/ftab021.

Kaeberlein T, Lewis K, Epstein SS. Isolating “uncultivable” microorganisms in pure culture in a simulated natural environment. *Science* 2002;**296**:1127–9.

Kahn AS, Chu JWF, Leys SP. Trophic ecology of glass sponge reefs in the Strait of Georgia, British Columbia. *Scientific Reports* 2018;**8**:756.

Kampa A, Gagunashvili AN, Gulder TAM *et al.* Metagenomic natural product discovery in lichen provides evidence for a family of biosynthetic pathways

in diverse symbioses. *Proceedings of the National Academy of Sciences of the United States of America* 2013;**110**:E3129–37.

Kato C, Sato T, Horikoshi K. Isolation and properties of barophilic and barotolerant bacteria from deep-sea mud samples. *Biodiversity & Conservation* 1994;**4**:1–9.

Katoh K, Misawa K, Kuma KI *et al.* MAFFT: A novel method for rapid multiple sequence alignment based on fast Fourier transform. *Nucleic Acids Research* 2002;**30**:3059–66.

Kautsar SA, Blin K, Shaw S *et al.* MIBiG 2.0: A repository for biosynthetic gene clusters of known function. *Nucleic Acids Research* 2020;**48**:D454–8.

Ke J, Yoshikuni Y. Multi-chassis engineering for heterologous production of microbial natural products. *Current Opinion in Biotechnology* 2020;**62**:88–97.

Kennedy J, Flemer B, Jackson SA *et al.* Evidence of a putative deep sea specific microbiome in marine sponges. *PLoS One* 2014;**9**:e91092.

Keren R, Lavy A, Ilan M. Increasing the Richness of Culturable Arsenic-Tolerant Bacteria from Theonella swinhoei by Addition of Sponge Skeleton to the Growth Medium. *Microbial Ecology* 2016;**71**:873–86.

Kim TK, Fuerst JA. Diversity of polyketide synthase genes from bacteria associated with the marine sponge *Pseudoceratina clavata*: culture-dependent and culture-independent approaches. *Environmental Microbiology* 2006;**8**:1460–70.

Kim TK, Hewavitharana AK, Shaw PN *et al.* Discovery of a new source of rifamycin antibiotics in marine sponge actinobacteria by phylogenetic prediction. *Applied and Environmental Microbiology* 2006;**72**:2118–25.

Klitgaard AB, Tendal OS. Distribution and species composition of mass occurrences of large-sized sponges in the northeast Atlantic. *Progress in Oceanography* 2004;**61**:57–98.

de Kluijver A, Nierop KGJ, Morganti TM *et al.* Bacterial precursors and unsaturated long-chain fatty acids are biomarkers of North-Atlantic deep-sea demosponges. *PLoS ONE* 2021;**16**:e0241095.

Kolář M, Urbánek K, Látal T. Antibiotic selective pressure and development of bacterial resistance. *International Journal of Antimicrobial Agents* 2001;**17**:357–63.

Kolmogorov M, Bickhart DM, Behsaz B *et al.* metaFlye: scalable long-read metagenome assembly using repeat graphs. *Nature Methods* 2020;**17**:1103–10.

Kolmogorov M, Yuan J, Lin Y *et al.* Assembly of long, error-prone reads using repeat graphs. *Nature Biotechnology* 2019;**37**:540–6.

Koschinsky A, Garbe-Schönberg D, Sander S *et al.* Hydrothermal venting at pressure-temperature conditions above the critical point of seawater, 5°S on the Mid-Atlantic Ridge. *Geology* 2008;**36**:615–8.

Kozlov AM, Darriba D, Flouri T *et al.* RAxML-NG: a fast, scalable and user-friendly tool for maximum likelihood phylogenetic inference. Wren J (ed.). *Bioinformatics* 2019;**35**:4453–5.

Kurnia NM, Uria AR, Kusnadi Y *et al.* Metagenomic Survey of Potential Symbiotic Bacteria and Polyketide Synthase Genes in an Indonesian Marine Sponge. *HAYATI Journal of Biosciences* 2017;**24**:6–15.

Kurtz S, Phillippy A, Delcher AL *et al.* Versatile and open software for comparing large genomes. *Genome biology* 2004;**5**:12.

Lagier JC, Edouard S, Pagnier I *et al.* Current and past strategies for bacterial culture in clinical microbiology. *Clinical Microbiology Reviews* 2015;**28**:208–36.

Lagier JC, Khelaifia S, Alou MT *et al.* Culture of previously uncultured members of the human gut microbiota by culturomics. *Nature Microbiology* 2016;**1**, DOI: 10.1038/nmicrobiol.2016.203.

Lange A, Beier S, Huson DH *et al.* Genome sequence of *Galleria mellonella* (greater wax moth). *Genome Announcements* 2018;**6**, DOI: 10.1128/genomeA.01220-17.

Laport M, Santos O, Muricy G. Marine Sponges: Potential Sources of New Antimicrobial Drugs. *Current Pharmaceutical Biotechnology* 2009;**10**:86–105.

Laport MS. Isolating Bacteria from Sponges: Why and How? *Curr Pharm Biotechnol* 2017;**18**:1224–36.

Larsen RA, Wilson MM, Guss AM *et al.* Genetic analysis of pigment biosynthesis in *Xanthobacter autotrophicus* Py2 using a new, highly efficient transposon mutagenesis system that is functional in a wide variety of bacteria. *Archives of Microbiology* 2002;**178**:193–201.

Lavaleye M. A comparison between the megafauna communities on the N.W. Iberian and Celtic continental margins—effects of coastal upwelling? *Progress in Oceanography* 2002;**52**:459–76.

Lavine MD, Strand MR. Insect hemocytes and their role in immunity. *Insect Biochemistry and Molecular Biology*. Vol 32. Pergamon, 2002, 1295–309.

Leal MC, Hilario A, Munro MH *et al.* Natural products discovery needs improved taxonomic and geographic information. *Nat Prod Rep* 2016;**33**:747–50.

Lee KA, Lee WJ. Immune–metabolic interactions during systemic and enteric infection in *Drosophila*. *Current Opinion in Insect Science* 2018;**29**:21–6.

Lerminiaux NA, Cameron ADS. Horizontal transfer of antibiotic resistance genes in clinical environments. *Canadian Journal of Microbiology* 2019;**65**:34–44.

Letunic I, Bork P. Interactive Tree Of Life (iTOL): an online tool for phylogenetic tree display and annotation. *Bioinformatics* 2007;**23**:127–8.

Letunic I, Bork P. Interactive Tree of Life (iTOL) v4: Recent updates and new developments. *Nucleic Acids Research* 2019;**47**:W256–9.

Leuko S, Raivio TL. Mutations that impact the enteropathogenic Escherichia coli Cpx envelope stress response attenuate virulence in *Galleria mellonella*. *Infection and Immunity* 2012;**80**:3077–85.

Leys SP, Kahn AS, Fang JKH *et al.* Phagocytosis of microbial symbionts balances the carbon and nitrogen budget for the deep-water boreal sponge *Geodia barretti*. *Limnology and Oceanography* 2017.

Leys SP, Mackie GO, Reiswig HM. The Biology of Glass Sponges. *Advances in Marine Biology*. Vol 52. Academic Press, 2007, 1–145.

Leys SP, Wilson K, Holeton C *et al.* Patterns of glass sponge (Porifera, Hexactinellida) distribution in coastal waters of British Columbia, Canada. *Marine Ecology Progress Series* 2004;**283**:133–49.

Leys SP, Yahel G, Reidenbach MA *et al.* The sponge pump: the role of current induced flow in the design of the sponge body plan. *PLoS One* 2011;**6**:e27787.

Li CT, Yan ZF, Chu X *et al. Delftia deserti* sp. nov., isolated from a desert soil sample. *Antonie van Leeuwenhoek, International Journal of General and Molecular Microbiology* 2015;**107**:1445–50.

Li H. Aligning sequence reads, clone sequences and assembly contigs with BWA-MEM. 2013.

Li H, Durbin R. Fast and accurate short read alignment with Burrows-Wheeler transform. *Bioinformatics* 2009;**25**:1754–60.

Li X, Guo J, Dai S *et al.* Exploring and exploiting microbial diversity through metagenomics for natural product drug discovery. *Current Topics in Medicinal Chemistry* 2009;**9**:1525–35.

Li Y, Spiropoulos J, Cooley W *et al. Galleria mellonella* - a novel infection model for the *Mycobacterium tuberculosis* complex. *Virulence* 2018a;**9**:1126–37.

Li Y, Sun LL, Sun ML *et al.* Vertical and horizontal biogeographic patterns and major factors affecting bacterial communities in the open South China Sea. *Scientific Reports* 2018b;**8**:1–10.

Li Z, Wang Y, Li J *et al.* Metagenomic Analysis of Genes Encoding Nutrient Cycling Pathways in the Microbiota of Deep-Sea and Shallow-Water Sponges. *Mar Biotechnol (NY)* 2016;**18**:659–71.

Li Z-YY, Wang Y-ZZ, He L-MM *et al.* Metabolic profiles of prokaryotic and eukaryotic communities in deep-sea sponge *Neamphius huxleyi* indicated by metagenomics. *Scientific Reports* 2014;**4**:3895.

Little TJ, Kraaijeveld AR. Ecological and evolutionary implications of immunological priming in invertebrates. *Trends in Ecology and Evolution* 2004;**19**:58–60.

Liu B, Zheng Y, Yin F *et al.* Toll Receptor-Mediated Hippo Signaling Controls Innate Immunity in *Drosophila*. *Cell* 2016;**164**:406–19.

Liu MY, Kjelleberg S, Thomas T. Functional genomic analysis of an uncultured δ-proteobacterium in the sponge *Cymbastela concentrica*. *The Isme Journal* 2011;**5**:427–35.

Liu T, Wu S, Zhang R *et al.* Diversity and antimicrobial potential of Actinobacteria isolated from diverse marine sponges along the Beibu Gulf of the South China Sea. *FEMS Microbiology Ecology* 2019;**95**:89.

Liu Y, Lai Q, Dong C *et al.* Phylogenetic Diversity of the *Bacillus pumilus* Group and the Marine Ecotype Revealed by Multilocus Sequence Analysis. Driks A (ed.). *PLoS ONE* 2013;**8**:e80097.

Loman NJ, Quinlan AR. Poretools: a toolkit for analyzing nanopore sequence data. *Bioinformatics* 2014;**30**:3399–401.

Lu S, Wang J, Chitsaz F *et al.* CDD/SPARCLE: The conserved domain database in 2020. *Nucleic Acids Research* 2020;**48**:D265–8.

Luepke KH, Suda KJ, Boucher H *et al.* Past, present, and future of antibacterial economics: Increasing bacterial resistance, limited antibiotic pipeline, and societal implications. *Pharmacotherapy* 2017;**37**:71–84.

Lurgi M, Thomas T, Wemheuer B *et al.* Modularity and predicted functions of the global sponge-microbiome network. *Nature Communications* 2019;**10**:992.

Luter HM, Bannister RJ, Whalan S *et al.* Microbiome analysis of a disease affecting the deep-sea sponge *Geodia barretti*. *FEMS Microbiol Ecol* 2017, DOI: 10.1093/femsec/fix074.

Luter HM, Whalan S, Webster NS. Thermal and Sedimentation Stress Are Unlikely Causes of Brown Spot Syndrome in the Coral Reef Sponge, *Ianthella basta*. Slomp CP (ed.). *PLoS ONE* 2012;**7**:e39779.

Luther MK, Arvanitis M, Mylonakis E *et al.* Activity of daptomycin or linezolid in combination with rifampin or gentamicin against biofilm-forming Enterococcus faecalis or E. faecium in an in vitro pharmacodynamic model using simulated endocardial vegetations and an in vivo survival assay using <i>. *Antimicrobial Agents and Chemotherapy* 2014;**58**:4612–20.

Macintyre LW, Charles MJ, Haltli BA *et al.* An Ichip-Domesticated Sponge Bacterium Produces an N-Acyltyrosine Bearing an α-Methyl Substituent. *Organic Letters* 2019;**21**:7768–71.

MacIntyre LW, Haltli BA, Kerr RG. Draft Genome Sequence of *Alteromonas* sp. Strain RKMC-009, Isolated from *Xestospongia muta* via *In Situ* Culturing Using an Isolation Chip Diffusion Chamber. *Microbiology Resource Announcements* 2019;**8**, DOI: 10.1128/mra.00508-19.

Maguire R, Duggan O, Kavanagh K. Evaluation of *Galleria mellonella* larvae as an in vivo model for assessing the relative toxicity of food preservative agents. *Cell Biology and Toxicology* 2016;**32**:209–16.

Mahmood S, Taylor KE, Overman TL *et al.* Acute infective endocarditis caused by *Delftia acidovorans*, a rare pathogen complicating intravenous drug use. *Journal of Clinical Microbiology* 2012;**50**:3799–800.

Majeed H, Gillor O, Kerr B *et al.* Competitive interactions in Escherichia coli populations: The role of bacteriocins. *ISME Journal* 2011;**5**:71–81.

Maldonado LA, Stach JEM, Pathom-Aree W *et al.* Diversity of cultivable actinobacteria in geographically widespread marine sediments. *Antonie van Leeuwenhoek, International Journal of General and Molecular Microbiology* 2005;**87**:11–8.

Maldonado M, López-Acosta M, Busch K *et al.* A Microbial Nitrogen Engine Modulated by Bacteriosyncytia in Hexactinellid Sponges: Ecological Implications for Deep-Sea Communities. *Frontiers in Marine Science* 2021;**8**:638505.

Mangano S, Michaud L, Caruso C *et al.* Antagonistic interactions between psychrotrophic cultivable bacteria isolated from Antarctic sponges: a preliminary analysis. *Research in Microbiologoy* 2008;**160**:27–37.

Mannala GK, Koettnitz J, Mohamed W *et al.* Whole-genome comparison of high and low virulent *Staphylococcus aureus* isolates inducing implant-associated bone infections. *International Journal of Medical Microbiology* 2018;**308**:505–13.

Marinho PR, Moreira APB, Pellegrino FLPC *et al.* Marine *Pseudomonas putida*: A potential source of antimicrobial substances against antibiotic-resistant bacteria. *Memorias do Instituto Oswaldo Cruz* 2009;**104**:678–82.

Martynov A v., Litvinova NM. Deep-water Ophiuroidea of the northern Atlantic with descriptions of three new species and taxonomic remarks on certain genera and species. *Marine Biology Research* 2008;**4**:76–111.

Matobole RM, van Zyl LJ, Parker-Nance S *et al.* Antibacterial Activities of Bacteria Isolated from the Marine Sponges *Isodictya compressa* and *Higginsia bidentifera* Collected from Algoa Bay, South Africa. *Marine Drugs* 2017;**15**, DOI: 10.3390/md15020047.

McMurdie PJ, Holmes S. phyloseq: An R Package for Reproducible Interactive Analysis and Graphics of Microbiome Census Data. *PLoS One* 2013;**8**:e61217.

Medema MH, Blin K, Cimermancic P *et al.* AntiSMASH: Rapid identification, annotation and analysis of secondary metabolite biosynthesis gene clusters in bacterial and fungal genome sequences. *Nucleic Acids Research* 2011;**39**:W339.

Mehbub MF, Lei J, Franco C *et al.* Marine Sponge Derived Natural Products between 2001 and 2010: Trends and Opportunities for Discovery of Bioactives. *Marine Drugs* 2014;**12**:4539–77.

Mehbub MF, Perkins M V., Zhang W *et al.* New marine natural products from sponges (Porifera) of the order Dictyoceratida (2001 to 2012); a promising source for drug discovery, exploration and future prospects. *Biotechnology Advances* 2016;**34**:473–91.

Meier-Kolthoff JP, Göker M. TYGS is an automated high-throughput platform for state-of-the-art genome-based taxonomy. *Nature Communications* 2019;**10**:1–10.

Meyer B, Kuever J. Phylogenetic diversity and spatial distribution of the microbial community associated with the Caribbean deep-water sponge *Polymastia* cf. *corticata* by 16S rRNA, aprA, and amoA gene analysis. *Microb Ecol* 2008;**56**:306–21.

Mikheenko A, Saveliev V, Gurevich A. MetaQUAST: evaluation of metagenome assemblies. *Bioinformatics* 2016;**32**:1088–90.

Mikheenko A, Valin G, Prjibelski A *et al.* Icarus: Visualizer for de novo assembly evaluation. *Bioinformatics* 2016;**32**:3321–3.

Mitra S, Gachhui R, Mukherjee J. Enhanced biofilm formation and melanin synthesis by the oyster settlement-promoting *Shewanella colwelliana* is related to hydrophobic surface and simulated intertidal environment. *Biofouling* 2015;**31**:283–96.

Moffat AD, Santos-Aberturas J, Chandra G *et al.* A User Guide for the Identification of New RiPP Biosynthetic Gene Clusters Using a RiPPER-Based Workflow. *Methods in Molecular Biology*. Vol 2296. Humana Press Inc., 2021, 227–47.

Moitinho-Silva L, Nielsen S, Amir A *et al.* The sponge microbiome project. *Gigascience* 2017;**6**:1–7.

Montalvo NF, Davis J, Vicente J *et al.* Integration of Culture-Based and Molecular Analysis of a Complex Sponge-Associated Bacterial Community. Chaturvedi V (ed.). *PLoS ONE* 2014;**9**:e90517.

Montalvo NF, Hill RT. Sponge-associated bacteria are strictly maintained in two closely related but geographically distant sponge hosts. *Appl Environ Microbiol* 2011;**77**:7207–16.

Montavon TJ, Bruner SD. Nonribosomal peptide synthetases. *Comprehensive Natural Products II: Chemistry and Biology*. Vol 5. Elsevier Ltd, 2010, 619–55.

Morel C, Mossialos E. Stoking the antibiotic pipeline. *BMJ (Online)* 2010;**340**:1115–8.

Morel MA, Ubalde MC, Braña V *et al. Delftia* sp. JD2: A potential Cr(VI)-reducing agent with plant growth-promoting activity. *Archives of Microbiology* 2011;**193**:63–8.

Mowlds P, Kavanagh K. Effect of pre-incubation temperature on susceptibility of *Galleria mellonella* larvae to infection by *Candida albicans*. *Mycopathologia* 2008;**165**:5–12.

Mukherjee J, Webster N, Llewellyn LE. Purification and characterization of a collagenolytic enzyme from a pathogen of the great barrier reef sponge, *Rhopaloeides odorabile*. *PLoS ONE* 2009;**4**, DOI: 10.1371/journal.pone.0007177.

Murillo FJ, Munoz PD, Cristobo J *et al.* Deep-sea sponge grounds of the Flemish Cap, Flemish Pass and the Grand Banks of Newfoundland (Northwest Atlantic Ocean): Distribution and species composition. *Marine Biology Research* 2012;**8**:842–54.

Mylonakis E, Moreno R, El Khoury JB *et al. Galleria mellonella* as a model system to study *Cryptococcus neoformans* pathogenesis. *Infection and Immunity* 2005;**73**:3842–50.

Nedialkova LP, Denzler R, Koeppel MB *et al.* Inflammation Fuels Colicin Ib-Dependent Competition of Salmonella Serovar Typhimurium and E. coli in

Enterobacterial Blooms. Galán JE (ed.). *PLoS Pathogens* 2014;**10**:e1003844.

Newman DJ, Cragg GM. Natural products as sources of new drugs over the 30 years from 1981 to 2010. *Journal of Natural Products* 2012;**75**:311–35.

Newman DJ, Cragg GM, Snader KM. Natural products as sources of new drugs over the period 1981-2002. *Journal of Natural Products* 2003;**66**:1022–37.

Nguyen KT, Ritz D, Gu JQ *et al.* Combinatorial biosynthesis of novel antibiotics related to daptomycin. *Proceedings of the National Academy of Sciences of the United States of America* 2006;**103**:17462–7.

Nguyen MT, Liu M, Thomas T. Ankyrin-repeat proteins from sponge symbionts modulate amoebal phagocytosis. *Mol Ecol* 2014;**23**:1635–45.

Nikouli E, Meziti A, Antonopoulou E *et al.* Gut Bacterial Communities in Geographically Distant Populations of Farmed Sea Bream (*Sparus aurata*) and Sea Bass (*Dicentrarchus labrax*). *Microorganisms* 2018;**6**:92.

Nishijima M, Lindsay DJ, Hata J *et al.* Association of Thioautotrophic Bacteria with Deep-Sea Sponges. *Marine Biotechnology* 2010;**12**:253–60.

Nithya C, Devi MG, Karutha Pandian S. A novel compound from the marine bacterium *Bacillus pumilus* S6-15 inhibits biofilm formation in gram-positive and gram-negative species. *Biofouling* 2011;**27**:519–28.

Ogata K, Yoshida N, Ohsugi M *et al.* Studies on Antibiotics Produced by Psychrophilic MicroorganismsPart I. Production of Antibiotics by a Psychrophile, *Streptomyces* sp. No. 81. *Agricultural and Biological Chemistry* 1971;**35**:79–85.

Oksanen J, Blanchet FG, Friendly M *et al.* vegan: Community Ecology Package. R package version 2.5-5. https://CRAN.R-project.org/package=vegan. 2019.

Olano C, Lombó F, Méndez C *et al.* Improving production of bioactive secondary metabolites in actinomycetes by metabolic engineering. *Metabolic Engineering* 2008;**10**:281–92.

Olsen RJ, Ebru Watkins M, Cantu CC *et al.* Virulence of serotype M3 group A *Streptococcus* strains in wax worms (*Galleria mellonella* larvae). *Virulence* 2011;**2**:111.

Olson J, McCarthy P. *Associated Bacterial Communities of Two Deep-Water Sponges*., 2005.

Olson JB, Lord CC, McCarthy PJ. Improved Recoverability of Microbial Colonies from Marine Sponge Samples. *Microb Ecol* 2000;**40**:139–47.

O'Neil J. *Review on Antimicrobial Resistance Antimicrobial Resistance: Tackling a Crisis for the Health and Wealth of Nations. London: Review on Antimicrobial Resistance*., 2014.

O'Sullivan D., Leahy Y, Healy L. *EMFF Offshore Reef Survey Sensitive Ecosystem Assessment and ROV Exploration of Reef - SeaRover 2018 Cruise Report*. Galway, 2018.

O'Sullivan David, Healy L, Leahy Y. *EMFF Offshore Reef Survey, Sensitive Ecosystem Assessment and ROV Exploration of Reef - SeaRover 2019 Cruise Report*. Galway, 2019.

Palomo S, González I, de la Cruz M *et al.* Sponge-Derived *Kocuria* and *Micrococcus* spp. as Sources of the New Thiazolyl Peptide Antibiotic Kocurin. *Marine Drugs* 2013;**11**:1071–86.

Parks DH, Imelfort M, Skennerton CT *et al.* CheckM: Assessing the quality of microbial genomes recovered from isolates, single cells, and metagenomes. *Genome Research* 2015;**25**:1043–55.

Payne DJ, Gwynn MN, Holmes DJ *et al.* Drugs for bad bugs: Confronting the challenges of antibacterial discovery. *Nature Reviews Drug Discovery* 2007;**6**:29–40.

Pearson WR. An introduction to sequence similarity ("homology") searching. *Current Protocols in Bioinformatics* 2013;**0 3**, DOI: 10.1002/0471250953.bi0301s42.

Peleg AY, Jara S, Monga D *et al. Galleria mellonella* as a model system to study *Acinetobacter baumannii* pathogenesis and therapeutics. *Antimicrobial Agents and Chemotherapy* 2009;**53**:2605–9.

Penders J, Stobberingh EE. Antibiotic resistance of motile aeromonads in indoor catfish and eel farms in the southern part of The Netherlands. *International Journal of Antimicrobial Agents* 2008;**31**:261–5.

Penn J, Li X, Whiting A *et al.* Heterologous production of daptomycin in *Streptomyces lividans*. *Journal of Industrial Microbiology and Biotechnology*. Vol 33. 2006, 121–8.

Pérez-Pascual D, Vendrell-Fernández S, Audrain B *et al.* Gnotobiotic rainbow trout (*Oncorhynchus mykiss*) model reveals endogenous bacteria that

protect against *Flavobacterium columnare* infection. *PLOS Pathogens* 2021;**17**:e1009302.

Pham TM, Wiese J, Wenzel-Storjohann A *et al.* Diversity and antimicrobial potential of bacterial isolates associated with the soft coral *Alcyonium digitatum* from the Baltic Sea. *Antonie Van Leeuwenhoek* 2016;**109**:105–19.

Piel J. Metabolites from symbiotic bacteria. *Nat Prod Rep* 2009;**26**:338–62.

Piel J, Hui D, Fusetani N *et al.* Targeting modular polyketide synthases with iteratively acting acyltransferases from metagenomes of uncultured bacterial consortia. *Environmental Microbiology* 2004a;**6**:921–7.

Piel J, Hui D, Wen G *et al.* Antitumor polyketide biosynthesis by an uncultivated bacterial symbiont of the marine sponge *Theonella swinhoei*. *Proceedings of the National Academy of Sciences of the United States of America* 2004b;**101**:16222–7.

Pineda M-CC, Strehlow B, Sternel M *et al.* Effects of sediment smothering on the sponge holobiont with implications for dredging management. *Scientific Reports* 2017;**7**:5156.

Pita L, Rix L, Slaby BM *et al.* The sponge holobiont in a changing ocean: from microbes to ecosystems. *Microbiome* 2018;**6**:46.

Proksch P, Edrada RA, Ebel R. Drugs from the seas - Current status and microbiological implications. *Applied Microbiology and Biotechnology* 2002;**59**:125–34.

Pye CR, Bertin MJ, Lokey RS *et al.* Retrospective analysis of natural products provides insights for future discovery trends. *Proceedings of the National Academy of Sciences of the United States of America* 2017;**114**:5601–6.

Qin Z, Munnoch JT, Devine R *et al.* Formicamycins, antibacterial polyketides produced by Streptomyces formicae isolated from African Tetraponera plant-ants. *Chemical Science* 2017;**8**:3218–27.

Quast C, Pruesse E, Yilmaz P *et al.* The SILVA ribosomal RNA gene database project: improved data processing and web-based tools. *Nucleic Acids Research* 2013;**41**:D590–6.

Radax R, Rattei T, Lanzen A *et al.* Metatranscriptomics of the marine sponge *Geodia barretti*: tackling phylogeny and function of its microbial community. *Environ Microbiol* 2012;**14**:1308–24.

Rafiq M, Hayat M, Zada S *et al.* Geochemistry and Bacterial Recovery from Hindu Kush Range Glacier and Their Potential for Metal Resistance and Antibiotic Production. *https://doi.org/101080/0149045120181551947* 2019;**36**:326–38.

Ramarao N, Nielsen-Leroux C, Lereclus D. The insect *Galleria mellonella* as a powerful infection model to investigate bacterial pathogenesis. *Journal of visualized experiments : JoVE* 2012, DOI: 10.3791/4392.

Ramiro-Sánchez B, González-Irusta JM, Henry L-A *et al.* Characterization and Mapping of a Deep-Sea Sponge Ground on the Tropic Seamount (Northeast Tropical Atlantic): Implications for Spatial Management in the High Seas. *Frontiers in Marine Science* 2019;**6**:278.

Ranc A, Dubourg G, Fournier PE *et al. Delftia tsuruhatensis*, an emergent opportunistic healthcare-associated pathogen. *Emerging Infectious Diseases* 2018;**24**:594–6.

Ratcliffe NA. Invertebrate immunity - A primer for the non-specialist. *Immunology Letters* 1985;**10**:253–70.

Reeves EP, Messina CGM, Doyle S *et al.* Correlation between gliotoxin production and virulence of *Aspergillus fumigatus* in *Galleria mellonella*. *Mycopathologia* 2004;**158**:73–9.

Reiswig HM. Bacteria as food for temperate-water marine sponges. *Canadian Journal of Zoology* 1975;**53**:582–9.

Reiswig HM, Mehl D. Tissue organization of Farrea occa (Porifera, Hexactinellida). *Zoomorphology* 1991;**110**:301–11.

Reji L, Tolar BB, Smith JM *et al.* Depth distributions of nitrite reductase (*nirK*) gene variants reveal spatial dynamics of thaumarchaeal ecotype populations in coastal Monterey Bay. *Environmental Microbiology* 2019;**21**:4032–45.

Renwick M, Mossialos E. What are the economic barriers of antibiotic R&D and how can we overcome them? *Expert Opinion on Drug Discovery* 2018;**13**:889–92.

Rice AL, Thurston MH, New AL. Dense Aggregations of a Hexactinellid Sponge, *Pheronema carpenteri*, in the Porcupine Seabight (Northeast Atlantic-Ocean), and Possible Causes. *Progress in Oceanography* 1990;**24**:179–96.

Richter M, Rosselló-Móra R. Shifting the genomic gold standard for the prokaryotic species definition. *Proceedings of the National Academy of Sciences of the United States of America* 2009;**106**:19126–31.

Richter M, Rosselló-Móra R, Oliver Glöckner F *et al.* JSpeciesWS: a web server for prokaryotic species circumscription based on pairwise genome comparison. *Bioinformatics* 2016;**32**:929–31.

Rigali S, Titgemeyer F, Barends S *et al.* Feast or famine: The global regulator DasR links nutrient stress to antibiotic production by Streptomyces. *EMBO Reports* 2008;**9**:670–5.

Rimoldi S, Gini E, Iannini F *et al.* The effects of dietary insect meal from *Hermetia illucens* prepupae on autochthonous gut microbiota of rainbow trout (*Oncorhynchus mykiss*). *Animals* 2019;**9**:143.

Riyanti, Balansa W, Liu Y *et al.* Selection of sponge-associated bacteria with high potential for the production of antibacterial compounds. *Scientific Reports* 2020;**10**:1–14.

Robinson SJ, Tenney K, Yee DF *et al.* Probing the bioactive constituents from chemotypes of the sponge *Psammocinia aff. bulbosa*. *Journal of Natural Products* 2007;**70**:1002–9.

Rognes T, Flouri T, Nichols B *et al.* VSEARCH: A versatile open source tool for metagenomics. *PeerJ* 2016;**2016**, DOI: 10.7717/peerj.2584.

Romanenko LA, Uchino M, Falsen E *et al. Pseudomonas pachastrellae* sp. nov., isolated from a marine sponge. *International Journal of Systematic and Evolutionary Microbiology* 2005;**55**:919–24.

Romanenko LA, Uchino M, Tanaka N *et al.* Lysobacter spongiicola sp. nov., isolated from a deep-sea sponge. *International Journal of Systematic and Evolutionary Microbiology* 2008;**58**:370–4.

Romano S, Jackson SA, Patry S *et al.* Extending the “One Strain Many Compounds” (OSMAC) Principle to Marine Microorganisms. *Mar Drugs* 2018;**16**, DOI: 10.3390/md16070244.

Ross RE, Howell K-L. Use of predictive habitat modelling to assess the distribution and extent of the current protection of ‘listed’ deep-sea habitats. *Diversity and Distributions* 2013;**19**:433–45.

Rothschild LJ, Mancinelli RL. Life in extreme environments. *Nature* 2001;**409**:1092–101.

Rubin-Blum M, Antony CP, Sayavedra L *et al.* Fueled by methane: deep-sea sponges from asphalt seeps gain their nutrition from methane-oxidizing symbionts. *The Isme Journal* 2019;**13**:1209–25.

Rutledge PJ, Challis GL. Discovery of microbial natural products by activation of silent biosynthetic gene clusters. *Nature Reviews Microbiology* 2015;**13**:509–23.

Sadd BM, Schmid-Hempel P. Insect Immunity Shows Specificity in Protection upon Secondary Pathogen Exposure. *Current Biology* 2006;**16**:1206–10.

Salem HM, Hussein MA, Hafez SE *et al.* Ultrastructure changes in the haemocytes of *Galleria mellonella* larvae treated with gamma irradiated *Steinernema carpocapsae* BA2. *Journal of Radiation Research and Applied Sciences* 2014;**7**:74–9.

Santos OC, Pontes P V, Santos JF *et al.* Isolation, characterization and phylogeny of sponge-associated bacteria with antimicrobial activities from Brazil. *Res Microbiol* 2010;**161**:604–12.

Santos-Aberturas J, Chandra G, Frattaruolo L *et al.* Uncovering the unexplored diversity of thioamidated ribosomal peptides in Actinobacteria using the RiPPER genome mining tool. *Nucleic Acids Research* 2019;**47**:4624–37.

Sauer P, Glombitza C, Kallmeyer J. A System for Incubations at High Gas Partial Pressure. *Front Microbiol* 2012;**3**:25.

Schell MA, Lipscomb L, DeShazer D. Comparative genomics and an insect model rapidly identify novel virulence genes of *Burkholderia mallei*. *Journal of Bacteriology* 2008;**190**:2306–13.

Scherlach K, Hertweck C. Triggering cryptic natural product biosynthesis in microorganisms. *Organic and Biomolecular Chemistry* 2009;**7**:1753–60.

Schirmer A, Gadkari R, Reeves CD *et al.* Metagenomic analysis reveals diverse polyketide synthase gene clusters in microorganisms associated with the marine sponge Discodermia dissoluta. *Applied and Environmental Microbiology* 2005;**71**:4840–9.

Schläppy M-LL, Schöttner SI, Lavik G *et al.* Evidence of nitrification and denitrification in high and low microbial abundance sponges. *Marine Biology* 2010;**157**:593–602.

Schmidt EW, Obraztsova AY, Davidson SK *et al.* Identification of the antifungal peptide-containing symbiont of the marine sponge *Theonella swinhoei* as a novel δ-proteobacterium, “Candidatus *Entotheonella palauensis*.” *Marine Biology* 2000;**136**:969–77.

Schmitt S, Tsai P, Bell J *et al.* Assessing the complex sponge microbiota: core, variable and species-specific bacterial communities in marine sponges. *Isme Journal* 2012;**6**:564–76.

Seed KD, Dennis JJ. Development of *Galleria mellonella* as an alternative infection model for the *Burkholderia cepacia* complex. *Infection and Immunity* 2008;**76**:1267–75.

Seemann T. Prokka: rapid prokaryotic genome annotation. *Bioinformatics* 2014;**30**:2068–9.

Seipke RF. Strain-Level Diversity of Secondary Metabolism in Streptomyces albus. *PLOS ONE* 2015;**10**:e0116457.

Sheehan G, Dixon A, Kavanagh K. Utilization of *Galleria mellonella* larvae to characterize the development of *Staphylococcus aureus* infection. *Microbiology (United Kingdom)* 2019;**165**:863–75.

Shen W, Le S, Li Y *et al.* SeqKit: A Cross-Platform and Ultrafast Toolkit for FASTA/Q File Manipulation. Zou Q (ed.). *PLOS ONE* 2016;**11**:e0163962.

Shigematsu T, Yumihara K, Ueda Y *et al. Delftia tsuruhatensis* sp. nov., a terephthalate-assimilating bacterium isolated from activated sludge. *International Journal of Systematic and Evolutionary Microbiology* 2003;**53**:1479–83.

Siegl A, Hentschel U. PKS and NRPS gene clusters from microbial symbiont cells of marine sponges by whole genome amplification. *Environ Microbiol Rep* 2010;**2**:507–13.

Siegl A, Kamke J, Hochmuth T *et al.* Single-cell genomics reveals the lifestyle of Poribacteria, a candidate phylum symbiotically associated with marine sponges. *The Isme Journal* 2011;**5**:61–70.

Silver LL. Challenges of antibacterial discovery. *Clinical Microbiology Reviews* 2011;**24**:71–109.

Simister RL, Schmitt S, Taylor MW. Evaluating methods for the preservation and extraction of DNA and RNA for analysis of microbial communities in marine sponges. *Journal of Experimental Marine Biology and Ecology* 2011;**397**:38–43.

Singkum P, Suwanmanee S, Pumeesat P *et al.* A powerful *in vivo* alternative model in scientific research: *Galleria mellonella*. *Acta Microbiologica et Immunologica Hungarica* 2019;**66**:31–55.

Sipkema D, Schippers K, Maalcke WJ *et al.* Multiple approaches to enhance the cultivability of bacteria associated with the marine sponge *Haliclona* (*gellius*) sp. *Appl Environ Microbiol* 2011;**77**:2130–40.

Smitten KL, Southam HM, de la Serna JB *et al.* Using Nanoscopy To Probe the Biological Activity of Antimicrobial Leads That Display Potent Activity against Pathogenic, Multidrug Resistant, Gram-Negative Bacteria. *ACS Nano* 2019;**13**:5133–46.

Spitaels F, Wieme AD, Vandamme P. MALDI-TOF MS as a Novel Tool for Dereplication and Characterization of Microbiota in Bacterial Diversity Studies. In: Demirev P, Sandrin TR (eds.). *Applications of Mass Spectrometry in Microbiology: From Strain Characterization to Rapid*

Screening for Antibiotic Resistance. Cham: Springer International Publishing, 2016, 235–56.

Stachelhaus T, Mootz HD, Marahiel MA. The specificity-conferring code of adenylation domains in nonribosomal peptide synthetases. *Chemistry and Biology* 1999;**6**:493–505.

Stamatakis A. RAxML version 8: A tool for phylogenetic analysis and post-analysis of large phylogenies. *Bioinformatics* 2014;**30**:1312–3.

Steinert G, Busch K, Bayer K *et al.* Compositional and Quantitative Insights Into Bacterial and Archaeal Communities of South Pacific Deep-Sea Sponges (Demospongiae and Hexactinellida). *Frontiers in Microbiology* 2020;**11**:716.

Strejcek M, Smrhova T, Junkova P *et al.* Whole-Cell MALDI-TOF MS Versus 16S rRNA Gene Analysis for Identification and Dereplication of Recurrent Bacterial Isolates. *Front Microbiol* 2018;**9**:1294.

Strieker M, Tanović A, Marahiel MA. Nonribosomal peptide synthetases: Structures and dynamics. *Current Opinion in Structural Biology* 2010;**20**:234–40.

Sunagawa S, Coelho LP, Chaffron S *et al.* Ocean plankton. Structure and function of the global ocean microbiome. *Science* 2015;**348**:1261359.

Sze MA, Schloss PD. The Impact of DNA Polymerase and Number of Rounds of Amplification in PCR on 16S rRNA Gene Sequence Data. *mSphere* 2019;**4**, DOI: 10.1128/msphere.00163-19.

Tabachnick KR. Adaptation of the Hexactinellid Sponges to Deep-Sea Life. In: Reitner J, Keupp H (eds.). *Fossil and Recent Sponges*. Berlin, Heidelberg: Springer Berlin Heidelberg, 1991, 378–86.

Tabachnick KR, Collins AG. Glass sponges (Porifera, Hexactinellida) of the northern Mid-Atlantic Ridge. *Marine Biology Research* 2008;**4**:25–47.

Talbot GH, Bradley J, Edwards JE *et al.* Bad bugs need drugs: An update on the development pipeline from the Antimicrobial Availability Task Force of the Infectious Diseases Society of America. *Chemotherapie Journal* 2006;**15**:97–105.

Tamaki H, Hanada S, Sekiguchi Y *et al.* Effect of gelling agent on colony formation in solid cultivation of microbial community in lake sediment. *Environmental Microbiology* 2009;**11**:1827–34.

Taylor MW, Radax R, Steger D *et al.* Sponge-Associated Microorganisms: Evolution, Ecology, and Biotechnological Potential. *Microbiology and Molecular Biology Reviews* 2007;**71**:295–347.

Taylor MW, Schupp PJ, Baillie HJ *et al.* Evidence for acyl homoserine lactone signal production in bacteria associated with marine sponges. *Applied and Environmental Microbiology* 2004;**70**:4387–9.

Tejman-Yarden N, Robinson A, Davidov Y *et al.* Delftibactin-A, a Non-ribosomal Peptide With Broad Antimicrobial Activity. *Frontiers in Microbiology* 2019;**10**:2377.

Tello A, Austin B, Telfer TC. Selective pressure of antibiotic pollution on bacteria of importance to public health. *Environmental Health Perspectives* 2012;**120**:1100–6.

Thacker RW, Freeman CJ. Sponge-microbe symbioses: recent advances and new directions. *Adv Mar Biol* 2012;**62**:57–111.

Thapa LP, Oh TJ, Lee HC *et al.* Heterologous expression of the kanamycin biosynthetic gene cluster (pSKC2) in *Streptomyces venezuelae* YJ003. *Applied Microbiology and Biotechnology* 2007;**76**:1357–64.

The PEW Charitable Trusts. Tracking the Global Pipeline of Antibiotics in Development, April 2020. *Antibiotic Resistance Project* 2020:1–5.

The World Health Organisation. *Global Priority List of Antibiotic-Resistant Bacteria to Guide Research, Discovery, and Development of New Antibiotics*., 2017.

Thomas JD, Watling L. A New Genus and Species of Didymocheliid Amphipod from Hexactinellid Sponges (Crustacea: Amphipoda: Didymocheliidae) from the Western Atlantic Ocean. *Bulletin of the Peabody Museum of Natural History* 2012;**53**:309–23.

Thomas T, Kavlekar DP, LokaBharathi PA. Marine Drugs from Sponge-Microbe Association—A Review. *Marine Drugs* 2010;**8**:1417–68.

Thomas T, Moitinho-Silva L, Lurgi M *et al.* Diversity, structure and convergent evolution of the global sponge microbiome. *Nature Communications* 2016;**7**:11870.

Thomas T, Rusch D, DeMaere MZ *et al.* Functional genomic signatures of sponge bacteria reveal unique and shared features of symbiosis. *The Isme Journal* 2010;**4**:1557–67.

Thoms C, Horn M, Wagner M *et al.* Monitoring microbial diversity and natural product profiles of the sponge Aplysina cavernicola following transplantation. *Marine Biology* 2003;**142**:685–92.

Tian RM, Sun J, Cai L *et al.* The deep-sea glass sponge *Lophophysema eversa* harbours potential symbionts responsible for the nutrient conversions of carbon, nitrogen and sulfur. *Environ Microbiol* 2016;**18**:2481–94.

Tian RM, Wang Y, Bougouffa S *et al.* Genomic analysis reveals versatile heterotrophic capacity of a potentially symbiotic sulfur-oxidizing bacterium in sponge. *Environmental Microbiology* 2014;**16**:3548–61.

Tian RM, Zhang W, Cai L *et al.* Genome Reduction and Microbe-Host Interactions Drive Adaptation of a Sulfur-Oxidizing Bacterium Associated with a Cold Seep Sponge. *mSystems* 2017;**2**, DOI: 10.1128/mSystems.00184-16.

Tojo S, Naganuma F, Arakawa K *et al.* Involvement of both granular cells and plasmatocytes in phagocytic reactions in the greater wax moth, *Galleria mellonella*. *Journal of Insect Physiology* 2000;**46**:1129–35.

Trevijano-Contador N, Zaragoza O. Immune response of *Galleria mellonella* against human fungal pathogens. *Journal of Fungi* 2019;**5**, DOI: 10.3390/jof5010003.

Trindade M, van Zyl LJ, Navarro-Fernandez J *et al.* Targeted metagenomics as a tool to tap into marine natural product diversity for the discovery and production of drug candidates. *Front Microbiol* 2015;**6**:890.

Tsai CJ-YY, Loh JMS, Proft T. *Galleria mellonella* infection models for the study of bacterial diseases and for antimicrobial drug testing. *Virulence* 2016;**7**:214–29.

Tu Q, Lin L, Cheng L *et al.* NCycDB: a curated integrative database for fast and accurate metagenomic profiling of nitrogen cycling genes. Wren J (ed.). *Bioinformatics* 2019;**35**:1040–8.

Tyler AD, Mataseje L, Urfano CJ *et al.* Evaluation of Oxford Nanopore's MinION Sequencing Device for Microbial Whole Genome Sequencing Applications. *Scientific Reports* 2018;**8**:10931.

Tzompa-Sosa DA, Yi L, van Valenberg HJF *et al.* Insect lipid profile: Aqueous versus organic solvent-based extraction methods. *Food Research International* 2014;**62**:1087–94.

Unson MD, Holland ND, Faulkner DJ. A brominated secondary metabolite synthesized by the cyanobacterial symbiont of a marine sponge and accumulation of the crystalline metabolite in the sponge tissue. *Marine Biology* 1994;**119**:1–11.

Uriz MJ, Martin D, Rosell D. Relationships of biological and taxonomic characteristics to chemically mediated bioactivity in Mediterranean littoral sponges. *Marine Biology* 1992;**113**:287–97.

Vacelet J, Boury-Esnault N, Fiala-Medioni A *et al.* A methanotrophic carnivorous sponge. *Nature* 1995;**377**:296.

Vacelet J, Fiala-Médioni A, Fisher CR *et al.* Symbiosis between methane-oxidizing bacteria and a deep-sea carnivorous cladorhizid sponge. *Marine Ecology Progress Series* 1996;**145**:77–85.

van Veen SQ, Claas EC, Kuijper EJ. High-throughput identification of bacteria and yeast by matrix-assisted laser desorption ionization-time of flight mass

spectrometry in conventional medical microbiology laboratories. *J Clin Microbiol* 2010;**48**:900–7.

Verhoeven J, Kavanagh AN, Dufour SC. Microbiome analysis shows enrichment for specific bacteria in separate anatomical regions of the deep-sea carnivorous sponge *Chondrocladia grandis*. *FEMS Microbiol Ecol* 2017;**93**, DOI: 10.1093/femsec/fiw214.

Verhoeven JT, Dufour SC. Microbiomes of the Arctic carnivorous sponges *Chondrocladia grandis* and *Cladorhiza oxeata* suggest a specific, but differential involvement of bacterial associates. *Arctic Science* 2017;**4**:186–204.

Versluis D, McPherson K, van Passel MWJ *et al.* Recovery of Previously Uncultured Bacterial Genera from Three Mediterranean Sponges. *Marine Biotechnology* 2017;**19**:454–68.

Vieira RP, Bett BJ, Jones DOB *et al.* Deep-sea sponge aggregations (*Pheronema carpenteri*) in the Porcupine Seabight (NE Atlantic) potentially degraded by demersal fishing. *Progress in Oceanography* 2020;**183**:102189.

Vogel H, Altincicek B, Glöckner G *et al.* A comprehensive transcriptome and immune-gene repertoire of the lepidopteran model host *Galleria mellonella*. *BMC Genomics* 2011;**12**, DOI: 10.1186/1471-2164-12-308.

Walsh CT. The chemical versatility of natural-product assembly lines. *Accounts of Chemical Research* 2008;**41**:4–10.

Wand ME, McCowen JWI, Nugent PG *et al.* Complex interactions of *Klebsiella pneumoniae* with the host immune system in a *Galleria mellonella* infection model. *Journal of Medical Microbiology* 2013;**62**:1790–8.

Webster N, Negri A, Webb RI *et al. A Spongin-Boring Alpha-Proteobacterium Is the Etiological Agent of Disease in the Great Barrier Reef Sponge* Rhopaloeides Odorabile., 2002.

Webster NS. Sponge disease: a global threat? *Environmental Microbiology* 2007;**9**:1363–75.

Webster NS, Taylor MW. Marine sponges and their microbial symbionts: love and other relationships. *Environ Microbiol* 2012;**14**:335–46.

Webster NS, Taylor MW, Behnam F *et al.* Deep sequencing reveals exceptional diversity and modes of transmission for bacterial sponge symbionts. *Environ Microbiol* 2010;**12**:2070–82.

Webster NS, Thomas T. The Sponge Hologenome. *mBio* 2016;**7**:e00135-16.

Webster NS, Wilson KJ, Blackall LL *et al. Phylogenetic Diversity of Bacteria Associated with the Marine Sponge* Rhopaloeides Odorabile. 2001/01/03. American Society for Microbiology, 2001.

Weissman JL, Hou S, Fuhrman JA. Estimating maximal microbial growth rates from cultures, metagenomes, and single cells via codon usage patterns. *Proceedings of the National Academy of Sciences* 2021;**118**:e2016810118.

Weisz JB, Lindquist N, Martens CS. Do associated microbial abundances impact marine demosponge pumping rates and tissue densities? *Oecologia* 2008;**155**:367–76.

Wen A, Fegan M, Hayward C *et al.* Phylogenetic relationships among members of the Comamonadaceae, and description of *Delftia acidovorans* (den Dooren de Jong 1926 and Tamaoka et al. 1987) gen. nov., comb. nov. *International Journal of Systematic Bacteriology* 1999;**49**:567–76.

Wick RR, Judd LM, Gorrie CL *et al.* Unicycler: Resolving bacterial genome assemblies from short and long sequencing reads. *PLoS Comput Biol* 2017;**13**:e1005595.

Wiegand I, Hilpert K, Hancock REW. Agar and broth dilution methods to determine the minimal inhibitory concentration (MIC) of antimicrobial substances. *Nature Protocols* 2008;**3**:163–75.

Williams SE, Stennett HL, Back CR *et al.* The Bristol Sponge Microbiome Collection: A Unique Repository of Deep-Sea Microorganisms and Associated Natural Products. *Antibiotics* 2020;**9**:509.

Wilson MC, Mori T, Rückert C *et al.* An environmental bacterial taxon with a large and distinct metabolic repertoire. *Nature 2014 506:7486* 2014;**506**:58–62.

Von Wintersdorff CJH, Penders J, Van Niekerk JM *et al.* Dissemination of antimicrobial resistance in microbial ecosystems through horizontal gene transfer. *Frontiers in Microbiology* 2016;**7**, DOI: 10.3389/fmicb.2016.00173.

Wojda I, Taszłow P. Heat shock affects host-pathogen interaction in *Galleria mellonella* infected with *Bacillus thuringiensis*. *Journal of Insect Physiology* 2013;**59**:894–905.

Wood DE, Lu J, Langmead B. Improved metagenomic analysis with Kraken 2. *Genome Biology* 2019;**20**:257.

Wood DE, Salzberg SL. Kraken: ultrafast metagenomic sequence classification using exact alignments. *Genome Biology* 2014;**15**:R46.

Wu G, Zhao Z, Liu C *et al.* Priming *Galleria mellonella* (Lepidoptera: Pyralidae) Larvae With Heat-Killed Bacterial Cells Induced an Enhanced Immune Protection Against *Photorhabdus luminescens* TT01 and the Role of Innate Immunity in the Process. *Journal of Economic Entomology* 2014;**107**:559–69.

Wyatt MA, Johnston CW, Magarvey NA. Gold nanoparticle formation via microbial metallophore chemistries. *Journal of Nanoparticle Research* 2014;**16**:1–7.

Xi L, Ruan J, Huang Y. Diversity and biosynthetic potential of culturable actinomycetes associated with marine sponges in the China seas. *International Journal of Molecular Sciences* 2012;**13**:5917–32.

Xin YJ, Kanagasabhapathy M, Janussen D *et al.* Phylogenetic diversity of Gram-positive bacteria cultured from Antarctic deep-sea sponges. *Polar Biology* 2011;**34**:1501–12.

Xu D, Han L, Li C *et al.* Bioprospecting deep-sea Actinobacteria for novel anti-infective natural products. *Front Microbiol* 2018;**9**:787.

Xue S, Zhang HT, Wu PC *et al.* Study on bioactivity of extracts from marine sponges in Chinese Sea. *Journal of Experimental Marine Biology and Ecology* 2004;**298**:71–8.

Yahel G, Eerkes-Medrano D, Leys S. Size independent selective filtration of ultraplankton by hexactinellid glass sponges. *Aquatic Microbial Ecology* 2006;**45**:181–94.

Yahel G, Sharp JH, Marie D *et al. In situ* feeding and element removal in the symbiont-bearing sponge *Theonella swinhoei*: Bulk DOC is the major source for carbon. *Limnology and Oceanography* 2003;**48**:141–9.

Yamada KD, Tomii K, Katoh K. Application of the MAFFT sequence alignment program to large data—reexamination of the usefulness of chained guide trees. *Bioinformatics* 2016;**32**:3246–51.

Yasuhara M, Danovaro R. Temperature impacts on deep-sea biodiversity. *Biological Reviews* 2016;**91**:275–87.

Yilmaz P, Parfrey LW, Yarza P *et al.* The SILVA and "all-species Living Tree Project (LTP)" taxonomic frameworks. *Nucleic Acids Research* 2014;**42**:D643–8.

Ylihonko K, Hakala J, Niemi J *et al.* Isolation and characterization of aclacinomycin A-non-producing *Streptomyces galilaeus* (ATCC 31615) mutants. *Microbiology* 1994;**140**:1359–65.

Zasloff M. Antimicrobial peptides of multicellular organisms. *Nature* 2002;**415**:389–95.

Zerikly M, Challis GL. Strategies for the discovery of new natural products by genome mining. *Chembiochem* 2009;**10**:625–33.

Zhang F, Jonas L, Lin H *et al.* Microbially mediated nutrient cycles in marine sponges. *FEMS Microbiol Ecol* 2019;**95**, DOI: 10.1093/femsec/fiz155.

Zhang H, Zhang F, Li Z. Gene analysis, optimized production and property of marine lipase from *Bacillus pumilus* B106 associated with South China Sea sponge *Halichondria rugosa*. *World Journal of Microbiology and Biotechnology* 2009;**25**:1267–74.

Zhang L li, He D, Chen J meng *et al.* Biodegradation of 2-chloroaniline, 3-chloroaniline, and 4-chloroaniline by a novel strain *Delftia tsuruhatensis* H1. *Journal of Hazardous Materials* 2010;**179**:875–82.

Zhang MM, Wang Y, Ang EL *et al.* Engineering microbial hosts for production of bacterial natural products. *Natural Product Reports* 2016;**33**:963–87.

Zhang T, Zhang J, Liu S *et al.* A novel and complete gene cluster involved in the degradation of aniline by *Delftia* sp. AN3. *Journal of Environmental Sciences* 2008;**20**:717–24.

Zhang Z, Wu Y, Zhang X-H. Cultivation of microbes from the deep-sea environments. *Deep Sea Research Part II: Topical Studies in Oceanography* 2018;**155**:34–43.

Ziemert N, Podell S, Penn K *et al.* The Natural Product Domain Seeker NaPDoS: A Phylogeny Based Bioinformatic Tool to Classify Secondary Metabolite Gene Diversity. de Crécy-Lagard V (ed.). *PLoS One* 2012;**7**:e34064.

Chapter 0. Appendix

Table S0-1 Summary of the published literature examining deep-sea sponge microbiotas. Only investigations that included sponges from depths deeper than ca. 200 m were included. (HMA, High Microbial Abundant; LMA, Low Microbial Abundant; N, number of biological replicas; SW, the inclusion of local seawater into the analysis; S, the inclusion of sediment into the analysis; SAB – sponge-associated bacteria; n.d., not done).

Sponge taxonomy	Class	HMA/ LMA	Depths (m)	Location	Summary of study method(s)				Ref.
					N	SW	S	Methods summary	
Scleritoderma cyanea	Demospongiae	n.l.	242	Curaçao	1	n.d	n.d	SAB isolation and phylogenetic identification; DGGE	(Olson, Lord and McCarthy 2000)
Scleritoderma sp.	Demospongiae	n.l.	255	Bonaire	1	n.d	n.d		
Polymastia* cf. *corticata	Demospongiae	n.l.	1,127	Kahouanne Basin, Caribbean Sea	1	n.d	n.d	DG-DGGE analysis, and sequencing of 16S rRNA, *aprA,* and *amoA* gene amplicons	(Meyer and Kuever 2008)
***Pachastrella* sp.**	Demospongiae	n.l	750	Philippine Sea	n.l	n.d	n.d	SAB isolation and phylogenetic identification; NP screening	(Romanenko *et al.* 2005, 2008)
Rossella nuda	Hexactinellida	n.l	350	Antarctica	n.l	n.d	n.d	SAB isolation and phylogenetic identification; antimicrobial activity plate screening; and detection of polyketide synthases (PKS)	(Xin *et al.* 2011)
Mixilla mollis	Demospongiae	n.l	1,040		n.l	n.d	n.d		
Radiella antartica	Demospongiae	n.l	4,700		n.l	n.d	n.d		
***Characella* sp.**	Demospongiae	n.l	686	Ogasawara Island, Japan	1	n.d	n.d	PCR-DGGE analysis and sequencing of 16S rRNA amplicon sequencing	(Nishijima *et al.* 2010)
***Pachastrella* sp.**	Demospongiae	n.l	572	Gulf of Mexico	1	n.d	n.d		
Unidentified *Poecilosclerida* sponge	Demospongiae	n.l			1	n.d	n.d		
Geodia barretti	Demospongiae	HMA	200-300	Bergen, Norway	n.l	n.d	n.d	16S rRNA amplicon sequencing; mRNA sequencing; FISH	(Radax *et al.* 2012)
Inflantella pellicula	Demospongiae	n.l	2,900	North Atlantic, Ireland	2	y	n.d	16S rRNA amplicon sequencing	(Jackson *et al.* 2013)
Neamphius huxleyi	Demospongiae	n.l	1,800	Southwest Indian Ocean Ridge	3	y	n.d	Whole metagenomic sequencing; 16S rRNA gene survey	(Li *et al.* 2014)
Lissodendoryx diversichela	Demospongiae	LMA	1,350	North Atlantic, Ireland	1	y	n.d	16S rRNA amplicon sequencing	(Kennedy *et al.* 2014)
Poecillastra compressa	Demospongiae	LMA	1,469		1	y	n.d		
Inflantella pellicula	Demospongiae	LMA	748		1	y	n.d		
Stelletta normani	Demospongiae	HMA	1,350		1	y	n.d		

Sponge taxonomy	Class	HMA/ LMA	Depths (m)	Location	Summary of study method(s)				Ref.
					N	SW	S	Methods summary	
Inflantella pellicula	Demospongiae	n.l	2,900 and 748	North Atlantic, Ireland	2	n.d	n.d	16S rRNA amplicon sequencing	(Borchert *et al.* 2016)
Stelletta normani	Demospongiae	n.l	2,400, 1,350 and 760		3	n.d	n.d		
Poecillastra compressa	Demospongiae	n.l	1,469 and 1,250		2	n.d	n.d		
Lophophysema eversa	Hexactinellida	n.l	3,683	South China Sea	1	n.d	n.d	Whole metagenomic sequencing; 16S rRNA amplicon sequencing	(Tian *et al.* 2016)
Geodia barretti	Demosponge	n.l	154-197, and 304-340	Kosterjorden, Sweden; and Florida, USA	6	y	y	16S rRNA amplicon sequencing	(Thomas *et al.* 2016)
Aphrocallistes beatrix	Hexactinellida	n.l	406, 493, 529, and 753	Florida, USA	4	y	y		
Geodia barretti	Demospongiae	n.l	100-220	Bergen, Norway	10	n.d	n.d	16S rRNA amplicon sequencing	(Luter *et al.* 2017)
Poecillastra compressa	Demospongiae	n.l	1,480	North Atlantic, Ireland	n.l	n.d	n.d	SAB isolation and WGS; enzyme activity plate screening;	(Borchert *et al.* 2017a)
Inflatella pellicula	Demospongiae	n.l	2,900		n.l	n.d	n.d		
Sericolophus hawaiicus	Hexactinellida	n.l	2,129		n.l	n.d	n.d		
***Suberites* sp.**	Demospongiae	n.l	850	Thuwal Seep II, Red Sea	1	n.d	n.d	Shotgun metagenomic sequencing; 16S rRNA gene survey; FISH	(Tian *et al.* 2017)
Chondrocladia grandis	Demospongiae	n.l	852	Gulf of Maine, USA	4	n.d	n.d	16S rRNA amplicon sequencing	(Verhoeven, Kavanagh and Dufour 2017)
Chondrocladia grandis	Demospongiae	n.l	537-539; 702 and 852	Scott Inlet, Canada; Davis Straights; and Gulf of Maine, USA	7	n.d	n.d	16S rRNA amplicon sequencing, biomarker analysis, oligotyping, and stable isotope analysis.	(Verhoeven and Dufour 2017)
Cladorhiza oxeata	Demospongiae	n.l	680, and 538	Davis Straights; and Scott Inlet, Canada	2	n.d	n.d		
***Axinellida* sp.**	Demospongiae	n.l	246	Gulf of Mexico, Florida, USA	1	n.d	n.d		(Xu *et al.* 2018)

Sponge taxonomy	Class	HMA/ LMA	Depths (m)	Location	Summary of study method(s)				Ref.
					N	SW	S	Methods summary	
***Sarcotagus* sp. or *Smenospongia* sp.**	Demospongiae	n.l	205	Georgia, USA	1	n.d	n.d	SAB isolation and phylogenetic identification; antimicrobial activity plate screening; extraction, purification and structural elucidation of antimicrobial compounds	
***Discodermia* sp.**	Demospongiae	n.l	440-575	Bahamas, Honduras and Guanaja	n.l	n.d	n.d		
***Forcepia* sp.**	Demospongiae	n.l	230-240	Gulf of Mexico, USA	n.l	n.d	n.d		
***Leiodermatium* sp.**	Demospongiae	n.l	1,288	Puerto Rico; Florida (Miami), USA	1	n.d	n.d		
***Oceanapiidae* sp.**	Demospongiae	n.l	2,790	Bahamas	1	n.d	n.d		
Scleritoderma cyanea	Demospongiae	n.l	795	Curacao	1	n.d	n.d		
***Spongosorites* sp.**	Demospongiae	n.l	730	Puerto Rico	1	n.d	n.d		
***Theonella* sp.**	Demospongiae	n.l	692	Puerto Rico	1	n.d	n.d		
***Theonellidae* n.sp.**	Demospongiae	n.l	655	Florida Keys, USA	1	n.d	n.d		
***Hymedesmia (Stylopus) methanophila* sp. nov.**	Demospongiae	LMA	2,925 and 3,106	Gulf of Mexico, USA	1	n.d	n.d	FISH; TEM; Whole metagenomic sequencing of DNA and RNA	(Rubin-Blum *et al.* 2019)
***Iophon methanophila* sp. nov.**	Demospongiae	LMA			1	n.d	n.d		
Paratimea sp. indet.	Demospongiae	n.l	472-532	South and North-east New Zealand	4	y	n.d	16S rRNA amplicon sequencing and quantitative real-time PCR (qPCR)	(Steinert *et al.* 2020)
Halichondria sp. indet.	Demospongiae	n.l	892–899		3	y	n.d		
Latrunculia morrisoni	Demospongiae	n.l	595, 670–706		3	y	n.d		
Geodia vaubani	Demospongiae	n.l	1172–1216, 802		4	y	n.d		
Penares turmericolor	Demospongiae	n.l	1187–1191		4	y	n.d		
Pleroma turbinatum	Demospongiae	n.l	472–497		3	y	n.d		
Bolosoma cyanae	Hexactinellida	n.l	1149–1167		4	y	n.d		
Corbitella plagiariorum	Hexactinellida	n.l	770–802		4	y	n.d		
Regadrella okinoseana	Hexactinellida	n.l	774–896		4	y	n.d		
Saccocalyx tetractinus	Hexactinellida	n.l	1352–1457, 4160		3	y	n.d		

Sponge taxonomy	Class	HMA/ LMA	Depths (m)	Location	Summary of study method(s)				Ref.
					N	SW	S	Methods summary	
Leucopsacus distantus	Hexactinellida	n.l	792–896		3	y	n.d		
Lanuginellinae gen. et sp. indet.	Hexactinellida	n.l	802–893		3	y	n.d		
Aphrocallistes beatrix	Hexactinellida	n.l	759–793		3	y	n.d		
Vazella pourtalesii	Hexactinellida	n.l	153-206	Scotian Shelf, Canada	33	y	y	16S rRNA amplicon sequencing	(Busch *et al.* 2020a)
Geodia hentscheli	Demosponge	HMA	580-2,184	Schulz Bank, Arctic Mid-Ocean Ridge	16	y	n.d	16S rRNA amplicon sequencing and biogeochemical measurements of SW.	(Busch *et al.* 2020b)
Lissodendoryx complicata	Demosponge	LMA	580-2,184		8	y	n.d		
Schaudinnia rosea	Hexactinellida	LMA	580-2,184		12	y	n.d		
Vazella pourtalesii	Hexactinellida	n.l	100-935	Sambro Bank, Canada	13	y	n.d	16S rRNA amplicon sequencing; TEM; *in situ* nutrient flux measurements	(Maldonado *et al.* 2021)
Schaudinnia rosea	Hexactinellida	n.l	150-200	Schulz Bank, Arctic Mid-Ocean Ridge	13	y	n.d		
Geodia arlantica	Demosponge	n.l	266-295	Sula Reef, Norway	2	n.d	n.d	Lipid extraction and fatty acid marker analysis	(de Kluijver *et al.* 2021)
Geodia barretti	Demosponge	n.l	~300	Barents Sea	6	n.d	n.d		
Geodia hentscheli	Demosponge	n.l	550-600	Schulz Bank, Arctic Mid-Ocean Ridge	1	n.d	n.d		
Geodia parva	Demosponge	n.l			1	n.d	n.d		
Stelletta rhaphidiophora	Demosponge	n.l			1	n.d	n.d		
Geodia hentscheli	Demosponge	n.l	690-1,000	Langseth Ridge, Central Arctic	3	n.d	n.d		
Geodia parva	Demosponge	n.l			3	n.d	n.d		
Stelletta rhaphidiophora	Demosponge	n.l			2	n.d	n.d		

Table S0-2 Selection of isolation media and incubation conditions most widely used in the literature for the cultivation of sponge-associated bacteria. Not all iterations of the same isolation media are represented in this table, such as the addition of antibiotics and/or specific vitamin/trace element solutions. The intention of this table is to highlight the main isolation media utilised across the literature. Where the percentage of agar was not given in the original publication, 'Agar' is stated without any percentage. (RT, room temperature; references denoted with '†' were found to be one of the best performing media(s) for that study in terms of diversity and recovery counts).

Isolation media	Type	Growth matrix	Incubation conditions		Reference
			Time	Temp.	
Actinomycete isolation medium††	Actinomycetes	Agar	16 weeks	25°C	(Laport 2017)
		1.5% agar	12 weeks	13°C	(Sipkema *et al.* 2011)†
		Agar	9 weeks	25°C	(Montalvo and Hill 2011)
		1.8% agar	6-8 weeks	30°C	(Abdelmohsen *et al.* 2010)†
Aqueous sponge extract	Oligotrophic/spongin binding bacteria	Agar and floating disk	16 weeks	13°C	(Laport 2017)
		1.5% agar and floating disk	12 weeks	13°C	(Sipkema *et al.* 2011)†
Basic artificial seawater medium	Oligotrophic	1.5% agar	24 weeks	18°C	(Esteves *et al.* 2016)
Basic natural seawater medium	Oligotrophic	1.5% agar and floating disk	24 weeks	18°C	(Esteves *et al.* 2016)
		1.5% agar, liquid and floating disk	12 weeks	13°C	(Sipkema *et al.* 2011)
Brain-Heart Infusion	Fastidious bacteria	1.8% agar	2-4 weeks	28°C	(Xin *et al.* 2011)
		Agar	1 week	RT	(Santos *et al.* 2010)
		Agar	1 week	RT	(Marinho *et al.* 2009)
Delicious medium	Oligotrophic	Agar	16 weeks	25°C	(Laport 2017)
		1.5% agar and floating disk	12 weeks	13°C	(Sipkema *et al.* 2011)†
Fluid thioglycolate agar	Obligate anaerobes	Agar	16 weeks	25°C	(Laport 2017)
		1.5% agar	12 weeks	13°C	(Sipkema *et al.* 2011)†
Glycerol Asparagine agar	Steptomycetes	1.8% agar	6-8 weeks	30°C	(Abdelmohsen *et al.* 2010)
		0.5% agar	9 weeks	25°C	(Montalvo and Hill 2011)
HVA medium	Heterotrophic/nitrifying soil bacteria	1.8% agar	2-4 weeks	28°C	(Xin *et al.* 2011)
HVG medium	Heterotrophic/nitrifying soil bacteria	1.8% gellan gum	2-4 weeks	28°C	(Xin *et al.* 2011)†
ISP2†	Streptomycetes	1.8% agar	6-8 weeks	30°C	(Abdelmohsen *et al.* 2010)†
		Agar	9 weeks	25°C	(Montalvo and Hill 2011)
M1†	Oligotrophs	1.8% agar	6-8 weeks	30°C	(Abdelmohsen *et al.* 2010)†
		1.8% agar	2-4 weeks	28°C	(Xin *et al.* 2011)
Marine Broth†	Generalists/ oligotrophs	Agar and floating disk	24 weeks	18°C	(Esteves *et al.* 2016)†
		1.5% agar	12 weeks	13°C	(Sipkema *et al.* 2011)
		1.8% agar	2-4 weeks	28°C	(Xin *et al.* 2011)
		Agar	9 weeks	25°C	(Montalvo and Hill 2011)
		1.8% agar	6-8 weeks	30°C	(Abdelmohsen *et al.* 2010)

Isolation media	Type	Growth matrix	Incubation conditions		Reference
			Time	Temp.	
		Agar	1 week	RT	(Santos *et al.* 2010)
		Agar	2 days	28°C	(Devi *et al.* 2010)
		Agar	1 week	RT	(Marinho *et al.* 2009)
		Agar	n.l	n.l	(Kim and Fuerst 2006)
Mucin agar†	Oligotrophic	Agar	16 weeks	25°C	(Laport 2017)
		1.5% agar and floating disk	12 weeks	13°C	(Sipkema *et al.* 2011)†
Mueller-Hinton	Non-selective	Agar	16 weeks	25°C	(Laport 2017)
		1.5% agar	12 weeks	13°C	(Sipkema *et al.* 2011)
Nutrient agar	Generalists	Agar	5-7 days	28°C	(Bibi *et al.* 2020)
Oligotrophic medium (OLIGO)	Oligotrophic	1.8% agar	6-8 weeks	30°C	(Abdelmohsen *et al.* 2010)
Organic sponge extract agar	Spongin binding bacteria	1.5% agar and floating disk	12 weeks	13°C	(Sipkema *et al.* 2011)
Peptone-starch†	Generalists	Agar	16 weeks	25°C	(Laport 2017)
		1.5% agar	12 weeks	13°C	(Sipkema *et al.* 2011)†
Raffinose-Histidine††	Oligotrophic Actinomycetes selective	Agar	16 weeks	25°C	(Laport 2017)
		1.5% agar and floating disk	12 weeks	13°C	(Sipkema *et al.* 2011)†
		1.8% agar	2-4 weeks	28°C	(Xin *et al.* 2011)†
Reasoner 2 agar†††	Oligotrophic Gammaproteobacteria selective	Agar	5-7 days	28°C	(Bibi *et al.* 2020)†
		1.5% agar	24 weeks	18°C	(Esteves *et al.* 2016)†
		1.8% agar	6-8 weeks	30°C	(Abdelmohsen *et al.* 2010)†
		Agar	9 weeks	25°C	(Montalvo and Hill 2011)†
		Agar	16 weeks	25°C	(Laport 2017)
Sponge spicule agar†	Oligotrophic/spicule binding bacteria	1.5% agar	24 weeks	18°C	(Esteves *et al.* 2016)
		2% agar	8 weeks	24-25°C	(Keren, Lavy and Ilan 2016)
		1.5% agar	12 weeks	13°C	(Sipkema *et al.* 2011)†
		Agar	9 weeks	25°C	(Montalvo and Hill 2011)
Tryptic soy	Generalist	Agar	5-7 days	28°C	(Bibi *et al.* 2020)
		Agar	4 weeks,	n.l	(Matobole *et al.* 2017)
		1.8% agar	2-4 weeks	28°C	(Xin *et al.* 2011)

Chapter 1. Appendix

Table S1-1. Agar composition. All were made in artificial sea water (ASW; 28.5 g/L Instant Ocean® Sea Salt), unless stated otherwise (*). All media was solidified with 1.5% agar (Sigma-Aldrich) unless stated otherwise, such as in premix media. (NA, not applicable).

Agar name		Components	Target	Supplier	Reference
Reasoner's 2 agar	R2a	**R2a premix (18.1 g/L)**: 0.5 g/L Yeast Extract, 0.5 g/L Proteose Peptone, 0.5 g/L Casamino Acids, 0.5 g/L Dextrose, 0.5 g/L Soluble Starch, 0.3 g/L Sodium Pyruvate, 0.3 g/L K2HPO4, 0.05 g/L MgSO4, 15 g/L agar	Heterotrophic aquatic bacteria	Difco™, UK	(Graça *et al.* 2013; Montalvo *et al.* 2014; Bibi *et al.* 2020)
Marine agar*	MA	**Marine broth premix (37.4 g/L)**: 5.0 g/L Peptone, 1.0 g/L Yeast Extract, 0.1 g/L Ferric Citrate, 19.45 g/L NaCl, 5.9 g/L MgCl, 3.24 g/L MgSO4, 1.8 g/L CaCl2, 0.55 g/L KCl, 0.16 g/L $NaHCO_3$, 0.08 g/L KBr, 34 mg/L SrCl2, 22.0 mg/L H3BO3, 4.0 mg/L Sodium Silicate, 2.4 mg/L NaF, 1.6 mg/L NH4NO3, 8.0 mg/L Na2HPO4	Heterotrophic marine bacteria	Difco™, UK	(Buck 1974; Montalvo and Hill 2011; Sipkema *et al.* 2011; Xin *et al.* 2011; Esteves *et al.* 2016)
Actinomycetes isolation agar	AIA	**AIA premix (22 g/L)**: 2.0 g/L Sodium Caseinate, 0.1 g/L L-Asparagine, 4.0 Sodium Propionate, 0.5 g/L K2HPO4, 0.1 g/L MgSO4, 0.001 g/L FeSO4	Actinomycetes	Sigma-Aldrich, UK	(Webster *et al.* 2001; Abdelmohsen *et al.* 2010; Williams *et al.* 2020)
Raffinose-Histidine agar	RHa	10.0 g/L Raffinose, 1.0 g/L L-Histidine, 0.5 g/L MgSO4, 0.01 g/L FeSO4	Actinomycetes	NA	(Webster *et al.* 2001)
Tryptic soy agar	TSa	**TSa premix (30 g/L)**: 17.0 g/L Pancreatic digest of casein, 3.0 g/L Enzymatic digest of soya bean, 2.5 g/L Glucose, 5.0 g/L NaCl, 2.5 g/L K_2HPO_4	Generalist	Thermo Fisher Scientific, UK	
Nutrient agar	NA	NA premix (28.0 g/L): 1.0 g/L 'Lab Lemco' powder, 2.0 g/L Yeast Extract, 5.0 g/L Peptone, 5.0 g/L NaCl	Generalist	Oxoid, UK	(Xi, Ruan and Huang 2012)
Luria Broth agar	LBa	LBa premix (27 g/L): 5.0 g/L NaCl, 10.0 g/l Tryptone, 5.0 g/L Yeast Extract	Generalist	Thermo Fisher Scientific, UK	
Oatmeal agar	OA	**OA premix (72.5 g/L)**: 60 g/L Oatmeal, 12.5 g/L agar		Sigma-Aldrich, UK	(Xi, Ruan and Huang 2012)
Filtered sterilised seawater	FFSW	Seawater collected at Plymouth (UK), sequentially filtered down to 0.22 µm pore-size filters.	Marine bacteria	NA	(Sipkema *et al.* 2011; Montalvo *et al.* 2014; Esteves *et al.* 2016)
Additives					
Low nutrient heterotrophic media	LNHM	0.22 µm filtered seawater supplemented with 1.0 µM NH_4Cl, 0.1 µM KH_2PO_4, and vitamin mix[a] at a 10^{-4} dilution of stock		NA	(Cho and Giovannoni 2004)

vitamin mix[a]		0.2 mg/L Thiamine HCl, 1.0 µm Biotin, 1.0 µm B12, 2.0 µm Folic Acid, 10.0 µm Paba, 0.1 mg/L Nicotinic Acid, 1.0 mg/L Inisotol, 0.2 mg/L Calcium pantothenate, 0.1 mg/L Pyradoxine HCl	NA	NA	(Davis and Guillard 1958; Cho and Giovannoni 2004)
Sponge spicule extract	SSE	2.0 g of sponge tissue ground up with pestle and mortar, homogenate was suspended in 40 ml sterile dH_2O overnight at 4°C. Suspension was filtered through 0.22 µm filter and remaining cake on the filer was dissolved in 50 ml of 5 mM EDTA in dH_2O for 24 h. Suspension was centrifuged at 138 x *g* for 10 min, and pellet rinsed twice in dH_2O, before being suspended in dH2O and stored at -20°C until used.	NA	NA	(Sipkema *et al.* 2011; Keren, Lavy and Ilan 2016; Laport 2017)

Table S1-2. Summary of primer pairs used for the amplification of smBGC's. Primer pairs were taken from (Palomo et al., 2013).

Primer pair	Type	5'-3'		Amplicon size (bp)	Annealing temp. (°C)	Ref.
K1F/ M6R	T1PKS	F	TSAAGTCSAACATCGGBCA	~1250-1400	57	(Palomo *et al.* 2013)
		R	CGCAGGTTSCSGTACCAGTA			
KSαF/ KSβR	T2PKS	F	TSGRCTACRTCAACGCSCACGG	~800-900	58	
		R	TACSAGTCSWTCGCCTGGTTC			
A3F/ A7R	NRPS	F	GCSTACSYSATSTACACSTCSGG	~700	61	
		R	SASGTCVCCSGTSCGGTAS			
27F/ 1492R	16S rRNA	F	AGAGTTTGATCCTGGCTCAG	~1,400	52	(Hongoh *et al.* 2003)
		R	TACGGYTACCTTGTTACGACTT			

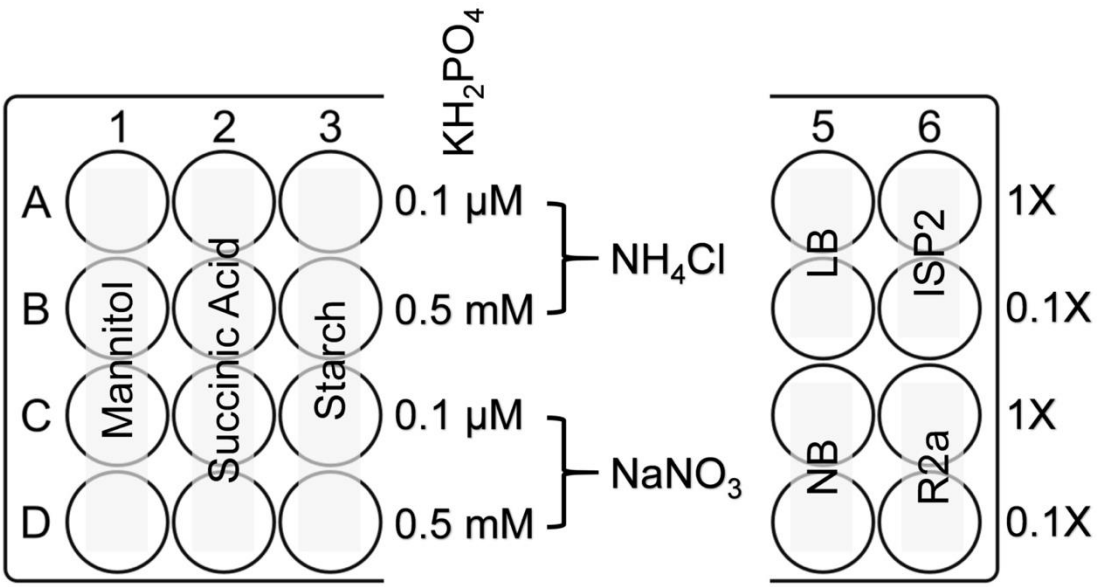

Figure S1-1. OSMAC growth matrix media. Bacterial cultures were incubated in flat-bottom 24-well plates in 800 µl of liquid media. Plates were sealed and incubated without orbital shaking for 14 days at 15°C. Each plate would be replicated in triplicate for each bacterial strain.

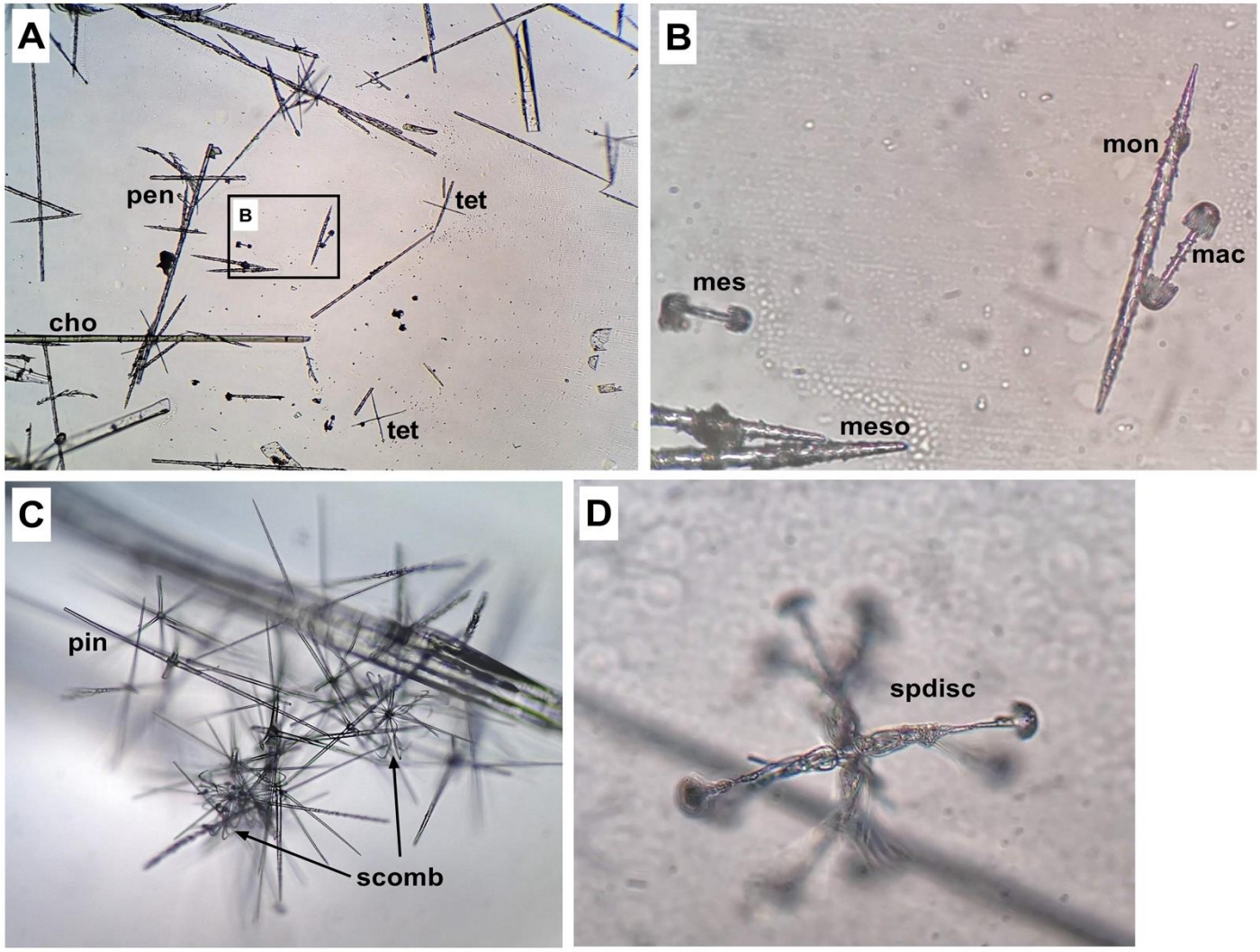

Figure S1-2. Spicule diversity of two hexactinellid sponges. (A-B) Spicules from Pheronema sp., and from Hertwigia sp. (C-D). (cho, choanosomal pentactines; mac, macramphidiscs; mes, mesamphidiscs; meso, mesouncinate; mon, monaxons; pen, pentacts; pin, pinular hexactines; tet, tetract; scomb, sigmatocomes; spdisc, spirodiscohexasters).

Table S1-3. Agar media and conditions used to culture bacteria from sponges.

Sponge	ID	Agar type/ Condition	Colonies isolated			
			4°C	15°C	RT	28°C
***Pheronema* spp.**	**JC135_125**	½ R2a	2	11	12	11
		½ R2a + LNHM	n.d.	11	n.d.	n.d.
		FSSW	n.d.	12	n.d.	n.d.
		½ R2a + SSE	n.d.	14	n.d.	n.d.
		OA	n.d.	1	n.d.	n.d.
		Total	**2**	**48**	**12**	**11**
	JC136_134	½ R2a	26	21	30	25
		½ R2a + LNHM	n.d.	15	n.d.	n.d.
		FSSW	n.d.	19	n.d.	n.d.
		½ R2a + SSE	n.d.	28	n.d.	n.d.
		Total	**26**	**83**	**30**	**25**
	JC136_135	½ R2a	7	22	13	7
		LNHM	n.d.	12	n.d.	n.d.
		FSSW	n.d.	12	n.d.	n.d.
		½ R2a + SSE	n.d.	20	n.d.	n.d.
		Total	**7**	**66**	**13**	**7**
	CE_19_29	MBa	n.d.	45	n.d.	n.d.
		RH	n.d.	11	n.d.	n.d.
		R2a	n.d.	153	n.d.	n.d.
		Total	**n.d.**	**209**	**n.d.**	**n.d.**
	CE_19_27	NB	n.d.	n.d.	n.d.	n.d.
		TSa	n.d.	n.d.	n.d.	n.d.
		MBa	n.d.	36	n.d.	n.d.
		RH	n.d.	11	n.d.	n.d.
		R2a	n.d.	21	n.d.	n.d.
		Total	**n.d.**	**68**	**n.d.**	**n.d.**
	CE_19_09	R2a + 1 ata	n.d.	56	n.d.	n.d.
		R2a + 4 ata + 21%	n.d.	22	n.d.	n.d.
		R2a + 4 ata + 4%	n.d.	50	n.d.	n.d.
		Total	**n.d.**	**128**	**n.d.**	**n.d.**
	CE_19_10	R2a + 1 ata	n.d.	60	n.d.	n.d.
		R2a + 4 ata + 21%	n.d.	60	n.d.	n.d.
		R2a + 4 ata + 4%	n.d.	60	n.d.	n.d.
		Total	**n.d.**	**180**	**n.d.**	**n.d.**
		Total	**915**			
***Hertwigia* spp.**	**GRNL_81**	½ R2a	7	19	15	18
		½ R2a + LNHM	n.d.	22	n.d.	n.d.
		FSSW	n.d.	15	n.d.	n.d.
		½ R2a + SSE	n.d.	30	n.d.	n.d.
		Total	**7**	**86**	**15**	**18**
	GRNL_82	½ R2a	41	59	51	45
		½ R2a + LNHM	n.d.	45	n.d.	n.d.
		FSSW	n.d.	73	n.d.	n.d.
		½ R2a + SSE	n.d.	82	n.d.	n.d.
		Total	**41**	**259**	**51**	**45**
		Total	**522**			
Total of bacterial isolates recovered			**1437**			

Table S1-4. Descriptive and ANOVA summary on the effect of temperature on bacteria recovery.(SS; Sum of Squares; MS, mean square; DF, degrees of freedom).

CFU	**Descriptive Statistics**					
	Sponge	Temp.	Mean	SD	N	
	P. carpenteri	4°C	4.66	4.84	6	
		15°C	5.33	3.44	6	
		22-25°C	6.66	4.41	6	
		28°C	6	3.40	6	
	Hertwigia sp.	4°C	8.00	6.54	6	
		15°C	13.00	9.40	6	
		22-25°C	11.00	6.72	6	
		28°C	10.50	5.99	6	
	Two-Way ANOVA test					
	Source	SS	DF	MS	F	*p*-value
	Sponge* Temp.	31.73	3	10.58	0.30	0.82
	Sponge	295.0	1	295.00	8.47	0.006
	Temp.	57.73	3	19.24	0.55	0.65
	Residual	1394	40	34.84		
Morphotypes	Descriptive Statistics					
	Sponge	Temp.	Mean	SD	N	
	P. carpenteri	4°C	1.50	1.05	6	
		15°C	2.00	0.89	6	
		22-25°C	2.67	1.03	6	
		28°C	2.33	1.03	6	
	Hertwigia sp.	4°C	1.83	0.41	6	
		15°C	3.16	1.47	6	
		22-25°C	3.00	1.26	6	
		28°C	3.33	1.03	6	
	Two-Way ANOVA test					
	Source	SS	DF	MS	F	*p*-value
	Sponge* Temp.	1.729	3	0.58	0.51	0.68
	Sponge	6.021	1	6.02	5.33	0.026
	Temp.	11.06	3	3.69	3.26	0.031
	Residual	45.17	40	1.13		

Significant p-values are in bold

Table S1-5. Descriptive and ANOVA summary on the effect of nutritional additives on bacteria recovery. (SS; Sum of Squares; MS, mean square; DF, degrees of freedom).

CFU	**Descriptive Statistics**					
	Sponge	Temp.	Mean	SD	N	
	P. carpenteri	½ R2a	6.00	4.41	9	
		+ LNHM	4.22	2.33	9	
		+ SSE	6.44	2.83	9	
		+ 24h Enrich	9.66	10.53	9	
	Hertwigia sp.	½ R2a	13.00	9.40	6	
		+ LNHM	11.16	6.64	6	
		+ SSE	19.50	9.58	6	
		+ 24h Enrich	16.66	9.03	6	
	Two-Way ANOVA test					
	Source	SS	DF	MS	F	*p*-value
	Sponge* Temp.	83.73	3	27.91	0.46	0.71
	Sponge	792.2	1	792.20	13.10	0.0008
	Temp.	329.9	3	110.00	1.82	0.16
	Residual	2419	40	60.48		
Morphotypes	Descriptive Statistics					
	Sponge	Temp.	Mean	SD	N	
	P. carpenteri	½ R2a	2.00	0.89	6	
		+ LNHM	2.66	0.82	6	
		+ SSE	2.50	0.87	6	
		+ 24h Enrich	2.00	0.89	6	
	Hertwigia sp.	½ R2a	3.16	1.47	6	
		+ LNHM	4.17	1.72	6	
		+ SSE	3.83	0.75	6	
		+ 24h Enrich	2.33	0.82	6	
	Two-Way ANOVA test					
	Source	SS	DF	MS	F	*p*-value
	Sponge* Temp.	2.542	3	0.85	0.83	0.4805
	Sponge	19.14	1	19.14	18.87	<0.0001
	Temp.	14.28	3	4.76	4.69	0.0056
	Residual	52.72	52	1.01		

Significant p-values are in bold

Table S1-6. Descriptive and ANOVA summary on the effect of pressure treatments on bacteria recovery. Type II SS; Type II Sum of Squares; MS, mean square; DF, degrees of freedom).

CFU	**Descriptive Statistics**					
	Sponge	Treatment	Mean	SD	N	
	CE_19_09	Atmosphere	18.66	2.08	3	
		4 ata, 21%	7.33	0.58	3	
		4 ata, 4%	16.66	1.15	3	
	CE_19_10	Atmosphere	21.33	6.66	3	
		4 ata, 21%	13.33	6.11	3	
		4 ata, 4%	23.00	2.00	3	
	Two-Way ANOVA test					
	Source	SS	DF	MS	F	*p*-value
	Sponge* Pres.	12.33	2	6.167	0.40	0.68
	Sponge	112.5	1	112.50	7.36	0.02
	Pres.	367.4	2	183.70	12.03	0.001
	Residual	183.3	12	15.28		
Morphotypes	Descriptive Statistics					
	Sponge	Treatment	Mean	SD	N	
	CE_19_09	Atmosphere	4.33	0.58	3	
		4 ata, 21%	2.33	1.53	3	
		4 ata, 4%	5.00	0.00	3	
	CE_19_10	Atmosphere	4.33	1.15	3	
		4 ata, 21%	2.33	0.58	3	
		4 ata, 4%	4.00	1.00	3	
	Two-Way ANOVA test					
	Source	SS	DF	MS	F	*p*-value
	Sponge* Pres.	1.00	2	0.50	0.56	0.58
	Sponge	0.50	1	0.50	0.56	0.47
	Pres.	17.44	2	8.72	9.81	0.003
	Residual	10.67	12	0.89		

Significant p-values are in bold

Table S1-7. Detection of biosynthetic gene clusters. Exemplar of a gel for the visualised products can be seen in Figure S1-3.

Phylum	Genera	No. of strains	Number of total strains (%)		
			PKS-I	PKS-II	NRPS
Actinobacteria	Streptomycete	1	1 (100)	0 (0)	1 (100)
	Microbacterium	5	4 (80)	2 (40)	0 (0)
	Brevundimona	2	2 (100)	0 (0)	0 (0)
	Rhodococcus	1	1 (100)	0 (0)	0 (0)
	Total	9	8 (88.8)	2 (22.2)	1 (11)
Proteobacteria	Pseudomonas	2	2 (100)	0 (0)	0 (0)
	Delftia	3	2 (66)	0 (0)	3 (100)
	Psychrobacter	1	1 (100)	1 (100)	0 (0)
	Stenotrophomonas	1	1 (100)	1 (100)	0 (0)
	Total	8	6 (75)	2 (25)	3 (37.5)
Firmicutes	Bacillus spp.	2	1 (50)	0 (0)	0 (0)
	Total	2	1 (50)	0 (0)	0 (0)
Absolute total		19	15 (78.0)	4 (21)	3 (15.8)

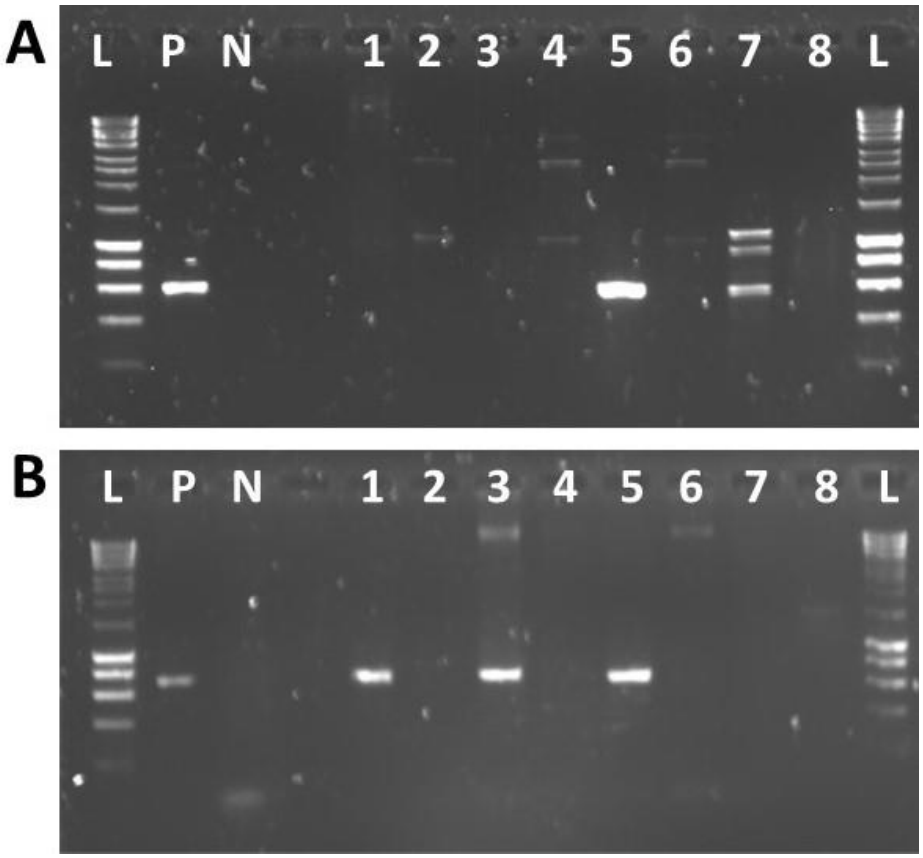

Figure S1-3. Example 1.5% agarose gel of the amplification of PKS and NRPS regions from bacterial isoaltes. Top gel (A) visualises the amplified products from the PKS primers, and the bottom gel (B) is for the NRPS amplified products. Lanes contained the following: P, positive control gDNA of *Streptomyces* sp; N, negative control of nuclease-free water; L, 1 Kb HyperLadder; Lane 1, RC-235; Lane 2, RC206-Y; Lane 3, PB-101; Lane 4, PC-227; Lane 5, Act2-R2a; Lane 6, RC201; Lane 7, RC206-O; Lane 8, RG-453.

Chapter 2. Appendix

Table S2-1. Reference databased utilised in analysis.

Database	Database contents	Date accessed	Reference
NaPDoS	Natural Product Domain Seeker. Bacterial Secondary Metabolite Gene (PKS and NRPS)	Oct 2020	https://npdomainseeker.sdsc.edu/; (Ziemert *et al.* 2012)
NCycDB	Bacterial Nitrogen metabolic cycling pathways	Jan 2021	(Tu *et al.* 2019)
RefSeq Kraken2 build	NCBI Reference Sequence Database composed of "compete" or "representative" genomes.	Jan 2021	https://lomanlab.github.io/mockcommunity/
UniProtKB	UnitProt Knowledgebase	Jan 2021	(Bateman and The UniProt Consortium 2018)
antiSMASH v.5	The antibiotics & Secondary Metabolite Analysis Shell	Jan 2021	https://antismash.secondarymetabolites.org/#!/start; (Blin et al., 2019)
SILVA SSU 138	Small (16S/18S, SSU) and large subunit (23S/28S, LSU) ribosomal RNA (rRNA) sequences for all three domains of life (Bacteria, Archaea and Eukarya)	Jan 2021	(Quast *et al.* 2013; Yilmaz *et al.* 2014; Laport 2017)

Table S2-2. Quality and quantity of metagenomic DNA samples. Molarity and media fragment size determined by the BioAnalzyer, concentration assessed by Qubit.

ID	Sample type	Transect	Quantity	Conc. (ng/µl)
CE19_15_09	Sediment	T52	0.5 mg	1.93
CE19_15_09	Sponge mesohyl	T52	2.0 mg	2.06
CE19_15_10	Sediment	T52	0.5 mg	17.06
CE19_15_10	Sponge mesohyl	T52	2.5 mg	48.80
CE19_15_11	Sediment	T52	0.5 mg	5.00
CE19_15_11	Sponge mesohyl	T52	2.0 mg	23.00
CE19_15_27	Sediment	T7	0.5 mg	4.20
CE19_15_27	Sponge mesohyl	T7	2.5 mg	1.15
CE19_15_28	Sediment	T7	0.5 mg	3.36
CE19_15_28	Sponge mesohyl	T7	2.5 mg	1.17
CE19_15_29	Sediment	T7	0.5 mg	6.58
CE19_15_29	Sponge mesohyl	T7	2.0 mg	41.8
Seawater T7	Water	T7	1.5 L	0.326
Seawater T52	Water	T52	1.5 L	0.412

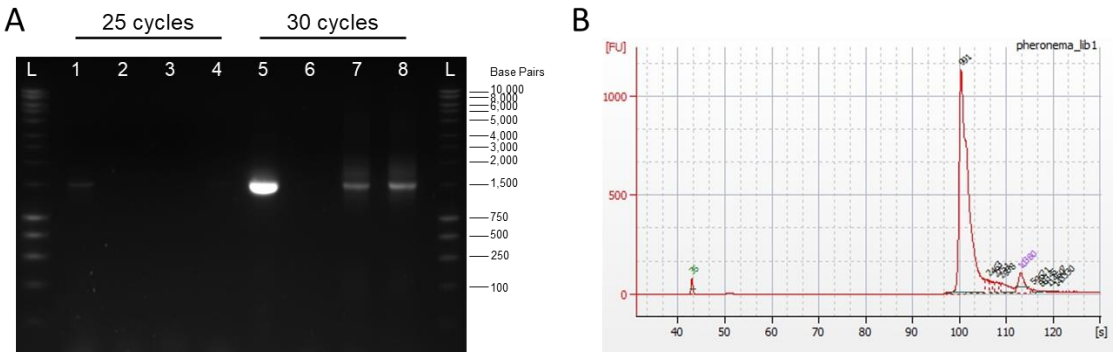

Figure S2-1. Assessing suitability of ONT PCR programme. (A) To check the suitability of the suggested amplification program suggested by ONT, the protocol was run with 25 cycles (lanes 1-4) and 30 cycles (lanes 5-8). Lanes 1 and 5, positive control of gDNA from E. coli. Lanes 2 and 6 are negative controls of nuclease-free water. The remaining lanes are the sediment sample BC10 and BC09. (B) One microliter of a 100 ng library was loaded onto a 2100 High Sensitivity DNA Chip (Agilent BioAnalyzer) to confirm the amplicon length in the library Confirmation of library amplicon were 1,451 bp in length.

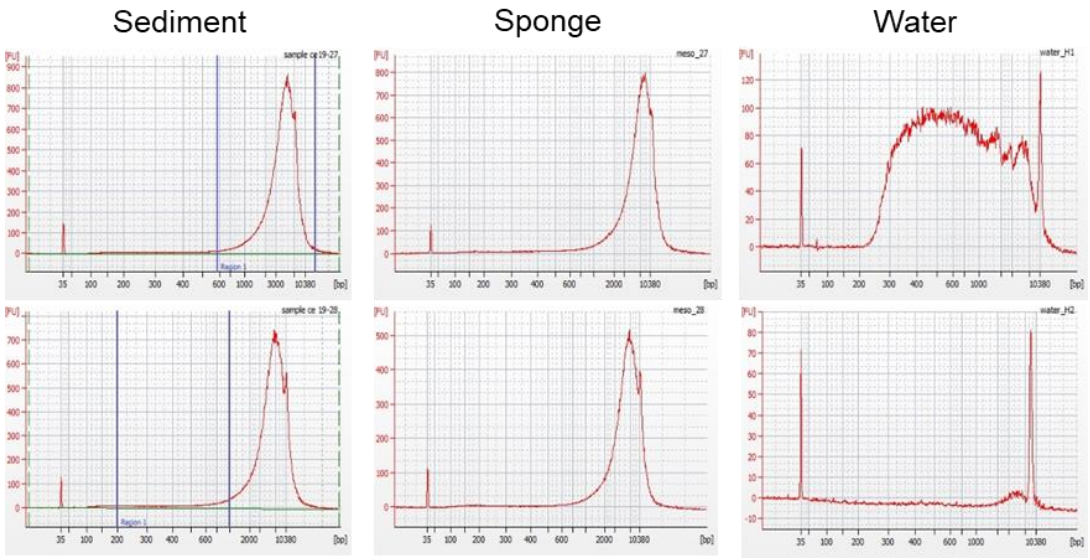

Figure S2-2. Examples of high sensitivity Bio Analyser fragment analysis. Ideal dsDNA is high molecular weight with minimal fragmentation, seen in the sediment and sponge samples.

Table S2-3. Sequencing library metadata.

ONT Barcode	Unique ID	Type	Transect	Sequencing Library	Input to sequencing library (ng)	# PCR
BC01	CE19_15_2Sed	Sediment	H1	1	14	1
BC02	CE19_15_10Sed	Sediment	H1	1	14	1
BC03	CE19_15_69Sed	Sediment	H1	1	14	1
BC06	CE19_15_011Spo	Sponge	H1	1	14	1
BC08	CE19_15_27Sed	Sediment	H2	1	14	1
BC09	CE19_15_28Sed	Sediment	H2	1	14	1
BC10	CE19_15_29Sed	Sediment	H2	1	14	1
BC11	CE19_15_27Spo	Sponge	H2	1	14	1
BC12	CE19_15_28Spo	Sponge	H2	1	14	1
BC02	Water_H1	Water	H1	2	7.14	1
BC04	CE19_15_009Spo	Sponge	H2	2	9.44	1
BC05	CE19_15_010Spo	Sponge	H2	2	3.52	1
BC04	CE19_15_009Spo	Sponge	H2	3	13	2
BC05	CE19_15_010Spo	Sponge	H2	3	13	2
BC07	Water_H2	Water	H2	3	13	2
BC01	CE19_15_029Spo	Sponge	H1	3	13	2
BC02	Water_H1	Water	H1	3	13	2

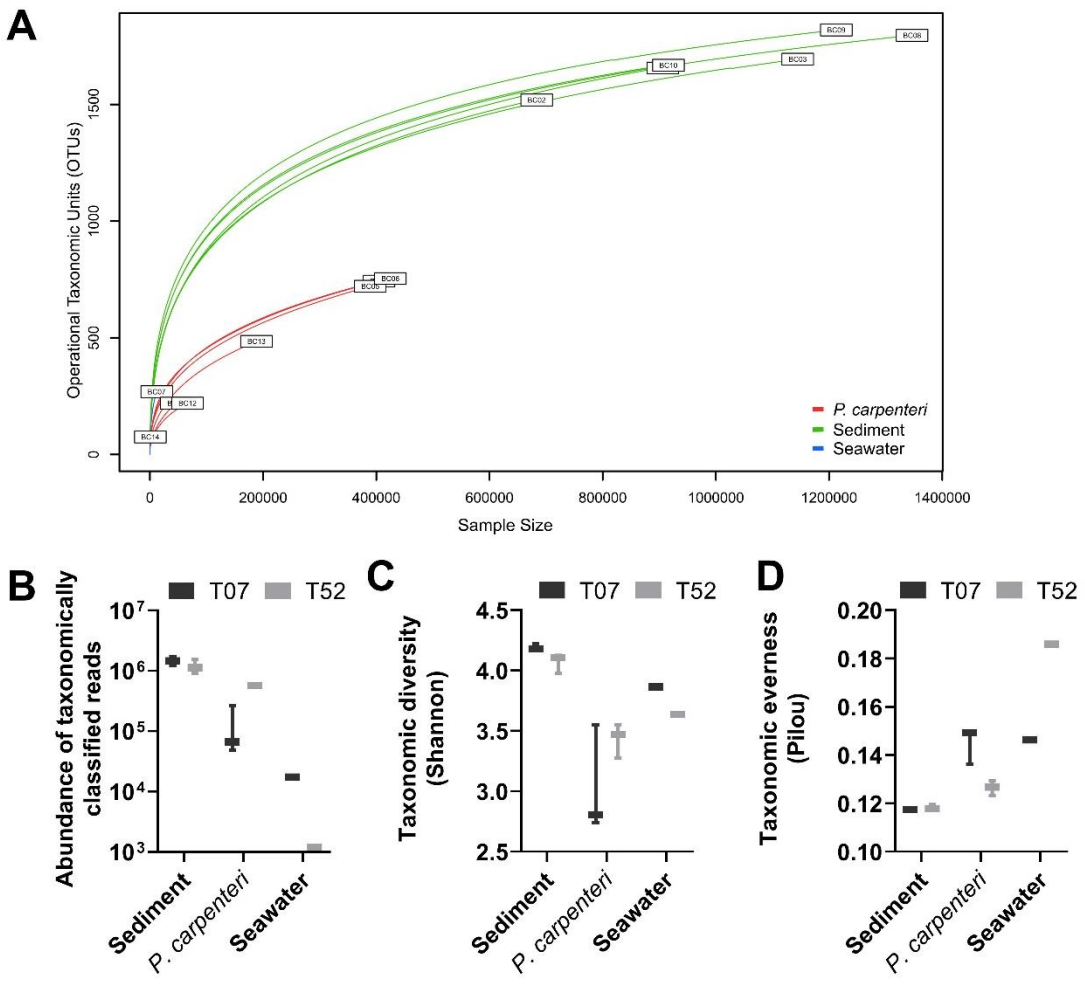

Figure S2-3. *P. carpenteri* exhibit a low observed and Shannon diversity compared to sediment communities, on part with water column diversity. (A) Rarefraction curve, (B) abundance of taxonomically classified reads, (C) taxonomic diversity as calculated by Shannon diversity metric, (D) taxonomic eveness as calculated by Pilou eveness metric. (A-D) *P. carpenteri*, sediment and water samples are grouped by sampling sites.

Table S2-4. Result of a pairwise comparison test for data presented in Fig. 2-3.

T07 PcAgg vs T52 PcAgg	Mean Diff.	95.00% CI of diff.	Adjusted p-value
α-proteobacteria	15.76	0.4256 to 31.10	0.0389
γ-proteobacteria	-2.729	-18.07 to 12.61	> 0.9999
Actinobacteriota	16.08	0.7464 to 31.42	0.0321
Methylomirabilota	0.006107	-15.33 to 15.34	> 0.9999
NB1-j	1.134	-14.20 to 16.47	> 0.9999
Acidobacteriota	0.9083	-14.43 to 16.24	> 0.9999
Planctomycetota	-31.77	-47.10 to -16.43	< 0.0001
Bacteroidota	0.8701	-14.47 to 16.21	> 0.9999
Myxococcota	-1.198	-16.53 to 14.14	> 0.9999
SAR324 clade (Marine group B)	1.185	-14.15 to 16.52	> 0.9999
Gemmatimodota	0.2204	-15.12 to 15.56	> 0.9999
Nitrospirota	0.4483	-14.89 to 15.78	> 0.9999
Firmicutes	1.473	-13.86 to 16.81	> 0.9999
Verrucomicrobiota	-0.03661	-15.37 to 15.30	> 0.9999
Chloroflexi	0.007886	-15.33 to 15.34	> 0.9999
Spirochaetota	0.3181	-15.02 to 15.65	> 0.9999
Other	-3.020	-18.36 to 12.32	> 0.9999
Unclassified	0.3335	-15.00 to 15.67	> 0.9999

Significant p values are highlighted in bold

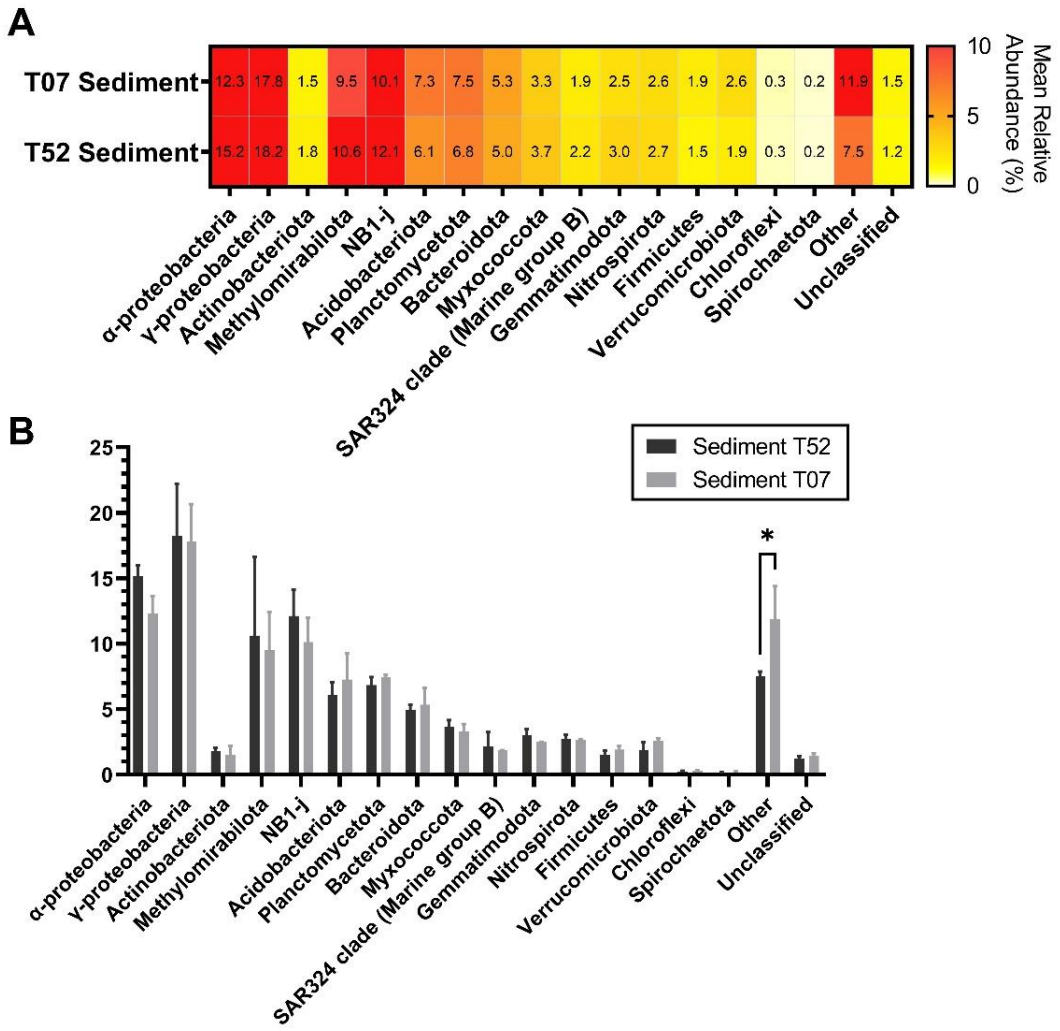

Figure S2-4. A comparison of sediment sampling sites reveals that rare taxa (< 0.1%) differentiates the two sites. (A) Mean relative abundance at phyla level, mean relative abundances > 0.1% are show. (B) Comparison of the relative abundances between two P. carpenteri, data are shown as mean ± SD (N = 3).Full results of Two-Way ANOVA can be found in Table S2-5 (Significant *p* values from a pairwise comparison are show in figure: ∗, p < 0.05; ∗∗∗∗, p < 0.0001).

Table S2-5. Summary of Two-Way ANOVA multiple comparison test for data presented in Figure S4B.

T07 Sediment vs T52 Sediment	Mean Diff.	95.00% CI of diff.	Adjusted *p*-value
α-proteobacteria	2.828	-1.283 to 6.939	0.4926
γ-proteobacteria	0.3893	-3.722 to 4.501	> 0.9999
Actinobacteriota	0.2608	-3.851 to 4.372	> 0.9999
Methylomirabilota	1.111	-3.001 to 5.222	> 0.9999
NB1-j	2.007	-2.104 to 6.119	0.9277
Acidobacteriota	-1.146	-5.257 to 2.966	0.9999
Planctomycetota	-0.6067	-4.718 to 3.505	> 0.9999
Bacteroidota	-0.3734	-4.485 to 3.738	> 0.9999
Myxococcota	0.3639	-3.748 to 4.475	> 0.9999
SAR324 clade (Marine group B)	0.3109	-3.801 to 4.422	> 0.9999
Gemmatimodota	0.4967	-3.615 to 4.608	> 0.9999
Nitrospirota	0.1100	-4.001 to 4.222	> 0.9999
Firmicutes	-0.4198	-4.531 to 3.692	> 0.9999
Verrucomicrobiota	-0.6992	-4.811 to 3.412	> 0.9999
Chloroflexi	-0.03393	-4.145 to 4.078	> 0.9999
Spirochaetota	-0.01890	-4.130 to 4.093	> 0.9999
Other	-4.361	-8.472 to -0.2493	0.0287
Unclassified	-0.2189	-4.330 to 3.893	> 0.9999

Significant p values are highlighted in bold

Table S2-6. Summary of metagenomic sequencing of Sponge 29.

Stage	No. of reads	Length (bp)		
		Minimum	Maximum	Average
Raw reads	232,000	69	45,864	2,453.1
Clean reads	192,655	150	45,864	2,369.9
Contigs	76,158	500	19,318	1,142.7

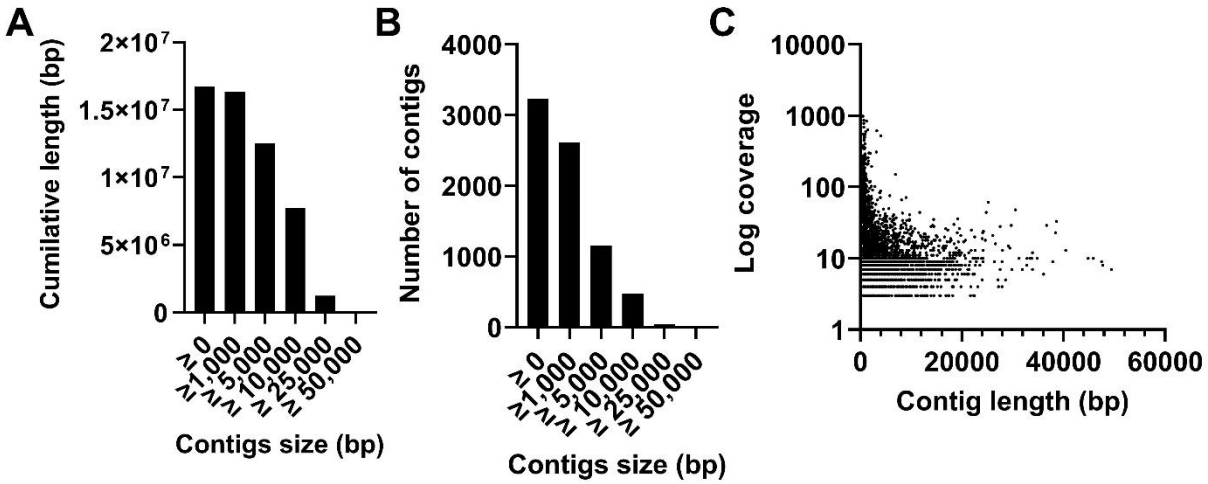

Figure S2-5. Quality analysis of contigs generate by Sponge 29 metagenome using metaFlye. Summary of contigs was generated by QUAST, (A) the cumulative lengths of contigs binned by contig length, (B) the number of contigs binned by length, and the coverage of contigs by length.

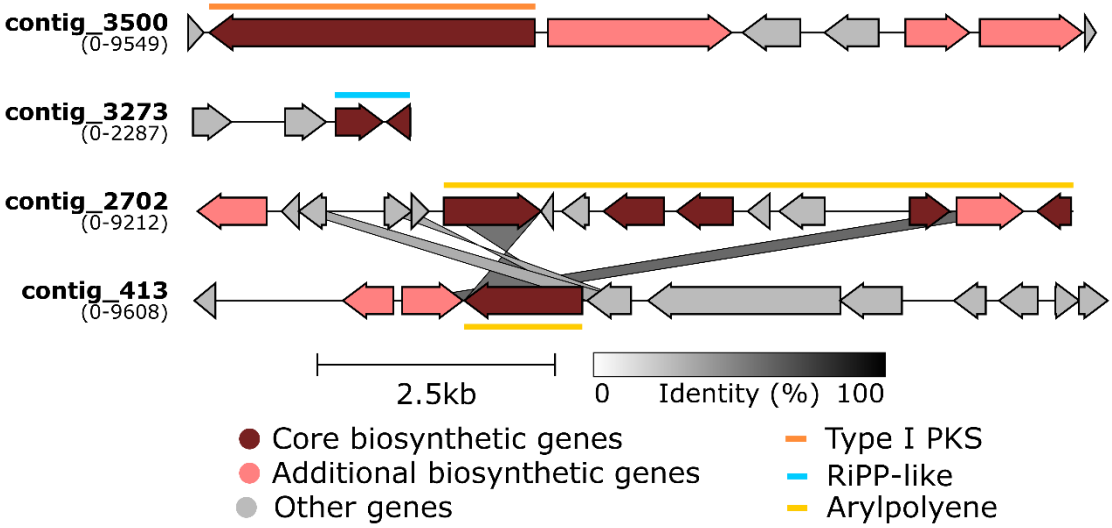

Figure S2-6. antiSMASH v.6 cluster predictions for Sponge 29. antiSMASH results were downloaded as GenBank (.gbk) file and aligned, and cluster arrow map was visualised using Clinker, annotations were added using Inkscape. Similar regions between the two Arylpolyene clusters are indicated. The coloured bars above arrows represent the region identified as belonging to a particular class of BGC. The start and end region of the cluster is indicated in the parentheses below the contig name. Genes with similar proposed functions are indicated with identical colors.

Table S2-7. BLASTp tabular output for the Best Reciprocal Hits (BRH) against NaPDoS database. Diamond BLASTpof predicted proteins from metagenomic data against the NaPDos database. (pident, Percentage of identical matches (%); length, alignment length; mismatch, Number of mismatches; gapopen, Number of gap openings; qstart, Start of alignment in query; qend, End of alignment in query; sstart, Start of alignment in subject; send, End of alignment in subject; evalue; Expected value; bitscore, Bit score).

Contig	NapDoS database hit	Pathway product	Pathway Type	pident	length	mismatch	gapopen	qstart	qend	sstart	send	evalue	bitscore
contig_1074_13	FabF_Ecoli_FAS	FAS	FAS	50.3	348	173	0	5	352	1	348	6.8E-101	359
contig_1231_5	FabF_Bacillus_FAS	FAS	FAS	57	223	95	1	1	223	184	405	1.4E-70	257.7
contig_1233_3	FabF_Bacillus_FAS	FAS	FAS	59	210	85	1	9	218	197	405	4.3E-69	252.7
contig_1493_5	FabF_Bacillus_FAS	FAS	FAS	29.7	397	260	4	6	397	1	383	9.4E-49	186
contig_1689_2	FabF_Bacillus_FAS	FAS	FAS	32.7	398	247	8	6	397	1	383	6.2E-53	199.9
contig_2003_5	FabF_Bacillus_FAS	FAS	FAS	42.4	422	222	6	7	425	1	404	3.1E-87	313.9
contig_2003_7	AknB_AF257324_KSa	aclacinomycin	PKS (Type II)	36	264	157	4	7	268	1	254	1.1E-37	148.7
contig_2406_6	FabF_Bacillus_FAS	FAS	FAS	32.4	408	258	5	13	405	1	405	2.5E-57	214.5
contig_2451_4	AlnM_ACI88862_KSb	alnumycin	PKS (Type II)	31.6	171	111	5	1	170	258	423	7.3E-16	75.5
contig_2639_15	FabF_Bacillus_FAS	FAS	FAS	39.8	181	109	0	226	406	1	181	2.7E-37	147.9
contig_2702_1	FabB_Ecoli_FAS	FAS	FAS	45.8	192	101	3	24	213	42	232	7.3E-38	149.1
contig_2702_10	FabB_Ecoli_FAS	FAS	FAS	44.5	164	88	3	24	185	42	204	3.9E-29	119.8
contig_2702_6	FabB_Ecoli_FAS	FAS	FAS	47.5	318	161	4	24	339	42	355	2E-73	267.7
contig_2702_9	FabB_Ecoli_FAS	FAS	FAS	62.3	69	26	0	34	102	292	360	5.4E-21	92.8
contig_2880_5	FabF_Ecoli_FAS	FAS	FAS	38.5	392	225	7	1	377	8	398	1.5E-59	221.9
contig_3023_1	FabF_Bacillus_FAS	FAS	FAS	61.8	178	68	0	225	402	1	178	2.5E-62	231.1
contig_3023_16	FabF_Ecoli_FAS	FAS	FAS	53.1	226	104	2	6	229	90	315	3.4E-65	240
contig_3023_19	A_AAG26879_SP	spore pigment	PKS (Type II)	38.7	111	68	0	49	159	9	119	6.9E-17	79
contig_3023_8	FabF_Streptomyces_FAS	FAS	FAS	58	81	34	0	1	81	198	278	4.1E-23	98.6
contig_3349_4	FabF_Ecoli_FAS	FAS	FAS	33.1	411	263	6	11	413	1	407	2.4E-57	214.5
contig_413_4	FabB_Ecoli_FAS	FAS	FAS	46.9	399	206	5	9	405	3	397	7.5E-91	325.9

Table S2-8. BLASTp tabular output for the Best Reciprocal Hits (BRH) against NCyc database. Diamond BLASTpof predicted proteins from metagenomic data against the NaPDos database. (pident, Percentage of identical matches (%); length, alignment length; mismatch, Number of mismatches; gapopen, Number of gap openings; qstart, Start of alignment in query; qend, End of alignment in query; sstart, Start of alignment in subject; send, End of alignment in subject; evalue; Expected value; bitscore, Bit score).

qid	sseqid		source	pident	length	mismatch	gapopen	qstart	qend	sstart	send	evalue	bitscore
	description	homolog											
contig_1168_7	asnB	SS23092	m5nr	51.7	58	27	1	1	58	1	57	1.20E-10	66.6
contig_1994_1	asnB	COG0367	eggNOG	68.4	335	106	0	1	335	284	618	3.10E-140	498.4
contig_1995_1	asnB	COG0367	eggNOG	69.6	250	76	0	31	280	1	250	3.30E-106	386.3
contig_2471_5	asnB	COG0367	eggNOG	40.1	619	318	9	1	613	1	572	3.40E-122	439.5
contig_2524_11	asnB	COG0367	eggNOG	58.3	254	106	0	375	628	1	254	3.20E-85	316.6
contig_2524_12	asnB	COG0367	eggNOG	57.2	491	203	5	140	628	1	486	3.40E-164	578.9
contig_1250_3	gdh_K00261	COG0443	COG	40.1	347	183	7	1	340	93	421	3.20E-58	226.1
contig_17_69	gdh_K00261	COG0334	eggNOG	50.5	305	142	2	127	423	1	304	7.90E-80	298.1
contig_2055_3	gdh_K00261	COG0443	COG	41.4	365	193	6	7	364	5	355	4.00E-70	265.8
contig_2055_9	gdh_K00261	COG0443	COG	41.4	365	193	6	7	364	5	355	4.00E-70	265.8
contig_2075_5	gdh_K00261	COG0443	COG	42.6	136	72	2	36	165	165	300	4.30E-21	101.7
contig_2568_2	gdh_K00261	COG0443	COG	43.5	170	89	3	4	172	3	166	7.50E-31	134.4
contig_3068_2	gdh_K00261	COG0745	COG	39	77	46	1	43	118	32	108	2.70E-08	58.9
contig_3281_2	gdh_K00261	COG0745	COG	35.6	90	57	1	38	126	19	108	9.70E-09	60.5
contig_3281_4	gdh_K00261	COG0745	COG	35.6	90	57	1	38	126	19	108	7.40E-09	60.8
contig_3667_14	gdh_K00261	COG0443	COG	56.4	55	24	0	7	61	23	77	2.20E-11	68.6
contig_3836_1	gdh_K00261	COG0443	COG	35.6	354	204	6	6	353	150	485	2.20E-46	187.2

contig_3873_2	gdh_K00261	COG0745	COG	34.4	90	58	1	36	124	19	108	3.30E-09	62
contig_3873_4	gdh_K00261	COG0745	COG	34.4	90	58	1	36	124	19	108	3.30E-09	62
contig_3879_2	gdh_K00261	COG0443	COG	50	110	54	1	1	109	50	159	3.80E-22	104.8
contig_699_4	gdh_K00261	COG0443	COG	38.2	503	283	8	26	519	3	486	1.40E-81	304.3
scaffold_2484_20	gdh_K00261	COG0443	COG	37.2	484	260	10	1	476	31	478	1.80E-78	293.9
contig_1008_2	gdh_K15371	SS23620	m5nr	46.8	380	192	4	3	379	7	379	4.90E-76	285.4
contig_1008_6	gdh_K15371	SS23620	m5nr	46.8	380	192	4	3	379	7	379	4.90E-76	285.4
contig_1036_5	gdh_K15371	COG1225	COG	49.7	143	72	0	8	150	26	168	2.00E-33	142.5
contig_1036_8	gdh_K15371	COG1225	COG	49.7	143	72	0	8	150	26	168	2.00E-33	142.5
contig_136_12	gdh_K15371	COG1200	COG	35.4	432	245	14	25	433	18	438	1.20E-54	214.5
contig_136_13	gdh_K15371	COG1200	COG	46.6	236	120	3	1	231	445	679	1.60E-51	203.4
contig_136_3	gdh_K15371	COG1200	COG	37.9	562	314	15	25	563	18	567	4.20E-87	322.8
contig_1758_66	gdh_K15371	SS23620	m5nr	46.3	337	172	4	5	340	9	337	3.90E-66	252.7
contig_1758_9	gdh_K15371	SS23620	m5nr	46.3	337	172	4	5	340	9	337	3.90E-66	252.7
contig_1785_7	gdh_K15371	COG1982	COG	38.9	404	228	7	16	417	380	766	1.10E-81	304.3
contig_2527_1	gdh_K15371	SS23620	m5nr	47.4	323	161	4	5	326	9	323	6.50E-66	251.5
contig_3305_10	gdh_K15371	COG0563	eggNOG	43.5	184	94	1	1	174	1	184	1.10E-36	153.7
contig_3305_4	gdh_K15371	COG0563	eggNOG	43.5	184	94	1	1	174	1	184	1.10E-36	153.7
contig_3367_5	gdh_K15371	ENOG410Y0QI	eggNOG	64.4	45	16	0	1	45	1	45	1.20E-07	56.2

contig_3523_2	gdh_K15371	COG0563	eggNOG	48.4	93	47	1	1	93	3	94	3.80E-19	95.1
contig_3596_9	gdh_K15371	COG0203	eggNOG	30.6	124	46	3	27	150	33	116	4.90E-06	52
contig_3697_8	gdh_K15371	SS23540	m5nr	45.5	132	72	0	331	462	2	133	4.30E-20	100.1
contig_3697_9	gdh_K15371	SS23540	m5nr	59.5	74	30	0	155	228	331	404	2.00E-13	76.6
contig_2096_8	glnA	COG0468	eggNOG	87.5	303	38	0	1	303	26	328	1.60E-146	519.2
contig_2211_4	glnA	SS23643	m5nr	32.8	290	134	8	29	310	230	466	6.50E-27	122.1
contig_2212_4	glnA	SS23643	m5nr	36.5	178	102	4	2	173	294	466	5.60E-21	101.7
contig_2212_5	glnA	COG1007	eggNOG	34	197	121	5	85	277	89	280	4.10E-19	96.7
contig_2738_2	glnA	COG0494	COG	35	143	92	1	4	146	23	164	2.90E-13	75.5
contig_2753_3	glnA	COG0659	COG	39.6	159	77	2	20	173	17	161	1.20E-22	107.5
contig_2753_4	glnA	COG0659	COG	32.4	324	160	8	20	306	17	318	5.40E-31	135.6
contig_3278_1	glnA	COG0494	eggNOG	40.9	115	62	4	86	198	43	153	6.30E-14	78.2
contig_3751_4	glnA	SS22207	m5nr	62.3	61	22	1	1	61	1	60	2.60E-17	89
contig_846_7	glnA	SS23643	m5nr	35.6	225	126	5	247	466	328	538	2.60E-21	104
contig_1178_3	glnA	COG0174	eggNOG	77.2	474	102	2	4	477	2	469	1.60E-230	798.9
contig_2999_9	glsA	SS25074	m5nr	39.8	88	52	1	44	131	13	99	1.40E-11	70.5
contig_1762_1	gs_K00265	SS22937	m5nr	60.8	51	20	0	25	75	29	79	4.00E-12	70.9
contig_1762_2	gs_K00265	SS22937	m5nr	55.6	45	20	0	8	52	61	105	6.80E-08	56.2
contig_3339_1	gs_K00265	SS22937	m5nr	59.5	74	30	0	3	76	14	87	8.40E-21	99.8
contig_3339_2	gs_K00265	SS22937	m5nr	61	123	48	0	82	204	3	125	7.80E-36	151.4
contig_3339_3	gs_K00265	SS22937	m5nr	65.3	72	25	0	149	220	3	74	2.00E-20	100.1
contig_3339_5	gs_K00265	SS22937	m5nr	60	60	24	0	56	115	25	84	7.00E-15	80.5
contig_1118_2	gs_K00266	SS10080	m5nr	50.9	53	26	0	5	57	9	61	2.10E-07	55.8

contig_1311_4	gs_K00266	SS16338	m5nr	36.4	272	168	3	9	280	172	438	4.90E-38	158.7
contig_1730_3	gs_K00266	SS10080	m5nr	54.2	48	22	0	5	52	9	56	2.20E-06	54.3
contig_1730_7	gs_K00266	SS10080	m5nr	54.2	48	22	0	5	52	9	56	2.20E-06	54.3
contig_1957_1	gs_K00266	SS10080	m5nr	54.2	48	22	0	5	52	9	56	7.00E-08	57.4
contig_2719_2	gs_K00266	COG0543	COG	63.2	95	35	0	192	286	3	97	6.30E-33	141.7
contig_2719_7	gs_K00266	COG0543	COG	61.6	99	38	0	188	286	3	101	6.30E-33	141.7
contig_340_20	gs_K00266	COG0167	eggNOG	40.4	285	163	4	26	305	154	436	8.70E-52	204.5
contig_811_28	gs_K00266	COG0543	COG	54.1	292	126	2	1	286	1	290	4.70E-89	328.2
contig_2093_10	hcp	SS20816	m5nr	40.6	202	107	3	1	189	1	202	7.00E-41	167.9
contig_2147_4	hcp	SS16625	m5nr	32.5	372	244	4	24	393	13	379	4.50E-45	182.6
contig_2147_8	hcp	SS16625	m5nr	32.5	372	244	4	24	393	13	379	4.50E-45	182.6
contig_2299_10	hcp	SS16625	m5nr	39.5	195	116	2	1	195	181	373	4.60E-32	138.7
contig_2669_7	hcp	COG1773	eggNOG	56	184	80	1	184	366	33	216	1.40E-60	234.2
contig_3471_3	hcp	COG2025	COG	38.8	374	224	1	12	380	6	379	1.80E-67	256.9
contig_3471_7	hcp	SS16625	m5nr	36.1	133	84	1	6	138	12	143	2.00E-18	94.7
contig_421_20	hcp	SS20816	m5nr	40.6	202	107	3	1	189	1	202	1.10E-41	170.6
contig_422_3	hcp	SS20816	m5nr	40.6	202	107	3	1	189	1	202	1.10E-41	170.6
scaffold_191_26	hcp	SS16625	m5nr	28.7	345	235	7	132	470	53	392	1.50E-32	141.7
contig_532_28	narB	SS24263	m5nr	30.8	130	90	0	1	130	36	165	2.90E-13	77
contig_2156_10	narC	SS18801	m5nr	42.6	223	117	4	1	212	2	224	1.80E-44	180.6
contig_3476_5	narC	SS18801	m5nr	40.6	202	109	3	1	191	2	203	7.70E-37	155.6
contig_1178_28	narY	SS22485	m5nr	43.5	333	150	3	1	296	1	332	8.30E-68	257.7
contig_1178_32	narY	SS22485	m5nr	49.4	237	119	1	97	332	1	237	1.00E-58	227.6
contig_2560_5	narY	SS22485	m5nr	41.5	260	148	4	75	331	11	269	4.60E-51	202.2
contig_2560_9	narY	SS22485	m5nr	56.3	71	31	0	3	73	167	237	1.90E-17	89.4

contig_3847_3	narY	SS22485	m5nr	35.7	112	71	1	218	328	2	113	4.80E-16	85.9
contig_1612_20	nasB	SS22185	m5nr	36	86	49	3	3	87	144	224	2.60E-06	53.1
contig_1832_3	nasB	SS19025	m5nr	50	104	51	1	10	113	12	114	1.30E-21	102.8
contig_708_36	nasB	SS22185	m5nr	33.7	187	119	2	49	231	17	202	4.60E-17	89
contig_1240_11	nifH	COG3839	eggNOG	45.9	172	91	1	85	254	82	253	3.20E-35	149.8
contig_1240_6	nifH	COG3839	eggNOG	45.9	172	91	1	85	254	82	253	3.20E-35	149.8
contig_220_3	nifH	COG2151	COG	50.5	95	34	1	1	95	179	260	1.50E-21	102.8
contig_220_4	nifH	COG2151	COG	40.1	364	202	4	5	365	2	352	3.10E-72	272.7
contig_222_7	nifH	COG2151	COG	51.1	221	92	3	1	219	179	385	1.50E-59	229.9
contig_2883_1	nifH	COG0003	eggNOG	44.3	79	41	2	4	79	3	81	2.40E-12	71.6
contig_2883_7	nifH	COG0003	eggNOG	32	256	164	4	3	255	4	252	1.50E-27	124.4
contig_2634_10	nifW	COG1045	COG	68.2	236	75	0	1	236	1	236	2.10E-98	359.4
contig_3370_11	nifW	COG1045	COG	50.9	320	138	3	14	319	23	337	1.30E-84	313.5
contig_3370_14	nifW	COG1045	COG	50.9	320	138	3	14	319	23	337	1.30E-84	313.5
contig_3700_7	nifW	COG1045	COG	64.1	217	75	1	103	319	25	238	9.10E-81	300.8
contig_3700_9	nifW	COG1045	COG	62.2	336	107	3	1	319	1	333	1.20E-120	433.3
contig_43_6	nifW	COG1045	COG	63.2	182	65	1	122	301	196	377	1.30E-63	243.8
contig_1918_19	nirA	COG0175	COG	59.3	221	87	1	22	239	15	235	1.70E-74	279.6
contig_1918_21	nirA	COG0175	COG	59.3	221	87	1	22	239	15	235	1.70E-74	279.6
contig_1918_5	nirA	COG0175	COG	59.3	221	87	1	22	239	15	235	1.70E-74	279.6
contig_1918_7	nirA	COG0175	COG	59.3	221	87	1	22	239	15	235	1.70E-74	279.6
contig_2683_1	nirA	COG0739	eggNOG	34.3	134	75	4	4	128	67	196	5.50E-11	68.2
contig_2887_13	nirA	COG0098	eggNOG	50.4	115	57	0	35	149	16	130	3.20E-23	109

contig_2887_15	nirA	COG0098	eggNOG	50.4	115	57	0	35	149	16	130	3.20E-23	109
contig_2887_4	nirA	COG0098	eggNOG	50.4	115	57	0	35	149	16	130	3.20E-23	109
contig_2887_6	nirA	COG0098	eggNOG	50.4	115	57	0	35	149	16	130	3.20E-23	109
contig_421_12	nirA	SS24359	m5nr	29.8	168	114	2	58	225	117	280	1.30E-12	73.9
contig_603_2	nirA	SS24359	m5nr	29.6	348	232	6	40	384	83	420	3.90E-31	136.3
contig_93_10	nirA	COG0175	COG	62.2	196	71	1	1	193	40	235	3.70E-72	271.6
contig_1898_4	nirB	COG1587	COG	39.5	329	198	1	79	407	1	328	3.00E-62	240
contig_109_18	nirD	SS05148	m5nr	43.4	76	43	0	4	79	3	78	4.90E-08	58.9
contig_109_9	nirD	SS05148	m5nr	43.4	76	43	0	4	79	3	78	4.90E-08	58.9
contig_1158_3	nirD	SS05148	m5nr	42.1	76	44	0	37	112	3	78	5.70E-07	55.5
contig_15_3	nirD	ENOG410XPPK	eggNOG	48.5	99	51	0	1	99	1	99	2.20E-25	115.9
contig_15_7	nirD	ENOG410XPPK	eggNOG	47.5	101	53	0	1	101	1	101	7.80E-26	116.7
contig_1661_9	nirD	COG2146	COG	60.9	69	27	0	34	102	11	79	1.20E-21	102.8
contig_2407_1	nirD	SS24200	m5nr	50	56	28	0	79	134	4	59	9.10E-09	62.4
contig_2793_3	nirD	SS10812	m5nr	28.1	270	182	5	186	444	1	269	1.30E-20	102.1
contig_2827_12	nirD	COG2146	COG	31.4	306	194	8	163	456	34	335	3.30E-29	130.6
contig_2827_3	nirD	SS10812	m5nr	34.2	187	109	4	12	184	116	302	1.30E-19	97.1
contig_2827_8	nirD	SS10812	m5nr	31.4	353	224	9	116	456	12	358	2.60E-34	147.5
contig_3469_4	nirD	COG2146	COG	57	93	40	0	1	93	1	93	6.50E-28	123.6
contig_3469_5	nirD	COG2146	COG	52.9	102	48	0	1	102	1	102	1.30E-28	125.9
contig_32_4	nirD	COG2146	eggNOG	59.8	102	40	1	1	101	1	102	5.50E-33	140.6
contig_1004_13	nirK	SS24021	m5nr	22.7	233	174	3	555	785	204	432	2.50E-08	61.6
contig_1005_1	nirK	COG3210	COG	27.3	304	165	11	2267	2559	200	458	1.00E-09	68.2
contig_1006_11	nirK	SS22230	m5nr	28	264	157	7	32	288	995	1232	1.40E-07	57.8

contig_1076_5	nirK	COG0488	COG	25.5	255	135	6	1	239	3	218	7.60E-11	69.3
contig_1140_14	nirK	COG0515	eggNOG	30	257	143	8	145	390	19	249	7.90E-21	102.4
contig_1140_3	nirK	COG0515	eggNOG	30	257	143	8	140	385	19	249	7.80E-21	102.4
contig_1163_1	nirK	COG0488	COG	28.9	246	124	5	2	237	7	211	2.10E-16	87.8
contig_1163_6	nirK	COG0488	COG	28.9	246	124	5	2	237	7	211	2.10E-16	87.8
contig_1170_4	nirK	COG0488	COG	39.8	352	197	8	163	505	43	388	1.00E-60	235
contig_1171_1	nirK	COG0488	COG	31.1	299	155	9	3	254	1	295	7.60E-30	131.3
contig_1187_13	nirK	SS24345	m5nr	50.6	785	372	5	1	773	136	916	3.40E-214	745.3
contig_1187_14	nirK	COG0574	eggNOG	47.9	73	29	2	14	77	4	76	5.80E-11	67
contig_1199_5	nirK	COG0552	COG	39.6	285	144	5	5	263	16	298	4.20E-42	172.2
contig_1236_6	nirK	COG0515	COG	36	150	88	4	86	228	28	176	3.00E-16	86.3
contig_1240_1	nirK	COG0515	eggNOG	34.3	108	57	3	8	110	121	219	2.80E-08	59.7
contig_129_9	nirK	COG0515	eggNOG	34.6	289	180	3	98	386	101	380	1.20E-42	175.6
contig_1331_4	nirK	COG0511	eggNOG	53.4	58	27	0	52	109	59	116	3.00E-09	62
contig_1412_3	nirK	COG0508	eggNOG	43.3	307	168	3	84	388	170	472	1.10E-61	237.7
contig_1441_15	nirK	COG0515	eggNOG	37.2	164	99	1	1	164	138	297	3.20E-25	115.5
contig_1444_8	nirK	COG2204	COG	43.7	453	252	1	6	458	9	458	1.70E-107	390.2
contig_1508_31	nirK	SS04014	m5nr	34.1	82	50	1	124	205	3	80	7.40E-10	64.7
contig_17_51	nirK	COG0515	eggNOG	39.6	268	151	5	261	527	126	383	1.90E-49	197.6
contig_1762_7	nirK	COG0545	COG	50	104	52	0	148	251	45	148	8.50E-24	111.3
contig_179_19	nirK	COG2204	COG	49.6	371	187	0	4	374	7	377	2.10E-100	366.7

contig_181_2	nirK	COG2204	COG	45.2	460	244	1	4	463	7	458	2.00E-108	393.3
contig_181_3	nirK	COG2204	COG	45.4	460	243	1	4	463	7	458	8.90E-109	394.4
contig_1848_6	nirK	COG0488	COG	26.9	193	114	7	343	520	55	235	9.30E-09	62.4
contig_1904_8	nirK	COG0488	COG	23.1	264	137	6	1	240	1	222	3.20E-09	63.9
contig_192_2	nirK	COG5278	COG	30.9	246	157	3	361	597	21	262	3.60E-25	117.1
contig_2018_1	nirK	SS15500	m5nr	52.5	295	129	3	41	324	1	295	4.70E-80	298.5
contig_2018_5	nirK	SS23696	m5nr	37.1	507	294	8	4	496	169	664	6.80E-83	308.5
contig_2025_2	nirK	COG0515	COG	34.1	182	91	5	4	156	73	254	3.90E-19	95.1
contig_2079_9	nirK	SS24345	m5nr	51.4	883	408	6	37	915	20	885	5.20E-246	851.3
contig_2180_18	nirK	COG0488	COG	27	178	111	5	71	241	347	512	1.10E-06	54.7
contig_2206_3	nirK	ENOG410XNMH	eggNOG	28.8	219	141	6	4	214	260	471	7.00E-16	84.7
contig_2206_4	nirK	COG2202	eggNOG	32.1	243	152	3	395	628	223	461	6.50E-25	116.3
contig_2228_12	nirK	SS10467	m5nr	40.7	518	298	8	50	560	77	592	2.20E-101	370.2
contig_2228_7	nirK	SS10467	m5nr	40.7	518	298	8	81	591	77	592	2.30E-101	370.2
contig_2261_4	nirK	SS22230	m5nr	54.5	220	100	0	2	221	303	522	9.30E-62	239.2
contig_2262_31	nirK	SS22230	m5nr	54.5	220	100	0	2	221	303	522	9.30E-62	239.2
contig_2402_1	nirK	COG1819	eggNOG	47.4	78	39	2	283	360	4	79	1.10E-12	75.1
contig_2417_18	nirK	COG0488	COG	25.7	206	130	5	319	512	4	198	7.10E-09	62.8
contig_2472_8	nirK	COG0515	eggNOG	31.6	272	157	8	7	260	67	327	1.70E-24	113.6
contig_2475_8	nirK	COG0552	COG	52.8	142	67	0	157	298	1	142	1.00E-32	141.4
contig_2478_5	nirK	COG3119	eggNOG	26.5	328	153	11	4	288	35	317	7.70E-17	89
contig_2500_1	nirK	SS22990	m5nr	50	98	49	0	4	101	66	163	1.40E-17	90.1

contig_2500_2	nirK	SS22990	m5nr	50	98	49	0	4	101	66	163	1.30E-17	90.1
contig_2613_10	nirK	COG0129	eggNOG	37.5	128	77	2	499	625	3	128	9.80E-18	92.4
contig_2613_11	nirK	COG0129	eggNOG	45.6	160	81	3	324	479	1	158	1.00E-30	135.6
contig_2613_4	nirK	COG0129	eggNOG	32.4	210	136	3	32	240	103	307	6.00E-22	105.1
contig_2613_5	nirK	COG0129	eggNOG	45.6	160	81	3	324	479	1	158	1.00E-30	135.6
contig_2613_6	nirK	COG0129	eggNOG	37.5	128	77	2	499	625	3	128	9.80E-18	92.4
contig_2640_3	nirK	COG0545	COG	50.5	105	52	0	81	185	45	149	1.30E-24	113.6
contig_2640_5	nirK	COG0545	COG	49.5	105	53	0	135	239	45	149	8.10E-24	111.3
contig_2684_21	nirK	COG0488	COG	33.8	160	101	4	10	166	355	512	2.40E-14	79.7
contig_2727_7	nirK	COG0488	COG	27	178	111	5	61	231	347	512	1.00E-06	54.7
contig_2742_3	nirK	SS23515	m5nr	46.2	65	35	0	3	67	225	289	6.60E-08	57
contig_2763_5	nirK	SS20977	m5nr	41.9	74	42	1	5	78	274	346	8.10E-10	63.2
contig_2763_6	nirK	SS20977	m5nr	41.9	74	42	1	5	78	274	346	6.80E-09	60.1
contig_2847_12	nirK	COG2331	eggNOG	64.1	39	14	0	21	59	1	39	2.00E-09	62.4
contig_3029_12	nirK	COG0552	COG	38.3	311	164	4	5	289	16	324	3.10E-47	189.5
contig_3029_13	nirK	COG0552	COG	39	290	151	2	42	331	2	265	3.20E-47	189.5
contig_3029_4	nirK	COG0552	COG	48.3	201	104	0	137	337	29	229	4.90E-48	192.2
contig_3029_8	nirK	COG0552	COG	47.8	201	105	0	137	337	29	229	1.40E-47	190.7
contig_3084_1	nirK	COG1435	eggNOG	47.7	65	33	1	29	92	1	65	2.70E-12	71.6
contig_3084_9	nirK	COG1435	eggNOG	47.5	80	41	1	1	80	116	194	8.70E-18	89.7
contig_3106_5	nirK	K00428	KEGG	26.7	348	164	14	133	419	81	398	1.70E-19	97.8
contig_3120_11	nirK	COG0323	eggNOG	27.8	349	213	8	1	322	127	463	6.50E-26	118.6

contig_3120_5	nirK	COG0323	eggNOG	40.9	115	67	1	86	199	5	119	9.00E-14	79.7
contig_3133_13	nirK	COG0515	eggNOG	32.1	165	96	5	1	151	47	209	1.30E-13	76.6
contig_3200_2	nirK	COG0488	COG	47.2	53	28	0	453	505	2	54	1.20E-08	62
contig_3200_5	nirK	COG0488	COG	49.1	53	27	0	453	505	2	54	2.40E-09	64.3
contig_3200_6	nirK	COG0488	COG	38.5	270	166	0	143	412	10	279	1.50E-51	204.5
contig_3296_4	nirK	COG0488	COG	27.1	240	140	7	1	237	1	208	2.70E-08	60.8
contig_35_11	nirK	COG0652	eggNOG	30.2	169	98	5	14	162	3	171	1.90E-09	63.2
contig_3583_4	nirK	ENOG410XNMH	eggNOG	55	411	164	4	94	494	24	423	7.20E-117	421.4
contig_3586_9	nirK	COG0515	eggNOG	34.5	267	157	6	65	326	126	379	3.60E-32	139.8
contig_3592_3	nirK	COG0515	eggNOG	36.6	224	137	2	1	224	138	356	8.30E-37	154.5
contig_3609_3	nirK	COG0488	COG	32.6	178	81	6	6	152	21	190	8.80E-11	67.4
contig_3626_12	nirK	SS16077	m5nr	64.9	188	66	0	2	189	46	233	3.50E-65	248.4
contig_3706_6	nirK	COG1249	eggNOG	62	79	30	0	1	79	80	158	1.60E-21	102.1
contig_3751_1	nirK	COG0488	COG	30.2	172	92	4	338	486	16	182	2.40E-12	74.3
contig_3792_1	nirK	COG1005	COG	58.6	203	63	4	209	404	12	200	6.20E-59	228.8
contig_3792_2	nirK	COG1005	COG	62.6	123	44	1	19	141	9	129	1.10E-39	164.9
contig_3792_3	nirK	COG1005	COG	52.7	165	57	4	247	404	1	151	2.50E-39	163.7
contig_3792_4	nirK	COG1005	COG	60.3	116	44	1	19	134	9	122	1.70E-35	151
contig_3792_5	nirK	COG1005	COG	55.7	174	56	4	238	404	7	166	1.10E-44	181.4
contig_3792_6	nirK	COG1005	COG	44.6	83	43	2	1	80	322	404	1.30E-12	73.2
contig_380_4	nirK	SS15942	m5nr	49.3	503	248	2	5	506	2	498	1.50E-133	476.9
contig_3867_11	nirK	SS22230	m5nr	65.7	70	24	0	266	335	1	70	7.00E-20	100.9
contig_39_19	nirK	COG0545	COG	59.6	89	36	0	2	90	52	140	5.20E-24	110.5

contig_3926_8	nirK	COG0488	COG	25.5	212	108	5	7	180	5	204	4.00E-12	72.4
contig_451_4	nirK	COG0515	eggNOG	34.3	204	131	3	22	224	166	367	8.20E-32	137.9
contig_451_8	nirK	COG0515	eggNOG	35.5	259	164	3	242	499	127	383	3.10E-43	176.8
contig_514_18	nirK	COG0515	eggNOG	37.7	154	96	0	37	190	230	383	1.90E-27	124.4
contig_616_5	nirK	COG0515	eggNOG	33.7	202	119	6	7	198	67	263	1.00E-24	114.8
contig_675_11	nirK	ENOG410XNMH	eggNOG	42	69	38	1	110	178	412	478	1.20E-08	60.5
contig_762_7	nirK	COG0515	eggNOG	37	181	110	4	1	180	204	381	9.10E-27	122.5
contig_762_8	nirK	COG0515	eggNOG	35.5	234	145	5	3	235	153	381	7.70E-35	148.7
contig_851_5	nirK	COG2197	eggNOG	43.7	135	75	1	24	157	30	164	4.70E-21	103.2
contig_851_6	nirK	COG0515	eggNOG	34.2	263	168	3	32	294	126	383	2.10E-38	160.2
contig_9_10	nirK	COG4191	COG	32.9	249	148	7	232	473	10	246	8.50E-30	132.1
contig_906_14	nirK	SS17868	m5nr	48.6	105	51	3	29	132	77	179	5.40E-16	84.7
contig_907_2	nirK	SS17868	m5nr	34.8	233	120	9	4	211	304	529	8.20E-22	104.4
contig_908_2	nirK	SS17868	m5nr	48.6	105	51	3	29	132	77	179	4.40E-16	84.7
contig_93_17	nirK	COG0488	COG	26.2	195	109	4	2	190	320	485	1.20E-09	64.3
contig_95_15	nirK	COG0488	COG	25.5	255	135	6	1	239	3	218	2.00E-11	71.2
contig_973_12	nirK	SS10467	m5nr	41.2	80	46	1	1	79	513	592	1.70E-08	58.9
scaffold_191_10	nirK	ENOG410XNMH	eggNOG	33.8	148	88	4	5	152	484	621	2.20E-14	79.3
scaffold_191_12	nirK	ENOG410XNMH	eggNOG	31.2	256	155	8	255	498	374	620	1.40E-22	108.2
contig_1225_20	nirS	COG0465	COG	31	248	160	6	231	469	159	404	1.10E-24	115.2
contig_1476_2	nirS	SS24700	m5nr	46.8	346	141	5	2	305	3	347	6.50E-76	284.6
contig_2026_2	nirS	SS24700	m5nr	43.1	304	131	5	3	264	14	317	5.50E-60	231.9

contig_2068_3	nirS	COG0465	eggNOG	54.9	339	152	1	1	338	243	581	3.90E-106	385.2
contig_2764_21	nirS	SS16989	m5nr	56.7	60	26	0	277	336	1	60	2.70E-14	80.1
contig_2764_3	nirS	SS16989	m5nr	55.7	61	27	0	279	339	3	63	2.70E-14	80.1
contig_2764_5	nirS	SS16989	m5nr	58.6	58	24	0	279	336	3	60	6.10E-14	79
contig_2764_6	nirS	SS16989	m5nr	58.6	58	24	0	279	336	3	60	6.10E-14	79
contig_2872_10	nirS	COG0465	COG	70.5	95	28	0	7	101	173	267	1.10E-35	149.8
contig_2872_11	nirS	COG0465	COG	59.5	185	74	1	288	471	1	185	7.00E-58	225.7
contig_2872_12	nirS	COG0465	COG	62.7	134	50	0	272	405	3	136	6.30E-43	176
contig_2872_14	nirS	COG0465	COG	44.9	207	109	3	399	601	8	213	7.00E-42	172.6
contig_2872_15	nirS	COG0465	COG	64.9	111	38	1	39	149	153	262	1.40E-34	146.4
contig_2872_16	nirS	COG0465	COG	66.7	60	20	0	288	347	1	60	9.20E-18	92.4
contig_2872_3	nirS	COG0465	COG	45.4	218	114	3	388	601	1	217	1.20E-44	181.8
contig_2872_4	nirS	COG0465	COG	43.9	198	106	3	408	601	1	197	7.20E-39	162.5
contig_2872_7	nirS	COG0465	COG	34.1	179	114	2	464	639	1	178	1.40E-22	108.6
contig_2872_8	nirS	COG0465	COG	60	65	25	1	387	450	1	65	1.50E-13	78.6
contig_2930_2	nirS	COG1622	eggNOG	31.6	190	116	4	28	204	100	288	2.30E-17	89.7
contig_3654_1	nirS	COG0465	COG	53.4	73	33	1	1	72	387	459	4.60E-15	80.5
contig_3654_2	nirS	COG0465	COG	79.5	39	8	0	250	288	5	43	5.50E-11	70.1
contig_3654_3	nirS	COG0465	COG	79.5	73	15	0	27	99	169	241	1.40E-27	122.5
contig_3654_9	nirS	COG0465	COG	42.2	109	63	0	4	112	475	583	1.80E-19	95.9
contig_439_1	nirS	SS16989	m5nr	39.5	114	64	2	7	115	91	204	1.30E-16	86.3
contig_546_5	nirS	COG0513	eggNOG	45.5	358	187	3	1	354	12	365	1.20E-85	317.4
contig_547_13	nirS	COG0513	eggNOG	45.5	358	187	3	1	354	12	365	1.20E-85	317.4
contig_547_24	nirS	COG0513	eggNOG	45.5	358	187	3	1	354	12	365	1.20E-85	317.4

contig_592_35	nirS	COG1622	eggNOG	32.7	208	119	4	63	251	59	264	3.20E-23	109.4
contig_592_5	nirS	COG1622	eggNOG	32.7	208	119	4	63	251	59	264	3.20E-23	109.4
contig_593_13	nirS	COG1622	eggNOG	32.7	208	119	4	63	251	59	264	3.20E-23	109.4
contig_593_3	nirS	COG1622	eggNOG	32.7	208	119	4	63	251	59	264	3.20E-23	109.4
contig_593_37	nirS	COG1622	eggNOG	34.9	129	74	2	3	121	137	265	9.70E-16	83.6
contig_696_17	nirS	COG0465	COG	65.4	130	45	0	230	359	1	130	3.60E-46	186.8
contig_696_4	nirS	COG0465	COG	56.2	466	201	3	138	601	26	490	2.60E-145	516.2
contig_906_6	nirS	COG0836	COG	32.7	352	224	7	51	390	4	354	4.50E-45	182.6
contig_906_8	nirS	COG0836	COG	28.1	302	204	7	101	390	1	301	2.30E-28	127.1
contig_911_1	nirS	COG0836	COG	28.7	289	193	7	114	390	3	290	6.60E-28	125.6
contig_974_2	nirS	COG0836	COG	35	297	181	6	51	336	4	299	1.20E-42	174.5
contig_1074_10	nmo	COG1028	eggNOG	53.8	65	28	2	155	218	11	74	3.20E-08	59.7
contig_1074_16	nmo	COG1028	eggNOG	36.3	146	88	3	11	152	19	163	2.10E-14	79.3
contig_1824_8	nmo	COG0432	eggNOG	65.7	137	47	0	5	141	3	139	5.00E-55	214.2
contig_1826_1	nmo	COG0432	eggNOG	65.7	137	47	0	5	141	3	139	5.00E-55	214.2
contig_1963_2	nmo	COG0107	eggNOG	50.6	87	43	0	9	95	5	91	1.10E-14	82
contig_1963_3	nmo	COG0107	eggNOG	39	159	77	3	13	164	31	176	2.50E-26	119
contig_2041_8	nmo	COG1028	eggNOG	27.1	236	139	7	8	215	64	294	1.50E-07	57
contig_2136_2	nmo	SS23303	m5nr	59.5	79	32	0	1	79	1	79	4.10E-22	104
contig_2136_3	nmo	SS23303	m5nr	59.5	79	32	0	1	79	1	79	4.10E-22	104
contig_2189_1	nmo	COG0107	COG	59.3	108	43	1	2	109	151	257	1.30E-29	129.4

contig_2189_7	nmo	COG0107	COG	52.7	131	58	2	1	128	128	257	3.20E-32	138.3
contig_2189_8	nmo	COG0107	eggNOG	53.2	77	36	0	63	139	1	77	8.20E-19	94.7
contig_2936_5	nmo	SS23303	m5nr	66.7	36	12	0	181	216	10	45	2.00E-06	53.5
contig_3277_6	nmo	COG0432	eggNOG	68.8	138	43	0	1	138	1	138	9.80E-56	216.5
contig_34_3	nmo	COG0107	COG	58.3	139	58	0	2	140	3	141	5.70E-44	177.6
contig_34_4	nmo	COG0107	COG	56.6	113	48	1	2	114	146	257	7.70E-30	130.2
contig_34_6	nmo	COG0107	COG	56.6	113	48	1	2	114	146	257	7.70E-30	130.2
contig_34_7	nmo	COG0107	COG	55.2	134	55	2	3	134	2	132	1.30E-34	147.1
contig_3500_2	nmo	COG4221	COG	42	1139	520	14	290	1297	2	1130	7.00E-250	864.8
contig_3500_3	nmo	COG4221	COG	39.1	649	365	8	688	1315	3	642	4.10E-133	476.9
contig_3794_2	nmo	SS23303	m5nr	50.6	235	114	2	19	251	3	237	7.90E-59	227.6
contig_3794_4	nmo	SS23303	m5nr	59.8	92	37	0	19	110	3	94	3.60E-27	122.5
contig_3794_5	nmo	SS23303	m5nr	50.5	93	44	2	161	251	2	94	2.00E-14	80.1
contig_675_21	nmo	COG0553	eggNOG	35	123	68	2	161	271	233	355	2.60E-10	66.6
contig_129_3	nosZ	SS25179	m5nr	38	179	105	3	34	212	103	275	1.40E-20	100.5
contig_129_8	nosZ	COG0515	COG	33.9	165	98	4	5	165	84	241	8.50E-20	98.6
contig_1334_1	nosZ	COG2931	eggNOG	52	500	217	6	37	531	2	483	3.90E-120	432.6
contig_136_10	nosZ	COG2205	COG	34.8	250	148	4	132	371	1101	1345	2.70E-34	146.7
contig_136_5	nosZ	COG2205	COG	34.8	250	148	4	132	371	1101	1345	2.70E-34	146.7
contig_1394_13	nosZ	COG0515	COG	35.6	275	167	5	9	280	76	343	1.10E-40	167.9
contig_142_32	nosZ	SS11211	m5nr	44.2	665	331	8	4	643	318	967	2.50E-154	546.2
contig_1420_3	nosZ	COG0031	eggNOG	57.3	302	127	2	9	308	7	308	2.60E-96	352.4

contig_1422_2	nosZ	COG0031	eggNOG	57.3	302	127	2	9	308	7	308	2.60E-96	352.4
contig_1442_3	nosZ	SS25179	m5nr	45.2	93	51	0	12	104	7	99	4.20E-17	88.2
contig_1691_41	nosZ	COG0515	COG	37.3	158	95	2	21	174	64	221	1.70E-23	109.8
contig_1699_12	nosZ	COG0515	COG	30.7	277	181	4	84	352	1	274	3.30E-34	146.4
contig_1781_14	nosZ	COG0448	COG	68.4	405	128	0	1	405	22	426	8.00E-170	597
contig_1781_18	nosZ	COG0448	COG	68.4	405	128	0	1	405	22	426	8.00E-170	597
contig_1842_21	nosZ	COG1825	eggNOG	36.7	109	67	1	78	186	21	127	2.30E-12	73.2
contig_2018_2	nosZ	ENOG410XNMH	eggNOG	22.4	183	120	4	57	226	21	194	1.50E-06	53.9
contig_210_2	nosZ	SS11211	m5nr	44.7	318	145	5	18	334	11	298	4.80E-67	255.4
contig_2124_19	nosZ	COG0515	COG	36.1	255	151	5	156	399	25	278	1.10E-35	151.4
contig_2124_6	nosZ	COG0515	COG	36.1	255	151	5	119	362	25	278	1.00E-35	151.4
contig_2175_5	nosZ	COG0085	eggNOG	67.2	256	84	0	904	1159	36	291	3.40E-99	364
contig_2175_7	nosZ	SS11615	m5nr	55.6	72	32	0	41	112	820	891	4.80E-16	84.3
contig_2175_8	nosZ	SS11615	m5nr	45.3	117	60	2	619	735	1	113	5.00E-19	97.8
contig_2280_4	nosZ	COG4690	COG	51	157	74	3	94	248	1	156	1.60E-35	151.4
contig_2500_3	nosZ	SS22990	m5nr	45.3	543	188	5	17	559	19	452	1.30E-106	387.5
contig_2500_4	nosZ	SS22990	m5nr	50.5	206	89	3	58	263	174	366	3.10E-42	172.6
contig_2646_9	nosZ	K06148	KEGG	30.9	220	140	4	3	218	506	717	1.50E-13	77.8
contig_2663_12	nosZ	K06148	KEGG	31.7	224	139	6	9	227	499	713	2.00E-20	100.1
contig_2663_4	nosZ	K06148	KEGG	37.3	110	63	3	9	116	499	604	2.50E-12	72
contig_2737_8	nosZ	SS11211	m5nr	39	105	54	3	1	96	664	767	1.10E-11	69.7
contig_2737_9	nosZ	SS11211	m5nr	50	70	35	0	1	70	780	849	1.60E-14	80.1
contig_2840_4	nosZ	SS22209	m5nr	30.9	298	173	9	239	535	238	503	3.40E-27	123.6

contig_2840_6	nosZ	SS22209	m5nr	30.9	298	173	9	239	535	238	503	3.40E-27	123.6
contig_2847_3	nosZ	COG2331	COG	66.1	59	20	0	1	59	1	59	2.50E-18	91.7
contig_2847_7	nosZ	COG2331	COG	66.1	59	20	0	1	59	1	59	2.50E-18	91.7
contig_2847_8	nosZ	COG2331	COG	66.1	59	20	0	1	59	1	59	2.50E-18	91.7
contig_2879_10	nosZ	K06148	KEGG	39.6	225	132	2	30	252	496	718	1.20E-42	174.1
contig_2879_1	nosZ	K06148	KEGG	42.2	83	46	1	15	97	638	718	6.10E-11	67.8
contig_2974_10	nosZ	SS22990	m5nr	68.4	38	12	0	8	45	221	258	3.20E-09	60.8
contig_2974_2	nosZ	SS22990	m5nr	60.8	51	20	0	3	53	137	187	1.10E-10	65.9
contig_2974_4	nosZ	SS22990	m5nr	33.5	191	101	6	3	185	61	233	1.30E-18	93.6
contig_2974_5	nosZ	SS22990	m5nr	34.5	110	63	2	3	111	61	162	3.50E-11	68.2
contig_3070_2	nosZ	K06148	KEGG	41.9	86	48	1	1	86	638	721	5.10E-11	67.4
contig_3070_5	nosZ	K06148	KEGG	44.1	93	50	1	30	122	637	727	2.90E-13	75.5
contig_3274_8	nosZ	K06148	KEGG	27.5	488	321	9	60	537	254	718	8.10E-40	165.6
contig_340_14	nosZ	SS22651	m5nr	25.1	343	206	11	61	394	69	369	1.40E-08	61.6
contig_3528_12	nosZ	K06148	KEGG	35.6	225	141	3	124	347	497	718	2.20E-33	143.7
contig_3528_2	nosZ	K06148	KEGG	24.8	532	372	12	205	718	117	638	1.10E-34	149.1
contig_3592_19	nosZ	COG0515	COG	38.7	261	150	5	22	280	1	253	6.30E-39	162.2
contig_3592_9	nosZ	COG0515	COG	38.7	261	150	5	22	280	1	253	6.30E-39	162.2
contig_3596_2	nosZ	K06148	KEGG	38.1	223	134	3	127	348	499	718	2.30E-35	150.2
contig_3658_5	nosZ	SS11615	m5nr	28.9	242	127	9	772	997	5	217	1.40E-15	86.3
contig_369_1	nosZ	COG4690	COG	54.1	270	121	3	2	270	133	400	3.20E-79	295.4
contig_370_1	nosZ	COG4690	COG	31.9	116	57	3	11	116	46	149	5.90E-06	53.1
contig_3814_3	nosZ	COG1219	COG	74.7	430	107	2	1	428	1	430	3.80E-183	641.3
contig_514_43	nosZ	COG0515	COG	40.1	257	143	3	7	252	9	265	6.10E-43	174.9
contig_686_8	nosZ	K06148	KEGG	30.1	166	86	5	63	215	519	667	7.80E-10	65.1

contig_766_3	nosZ	K06148	KEGG	31.7	224	139	6	22	240	499	713	1.60E-20	100.5
contig_766_6	nosZ	K06148	KEGG	31.7	224	139	6	22	240	499	713	1.60E-20	100.5
contig_769_1	nosZ	COG0542	COG	86.4	641	82	1	1	636	1	641	0.00E+00	1079.3
contig_769_7	nosZ	COG0542	COG	85.5	733	101	1	1	728	1	733	0.00E+00	1221.5
contig_93_22	nosZ	K06148	KEGG	31.7	218	124	7	21	227	523	726	8.30E-15	81.3
scaffold_1601_1	nosZ	SS18642	m5nr	33.6	443	235	10	6	402	108	537	1.30E-55	217.6
scaffold_1601_8	nosZ	SS18642	m5nr	33.1	462	250	10	1	416	140	588	1.70E-53	210.7
scaffold_191_25	nosZ	COG1022	eggNOG	34.1	214	140	1	372	585	2	214	1.30E-32	141.7
contig_1441_4	ureB	SS15895	m5nr	47.8	268	131	3	36	302	206	465	5.80E-72	271.6
contig_1441_5	ureB	SS15895	m5nr	61.1	108	36	1	3	104	473	580	9.10E-35	146.7
contig_1441_6	ureB	SS15895	m5nr	50.3	181	84	2	1	176	590	769	3.00E-49	195.3
contig_1441_7	ureB	SS15895	m5nr	60.6	132	52	0	418	549	2	133	3.40E-47	190.7
contig_17_55	ureB	SS16338	m5nr	27.3	403	269	10	193	580	97	490	1.40E-24	115.2
contig_18_5	ureB	SS16338	m5nr	27	403	270	10	193	580	97	490	5.40E-24	113.2
contig_2550_15	ureB	SS15895	m5nr	56.6	470	189	4	36	498	206	667	3.30E-168	592
contig_2550_5	ureB	SS15895	m5nr	56.6	470	189	4	1	463	206	667	3.10E-168	592
contig_3195_2	ureB	SS15895	m5nr	48.8	129	46	2	429	549	86	202	1.80E-32	141.7
contig_3195_3	ureB	SS15895	m5nr	53.2	517	225	6	11	520	213	719	2.90E-169	595.5
contig_1508_21	ureC	SS22785	m5nr	42.6	68	39	0	257	324	10	77	2.10E-09	63.9

Chapter 3. Appendix

Table S3-1. Summary of experimental design utilised for *G. mellonella* experiments. Table adapted from (Andrea et al., 2019) to include details of strains and a brief summary of their characteristics. (LP, left pro-leg; NA, not available, P-, privately purchased larvae from country specified).

S. aureus strain	Strain characteristics	Larval weight/size	Larval origin	Storage	Injection site	Infection	Reference
EDCC 5455-5461	clinical isolates	150–200 mg	Reared	30°C	Not given	1.0 x10^6	(Mannala *et al.* 2018)
EDCC 5464	clinical isolate, MRSA strain						
RN4220		NA	P-UK	4°C	Between segments	~1.3 x10^6	(Ba *et al.* 2015)
LGA251	veterinary isolate, mecC positive						
02.5099.D	clinical isolate, mecC positive						
ATCC 43300	MRSA, type culture	15–25 mm long	P-UK	7 days	LP	0.8–2.6 x10^6	(Bazaid *et al.* 2018)
Newman							
NCTC 13277	MRSA, type culture						
2x clin. isol.							
ATCC 29213	MSSA	~250 mg	P-China	NA	LP	~1.0 x10^6	(Dong *et al.* 2017)
ATCC 43300	MRSA						
N54	MSSA, clinical isolate						
MRSA N9	MRSA, clinical isolate						
USA300 JE2	MRSA	300–700 mg	P-Netherlands	NA	LP	1.0 x10^6	(Ebner *et al.* 2016)
ATCC 25923	type culture	~200 mg	NA	NA	LP	1.0 x10^3	(Ferro *et al.* 2016)
ATCC 6538	type culture						
SA01-04	clinical isolates						
USA300-0114		200–300 mg	P-USA	4°C, 14 days	LP	5.0 x10^6	(Jacobs *et al.* 2013)
UAMS-1							
UAMS-1112							
RN4220							
ATCC 6538	type culture	NA	Reared	28°C	NA	10^8 CFU/ml	(Jorjão *et al.* 2018)
ATCC 11195	MSSA, type culture	NA	P-UK	4°C, 14 days	NS	~2.5 x10^6	(Gibreel and Upton 2013)

Table S3-2. Multiple comparison results for change in lipid weight 24 h post-MRSA infection described in Figure 4.5A. (PBS; phosphate-buffered saline injection; NM, no manipulation control; ns, not significant).

Interaction	Mean rank diff.	Adjusted *p*-value
NM vs. PBS	78.87	>0.9999
NM vs. Live	339.5	<0.0001
NM vs. Dead	490.7	<0.0001
PBS vs. Live	260.6	<0.0001
PBS vs. Dead	411.8	<0.0001
Live vs. Dead	151.2	<0.0001

Significant p-values are in bold.

Chapter 4. Appendix

Equation S4-1. Larval total volume calculation. V_l, liquid volume of larvae; M_l, total mass of larvae. Equation taken from Andrea, Krogfelt and Jenssen (2019)

$$V_l = (0.6102 \times M_l) + 9.4889$$

Equation S4-2. *in vivo* concentration of injected compound calculation. $C_{comp.}$, concentration of compound injected into larvae; $C_{in\ vivo}$, *in vivo* concentration of compound injected; V_l, liquid volume of larvae as calculated in Eq. 4-1; $V_{comp.}$, volume of compound injected. Equation taken from Andrea, Krogfelt and Jenssen (2019)

$$C_{comp.} = \frac{C_{in\ vivo} \times V_l}{V_{comp.}}$$

Table S4-1. ANIb and antiSMASH results for PB091 and related organism. All genomes were accessed from NCBI and uploaded onto the JSpeciesWS online tool in addition to antiSMASH. (ANIb, genome-wide Average Nucleotide Identity based on BLAST+; hserlactone, homoserine lactone; T1/2PKS, Type 1/2 Polyketide Synthase; NRPS, Non-Ribosomal Peptide Synthase).

Organism	Strain	Number of contigs	Length (Mbp)	Type Strain?	NCBI assembly reference number	Similarity to strain PB091 (ANIb %)	Number of antiSMASH identified potential smBGC											
							T1PKS	T2PKS	NRPS	NRPS-PKS Hybrid	Terpene	RiPP-like	RRE- containing RiPP-like	Resorcinol	Arylpolyene	Butyrolactone	hserlactone	Total
D. acidovorans	NBRC 14950	91	6.63	Y	GCA_001598795.1	**97.30**	0	0	2	2	1	0	1	1	0	0	0	7
	Strain 2167	6	6.77	N	GCA_000741825.1	**97.26**	0	0	0	2	1	0	1	1	0	0	0	5
	CCUG 15835	68	6.82	N	GCA_000411215.1	94.53	0	1	5	1	1	0	1	1	0	0	0	10
	CCUG 274B	90	6.95	N	GCA_000411195.1	94.33	0	1	4	1	1	0	1	1	0	0	0	9
	SPH-1	1	6.76	N	GCA_000018665.1	**97.44**	0	0	0	1	1	0	1	1	0	0	0	4
***Delftia* sp.**	Strain 670	158	6.75	N	GCA_000710145.1	94.18	0	0	1	0	1	1	0	1	0	0	0	4
	Cs1-4	1	6.68	N	GCA_000214395.1	**97.51**	0	0	0	1	1	0	1	1	0	0	1	4
	D-2189*	110	6.96	N	GCF_900078185.1	94.35	0	1	0	1	1	0	1	1	0	0	0	5
	JD2	181	6.75	N	GCA_001682645.1	**97.46**	0	0	2	1	1	0	1	1	0	0	0	6
	RIT313	122	6.69	N	GCA_000632165.1	**97.64**	0	0	3	1	1	0	1	1	0	0	0	7
D. tsuruhatensis	Strain 391	153	6.73	N	GCA_000710165.1	94.11	0	0	0	2	1	0	1	1	0	0	0	5
	CM13	1,744	6.79	N	GCA_001753225.1	94.15	0	0	5	1	1	0	1	1	1	0	0	10
	MTQ3	62	6.79	N	GCA_001021565.1	93.52	0	0	0	1	1	0	1	1	1	0	0	5
D. lacustris	LMG 24775	74	7.17	Y	GCA_900107225.1	94.35	0	0	1	1	1	0	1	1	1	0	0	6

ANIb values above a minimum 95% cutoff value are in bold.

Table S4-2. Tukeys' multiple comparisons test for *G. mellonella* survival at 120 h (Fig. 4-4).

Tukey's multiple comparisons test			Mean difference	Adjusted *p*-value
No Manipulation	vs	PB Control	6.667	0.8636
No Manipulation	vs	PBS + PB091_S70	6.667	0.8636
No Manipulation	vs	LD50 + PBS	93.33	**<0.0001**
No Manipulation	vs	LD50 + PB091_S70	80.00	**<0.0001**
PBS Control	vs	PBS + PB091_S70	0.000	>0.9999
PBS Control	vs	LD50 + PBS	86.67	**<0.0001**
PBS Control	vs	LD50 + PB091_S70	73.33	**<0.0001**
PBS + PB091_S70	vs	LD50 + PBS	86.67	**<0.0001**
PBS + PB091_S70	vs	LD50 + PB091_S70	73.33	**<0.0001**
LD50 + PB091_S70	vs	PBS + PB091_S70	-13.33	0.2903

Significant p-values are in bold.

Table S4-3. Tukeys' multiple comparisons test for time-kill assay survival at 6 h (Fig. 4-5).

Tukey's multiple comparisons test			**Mean difference**	**Adjusted *p*-value**
PBS Control	vs	25 µg/ml	9.25×10^{8}	0.6763
PBS Control	vs	43.7 µg/ml	1.02×10^{9}	0.6227
25 µg/ml	vs	43.7 µg/ml	9.93×10^{7}	0.9958

Significant p-values are in bold.

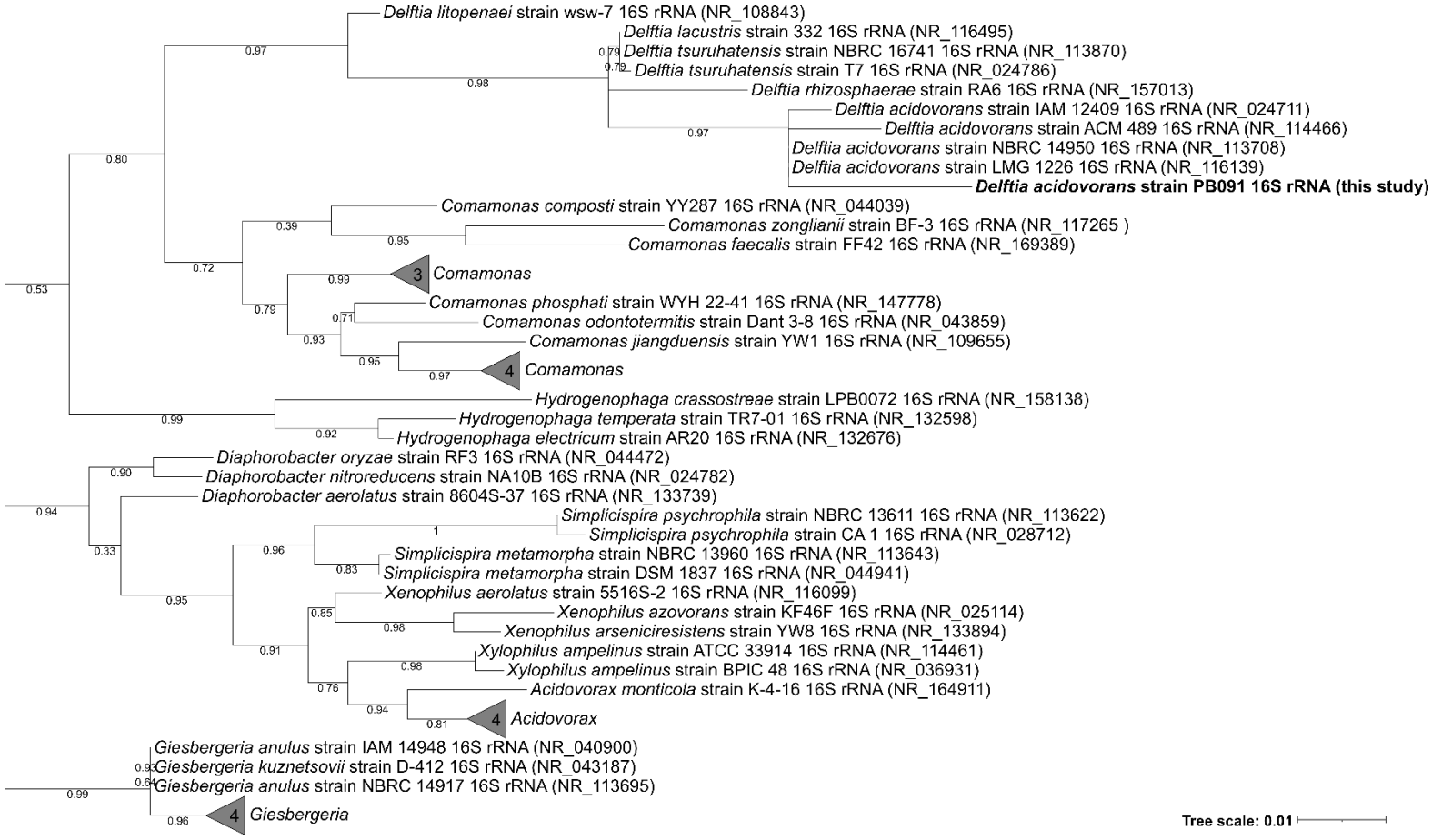

Figure S4-1. Phylogenetic placement of strain PB091 within the family Comamonadaceae based on full-length 16S ribosomal RNA (rRNA) gene sequences. The depicted tree is a neighbor-joining consensus tree, generated using eneiousTreeBuilder. Bootstrap values are depicted at branch nodes to two decimal places. Study strain is shown in bold, and GenBank accession numbers are shown in parenthesis.

Table S4-4. Consensus amino acid specificity of NRPS in PB091 and D-2189 based on motifs. NRPS cluster amino acid sequences were parsed through UMaryland PKS/NRPS and NRPSPredictor2.

Isolate	Location (contig_gene)	A domain	Coordinates	Residues in the Binding Pocket								Stachelhaus Prediction	
												aa	Confidence (%)
PB091	ctg1_984	A1	592-801	D	V	W	N	I	G	L	I	Thr	75
		A2	1672-1889	D	F	W	N	V	G	M	V	Thr	100
		A3	2755-2972	D	F	W	N	V	G	M	V	Thr	100
		A4	3825-4037	D	G	E	A	V	G	G	V	Orn	75
	ctg1_985	A1	650-861	D	A	E	D	I	G	A	V	Arg	87
		A2	1724-1933	D	V	W	H	F	S	L	I	Ser	100
		A3	2784-3001	D	F	W	N	V	G	M	V	Thr	100
		A4	3858-4066	D	A	F	W	L	G	T	F	Val	83
	ctg1_986	A1	642-854	D	L	T	K	V	G	H	V	Asp	87
		A2	2157-2377	D	F	W	N	V	G	M	V	Thr	100
	ctg1_988	A1	1305-1514	D	I	W	H	V	S	L	I	Ser	87
D-2189	ctg47_6	A1	1303-1512	D	I	W	H	I	S	L	I	Ser	87
	ctg47_8	A1	681-893	D	L	T	K	V	G	H	V	Asp	87
		A2	1757-1971	D	F	W	N	I	G	M	V	Thr	100
		A3	2857-3059	D	I	L	Q	L	I	W	K	Gly	100
	ctg47_9	A1	662-882	D	F	W	N	I	G	M	V	Thr	100
		A2	1756-1965	D	V	W	N	I	G	L	I	Thr	75
		A3	2841-3050	D	V	W	H	L	S	L	I	Ser	100
		A4	3931-4149	D	G	E	D	H	G	A	V	Arg	**62**
		A5	4554-5658	D	G	E	A	V	G	G	V	Orn	75

Confidence values in bold are regarded as weak Stachelhaus code matches (≤70%)

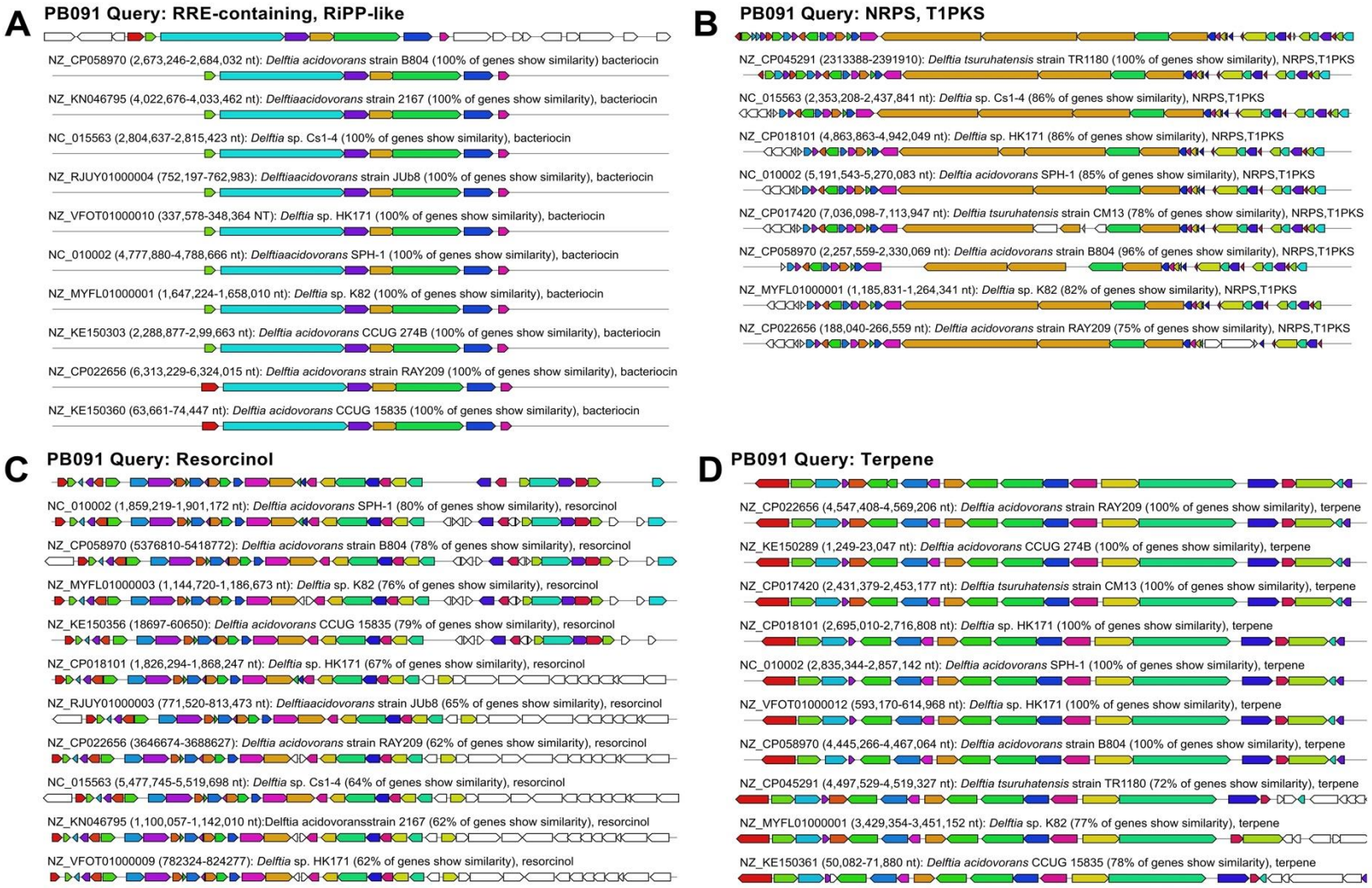

Figure S4-2. antiSMASH cluster comparison of PB091 with publicly available *Delftia* spp. genomes showing ubiquitous clusters within the genera. All clusters identified from PB091 are ubiquitous in *Delftia* spp. such as: (A) Putative bacteriocin from RRE-containing, RiPP-like cluster, (B) Delftibactin-A/B, (C) Resorcinol, and (D) Terpene. Region in which cluster was identified is presented in parenthesis, after the MiBIG cluster Accession number. Additionally the similarity of *Delftia* spp. Cluster to PB091 is show in in parenthesis.

Publications

Chapter 3 in Pathogens and Disease (FEMS)

OXFORD FEMS

Pathogens and Disease, 79, 2021, ftab003

doi: 10.1093/femspd/ftab003
Advance Access Publication Date: 27 January 2021
Research Article

RESEARCH ARTICLE

Galleria mellonella larvae exhibit a weight-dependent lethal median dose when infected with methicillin-resistant *Staphylococcus aureus*

Poppy J. Hesketh-Best[1,*,†], Michelle V. Mouritzen[2], Kayleigh Shandley-Edwards[1], Richard A. Billington[1] and Mathew Upton[2]

[1]School of Biological and Marine Sciences, University of Plymouth, Drake Circus, Plymouth, PL4 8AA, UK and [2]School of Biomedical Sciences, University of Plymouth, Derriford Research Facility, Plymouth Science Park, Plymouth, PL6 8BT, UK

*Corresponding author: Derriford Research Facility, Plymouth Science Park, Plymouth, PL6 8BT, UK. Tel: (+44) 1752 584466; E-mail: poppy.heskethbest@plymouth.ac.uk

One sentence summary: *Galleria mellonella* a commonly used infection model, is a weight-dependent model as MRSA activates lipolytic immune response rendering size a key factor for standardization of this model.

Editor: Juliana Campos Junqueira

†Poppy J. Hesketh-Best, http://orcid.org/0000-0002-0284-6689

ABSTRACT

Galleria mellonella is a recognised model to study antimicrobial efficacy; however, standardisation across the scientific field and investigations of methodological components are needed. Here, we investigate the impact of weight on mortality following infection with Methicillin-resistant *Staphylococcus aureus* (MRSA). Larvae were separated into six weight groups (180–300 mg at 20 mg intervals) and infected with a range of doses of MRSA to determine the 50% lethal dose (LD_{50}), and the 'lipid weight' of larvae post-infection was quantified. A model of LD_{50} values correlated with weight was developed. The LD_{50} values, as estimated by our model, were further tested *in vivo* to prove our model.
We establish a weight-dependent LD_{50} in larvae against MRSA and demonstrate that *G. mellonella* is a stable model within 180–260 mg. We present multiple linear models correlating weight with: LD_{50}, lipid weight, and larval length. We demonstrate that the lipid weight is reduced as a result of MRSA infection, identifying a potentially new measure in which to understand the immune response. Finally, we demonstrate that larval length can be a reasonable proxy for weight. Refining the methodologies in which to handle and design experiments involving *G. mellonella*, we can improve the reliability of this powerful model.

Keywords: Methicillin-resistant *Staphylococcus aureus*; *Galleria mellonella*; antibiotic testing; LD_{50}; pre-clinical model; fat body

INTRODUCTION

Galleria mellonella (Greater wax moth) larvae are widely utilised for toxicity screening (Desbois and Coote 2012; Maguire, Duggan and Kavanagh 2016; Coates *et al.* 2019) and to study host-pathogen interactions (Peleg *et al.* 2009; Olsen *et al.* 2011; Junqueira 2012; Wojda and Taszłow 2013). Unlike many insect models, *G. mellonella* can be incubated at 37°C, which facilitates the investigation of human pathogens. This has included most of the ESKAPE pathogens: *Enterococcus faecium* (Chibebe Junior *et al.* 2013; Luther *et al.* 2014); *Staphylococcus aureus* (Brackman *et al.* 2011; Ramarao, Nielsen-Leroux and Lereclus

Received: 30 September 2020; **Accepted:** 11 January 2021

2012; Sheehan, Dixon and Kavanagh 2019); *Klebsiella pneumoniae* (Wand *et al.* 2013; Diago-Navarro *et al.* 2014); *Acinetobacter baumannii* (Peleg *et al.* 2009); and *Pseudomonas aeruginosa* (Jander, Rahme and Ausubel 2000; Seed and Dennis 2008). Additionally, *Escherichia coli* (Leuko and Raivio 2012; Alghoribi *et al.* 2014; Jønsson *et al.* 2017; Guerrieri *et al.* 2019), *Bulkholderia mallei* (Schell, Lipscomb and DeShazer 2008) and several fungi (Cotter, Doyle and Kavanagh 2000; Reeves *et al.* 2004; Mylonakis *et al.* 2005) have also been studied using *G. mellonella*. Crucially, a positive correlation between the virulence and immune responses between mammalian models and *G. mellonella* has been established for *P. aeruginosa* (Jander, Rahme and Ausubel 2000), *Cryptococcus neoformans* (Mylonakis *et al.* 2005) and *S. aureus* (Sheehan, Dixon and Kavanagh 2019), demonstrating the powerful potential of this invertebrate model.

Antibiotic efficacy at dosages recommended for human use can be tested in *G. mellonella*, in addition to their toxicity correlating with toxicity observed in murine models (Ignasiak and Maxwell 2017). This has been shown with both natural and synthetic compounds (Gibreel and Upton 2013; Smitten *et al.* 2019), opening up the possibility of a rapid and cheap model for the early stages of discovery and development of natural and synthetic products, without the challenges of ethical approval, specialist training and the difficulties of using mice-models in early-stage drug development. Infections caused by antibiotic-resistant *S. aureus* are of global concern and it is listed as a high priority pathogen for which new antibiotics are urgently needed (The World Health Organisation 2017). Methicillin-resistant *S. aureus* (MRSA) has been utilised with *G. mellonella* for the study of virulence (Mannala *et al.* 2018), pathogenicity (Ebner *et al.* 2016), antimicrobial efficacy of existing antimicrobials (Ba *et al.* 2015; Ferro *et al.* 2016), and for novel candidates (Gibreel and Upton 2013; Jacobs *et al.* 2013; Dong *et al.* 2017) (Table S1, Supporting Information).

Despite the increased popularity of *G. mellonella*, there is much variability in method application (Andrea, Krogfelt and Jenssen 2019). This includes differences in larval size, storage, infective dose, and injection intervals. In this study, we address larval size and its potential impact in experimental design. In antibiotic efficacy studies, typically the model is infected with a pathogen shortly before the candidate treatment is presented. This has not been standardised with respect to the parameters previously mentioned for *G. mellonella*. In our preliminary experimentation in determining a 50% lethal dose (LD_{50}) for MRSA in *G. mellonella*, it was noted that smaller larvae were more susceptible to infection than larger larvae. This was when using a broad range of larval weights (~200–300 mg), as previously reported (Jacobs *et al.* 2013). Furthermore, the larval weight has been demonstrated to positively correlate with the larval liquid volume, leading to recommendations on how *in vivo* concentrations of injected compounds and pathogens should be calculated (Andrea, Krogfelt and Jenssen 2019). This led us to hypothesise that the larvae LD_{50} for a pathogen, in our case here MRSA, is directly proportional to the larvae weight and that larvae weight is an essential parameter in experimental design that must be tightly controlled.

When physical and anatomical barriers are breached, the wax moth larvae have an innate immune response relying on germline-encoded factors for the detection and clearance of microbial pathogens (Trevijano-Contador and Zaragoza 2019). There are two branches, cellular and humoral immunity. Cellular immunity is conducted by haemocytes, which are present in an open circulatory system called the haemolymph, which is analogous to vertebrate blood. There are at least six subpopulations of haemocytes which perform similar roles to those of the myeloid lineage in vertebrates (Boman and Hultmark 1987; Lavine and Strand 2002), and they are also associated with digestive system, trachea and fat body (Ratcliffe 1985). Five types of haemocytes were identified in fifth larval instar of *G. mellonella*; prohaemocytes, plasmatocytes, granulocytes, oenocytoids and spherulocytes (Salem *et al.* 2014). The main immune processes include coagulation, phagocytosis and encapsulation (Tojo *et al.* 2000). Circulating haemocyte density increases during pathogenesis due to the release of suspended cells from the fat body (Tojo *et al.* 2000). Haemocyte density and subpopulation variations changes with time of exposure to pathogen and pathogen virulence (Arteaga Blanco *et al.* 2017).

Melanisation additionally occurs in the haemolymph, the process of melanin production resulting in the darkened appearance of the larvae (Tojo *et al.* 2000). The humoral branch is involved in the production of lytic enzymes (Vogel *et al.* 2011), and antimicrobial peptides (AMPs) that are active against bacterial pathogens (Cytryńska *et al.* 2007; Tsai, Loh and Proft 2016). These molecules are mostly produced by the larval 'fat body', analogous to the mammalian liver, and are released into the haemolymph (Zasloff 2002).

A proteomic investigation has shown *S. aureus* infections lead to an increase in production of proteins such as AMPs and peptidoglycan recognition proteins (Sheehan, Dixon and Kavanagh 2019). Critically, the same study identified similarities between *G. mellonella* and mammal immune response to *S. aureus* infections. What has not been investigated is the physiological change in *G. mellonella* lipid as a result of *S. aureus* infections. For this investigation, we were motivated to quantify the lipid weight, a proxy for the fat body, of the larvae to observe how the fat body might have been affected as a result of MRSA infection.

The aim of the work here is to investigate methodological adjustments which may improve the reproducibility and reliability of using pet-food grade *G. mellonella* as an experimental model. This was achieved by (i) examining the effect of larval weight on the LD_{50} to MRSA infection, and (ii) characterising physiological changes occurring to lipid weight as a result of the larval immune response to MRSA.

MATERIALS AND METHODS

Cultivation of MRSA

A single colony of methicillin-resistant *Staphylococcus aureus* (MRSA) NTCT 12 493 was streaked onto fresh Luria broth (LB, Fischer Scientific, UK; Tryptone 10 g/L, yeast extract 5 g/L, and sodium chloride 10 g/L) solidified with 1.5% agar (Acros Organics, UK) 24 h before experimentation. Single colonies were suspended in Dulbecco A Phosphate buffered saline (PBS, Oxoid UK) to a range of optical density (OD) read at 600 nm (Eppendorf BioPhotometer, Netherlands). These dilutions were OD_{600} = 0.1–1.0 in 0.1 increments. Viable cell counts were made of each dilution.

Determining a weight-based LD_{50} for Galleria mellonella larvae

Larvae were purchased commercially from Livefoods UK Ltd. (Somerset, UK; www.livefoods.co.uk). On receipt, larvae were individually weighed using an accurate scale and grouped into the following weight bands: 180–200, 201–220, 221–240, 241–260, 261–280, and 281–300 mg. Larvae were stored at 4°C for up to 7 days in the dark with no food and water. Healthy larvae were

identified by a uniform cream colour, with no indications of melanisation such as spots or markings (Fig. 1A) (Li et al. 2018). Larvae were euthanised by chilling them at 4°C for 1 h, before freezing them at −20°C for a minimum of 24 h.

Larvae (n = 10) from each weight band were infected by injecting 10 μL of one of the 10 dilutions of MRSA into the left penultimate pro-leg (Fig. 1C), using a 50 μL Hamilton 750 syringe (Hamilton Company, UK) with a removable needle. Injected larvae were placed into Petri dishes lined with tissue paper (KIMTECH, UK). Three independent replicates of this experiment were carried out. Syringes were cleaned before and after each bacterial dilution. Cleaning consisted of taking up and discarding of each wash solution thrice before progressing to the next wash solution. Wash solution order was as follows: distilled H_2O (dH_2O), 70% ethanol, and dH_2O.

After infection, the larvae were maintained at 37°C in the dark without food or water. A placebo control of sterile PBS was used to account for the effect of the physical trauma of injection, along with a non-manipulation (NM) control. After 24 h the live/dead counts were recorded. Larvae were recorded as dead when they met the following: (i) complete melanisation (Fig. 1A), (ii) did not respond to touch, and (iii) could not correct itself when rolled onto its back.

Determining the weight-dependent LD_{50}, live/dead counts were converted into percentage mortality at 24 h for each group. For this investigation we have defined LD_{50} as CFU of MRSA per mg of organism resulting in 50% mortality. To model the dose-response and describe the relationship between increasing the infection dose on survival for each weight group, a non-linear sigmoidal regression curve was plotted. The infection dose, represented as CFU/mg of total weight of larva, was log-transformed. A non-linear regression curve was calculated to fit best the data generated from three independent replicas. From the equation generated from this curve, the theoretical LD_{50} was calculated along with the standard deviation (SD). Estimated LD_{50} from each weight groups were plotted against the mean larvae weight. A regression line was drawn, and the coefficient of determinant R^2 was calculated.

Correlating larval size with rate of pupation

On the day of receipt, larvae were placed into weight groups in Petri dishes. They were immediately placed at 37°C, in the dark with no food or water and permitted to pupate over 15 days. Larvae were observed daily and pupation events recorded.

Quantifying lipid weight of *G. mellonella*

Following investigation of the LD_{50} for MRSA, the lipid weight for all living and dead larvae was quantified. Live larvae from treatments, the NM and PBS controls were ethically euthanised. Dead larvae were stored at −20°C until needed. Larvae were left to thaw at room temperature for 24 h and were weighed and individually placed in Eppendorf tubes to be dried over 7 days at 55°C, and re-weighed to reveal their dry weight. Larvae were then submerged in ≥ 99.9% diethyl ether (Sigma-Aldrich, UK) and left for 3 days at 4°C to dissolve lipid. Diethyl ether was utilised as the lipid extraction solvent (Tzompa-Sosa et al. 2014). After, ether was left to evaporate in a fume hood for 24 h. Once dried, larvae were weighed again to acquire the post-ether weight. Quantities are then presented as followed: 'total weight' is the weight of the larvae pre-experimentation; 'water weight' ($water\ weight = pre\ experimentation\ weight - dry\ weight$); 'lipid weight' ($lipid\ weight = dry\ weight - post\ ether\ weight$).

Table 1. Summary of the LD_{50}s as calculated by non-linear models for each weight group (N, number of replicas; R^2, coefficient of determination).

Weight group (mg)	LD_{50} (CFU/mg)[a]	SD (CFU/mg)	N	R^2
180–200	1.19×10^7	1.47	30	0.85
201–220	1.26×10^7	2.45	30	0.77
221–240	2.34×10^7	1.57	30	0.80
241–260	4.40×10^7	3.35	30	0.76
261–280	8.97×10^7	1.46	30	0.69
281–300	4.19×10^7	1.81	30	0.78

[a]Example of how this is calculated can be found in Table S3 (Supporting Information).

Statistical analysis

All statistical analysis was performed using PRISM GraphPad 8.4.2 (GraphPad Software, San Diego, CA, USA). One-way ANOVA (two-tailed), two-way ANOVA, and Pearson's correlation coefficients were used when applicable to compare treatment groups. Log-rank Mantel-Cox tests compared survival curves for antimicrobial efficacy tests and pupation. A P-value of: < 0.05 (*), < 0.01 (**) or < 0.001 (***), < 0.0001 (****) was considered to be significantly different.

RESULTS

Larval weight affects LD_{50}

To begin testing our hypothesis, LD_{50} values were determined for each weight group. A sigmoidal non-linear model best fit the dose-dependent response of the data, resulting in an LD_{50} calculated for each weight group (Fig. 2). When adjusted to the number of cells injected into each larvae per one unit of body weight (CFU/mg), the resulting LD_{50} ranged from 1.19×10^7 CFU/mg, for the 180–200 mg group, to the highest LD_{50} which was 8.97×10^7 CFU/mg for the 261–280 mg group (Table 1). The LD_{50} increased across weight groups except for the 281–300 mg group, which had a lower LD_{50} than the 261–280 mg weight group. Throughout this experiment, we encountered some difficulties when handling larvae from the two higher weight-bands (261–280 and 281–300 mg), such as high variation in mortality at the lowest infective dosages (0%–40% mortality) and highest dosages (60%–100% mortality). Nevertheless, we were able to calculate an LD_{50} with the final data.

We observed a positive correlation between weight of the larvae and LD_{50}, as calculated by Pearson correlation test ($r = 0.87$, $P = 0.025$, $n = 18$). A linear regression model arriving at an equation ($y = 0.007966x + 5.548$) was used to estimate LD_{50} (Fig. 3A). The LD_{50} values, as estimated by our model, were tested *in vivo*, demonstrating an approximate 50%–56% (± 5.7%–10%) survival for four of the weight groups (Fig. 3B). Survival at 24 h for the weight groups 261–280 and 281–300 mg was 30% (± 0%) and 43% (±15.3%), respectively.

MRSA infection leads to a reduction in lipid weight

With the non-manipulated (NM) group, we assessed the overall relationship between total weight, dry weight, and lipid weight and length of the larvae (Fig. 4). Determined by Pearson's correlation test, we found a positive correlation between the total and dry weight, ($r = 0.972$, $P < 0.0001$, $n = 83$) (Fig. 4A), and total and water weight ($r = 0.989$, $P < 0.0001$, $n = 83$) (Fig. 4B). These

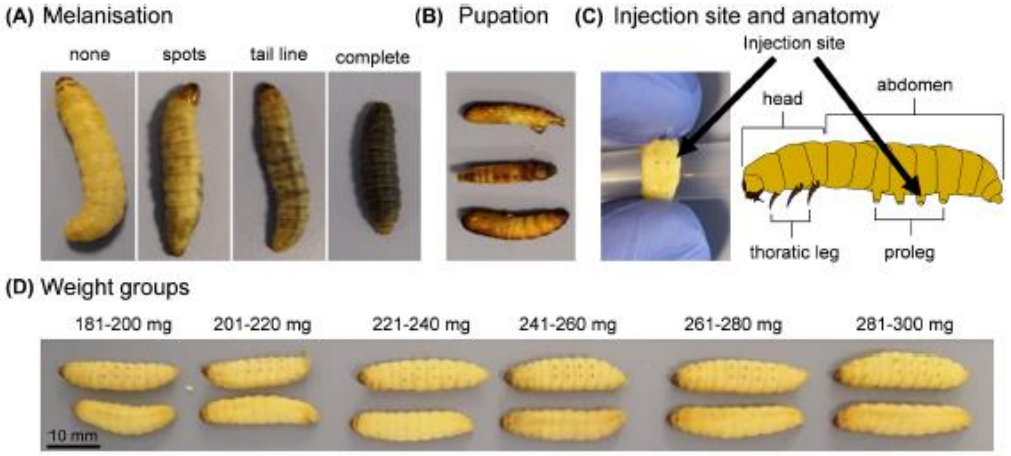

Figure 1. Galleria mellonella larvae. (A) Melanisation is a visual indication of the health of the larvae, as larvae progress from none to complete melanisation as a result of stress and/or infection. (B) Larvae pupation. (C) Route of infection for larvae is by intra-haemocoelic injection at the penultimate pro-leg (arrow). (D) Larvae are divided up into six weight groups.

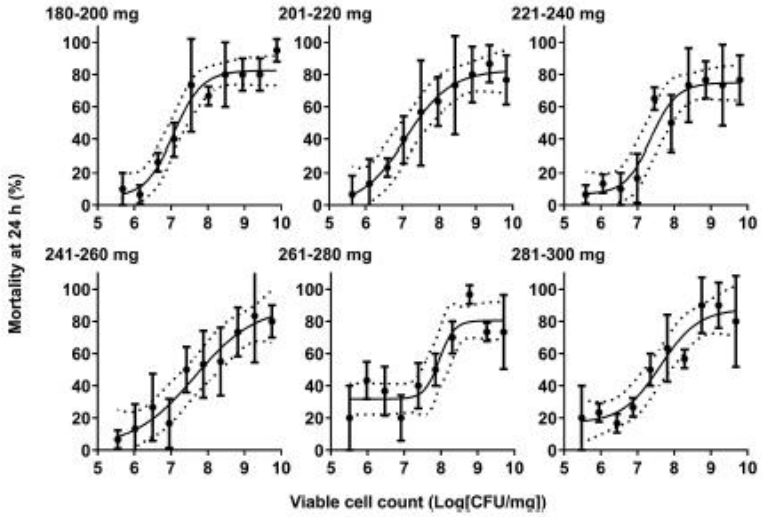

Figure 2. Sigmoidal non-linear logistic regressions best fit the dose-dependent response observed when calculating an LD_{50} for MRSA. LD_{50} was calculated for each weight group with 10 larvae/group. Data are shown as mean ± SD (n = 10) of three independent replicas.

two results support the findings of previous research (Andrea, Krogfelt and Jenssen 2019). Two additional positive correlations were observed between total weight and lipid ($r = 0.788$, $P < 0.0001$, $n = 83$) (Fig. 4C), and total weight and length ($r = 0.9944$, $P < 0.0001$, $n = 252$) (Fig. 4D).

We also investigated the effect of infection on the lipid weight of all the larvae used in determining the LD_{50} for MRSA (Fig. 5). As calculated by one-way ANOVA, injection with MRSA resulted in an overall decrease in the lipid weight for both dead (18.7 mg ± 8.541, $P < 0.0001$, $n = 573$) and live larvae (22.4 mg ± 6.556, $P < 0.0001$, $n = 524$), when compared to the NM control (31.92 mg ± 8.815, $n = 83$) (Fig 5A). When compared to one another, live larvae had a significantly greater lipid weight compared to dead larvae ($P < 0.0001$). There was no significant reduction in the lipid weight between NM and PBS control (27.81 mg ± 5.825, $P > 0.999$, $n = 50$) (Fig 5A and Table S2, Supporting Information).

Finally, we observed that at a high infective dosage of MRSA, the larvae had a lipid weight close to the mean of the NM and PBS control compared to the lower dosages (Fig. 5C and D). This

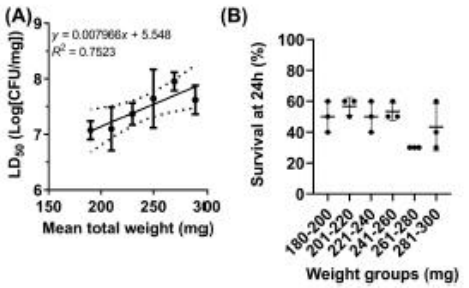

Figure 3. LD_{50} as calculated by non-linear regression models positively correlated with weight and was validated *in vivo* for all but the two highest weight groups. (A) Calculated LD_{50} by non-linear models correlation positively with total weight. (B) LD_{50} value as calculated by the model was validated by injecting into larvae and observing mortality. Data are shown as mean ± SD (n = 10) of three independent replicas.

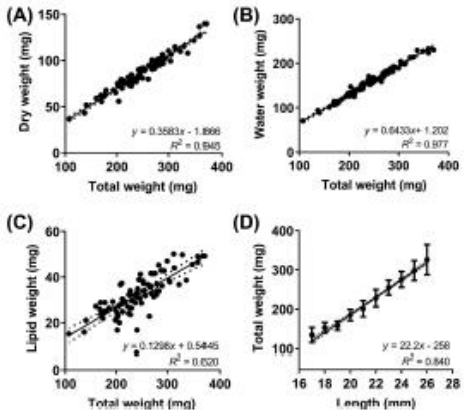

Figure 4. Multiple correlations observed between larvae total weight and dry weight, water weight, lipid weight, and larvae length. Non-manipulated (NM) larvae were used to analyse the relationships between (A) total weight and dry weight, (B) total weight and the lipid weight after here presented as lipid weight, (C) total weight and lipid weight as proportional to the total weight, water weight, and (D) total weight and larvae length where data is presented as mean ± SD (n = 252).

was supported by a positive correlation between lipid weight and infective dose for both live (r = 0.778, P = 0.008) (Fig. 5C) and dead larvae (r = 0.669, P = 0.035) (Fig. 5D).

Pupation is unaffected by weight

To explore whether larger larvae were closer to the final instar stage (pupae) in which they begin to pupate into adult moths, an observational experiment was performed. NM larvae were left to pupate at 37°C, and it was observed that 80–100% of larvae pupated within the 15 day incubation period, independent on their weight grouping, as calculated by Log-rank (Mantel-Cox) test (X^2(5, N = 60) = 4.004, P = 0.549) (Fig. 6).

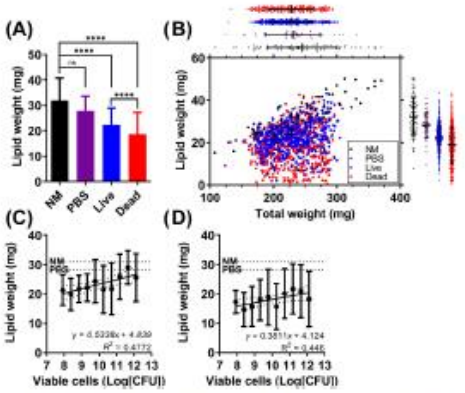

Figure 5. Injection of the larvae with MRSA results in an overall decreased in the lipid weight of the larvae. (A) Statistical results from a one-way ANOVA are illustrated above the bars as compared to the NM control. Summary of multiple analysis can be found in Table S2 (Supporting Information). (B) Box-plots above and to the right of the scatter plot are to illustrate the distribution of the data. Colours are as follows: black, NM control; purple, PBS control; blue, live larvae; and red, dead larvae 24 h post-MRSA infection. Correlations of infective dose and lipid weight for (C) living and (D) dead larvae. Data is presented as Log[CFU], as the infective doses are not adjusted for larvae weight. Data presented as mean ± SD (n = 10) of three independent replicas.

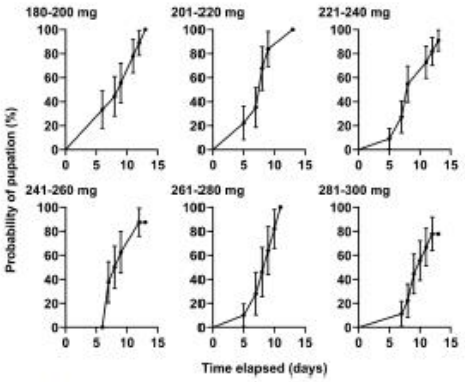

Figure 6. The weight did not influence the probability of pupation of NM larvae. NM larvae were incubated at 37°C for 15 days and observed daily for pupation events. No significant difference was found between the weight group and the probability of pupation as calculated by a Log-rank Mantel-Cox test (P = 0.5489). Data are shown as mean ± SD (n = 10) repeated twice.

DISCUSSION

MRSA exhibits a weight-dependent LD_{50}

In this study, we have demonstrated it is possible to develop a model in which a LD_{50} can be predicted based on the weight of the larvae, and that the prediction can be experimentally validated (Fig. 3). The linear model correlating total and water weight (Fig. 4B) imply that in increasingly larger larvae, the *in vivo* dilution of MRSA increases requiring a greater density

of pathogen to reach the LD_{50}. Likewise for the positive correlation confirmed with total and lipid weight (Fig. 4C), the presence of a larger fat body that can be degraded for the production of immune factors, may well be why we observe the weight-dependent effect on LD_{50}. The LD_{50}s (1.19–8.97 × 10^7 CFU/mg) for the MRSA strain was not within range of infective dosages utilised in previously investigated MRSA and Methicillin-sensitive *S. aureus* (MSSA) strains (0.8–5.0 × 10^6 CFU) (Table S1, Supporting Information). However, a direct comparison may not be appropriate given the variation in reporting densities as in our study the LD_{50} was adjusted to account for *in vivo* dilution in the larvae as described in Andrea, Krogfelt and Jenssen (2019), but this is not always done.

During the process of this investigation, we found two of the largest weight groups (261–280 and 281–300 mg) to be unreliable, which hindered progress. This was consistent across multiple batches of larvae orders. LD_{50}, as calculated by our model for 261–280 and 281–300 mg larvae, resulted in less than 50% survival at 24 h (Fig. 3B), indicating that our model for a weight-dependent LD_{50} had overestimated the LD_{50}. Our first assumptions were that larger larvae were older and closer to pupation than the smaller weight groups, as larvae increase in size until pupation (Jorjão *et al.* 2018), which might somehow impact on survival. Given the difficulty in identifying an age for each larva, it is a difficult hypothesis to test beyond quantifying the number of days it took for NM larvae from each weight group to pupate.

When this was conducted, we found that larval size did not influence the probability of pupation (Fig. 6), and we conclude that the larvae received from the supplier had an 80–100% probability of pupating within 15 days if kept at 37°C, regardless of weight. It would appear that larger larvae were not likely to be closer to pupation than smaller ones, so the reason for our observed decrease in LD_{50} for large larvae remains unknown. Since larvae were kept without food, this may be a reason for the observed similar pupation times across all weight groups as lack of food source may be forcing the larvae into pupation. Feeding regimes are not the standard protocol when investing antibiotic efficacy, as such we feel this best represented the conditions larvae would be exposed to at the start of experimentation.

Using *G. mellonella* does have drawbacks, one such being the functional equivalent of adaptive immunity termed 'immune priming' (Little and Kraaijeveld 2004; Sadd and Schmid-Hempel 2006). Individual larvae that survive infection or exposure to a particular pathogen may exhibit increased immune resistance against the same or similar pathogens. Priming with heat-killed pathogens was observed to result in increased larval survival (Wu *et al.* 2014). Ultimately there will be no control over the immune history of the larvae and this should always be recognised when working with pet-food grade *G. mellonella*. Across the literature, a wide range of weight bands have been utilised: 150–200 mg (Mannala *et al.* 2018); 300–700 mg (Ebner *et al.* 2016); 200–300 mg (Jacobs *et al.* 2013); and in other studies this is not declared (Ba *et al.* 2015; Jorjão *et al.* 2018). Our results suggest that choosing weight ranges as wide as 300–700 mg and 200–300 mg could result in inconsistent data. While a weight range of only 20 mg is likely a conservative approach, ranges such as 100 mg or greater in our weight-dependent LD_{50} model for MRSA indicates that there would be significant differences in survival (Fig. 3A).

Weighing individual larvae is a time-consuming procedure. This study also demonstrated that larvae length is reasonable proxy for the weight (Fig. 4D). Larval length has been previously used to characterise larvae for experimentation where larvae of 15–25 mm were utilised (Bazaid *et al.* 2018). Like total weight, a large length grouping may also encounter similar challenges. A 20 mg weight grouping would equate to roughly 1 mm, for example, 180–200 mg would be 20–21 mm. Measuring length may be a preferred alternative to accurately weighing all larval. When sourcing larvae from our supplier, we frequently found that larvae belonging to the weight groups 201–220 and 221–240 mg were most abundant, which will inevitably be the practical determining factor in weight group selection. Our findings would support selection of larvae in this range.

Lipid metabolism occurs in response to MRSA infection

MRSA infection leads to a decreased lipid weight in the larvae after 24 h, whether they died or survived the infection (Fig. 5A). The reduction in lipid weight is likely the result of lipolysis during an immune response. This is to be expected, the fat body of the larvae produce many defence compounds essential to the larvae's immune response (Cytryńska *et al.* 2007; Tsai, Loh and Proft 2016). This reaction can be rapid, in some models showing production of AMPs within the first 4 to 6 h post-infection (Sheehan, Dixon and Kavanagh 2019; Trevijano-Contador and Zaragoza 2019). This is supported by proteomic work, which demonstrated that at 6 and 24 h post-*S. aureus* infection larvae had increased expression of AMPs (Sheehan, Dixon and Kavanagh 2019).

On exposure to the infecting pathogen, there may be a rapid metabolism of the fat body to provide the required energy to fight the infection. Larvae with larger lipid weight before infection might be more likely to survive, as seen with the surviving larvae having a greater lipid weight than dead larvae (Fig. 5A). Within this experimental design, the larvae are not fed before or during the experiment, and therefore they cannot be acquiring more lipid. Where lipid weight was seen as closer to the NM and PBS control baseline, as observed in the trend of lipid weight positively correlating with infective dose (Fig. 5C and D), it is more likely that lipid metabolism has been compromised.

What could reasonably be expected is that lipolysis of the fat body occurs to increase the production of AMPs and additional defence compounds. When *Drosophila* are stimulated by a systemic infection with *S. aureus*, signalling from the Toll receptor increases, which leads to increased production of AMPs and reduced accumulation of lipids (Liu *et al.* 2016; Lee and Lee 2018). This could suggest that for larvae surviving high infective dosages, there are additional immune responses that do not deplete the fat body.

We intended to quantify the larval lipid weight to aid in understanding the weight-dependent LD_{50} effect and the observed unreliability of the two largest weight groups (261–280 and 281–300 mg). We report several observations regarding the lipid weight and MRSA infection; however, none can fully explain the irregularity we encountered for the largest weight groups. Analysing larval lipid weight has proved some insight, but would benefit from further investigation, though alternative methods to estimate lipid mass would be required.

Overall assessment of *G. mellonella* as a model

There remains a lack of widely available and cheap standardised stocks of larvae reared under controlled conditions. Temperature (Mowlds and Kavanagh 2008), diet (Banville, Browne and Kavanagh 2012; Jorjão *et al.* 2018), past infections (Fallon, Kelly and Kavanagh 2012), and antibiotics and hormones in the feed (Büyükgüzel and Kalender 2008) are all reported to influence laboratory experimentation. Most larvae currently used are acquired from commercial insect food providers (Andrea,

Krogfelt and Jenssen 2019), where it is understood that use of antibiotics and hormones in the culture medium is common practice, and acquiring accurate information regarding the conditions in which the larvae are reared is challenging. All of which may vary between larvae suppliers, which is a challenge that warrants further investigation.

Ultimately from our investigation, it would appear that lipid deposits are essential in *G. mellonella* response to MRSA. Prior investigation has evaluated the effect of nutrient deprivation on larvae (Banville, Browne and Kavanagh 2012), and the selection of diet (Jorjão *et al.* 2018), which both influence susceptibility to *S. aureus* infection. This emphasises the issues associated with a having lack of knowledge of rearing conditions used by suppliers and how they will influence experimental results. TruLarv™ (BioSystems Technology, UK) currently provide the only standardised *G. mellonella* in the UK. While cheap compared to murine models, it is considerably costlier (£1.20 per larvae) than purchasing larvae from commercial pet food providers.

However for pet-food grade larvae to be reliably used in research, more significant consideration should be taken over the parameters that can be controlled, and in this study, we emphasise that such experiments can be reproducible and reliable. We recommend that investigators consider the potential variability associated with using different larval weight as we have shown herein. We would recommend using weight groupings as a means to control this. Our data suggests that all larvae used should be within 10 mg of the mean weight of all larvae to provide consistency. Additionally, larvae of > 260 mg should not be avoided.

In this work, we present several linear regression curves that could be used as tools to aid in experimental design, such as the linear model for LD_{50} (Fig. 3A), weight and lipid content (Fig. 4C), and length (Fig. 4D). Finally, we demonstrate that the lipid weight is reduced as a result of MRSA infection, identifying a potentially new measure in which to understand the immune response. Similarities between *G. mellonella* and mammals in response to *S. aureus* infections can be used to study the efficacy and interactions of novel antimicrobials, even at early development stages. By refining and standardising methodologies in which to handle and select *G. mellonella* for study, we can improve the reliability of this powerful model for multiple purposes.

SUPPLEMENTARY DATA

Supplementary data are available at FEMSPD online.

TRANSPARENCY DECLARATION

The authors declare no conflict of interests. The funders had no role in the design of the study; in the collection, analyses, or interpretation of data; in the writing of the manuscript, or in the decision to publish the results.

AUTHOR CONTRIBUTIONS

Conceptualisation, PJHB and MVM; Methodology, PJHB, MVM, KSE, RAB, and MU; Validation, PJHB, MVM, and KSE; Formal Analysis, PJHB; Investigation, PJHB and MVM; Resources, PJHB and MVM; Data Curation, PJHB and MVM; Writing—Original Draft Preparation, PJHB; Writing—Review & Editing, PHB, MVM, KSE, RAB, and MU; Visualization, PJHB; Supervision, RAB, and MU; Funding Acquisition, MU.

FUNDING

This study was funded in part by the University of Plymouth, School of Biology and Marine Science postgraduate research studentship and Innovate UK Antibiotic Development grant (Innovate UK 103358).

Conflicts of Interest. None declared.

REFERENCES

Alghoribi MF, Gibreel TM, Dodgson AR *et al. Galleria mellonella* infection model demonstrates high lethality of ST69 and ST127 uropathogenic *E. coli*. *PLoS One* 2014;9:e101547–.

Andrea A, Krogfelt KA, Jenssen H. Methods and Challenges of Using the Greater Wax Moth (*Galleria mellonella*) as a Model Organism in Antimicrobial Compound Discovery. *Microorganisms* 2019;7:85.

Arteaga Blanco LA, Crispim JS, Fernandes KM *et al.* Differential cellular immune response of *Galleria mellonella* to *Actinobacillus pleuropneumoniae*. *Cell Tissue Res* 2017;370:153–68.

Banville N, Browne N, Kavanagh K. Effect of nutrient deprivation on the susceptibility of *Galleria mellonella* larvae to infection. *Virulence* 2012;3:497.

Ba X, Harrison EM, Lovering AL *et al.* Old drugs to treat resistant bugs: Methicillin-resistant *Staphylococcus aureus* isolates with mecC are susceptible to a combination of penicillin and clavulanic acid. *Antimicrob Agents Chemother* 2015;59:7396–404.

Bazaid AS, Forbes S, Humphreys GJ *et al.* Fatty acid supplementation reverses the small colony variant phenotype in triclosan-adapted *Staphylococcus aureus*: genetic, proteomic and phenotypic analyses. *Sci Rep* 2018;8:3876.

Boman HG, Hultmark D. Cell-free immunity in insects. *Annu Rev Microbiol* 1987;41:103–26.

Brackman G, Cos P, Maes L *et al.* Quorum sensing inhibitors increase the susceptibility of bacterial biofilms to antibiotics in vitro and in vivo. *Antimicrob Agents Chemother* 2011;55:2655–61.

Büyükgüzel E, Kalender Y. *Galleria mellonella* (L.) survivorship, development and protein content in response to dietary antibiotics. *J Entomol Sci* 2008;43:27–40.

Chibebe Junior J, Fuchs BB, Sabino CP *et al.* Photodynamic and antibiotic therapy impair the pathogenesis of *Enterococcus faecium* in a whole animal insect model. *PLoS One* 2013;8:55926.

Coates CJ, Lim J, Harman K *et al.* The insect, *Galleria mellonella*, is a compatible model for evaluating the toxicology of okadaic acid. *Cell Biol Toxicol* 2019;35:219–32.

Cotter G, Doyle S, Kavanagh K. Development of an insect model for the in vivo pathogenicity testing of yeasts. *FEMS Immunol Med Microbiol* 2000;27:163–9.

Cytryńska M, Mak P, Zdybicka-Barabas A *et al.* Purification and characterization of eight peptides from *Galleria mellonella* immune hemolymph. *Peptides* 2007;28:533–46.

Desbois AP, Coote PJ. Chapter 2 - utility of greater wax moth larva (*Galleria mellonella*) for evaluating the toxicity and efficacy of new antimicrobial agents. In: Laskin AI, Sariaslani S, Gadd GM (eds). *Advances in Applied Microbiology*. Vol 78, Cambridge, Massachusetts, United States: Academic Press, 2012, 25–53.

Diago-Navarro E, Chen L, Passet V *et al.* Carbapenem-resistant *Klebsiella pneumoniae* exhibit variability in capsular polysaccharide and capsule associated virulence traits. *J Infect Dis* 2014;210:803–13.

Dong CL, Li LX, Cui ZH *et al.* Synergistic effect of pleuromutilins with other antimicrobial agents against *Staphylococcus aureus* in vitro and in an experimental *Galleria mellonella* model. *Front Pharmacol* 2017;**8**:553.

Ebner P, Rinker J, Nguyen MT *et al.* Excreted cytoplasmic proteins contribute to pathogenicity in *Staphylococcus aureus*. *Infect Immun* 2016;**84**:1672–81.

Fallon J, Kelly J, Kavanagh K. *Galleria mellonella* as a model for fungal pathogenicity testing. *Methods Mol Biol* 2012;**845**: 469–85.

Ferro TAF, Araújo JMM, dos Santos Pinto BL *et al.* Cinnamaldehyde Inhibits *Staphylococcus aureus* Virulence Factors and Protects against Infection in a *Galleria mellonella* Model. *Front Microbiol* 2016;**7**:2052.

Gibreel TM, Upton M. Synthetic epidermicin NI01 can protect *Galleria mellonella* larvae from infection with *Staphylococcus aureus*. *J Antimicrob Chemother* 2013;**68**:2269–73.

Guerrieri CG, Pereira MF, Galdino ACM *et al.* Typical and atypical enteroaggregative *Escherichia coli* are both virulent in the *Galleria mellonella* model. *Front Microbiol* 2019;**10**:1791.

Ignasiak K, Maxwell A. *Galleria mellonella* (greater wax moth) larvae as a model for antibiotic susceptibility testing and acute toxicity trials. *BMC Res Notes* 2017;**10**:428.

Jacobs AC, DiDone L, Jobson J *et al.* Adenylate kinase release as a high-throughput-screening-compatible reporter of bacterial lysis for identification of antibacterial agents. *Antimicrob Agents Chemother* 2013;**57**:26–36.

Jander G, Rahme LG, Ausubel FM. Positive correlation between virulence of *Pseudomonas aeruginosa* mutants in mice and insects. *J Bacteriol* 2000;**182**:3843–5.

Jorjão AL, Oliveira LD, Scorzoni L *et al.* From moths to caterpillars: Ideal conditions for *Galleria mellonella* rearing for in vivo microbiological studies. *Virulence* 2018;**9**:383–9.

Junqueira JC. *Galleria mellonella* as a model host for human pathogens: Recent studies and new perspectives. *Virulence* 2012;**3**:474–6.

Jønsson R, Struve C, Jenssen H *et al.* The wax moth *Galleria mellonella* as a novel model system to study Enteroaggregative *Escherichia coli* pathogenesis. *Virulence* 2017;**8**: 1894–9.

Lavine MD, Strand MR. Insect hemocytes and their role in immunity. *Insect Biochemistry and Molecular Biology*. Vol 32, Oxford, UK: Pergamon, 2002, 1295–309.

Lee KA, Lee WJ. Immune–metabolic interactions during systemic and enteric infection in *Drosophila*. *Curr Opin Insect Sci* 2018;**29**:21–6.

Leuko S, Raivio TL. Mutations that impact the enteropathogenic *Escherichia coli* Cpx envelope stress response attenuate virulence in *Galleria mellonella*. *Infect Immun* 2012;**80**: 3077–85.

Little TJ, Kraaijeveld AR. Ecological and evolutionary implications of immunological priming in invertebrates. *Trends Ecol Evol* 2004;**19**:58–60.

Liu B, Zheng Y, Yin F *et al.* Toll receptor-mediated hippo signaling controls innate immunity in *Drosophila*. *Cell* 2016;**164**:406–19.

Li Y, Spiropoulos J, Cooley W *et al.* Galleria mellonella - a novel infection model for the *Mycobacterium tuberculosis* complex. *Virulence* 2018;**9**:1126–37.

Luther MK, Arvanitis M, Mylonakis E *et al.* Activity of daptomycin or linezolid in combination with rifampin or gentamicin against biofilm-forming *Enterococcus faecalis* or *E. faecium* in an in vitro pharmacodynamic model using simulated endocardial vegetations and an *in vivo* sur. *Antimicrob Agents Chemother* 2014;**58**:4612–20.

Maguire R, Duggan O, Kavanagh K. Evaluation of *Galleria mellonella* larvae as an in vivo model for assessing the relative toxicity of food preservative agents. *Cell Biol Toxicol* 2016;**32**:209–16.

Mannala GK, Koettnitz J, Mohamed W *et al.* Whole-genome comparison of high and low virulent *Staphylococcus aureus* isolates inducing implant-associated bone infections. *Int J Med Microbiol* 2018;**308**:505–13.

Mowlds P, Kavanagh K. Effect of pre-incubation temperature on susceptibility of *Galleria mellonella* larvae to infection by *Candida albicans*. *Mycopathologia* 2008;**165**:5–12.

Mylonakis E, Moreno R, El Khoury JB *et al.* *Galleria mellonella* as a model system to study *Cryptococcus neoformans* pathogenesis. *Infect Immun* 2005;**73**:3842–50.

Olsen RJ, Ebru Watkins M, Cantu CC *et al.* Virulence of serotype M3 group A *Streptococcus* strains in wax worms (*Galleria mellonella* larvae). *Virulence* 2011;**2**:111.

Peleg AY, Jara S, Monga D *et al.* *Galleria mellonella* as a model system to study *Acinetobacter baumannii* pathogenesis and therapeutics. *Antimicrob Agents Chemother* 2009;**53**:2605–9.

Ramarao N, Nielsen-Leroux C, Lereclus D. The insect *Galleria mellonella* as a powerful infection model to investigate bacterial pathogenesis. *J Vis Exp* 2012:e4392, DOI: 10.3791/4392.

Ratcliffe NA. Invertebrate immunity - A primer for the non-specialist. *Immunol Lett* 1985;**10**:253–70.

Reeves EP, Messina CGM, Doyle S *et al.* Correlation between gliotoxin production and virulence of *Aspergillus fumigatus* in *Galleria mellonella*. *Mycopathologia* 2004;**158**:73–9.

Sadd BM, Schmid-Hempel P. Insect immunity shows specificity in protection upon secondary pathogen exposure. *Curr Biol* 2006;**16**:1206–10.

Salem HM, Hussein MA, Hafez SE *et al.* Ultrastructure changes in the haemocytes of *Galleria mellonella* larvae treated with gamma irradiated *Steinernema carpocapsae* BA2. *J Radiat Res Appl Sci* 2014;**7**:74–9.

Schell MA, Lipscomb L, DeShazer D. Comparative genomics and an insect model rapidly identify novel virulence genes of *Burkholderia mallei*. *J Bacteriol* 2008;**190**:2306–13.

Seed KD, Dennis JJ. Development of *Galleria mellonella* as an alternative infection model for the *Burkholderia cepacia* complex. *Infect Immun* 2008;**76**:1267–75.

Sheehan G, Dixon A, Kavanagh K. Utilization of *Galleria mellonella* larvae to characterize the development of *Staphylococcus aureus* infection. *Microbiol (United Kingdom)* 2019;**165**: 863–75.

Singkum P, Suwanmanee S, Pumeesat P *et al.* A powerful in vivo alternative model in scientific research: *Galleria mellonella*. *Acta Microbiol Immunol Hung* 2019;**66**:31–55.

Smitten KL, Southam HM, de la Serna JB *et al.* Using nanoscopy to probe the biological activity of antimicrobial leads that display potent activity against pathogenic, multidrug resistant, gram-negative bacteria. *ACS Nano* 2019;**13**:5133–46.

The World Health Organisation. *Global Priority List of Antibiotic-Resistant Bacteria to Guide Research, Discovery, and Development of New Antibiotics*, Geneva, Switzerland, 2017.

Tojo S, Naganuma F, Arakawa K *et al.* Involvement of both granular cells and plasmatocytes in phagocytic reactions in the greater wax moth, *Galleria mellonella*. *J Insect Physiol* 2000;**46**:1129–35.

Trevijano-Contador N, Zaragoza O. Immune response of *Galleria mellonella* against human fungal pathogens. *J Fungi* 2019;**5**:3.

Tsai CJ-YY, Loh JMS, Proft T. *Galleria mellonella* infection models for the study of bacterial diseases and for antimicrobial drug testing. *Virulence* 2016;**7**:214–29.

Tzompa-Sosa DA, Yi L, van Valenberg HJF *et al.* Insect lipid profile: Aqueous versus organic solvent-based extraction methods. *Food Res Int* 2014;62:1087–94.

Vogel H, Altincicek B, Glöckner G *et al.* A comprehensive transcriptome and immune-gene repertoire of the lepidopteran model host *Galleria mellonella*. *BMC Genomics* 2011;12:308.

Wand ME, McCowen JWI, Nugent PG *et al.* Complex interactions of *Klebsiella pneumoniae* with the host immune system in a *Galleria mellonella* infection model. *J Med Microbiol* 2013;62:1790–8.

Wojda I, Taszłow P. Heat shock affects host-pathogen interaction in *Galleria mellonella* infected with *Bacillus thuringiensis*. *J Insect Physiol* 2013;59:894–905.

Wu G, Zhao Z, Liu C *et al.* Priming *Galleria mellonella* (Lepidoptera: Pyralidae) larvae with heat-killed bacterial cells induced an enhanced immune protection against *Photorhabdus luminescens* TT01 and the role of innate immunity in the process. *J Econ Entomol* 2014;107:559–69.

Zasloff M. Antimicrobial peptides of multicellular organisms. *Nature* 2002;415:389–95.